

**INVESTIGATION OF THE DUAL CYTO-TOXIC/-PROTECTIVE  
ROLES OF  $\alpha$ -SYNUCLEIN IN HUMAN NEUROBLASTOMA, SH-SY5Y  
AND HUMAN MELANOMA, SK-MEL28 CELLS**

By

**CHOONG CHI-JING**

A thesis submitted to Faculty of Engineering and Science,

Universiti Tunku Abdul Rahman,

in partial fulfillment of the requirements for the degree of

Master of Science

March 2011

## ABSTRACT

### INVESTIGATION OF THE DUAL CYTO-TOXIC/-PROTECTIVE ROLES OF $\alpha$ -SYNUCLEIN IN HUMAN NEUROBLASTOMA, SH-SY5Y AND HUMAN MELANOMA, SK-MEL28 CELLS

**Choong Chi-Jing**

$\alpha$ -Synuclein ( $\alpha$ -Syn) is a central player in the pathophysiology of the dopaminergic neurodegeneration that occurs in Parkinson's disease (PD). However, emerging results suggest that the fundamental property of its wild type form may be protective. Therefore the objective of this study was to investigate the cyto-toxic/-protective roles of  $\alpha$ -Syn in neuronal SH-SY5Y and melanoma SK-MEL28 cells, by overexpression and knockdown, respectively. For  $\alpha$ -Syn overexpression, wild type human  $\alpha$ -Syn and three familial pathogenic  $\alpha$ -Syn mutants (A30P, A53T and E46K) were cloned in the pcDNA<sup>TM</sup>3.1 vector and were transfected into SH-SY5Y cells by electroporation. While for  $\alpha$ -Syn knockdown, three short hairpin RNAs (shRNAs) sequences targeting human  $\alpha$ -Syn mRNA were cloned in the expression vector, PLKO.1, and were transfected into SK-MEL28 cells, with pLKO.1-TRC control and pLKO.1-scramble shRNA as controls. Stable cells were established by selection with antibiotics and the expression of  $\alpha$ -Syn was then confirmed by Western blotting. Effects of  $\alpha$ -Syn overexpression or knockdown on cell viability and expression of apoptotic markers were studied after subjecting the cells to an apoptotic stimulus, staurosporine. Depletion of endogenous  $\alpha$ -Syn was found to enhance staurosporine-induced cyto-toxicity

in SK-MEL28 with lower cell viability, greater Bax/Bcl-2 and Bax/Bcl-xL ratios and cleaved caspase 9 level compared with controls. SH-SY5Y cells overexpressing wild type  $\alpha$ -Syn were less vulnerable, while cells overexpressing  $\alpha$ -Syn mutant constructs were more sensitive to staurosporine compared with controls. Stable SH-SY5Y cell lines overexpressing wild type and mutant  $\alpha$ -Syn were then subjected to acute and chronic treatment of rotenone and maneb, the environmental toxins that could trigger physical symptoms associated with PD. MTT assay and flow cytometric determination of mitochondrial membrane potential changes ( $\Delta\Psi_m$ ) and reactive oxygen species (ROS) levels showed that wild type  $\alpha$ -Syn attenuated rotenone and maneb-induced cell death accompanied with reduced  $\Delta\Psi_m$  and ROS level, whereas  $\alpha$ -Syn mutants exacerbated environmental toxins-induced cytotoxicity. In conclusion, these results suggest that the fundamental property of wild type  $\alpha$ -Syn may be protective and such property may be lost by its familial PD-linked mutations.

## ACKNOWLEDGEMENT

Throughout the venture of this research project, I would like to express my utmost gratitude to my supervisor, Dr Say Yee How for giving me permission to commence the necessary research work in the first instance and to encourage me to progress with my thesis. Thank you for the tremendous amount of time, patience, guidance and support imparted. Also, I would like to thank Dr Lim Yang Mooi (Faculty of Medicine and Health Sciences, UTAR) for the kind gift of SK-MEL28 cell line. Special thanks to the Malaysian Ministry of Science, Technology and Innovation e-Science grant 02-02-11-SF0068 for supporting this project.

Next, my cordial appreciation goes to all my lab buddies for the efforts of making the lab a convivial place to work and inspiring me in research through our interactions during the lengthy hours in lab. Through our many triumphs and blunders, I thank each of them for bringing me up. Of course, I am very much obliged to lab seniors for their expertise advices, insightful hints and priceless experience sharing.

Last but not least, I am deeply indebted to my family for their unflagging love and superb support throughout my life, and for cultivating my absolute potential; this is simply impossible without them.

**FACULTY OF ENGINEERING AND SCIENCE**  
**UNIVERSITI TUNKU ABDUL RAHMAN**

Date: \_\_\_\_\_

**SUBMISSION OF THESIS**

It is hereby certified that **CHOONG CHI-JING** (ID No: **09UEM02356**) has completed this thesis entitled “INVESTIGATION OF THE DUAL CYTOTOXIC/-PROTECTIVE ROLES OF  $\alpha$ -SYNUCLEIN IN HUMAN NEUROBLASTOMA, SH-SY5Y AND HUMAN MELANOMA, SK-MEL28 CELLS” under the supervision of Dr. Say Yee How (Supervisor) from the Department of Biomedical Science, Faculty of Science.

I understand that University will upload softcopy of my thesis in pdf format into UTAR Institutional Repository, which may be made accessible to UTAR community and public.

Yours truly,

\_\_\_\_\_

(CHOONG CHI-JING)

## APPROVAL SHEET

This thesis entitled “**INVESTIGATION OF THE DUAL CYTO-TOXIC/-  
PROTECTIVE ROLES OF  $\alpha$ -SYNUCLEIN IN HUMAN  
NEUROBLASTOMA, SH-SY5Y AND HUMAN MELANOMA, SK-  
MEL28 CELLS**” was prepared by CHOONG CHI-JING and submitted as  
partial fulfillment of the requirements for the degree of Master of Science at  
Universiti Tunku Abdul Rahman.

Approved by:

\_\_\_\_\_

(Dr. Say Yee How)  
Assistant Professor/Supervisor  
Department of Biomedical Science  
Faculty of Science  
Universiti Tunku Abdul Rahman

Date:.....

## DECLARATION

I hereby declare that the thesis is based on my original work except for quotations and citations which have been duly acknowledged. I also declare that it has not been previously or concurrently submitted for any other degree at UTAR or other institutions.

Name CHOONG CHI-JING

Date \_\_\_\_\_

## TABLE OF CONTENTS

	<b>Page</b>
<b>ABSTRACT</b>	<b>ii</b>
<b>ACKNOWLEDGEMENT</b>	<b>iv</b>
<b>SUBMISSION OF THESIS</b>	<b>v</b>
<b>APPROVAL SHEET</b>	<b>vi</b>
<b>DECLARATION</b>	<b>vii</b>
<b>LIST OF TABLES</b>	<b>xiii</b>
<b>LIST OF FIGURES</b>	<b>xiv</b>
<b>LIST OF ABBREVIATIONS</b>	<b>xviii</b>
<b>LIST OF MANUSCRIPTS</b>	<b>xxi</b>
<b>CHAPTER</b>	
<b>1.0 INTRODUCTION</b>	<b>1</b>
<b>2.0 LITERATURE REVIEW</b>	<b>7</b>
2.1 $\alpha$ -Syn	7
2.1.1 The Synuclein family	7
2.1.2 Molecular structure and functional characteristics of $\alpha$ -Syn	9
2.1.3 Functions of $\alpha$ -Syn	13
2.2 Parkinson's disease	17
2.2.1 Clinical and pathological features of Parkinson's disease	17
2.2.2 The synucleopathies	19
2.2.3 Familial PD-associated mutants of $\alpha$ -Syn	20
2.2.4 Environmental chemical inducer of Parkinsonism syndrome	23
2.2.5 Oxidative stress and mitochondrial dysfunction in PD	30
2.3 Cancer and apoptosis	32
2.3.1 The Synucleins and cancer	32
2.3.2 Melanoma	33
2.3.3 Relationship between cancer development and dysregulation of apoptosis	37
2.3.4 Apoptotic pathways	39
2.3.5 Staurosporine-mediated apoptosis	45
<b>3.0 MATERIALS AND METHODS</b>	<b>47</b>
3.1 List of solution formulations	47
3.2 Molecular biology of $\alpha$ -Syn constructs	48
3.2.1 Plasmid pCMV-Sport6 with wild type $\alpha$ -Syn cDNA	48
3.2.2 Plasmid pBABE-hygro	48

3.2.3	Design of primers for generation of $\alpha$ -Syn mutant constructs	49
3.2.4	Site-directed mutagenesis	50
3.2.5	Plasmid extraction	52
3.2.6	DNA quantification by spectrophotometry	52
3.2.7	Restriction digestion of DNA	53
3.2.8	Agarose gel electrophoresis	53
3.2.9	Mammalian expression vector, pcDNA <sup>TM</sup> 3.1D/V5-His-TOPO <sup>®</sup>	54
3.2.10	Molecular cloning using pcDNA <sup>TM</sup> 3.1 Directional TOPO <sup>®</sup> Expression Kit	54
3.3	Molecular biology of $\alpha$ -Syn gene silencing	57
3.3.1	Plasmid pLKO.1	57
3.3.2	Design of shRNA oligonucleotides for pLKO.1	58
3.3.3	Annealing of shRNA oligonucleotides	60
3.3.4	Double restriction digestion of pLKO.1-TRC cloning vector	60
3.3.5	Purification of DNA from agarose gel	61
3.3.6	Preparation of competent <i>E. coli</i> DH5 $\alpha$ using Calcium Chloride	62
3.3.7	Ligation and transformation into <i>E. coli</i> DH5 $\alpha$	63
3.3.8	Screening for inserts	63
3.4	Cell culture	64
3.4.1	Maintenance of cell lines	64
3.4.2	Cell passaging	65
3.4.3	Cryopreservation	66
3.4.4	Stable transfection of cells	66
3.5	Protein expression analysis	69
3.5.1	Preparation of cell lysates	69
3.5.2	BCA Protein Assay	70
3.5.3	Sodium Dodecyl Sulphate-Polyacrylamide Gel Electrophoresis (SDS-PAGE)	71
3.5.4	Western blot analysis	72
3.5.5	Immunofluorescence microscopy	74
3.6	Staurosporine treatment	75
3.6.1	MTT (3-(4, 5-Dimethylthiazol-2-yl)-2, 5-diphenyltetrazolium bromide) assay	75
3.6.2	Determination of median lethal dose (LD <sub>50</sub> )	76
3.6.3	Detection of apoptotic markers level by Western blot analysis	76
3.6.4	Staining DNA with propidium iodide for flow cytometric analysis	77
3.7	<i>In vitro</i> model of Parkinson's disease	78
3.7.1	Environmental toxins treatment paradigm	78
3.7.2	Flow cytometric detection of reactive oxygen species level	79
3.7.3	Measurement of mitochondrial membrane potential	80
3.8	Statistical analysis	80

<b>4.0</b>	<b>RESULTS</b>	<b>81</b>
4.1	Down-regulation of $\alpha$ -Syn expression in SK-MEL28 by RNAi interference	81
4.1.1	Molecular cloning of shRNA sequences into pLKO.1-TRC cloning vector	81
4.1.2	$\alpha$ -Syn-shRNA down-regulates $\alpha$ -Syn expression	83
4.2	Effect of $\alpha$ -Syn knockdown on staurosporine insult	85
4.2.1	$\alpha$ -Syn knockdown enhances staurosporine-induced cyto-toxicity	85
4.2.2	Observation of morphological changes in SK-MEL28 following staurosporine treatment	87
4.2.3	Expression of apoptotic markers in SK-MEL28	89
4.2.4	$\alpha$ -Syn knockdown reduces the proliferative index of SK-MEL28	97
4.3	Overexpression of $\alpha$ -Syn in SH-SY5Y	100
4.3.1	Generation of mutant $\alpha$ -Syn construct by site-directed mutagenesis	100
4.3.2	Co-transfection using plasmid pCMV-Sport6- $\alpha$ -Syn and pBABE-hygro	103
4.3.3	Molecular cloning of $\alpha$ -Syn constructs into plasmid vector pcDNA <sup>TM</sup> 3.1	104
4.3.4	Generation of stable human $\alpha$ -Syn overexpressing cell lines	106
4.4	Effects of overexpression of wild type and mutant human $\alpha$ -Syn against staurosporine insult	108
4.4.1	Differential effects of overexpression of wild type and mutant human $\alpha$ -Syn on staurosporine-induced cell death in SH-SY5Y	108
4.4.2	Observation of morphological changes in SH-SY5Y following staurosporine treatment	108
4.4.3	Expression of apoptotic markers in SH-SY5Y	111
4.4.4	Overexpression of mutant $\alpha$ -Syn reduces proliferative index of SH-SY5Y	118
4.5	Effects of $\alpha$ -Syn overexpression against insults of environmental toxins, rotenone and maneb in SH-SY5Y	122
4.5.1	Differential effects of overexpression of wild type and mutant human $\alpha$ -Syn against acute rotenone-induced cell death in SH-SY5Y	122
4.5.2	Differential effects of overexpression of wild type and mutant human $\alpha$ -Syn on acute maneb-induced cell death in SH-SY5Y	123
4.5.3	Differential effects of overexpression of wild type and mutant human $\alpha$ -Syn on H <sub>2</sub> O <sub>2</sub> -induced cell death in SH-SY5Y that had been subjected to chronic rotenone treatment	124
4.5.4	Differential effects of overexpression of wild type and mutant human $\alpha$ -Syn on H <sub>2</sub> O <sub>2</sub> -induced cell death in SH-SY5Y that had been subjected to chronic maneb treatment	126

4.5.5	Differential effects of overexpression of wild type and mutant human $\alpha$ -Syn on rotenone and maneb-induced reactive oxygen species generation in SH-SY5Y	127
4.5.6	Differential effects of overexpression of wild type and mutant human $\alpha$ -Syn on rotenone and maneb-induced mitochondrial membrane potential changes ( $\Delta \Psi_m$ ) in SH-SY5Y cells	131
<b>5.0</b>	<b>DISCUSSION</b>	<b>136</b>
5.1	Gene silencing using RNA interference	136
5.1.1	Knockdown efficiency of short hairpin RNAs	136
5.1.2	Advantages of using shRNA versus siRNA	137
5.2	Assessment of anti-apoptotic property of $\alpha$ -Syn in both human melanoma and neuronal cell lines	138
5.2.1	Anti-apoptotic effect of $\alpha$ -Syn in human melanoma, SK-MEL28	139
5.2.2	Proposed anti-apoptotic and apoptotic mechanisms of wild type $\alpha$ -Syn	141
5.2.3	Differential effects of wild type and mutant $\alpha$ -Syn on human neuronal, SH-SY5Y following staurosporine treatment	143
5.2.4	Modulation of expression levels of apoptotic markers by wild type and mutant $\alpha$ -Syn in SH-SY5Y	144
5.2.5	Attributed reasons for differential toxicity conferred by wild type and mutant $\alpha$ -Syn	146
5.3	Role of $\alpha$ -Syn on cell proliferation rate	149
5.4	G <sub>2</sub> /M phase arrest caused by staurosporine	150
5.5	$\alpha$ -Syn (gene) and toxicants (environmental) interactions in <i>in vitro</i> Parkinsonian SH-SY5Y cell culture model	150
5.5.1	Possible mechanisms of rotenone and maneb-induced cell death	153
5.5.2	Decreased basal level ROS in wild type $\alpha$ -Syn-transfected SH-SY5Y	154
5.5.3	Role of wild type $\alpha$ -Syn in counteracting rotenone- and maneb-mediated reactive oxygen species generation	155
5.5.4	Role of wild type $\alpha$ -Syn in inhibiting rotenone- and maneb-mediated mitochondrial depolarisation	158
5.6	Role of $\alpha$ -Syn against additional acute oxidative stress in chronic environmental toxins-treated <i>in vitro</i> Parkinsonian SH-SY5Y cell culture model	160
5.7	Future studies and implication	162
<b>6.0</b>	<b>CONCLUSIONS</b>	<b>164</b>

**REFERENCES**

**166**

**APPENDICES**

**197**

## LIST OF TABLES

Table		Page
2.1	Cardinal and secondary clinical features of Parkinson's disease.	19
3.1	List of solution formulations.	47
3.2	Mutagenic primers used to create $\alpha$ -Syn mutant constructs.	50
3.3	(a) PCR reagent mixture and (b) thermal cycling conditions for site-directed mutagenesis to generate $\alpha$ -Syn mutant constructs.	51
3.4	PCR primers for amplification of gene encoding for $\alpha$ -Syn.	55
3.5	(a) PCR reaction mixture and (b) thermal cycling conditions applied to generate blunt end wild type and mutant $\alpha$ -Syn cDNA fragments.	55
3.6	TOPO <sup>®</sup> cloning reaction.	56
3.7	21-mer targets in the SNCA gene for efficient gene silencing.	59
3.8	Forward and reverse shRNA oligonucleotides containing sense and antisense strands.	60
3.9	Preparation of mixture for shRNA oligonucleotides annealing.	60
3.10	Reaction mixture for restriction digestion with (a) <i>AgeI</i> and (b) <i>EcoRI</i> .	61
3.11	Ligation mixture for cloning the inserts into pLKO.1-TRC cloning vector.	63
3.12	(a) Electroporation setting and (b) reaction mixture preparation for SH-SY5Y cells.	68
3.13	(a) Electroporation setting and (b) reaction mixture preparation for SK-MEL28 cells.	69
3.14	Formulations for SDS-PAGE 15% resolving gel and 4% stacking gel.	71
3.15	Details of primary antibodies for Western blotting.	74
3.16	Details of primary and secondary antibodies for detection of apoptotic markers following staurosporine treatment.	77

## LIST OF FIGURES

Figure		Page
2.1	Organisation of the human Synuclein genes.	8
2.2	The $\alpha$ -Syn protein.	10
2.3	NMR image of $\alpha$ -Syn shows the $\alpha$ -helices formed by the N-terminal region upon interaction with lipid while C-terminal part remains free and unfolded.	12
2.4	Schematic illustration of the function of $\alpha$ -Syn in dopamine metabolic pathway in neurons.	17
2.5	Amino acid sequence of $\alpha$ -Syn.	21
2.6	Chemical structure of rotenone.	24
2.7	Chemical structure of maneb.	27
2.8	The hallmarks of cancer.	38
2.9	Schematic representation of the main intrinsic and extrinsic apoptotic signalling pathways.	41
2.10	The three classes of Bcl-2 proteins.	42
2.11	The regulation of intrinsic pathway of apoptosis by pro-apoptotic BH-3 only and anti-apoptotic Bcl-2 proteins.	44
2.12	Molecular structure of staurosporine.	45
3.1	Vector map of plasmid pCMV-Sport6.	48
3.2	Vector map of plasmid pBABE-hygro.	49
3.3	Elements of pcDNA <sup>TM</sup> 3.1D/V5-His-TOPO <sup>®</sup> vector.	54
3.4	Map of pLKO.1 containing a shRNA insert.	58
3.5	Details of shRNA insert.	59
3.6	Morphology of (a) SH-SY5Y and (b) SK-MEL28 cells.	65
4.1	Agarose electrophoresis gel pictures for shRNA molecular cloning.	82

4.2	Sequencing alignments produced by Multalin.	82
4.3	Expression of $\alpha$ -Syn in SK-MEL28 cells by (a) Western blot analysis and (b) the relative densitometry.	84
4.4	Immunofluorescence microscopy depicting expression of human $\alpha$ -Syn protein in SK-MEL28 cell lines.	85
4.5	Effect of staurosporine on percentage of cell viability of untransfected and stably transfected SK-MEL28.	86
4.6	Morphological changes of SK-MEL28 cells after treatment with varying concentrations of staurosporine for 24 hr.	88
4.7	Expression of Bax in SK-MEL28 cell lines by (a) Western blot analysis and (b) its relative densitometry.	90
4.8	Expression of Bcl-2 in SK-MEL28 cell lines by (a) Western blot analysis and (b) its relative densitometry.	92
4.9	Expression of Bcl-xL in SK-MEL28 cell lines by (a) Western blot analysis and (b) its relative densitometry.	93
4.10	Expression of cleaved caspase 9 in SK-MEL28 cell lines by (a) Western blot analysis and (b) its relative densitometry.	95
4.11	Ratios of (a) Bax/Bcl-2 and (b) Bax/Bcl-xL in SK-MEL28 were quantified and plotted.	96
4.12	Effect of $\alpha$ -Syn knockdown on the proliferative index of SK-MEL28.	97
4.13	Cell cycle distribution of (a) untreated and (b) staurosporine-treated SK-MEL28 cell lines.	99
4.14	Sequencing alignments produced by Multalin.	101
4.15	NCBI Blastx results.	102
4.16	Agarose electrophoresis gel pictures for molecular cloning of $\alpha$ -Syn.	104
4.17	Sequencing alignments produced by Multalin.	105
4.18	Stable overexpression of human wild type or mutant $\alpha$ -Syn in SH-SY5Y.	107

4.19	Differential effects of staurosporine in untransfected SH-SY5Y and stably SH-SY5Y cells overexpressing different $\alpha$ -Syn.	109
4.20	Morphological changes of SH-SY5Y cells after treatment with varying concentrations of staurosporine for 24 hr.	110
4.21	Expression of Bax in SH-SY5Y cell lines by (a) Western blot analysis and (b) its relative densitometry.	112
4.22	Expression of Bcl-2 in SH-SY5Y cell lines by (a) Western blot analysis and (b) its relative densitometry.	113
4.23	Expression of Bcl-xL in SH-SY5Y cell lines by (a) Western blot analysis and (b) its relative densitometry.	114
4.24	Expression of cleaved caspase 9 in SH-SY5Y cell lines by (a) Western blot analysis and (b) its relative densitometry.	116
4.25	Ratios of (a) Bax/Bcl-2 and (b) Bax/Bcl-xL in SH-SY5Y cell lines were quantified and plotted.	117
4.26	Effect of $\alpha$ -Syn overexpression on the proliferative index of SH-SY5Y.	119
4.27	Cell cycle distribution of untreated SH-SY5Y cell lines.	120
4.28	Cell cycle distribution of staurosporine-treated SH-SY5Y cell lines.	121
4.29	Effects of acute rotenone treatment in untransfected SH-SY5Y and stably SH-SY5Y cells overexpressing different $\alpha$ -Syn.	123
4.30	Effects of acute maneb treatment in untransfected SH-SY5Y and stably SH-SY5Y cells overexpressing different $\alpha$ -Syn.	124
4.31	Effects of H <sub>2</sub> O <sub>2</sub> in chronically rotenone-treated untransfected SH-SY5Y and stably SH-SY5Y cells overexpressing different $\alpha$ -Syn.	125
4.32	Effects of H <sub>2</sub> O <sub>2</sub> in chronically maneb-treated untransfected SH-SY5Y and stably SH-SY5Y cells overexpressing different $\alpha$ -Syn.	126

4.33	Flow cytometric histograms of DCF show the effect of wild type and mutant $\alpha$ -Syn on ROS generation of SH-SY5Y cells under various treatments.	128
4.34	Effect of wild type and mutant $\alpha$ -Syn overexpression on ROS generation in SH-SY5Y cells.	131
4.35	Histograms of DiOC6(3) fluorescence, indicative of mitochondrial membrane potential changes ( $\Psi_m$ ).	133
4.36	Effects of wild type and mutant $\alpha$ -Syn overexpression on mitochondrial membrane potential changes ( $\Delta\Psi_m$ ).	135
5.1	Protein alignment for the human Synuclein proteins.	140
5.2	A schematic representation of the anti-apoptotic mechanisms exhibited by wild type $\alpha$ -Syn in previous literatures, which eventually lead to cell survival.	142
5.3	A schematic model of $\alpha$ -Syn-mediated dopaminergic protection from MPP <sup>+</sup> -induced cyto-toxicity.	152
5.4	A presynaptic terminal from a dopaminergic neuron depicting the potential function of $\alpha$ -Syn in intracellular dopamine storage.	156

## LIST OF ABBREVIATIONS

6-OHDA	6-hydroxydopamine
ADP	Adenosine Diphosphate
AIF	Apoptosis Inducing Factor
ALS	Amyotrophic Lateral Sclerosis
APAF-1	Apoptotic Protease-Activating Factor 1
ATP	Adenosine Triphosphate
BCSG1	Breast Cancer-Specific Gene 1
CO <sub>2</sub>	Carbon Dioxide
CSP $\alpha$	Cysteine-String Protein $\alpha$
DAT	Dopamine Transporter
DCFH-DA	2', 7'-Dichlorfluorescein-diacetate
DiOC6 (3)	3, 3'-dihexyloxacarbocyanine iodide
DISC	Death Inducing Signalling Complex
DMSO	Dimethylsulphoxide
DNA	Deoxyribonucleic Acid
DTC	Dithiocarbamate
EBDC	Ethylene-(bis)-dithiocarbamates
ERK	Extracellular Signal-Regulated Protein Kinase
FABP	Fatty Acid Binding Protein
FAD	Flavin Adenine Dinucleotide
FADH <sub>2</sub>	Flavin Adenine Dinucleotide (Reduced form)
FBS	Fetal Bovine Serum
GSH	Glutathione

GSK-3	Glycogen Synthase Kinase-3
GSSG	Glutathione Disulphide
H <sub>2</sub> O <sub>2</sub>	Hydrogen Peroxide
hr	Hour
JIP-1b/IB1	c-Jun N-terminal kinase interacting protein-1/Islet-Brain 1
JNK	c-Jun N-terminal kinase
LD	Lethal Dose
L-DOPA	Dihydroxyphenylalanine
LRRK2	Leucine-Rich Repeat Kinase 2
MAPK	Major Mitogen-Activated Kinases
MEM	Minimum Essential Medium, Eagle's
min	Minute
MPP <sup>+</sup>	1-Methyl-4-Phenylpyridinium
MPTP	Methyl-4-Phenyl-1,2,3,6-Tetrahydropyridin
MSA	Multiple System Atrophy
MTT	3-(4, 5-dimethylthiazol-2-yl)-2, 5-diphenyltetrazolium bromide
NAC	Non-Amyloid β-Component
NACP	Precursor of the Non-Amyloid β-Component
NADH	Nicotinamide Adenine Dinucleotide (Reduced form)
NADPH	Nicotinamide Adenine Dinucleotide Phosphate
NBIA 1	Neurodegeneration with Brain Iron Accumulation Type 1
OD	Optical Density
PBS	Phosphate Buffered Saline
PD	Parkinson's disease
PI3K	Phosphoinositide 3-kinase

PINK1	PTEN-induced putative kinase 1
PKC $\delta$	Protein Kinase C Delta
PLD2	Phospholipase D2
PVDF	Polyvinylidene difluoride
RISC	RNA-Induced Silencing Complex
RNA	Ribonucleic Acid
ROS	Reactive Oxygen Species
SDS-PAGE	Sodium Dodecyl Sulfate Polyacrylamide Gel Electrophoresis
sec	Second
shRNA	Short hairpin RNA
siRNA	Small Interfering RNA
Smac/Diablo	Second Mitochondrial-derived Activator of Caspase/Direct IAP-Binding protein with a Low pI
SNARE	Soluble N-Ethylmaleimide-Sensitive Factor (NSF) Attachment Protein Receptor
SOD	Superoxide Dismutase
Syn	Synuclein
TH	Tyrosine Hydroxylase
TNFR	Tumor Necrosis Factor Receptor
TRAIL	TNF-related apoptosis-inducing ligand
TUNEL	Terminal Deoxynucleotide Transferase-mediated dUTP Nick End Labeling
UCH-L1	Ubiquitin C-terminal Hydrolase-L1
VMAT2	Vesicular Monoamine Transporter 2

## LIST OF MANUSCRIPTS

- 1 Chi-Jing Choong & Yee-How Say (2011). Neuroprotection of  $\alpha$ -Synuclein under acute and chronic rotenone and maneb treatment is abolished by its familial Parkinson's disease mutations A30P, A53T and E46K. *NeuroToxicology*, doi:10.1016/j.neuro.2011.05.012
- 2 Chi-Jing Choong & Yee-How Say (2011). Knockdown of  $\alpha$ -Synuclein Enhances Susceptibility to Staurosporine-induced Apoptosis in Human Melanoma SK-MEL28 Cells. *Journal of Biological Science*, 11, 135-145.

## CHAPTER 1

### INTRODUCTION

The Synucleins are a family of small, soluble, highly conserved proteins that consist of  $\alpha$ -,  $\beta$ -, and  $\gamma$ -Synuclein, which are predominantly expressed in the neurons. They are a natively unfolded group of proteins that are characterised by 5-6 repeats of the amino acid motif (KTKEGV), constituting most of the N-terminal half of the proteins (Clayton & George, 1998; Lavedan, 1998; Lavedan et al., 1998).  $\alpha$ -Synuclein ( $\alpha$ -Syn) is a 140 amino-acid acidic protein of 19 kDa originally isolated from amyloid plaques of Alzheimer's disease brains, as a fragment known as the precursor of the non-A $\beta$ -component (NACP) (Ueda et al., 1993). It is widely expressed in various brain regions including the neocortex, hippocampus, dentate gyrus, olfactory bulb, thalamus, cerebellum, amygdala and nucleus accumbens and is predominantly localised in the presynaptic terminals (Iwai et al., 1995; Wersinger, Banta, & Sidhu, 2004). Although the function of  $\alpha$ -Syn is still poorly understood, several studies suggest that it has a potential role in modulating synaptic transmission, the density of synaptic vesicles and neuronal plasticity (Abeliovich et al., 2000; Cabin et al., 2002; Murphy, Rueter, Trojanowski, & Lee, 2000), as well as in the folding/refolding of soluble N-Ethylmaleimide-sensitive factor (NSF) attachment protein receptor (SNARE) critical for neurotransmitter release, vesicle recycling and synaptic integrity (Chandra, Gallardo, Fernandez-Chacon, Schluter, & Sudhof, 2005).

$\alpha$ -Syn has attracted considerable attention due to its involvement in neurodegenerative diseases. Extensive studies show that  $\alpha$ -Syn is neurotoxic and it is somehow implicated in the pathophysiology of Parkinson's disease (PD) (Maries, Dass, Collier, Kordower, & Steece-Collier, 2003). PD is characterised by the selective and progressive loss of dopaminergic neurons in substantia nigra pars compacta (Hoehn & Yahr, 1967). Depletion of dopamine within the striatum causes dysregulation of the motor circuits that project throughout the basal ganglia, resulting in the clinical manifestations of PD (Bernheimer, Birkmayer, Hornykiewicz, Jellinger, & Seitelberger, 1973). The neuropathological hallmark of PD is the presence of intraneuronal proteinaceous inclusions enriched in  $\alpha$ -Syn, known as Lewy bodies within the surviving neurons of the substantia nigra and other brain regions (Kuzuhara, Mori, Izumiyama, Yoshimura, & Ihara, 1988; Spillantini, Crowther, Jakes, Hasegawa, & Goedert, 1998). Furthermore, three missense mutations for  $\alpha$ -Syn, A30P, A53T and E46K have been known to be associated with rare autosomal dominant forms of familial PD (Kruger et al., 1998; Polymeropoulos et al., 1997; Zarranz et al., 2004).

$\alpha$ -Syn neuropathology is associated with its aberrant oligomerisation into soluble protofibrils, which emerge as perhaps the most toxic  $\alpha$ -Syn species, followed by the coalescence of these oligomeric forms into neurotoxic insoluble fibrils composed of  $\beta$ -sheet structure and amyloid-like filaments, prior to their aggregation into insoluble fibrillar structures and inclusions, which then accumulate as Lewy bodies (El-Agnaf & Irvine, 2002; Goedert, Spillantini, & Davies, 1998). Several experimental conditions including

presence of mutations, protein overexpression, exposure to death inducing stimuli (neurotoxins and oxidative factors), alterations in post-translational modifications (such as phosphorylation, oxidation, sumoylation or transglutamination), impairment of the ubiquitin-proteasome pathway of protein degradation, or a crowded milieu were shown to accelerate  $\alpha$ -Syn aggregation and subsequent neuronal cell death (Beyer, 2006; Goedert, 2001; Uversky, Cooper, Bower, Li, & Fink, 2002).

On the contrary, many evidences from previous literatures have reported a neuroprotective effect for  $\alpha$ -Syn since it was found to inhibit apoptosis induced by a broad range of apoptotic stimuli or to modulate the expression levels or activity of proteins implicated in the regulation of apoptosis onset (Da Costa, Ancolio, & Checler, 2000; Da Costa, Paitel, Vincent, & Checler, 2002). It is conceivable that  $\alpha$ -Syn has the putative physiological function of providing neuroprotection that may be lost either by the familial PD-linked mutants or after exposure to certain toxic insults (Sidhu, Wersinger, Moussa, & Vernier, 2004c).

The discovery of a severe and unremitting Parkinsonian syndrome in young drug-addicts involuntary intoxicated with the synthetic narcotic contaminant 1-methyl-4-phenyl-1,2,3,6-tetrahydropyridine (MPTP) in 1983 provided support for the hypothesis that exposure to environmental neurotoxins can lead to PD (Langston, Ballard, Tetrud, & Irwin, 1983). Recent epidemiological and experimental studies further indicate the exposure to environmental agents including agricultural chemicals contribute to the development of this disorder.

Since many human disorders including PD do not come about spontaneously in experimental cell culture and animal models, characteristic functional changes have to be mimicked by these neurotoxic agents (Uversky, 2004).

Rotenone, a naturally derived pesticide, is a potent neurotoxicant through its inhibition of mitochondrial complex I and increased oxidative stress, which have been implicated in the pathogenesis of PD (Betarbet et al., 2000). Rotenone-administered rats reproduced the typical Parkinson's disease phenotype, both behaviourally and pathologically, including selective nigrostriatal dopaminergic degeneration and  $\alpha$ -Syn-positive cytoplasmic inclusions (Betarbet et al., 2000; Sherer, Kim, Betarbet, & Greenamyre, 2003b). Maneb is a member of dithiocarbamates (DTCs), which exposure has been linked to a range of neurobehavioural abnormalities with adverse effects on glutamate and dopaminergic systems (Barlow, Lee, Cory-Slechta, & Opanashuk, 2005). Maneb's potential role in the pathogenesis of PD was noted as permanent Parkinsonism has been reported following chronic occupational exposure to this fungicide (Meco, Bonifati, Vanacore, & Fabrizio, 1994). Although rotenone and maneb may not be a major contributor to PD, their exposure can lead to deleterious consequences on dopaminergic cell viability and thus, provide a unique model for examining the degeneration of dopaminergic neurons in the etiology of PD (Drechsel & Patel, 2008).

Apart from its central role in the pathophysiology of PD,  $\alpha$ -Syn has recently been identified as another attractive candidate in oncogenesis besides  $\gamma$ -Syn, which has been detected in elevated levels in various types of cancer including

breast, ovarian, gastric, liver, colorectal, uterine and lung cancers, particularly in advanced stages of the diseases (Ahmad, Attoub, Singh, Martin, & El-Agnaf, 2007). Matsuo and Kamitani (2010) demonstrated that  $\alpha$ -Syn is positively detected in primary and metastatic melanoma sections but is undetectable in non-melanocytic cutaneous carcinoma and normal skin. SK-MEL28 is one of the melanoma cell lines found to be highly overexpressing  $\alpha$ -Syn (Matsuo and Kamitani, 2010). Thus far, not many studies have explored the role of  $\alpha$ -Syn in cancer cells. Therefore, whether  $\alpha$ -Syn has any cyto-protective effect in melanoma cell lines that would eventually lead to drug resistance and disease progression needs to be elucidated.

To date, despite the long focus on  $\alpha$ -Syn, the precise role of  $\alpha$ -Syn remains unknown and this has become an obstacle for revelation of its pathological mechanisms. Therefore, in order to clarify the cyto-toxic/-protective roles of  $\alpha$ -Syn, the objectives of this present study were:

1. To assess the ability of  $\alpha$ -Syn to resist staurosporine-mediated apoptosis in a human melanoma cell line, SK-MEL28 and a human neuronal cell line, SH-SY5Y by stable short hairpin RNA (shRNA) knockdown and overexpression, respectively. Hallmarks of apoptosis studied included cell viability, cell morphology, expression of apoptotic markers and proliferative index.
2. To investigate the cellular effects of gene-environment interaction in an *in vitro* Parkinsonian model, by subjecting SH-SY5Y cells stably overexpressing wild type  $\alpha$ -Syn or A30P, A53T and E46K  $\alpha$ -Syn

mutants to acute or chronic rotenone and maneb treatment. Cellular effects studied included cell viability, oxidative stress and mitochondrial membrane potential.

## CHAPTER 2

### LITERATURE REVIEW

#### 2.1 $\alpha$ -Syn

##### 2.1.1 The Synuclein family

The Synuclein family consists of three distinct small, soluble proteins,  $\alpha$ -,  $\beta$ -, and  $\gamma$ -Syn, which have been extensively described in vertebrates such as *Homo sapiens*, *Rattus norvegicus* and *Mus musculus* (George, 2001), but only in one invertebrate, *Xenopus laevis* (Yuan et al., 2007).

The Synuclein was initially identified by expression screening of cDNA clones generated from the electric lobe of Pacific electric ray, *Torpedo californica* with an antiserum raised against purified cholinergic vesicles (Maroteaux, Campanelli, & Scheller, 1988). As the protein was detected subcellularly on portions of the nuclear membrane and in high concentration in presynaptic terminals of the nervous system but not in peripheral tissue, the investigators named the novel protein syn (synapse) nuclein (nucleus). The original Torpedo cDNA clone (encoding the 143 amino-acid electric-ray  $\gamma$ -Syn) was then used to isolate a rat clone encoding a 140 amino-acid protein (rat  $\alpha$ -Syn) (Maroteaux et al., 1988). Subsequently, the first product of the  $\beta$ -Syn gene was isolated as a 134 amino-acid bovine brain-specific phosphoprotein (phosphoneuroprotein 14) (Nakajo, Tsukada, Omata, Nakamura, & Nakaya, 1993).

The human  $\alpha$ -,  $\beta$ -, and  $\gamma$ -Syn genes (*SNCA*, *SNCB*, and *SNCG*) have been mapped to chromosome 4q21.3-q22, 5q35, and 10q23, respectively (Chen et al., 1995; Ninkina et al., 1998; Spillantini, Divane, & Goedert, 1995). As shown in Figure 2.1, the  $\alpha$ -Syn gene is organised as 7 exons, 5 of which are protein-coding, while the  $\beta$ -Syn gene has 6 exons (5 protein-coding) and the  $\gamma$ -Syn gene has 5 exons (all protein-coding) (Lavedan, 1998).

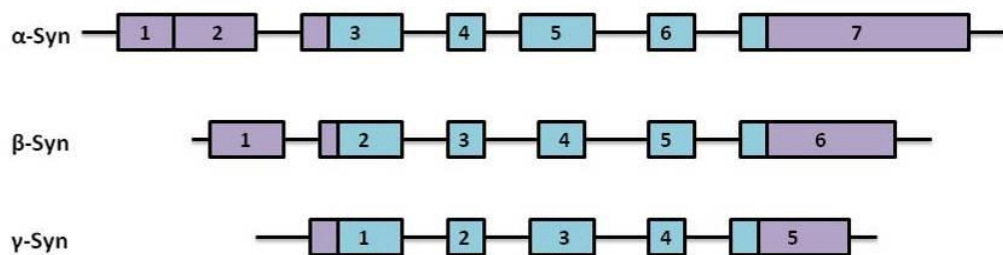


**Figure 2.1: Organisation of the human Synuclein genes.** Exons are represented by boxes, blue or purple, for the coding or untranslated regions respectively. Introns are shown as interrupted horizontal lines (Modified from Lavedan, 1998).

The Synucleins are small proteins with a calculated molecular mass close to 14 kDa. However, it has been shown that their apparent molecular mass is approximately 19 kDa, indicating that they are post-transcriptionally modified (Jakes, Spillantini, & Goedert, 1994). All Synuclein protein sequences consist of a well-conserved amino-terminal that includes a variable number of 11-residue repeats, each with a highly conserved hexamer motif (KTKEGV) and a less-conserved carboxy-terminal that includes a predominance of acidic residues (George, Jin, Woods, & Clayton, 1995).

All three Synuclein proteins are predominantly expressed in brain, particularly in the neocortex, hippocampus, striatum, thalamus, and cerebellum (Lavedan,

1998). The  $\gamma$ -Syn is also highly expressed in the peripheral nervous system (primary sensory neurons, sympathetic neurons, and motor neurons) and many non-neuronal tissues including retina, olfactory epithelium and various advanced-stage tumours (Buchman, Adu, Pinon, Ninkina, & Davies, 1998; Lavedan et al., 1998).

Extensively found in presynaptic terminals,  $\alpha$ -Syn appears to be equally distributed between cytosolic and membrane fractions, where it is in close proximity to, but loosely associated with, synaptic vesicles (Jakes et al., 1994; Kahle et al., 2000). It has also been established that  $\alpha$ -Syn is intensely localised in the nucleus of mammalian brain neurons (Yu et al., 2007).  $\beta$ -Syn is predominantly found in nerve terminal but mainly expressed in the cytoplasmic region only (Jakes et al., 1994; Shibayama-Imazu et al., 1998). Conversely,  $\gamma$ -Syn is not an exclusively cytoplasmic protein, but has a dynamic localisation and can associate with subcellular structures.  $\gamma$ -Syn is present in the perinuclear area and is localised to centrosomes in several types of human interphase cells. In mitotic cells,  $\gamma$ -Syn staining is localised to the poles of the spindle (Surgucheva, McMahon, & Surguchov, 2006).

### **2.1.2 Molecular structure and functional characteristics of $\alpha$ -Syn**

Structurally,  $\alpha$ -Syn with molecular size of 19 kDa comprises 140 amino acids distributed in three overlapping regions including (1) the N-terminal repeat region, residues 1-95; (2) the highly hydrophobic central portion, residues 61-95 and (3) the acidic C-terminal region, residues 96-140 (George et al., 1995) (Figure 2.2).

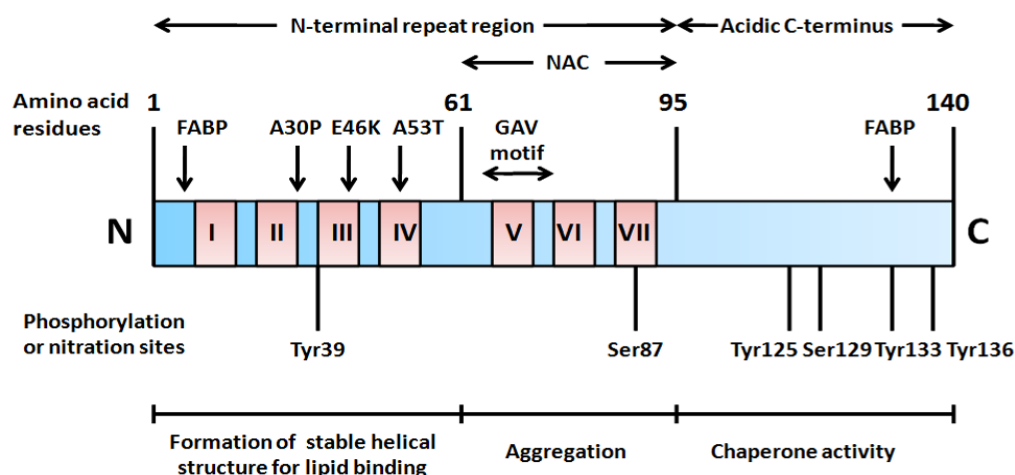


**Figure 2.2: The  $\alpha$ -Syn protein.** The  $\alpha$ -Syn protein is divided into three overlapping regions, namely N-terminal repeat region (1-95), which contains seven conserved repeat motifs (red coloured boxes) and is believed to be involved in  $\alpha$ -Syn interactions with lipids; a central hydrophobic NAC region (61-95) which is essential for the aggregation of  $\alpha$ -Syn; and an acidic C-terminus (96-140) which exhibits chaperone activity. Phosphorylation and nitration sites are shown (Modified from Cheng, Vivacqua, & Yu, 2010).

The positively charged N-terminal region is dominated by seven imperfect 11-residue repeats, each with the core consensus sequence motif KTKEGV that contribute to this domain's structural apolipoprotein-like class-A<sub>2</sub> amphipathic  $\alpha$ -helical features (George et al., 1995). This region also harbors one of two conserved Fatty Acid Binding Protein (FABP) signatures (residues 2-19), which are important for lipid binding (Perrin, Woods, Clayton, & George, 2000; Sharon et al., 2001). Most likely, this domain is responsible for  $\alpha$ -Syn to form a stable helical structure in association with lipid micelles, for the weak association of  $\alpha$ -Syn with synaptic vesicles and for its bilayer disrupting capacity (Dev, Hofele, Barbieri, Buchman, & van der Putten, 2003). Nitration of Tyr39 of  $\alpha$ -Syn largely hinders its ability to bind to lipid vesicles as addition of the rather bulky nitro group at the ortho position of the aromatic ring not only induces a significant shift in the pKa of the tyrosine residue, adding a

negative charge, but also prevent the rotational ability of the tyrosine residue, all of which may destabilise the  $\alpha$ -helical conformation induced upon binding to lipid vesicles (Hodara et al., 2004). Furthermore, all familial mutations (A30P, A53T and E46K) that are related to the autosomal dominant form of PD cluster in this region (Lundvig, Lindersson, & Jensen, 2005).

The central portion, known as non-A $\beta$ -component (NAC) region comprises the highly amyloidogenic part (Ueda et al., 1993) and serves as the building block of  $\alpha$ -Syn aggregates with critical residues within the GAV motif (residues 66-74) (Du et al., 2003). It is responsible for the ability of  $\alpha$ -Syn (i) to undergo a conformational change from random coil to  $\beta$ -sheet structure (Serpell, Berriman, Jakes, Goedert, & Crowther, 2000), (ii) to form cylindrical  $\beta$ -sheets (Perutz, Pope, Owen, Wanker, & Scherzinger, 2002), and (iii) to form amyloid-like protofibrils and fibrils (El-Agnaf & Irvine, 2000). These features distinguish  $\alpha$ -Syn from its two close relatives,  $\beta$ - and  $\gamma$ -Syn which fail to form copolymers due to their lack of most NAC sequence (Biere et al., 2000).

The negatively charged C-terminal region is found to be rich in Pro and the acidic residues, Glu and Asp (Giasson, Murray, Trojanowski, & Lee, 2001) but it has no distinct structural propensity. NMR spectroscopy studies of  $\alpha$ -Syn in solution have shown that its C-terminal part remains free and unfolded, and does not associate with vesicles or micelles (Eliezer, Kutluay, Bussell, & Browne, 2001) (Figure 2.3). However, it is one of the two regions in  $\alpha$ -Syn (residues 123-140) that show sequence resemblance with cytosolic FABP (Sharon et al., 2001). Furthermore, the C-terminal region seems to play a role

in preventing  $\alpha$ -Syn aggregation as C-terminal-region-truncated form of  $\alpha$ -syn (residues 1-120) was reported to be more prone in forming filaments than the full length protein (Crowther, Jakes, Spillantini, & Goedert, 1998). The acidic C-terminal tail of  $\alpha$ -Syn also appears critical for its chaperone-like activity (Souza, Giasson, Lee, & Ischiropoulos, 2000b) as C-terminal deletion leads to abolishment of chaperone activity and the second acidic repeat (residues 125–140) of  $\alpha$ -Syn has been suggested to be important for the chaperone activity (Kim, Paik, & Yang, 2002). Moreover, modifications of this second repeat region are implicated in the aggregation process of  $\alpha$ -Syn. Phosphorylation of Ser129 or nitration of Tyr125, Tyr133, and Tyr136 promote the formation of  $\alpha$ -Syn filaments or oligomers (Fujiwara et al., 2002; Giasson et al., 2000; Souza, Giasson, Chen, Lee, & Ischiropoulos, 2000a). Conversely, phosphorylation of Ser87 and Tyr125 has been reported in inhibiting  $\alpha$ -Syn fibrillisation *in vitro* (Chen et al., 2009; Paleologou et al., 2010).

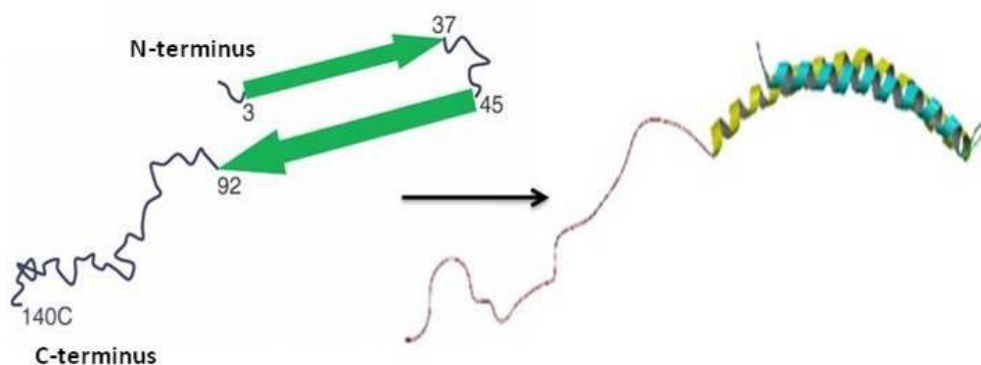


**Figure 2.3:** NMR image of  $\alpha$ -Syn shows the  $\alpha$ -helices formed by the N-terminal region upon interaction with lipid while C-terminal part remains free and unfolded (Adapted from Lyubchenko, Kim, Krasnoslobodtsev, & Yu, 2010; RCSB Protein Data Bank, 2009).

$\alpha$ -Syn has a natively unfolded monomeric state with no significant secondary structure (Weinreb, Zhen, Poon, Conway, & Lansbury, 1996). However, it is thought to gain structure upon binding to substrates. With numerous phosphorylation sites possessed, it can undergo several post-translational modifications that regulate substrate affinity and stabilise intermediate conformations (Esposito, Dohm, Kermer, Bahr, & Woutersa, 2007). Taken together,  $\alpha$ -Syn is believed to undergo major structural change from its natively unfolded state to  $\alpha$ -helical conformation upon interaction with membrane lipids or to the characteristic crossed  $\beta$ -conformation in highly organised amyloid-like fibrils under conditions that trigger aggregation (Moussa, Mahmoodian, Tomita, & Sidhu, 2007).

### **2.1.3 Functions of $\alpha$ -Syn**

Despite the long focus on  $\alpha$ -Syn, its exact normal function still remains unclear. General functions ascribed to  $\alpha$ -Syn include modulation of physiological processes such as synaptic plasticity, synaptic vesicle formation, regenerative sprouting of damaged axons and axonal transport (Sidhu et al., 2004c).

Due to its high expression in presynaptic terminals, involvement of  $\alpha$ -Syn in synaptic plasticity has long been envisaged, given that the  $\alpha$ -Syn expression is modulated in various physiological situations of plastic remodeling of neuronal networks.  $\alpha$ -Syn was specifically up-regulated in a discrete population of presynaptic terminals of the songbird brain during a period of song-acquisition-related synaptic rearrangement (George et al., 1995). On the other hand,  $\alpha$ -Syn showed a trend towards being down-regulated at the mRNA level following

long-term potentiation in hippocampus of young and aged rats (Stephan et al., 2002).

A study done by Cabin et al. (2002) demonstrated that following prolonged repetitive stimulation, mice lacking  $\alpha$ -Syn exhibited attenuated synaptic response. Moreover, hippocampal synapses of  $\alpha$ -Syn knock-out mice showed fewer synaptic vesicles, particularly in the reserve pool, and the replenishment of docked vesicles by reserve pool vesicles after depletion was also slower, compared to that of their control littermates, thus, suggesting that  $\alpha$ -Syn may be required for the genesis and/or maintenance of a reserve pool of presynaptic vesicles and regulation of synaptic vesicle mobilisation at nerve terminals (Cabin et al., 2002).

$\alpha$ -Syn-depleted neurons also showed reduced expression levels of synapsin, a protein vital for synaptic vesicle recycling, suggesting that a putative key function of  $\alpha$ -Syn may be to regulate synaptic vesicle recycling through modulation of phospholipase D2 (PLD2) activity and its FABP properties (Cabin et al., 2002; Sidhu et al, 2004c).  $\alpha$ -Syn may also regulate synaptic vesicle recycling by assisting in the folding and refolding of SNAREs (Bonini & Giasson, 2005). SNAREs are protein complex consisting of synaptobrevin, syntaxin, and SNAP25, which play a role in vesicle priming, transferring of docked vesicles into an exocytosis-competent state, and vesicle fusion to the membrane (Goda, 1997). A study involving analysis of cysteine-string protein  $\alpha$  (CSP $\alpha$ )-deficient mice demonstrated that up-regulation of  $\alpha$ -syn compensates for the loss of CSP $\alpha$  activity by restoring SNARE complexes to their correct

levels and suppressing presynaptic degeneration, motor dysfunction, and death of mice lacking CSP $\alpha$  (Chandra et al., 2005). Furthermore,  $\alpha$ -Syn has been suggested to interfere with axonal transport of synaptic vesicles by its interaction with proteins that either bind to or are part of the cytoskeleton, such as tau, heterodimeric but not microtubule tubulin, MAP1B, MAP2, synphilin-1, and torsin A (Payton, Perrin, Clayton, & George, 2001).

Specifically,  $\alpha$ -Syn may be instrumental in the physiological maintenance of dopamine homeostasis and dopamine synaptic tone in dopaminergic neurons of the substantia nigra pars compacta through regulation of the functional activity of tyrosine hydroxylase (TH) and dopamine transporter (DAT), as extensively reviewed by a few groups (Lotharius & Brundin, 2002; Perez & Hastings, 2004; Sidhu, Wersinger, & Vernier, 2004a).

Dopamine biosynthesis begins with a rate-limiting step: the hydroxylation of tyrosine into dihydroxyphenylalanine (L-DOPA) catalysed by phosphorylated TH followed by conversion of L-DOPA into dopamine by aromatic amino acid decarboxylase. Since TH is only active in phosphorylated form, the regulation phosphorylation/dephosphorylation of TH is essential in dopamine biosynthesis (Perez & Hastings, 2004; Sidhu Wersinger, & Vernier, 2004b). In particular, there may be a reciprocal interplay between  $\alpha$ -Syn and 14-3-3 proteins for the regulation of TH activity. TH has been reported to require binding of chaperone protein, 14-3-3 for optimal activation through maximal phosphorylation (Xu et al., 2002). Conversely,  $\alpha$ -Syn appears to colocalise with TH and directly bind to the dephosphorylated form of TH. It tends to

maintain TH in an inactive form in an opposite manner to 14-3-3 proteins, causing an overall net decrease in enzymatic activity and dopamine synthesis (Perez et al., 2002).

DAT is expressed in the presynaptic terminals of dopaminergic neurons where it mediates the re-uptake of dopamine back into the dopaminergic nerve terminals (Chen & Reith, 2000). Enhanced DAT activity would increase intracellular levels of dopamine with a resulting increased oxidative stress within the dopaminergic neuron and neuronal death (Sidhu et al, 2004a). The regulation of DAT which involve the rapid and transient shuttling of the transporter molecule to and from the plasma membrane may thus be a key component in the maintenance of dopaminergic neurotransmission and the integrity of dopaminergic neurons (Sidhu et al., 2004a). In agreement with these theories, a study demonstrated that in the presence of wild type  $\alpha$ -Syn, the transporter was dynamically trafficked away from the plasma membrane into the cytoplasm, as indexed by reduced DAT presence at the plasma membrane by biotinylation experiments (Wersinger, Prou, Vernier, & Sidhu, 2003). Moron et al. (2003) reported that activation of mitogen-activated protein (MAP) kinases, extracellular signal-regulated kinase (ERK) 1/2 was shown to increase the amount of DAT at the cell surface and dopamine re-uptake. Since  $\alpha$ -Syn can bind to the MAP kinase ERK and inhibit its activity, it is very likely that the presence of  $\alpha$ -Syn at the nerve terminals tends to blur the MAP kinase activity and decrease the amount of DAT at the cell surface of dopaminergic nerve terminals (Iwata, Miura, Kanazawa, Sawada, & Nukina, 2001; Sidhu et

al., 2004c). Figure 2.4 illustrates the collective functions of  $\alpha$ -Syn in dopaminergic neurons.

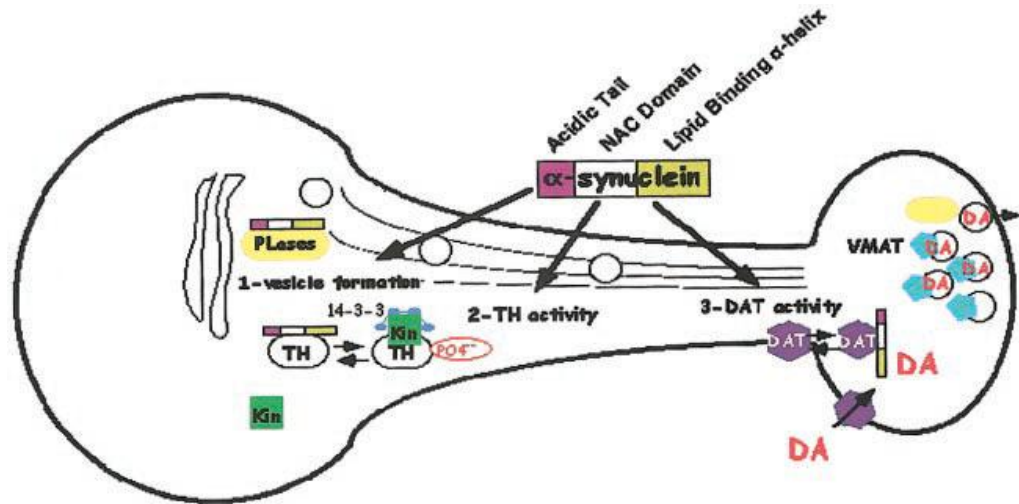


**Figure 2.4: Schematic illustration of the function of  $\alpha$ -Syn in dopamine metabolic pathway in neurons.** (1) In normal situations or when synaptic plasticity needs to be increased,  $\alpha$ -Syn contributes to the formation of synaptic vesicles, both by enhancing PLD2 activity and by its lipid binding properties. At the synaptic terminals, vesicles bearing the vesicular transporter quickly and efficiently accumulate dopamine. (2)  $\alpha$ -Syn modulates the activity of TH, the limiting enzyme of catecholamine biosynthesis, by preventing its interactions with kinases. In contrast, 14-3-3 proteins favour TH activity by enhancing TH phosphorylation by calmodulin kinases or ERKs. (3) The shuttling of DAT to and away from the plasma membrane is also modified by the action of  $\alpha$ -Syn, thereby changing the efficiency of dopamine uptake at the nerve terminal (Figure taken from Sidhu et al., 2004c).

## 2.2 Parkinson's disease

### 2.2.1 Clinical and pathological features of Parkinson's disease

Parkinson's disease (PD), first described by James Parkinson in 1817 in his work, *An Essay on the Shaking Palsy*, is the second most common age-related, progressive neurodegenerative disorder after Alzheimer's disease (Corti et al., 2005). With a mean age at onset of 55, PD affects nearly 2% of the population over age 65. The percentage of affected individuals within a population rises

from about 1% at 65 years to about 5% at 85 years, making age the main risk factor for PD (De Lau & Breteler, 2006). The majority of cases are of idiopathic origin. However, a number of specific genetic mutations causing PD have been discovered (Dauer & Przedborski, 2003).

Clinically, it is characterised by a triad of cardinal neurological symptoms including bradykinesia, muscular rigidity, resting tremour and postural instability that become apparent when more than 60% of the melanised dopaminergic neurons of the substantia nigra pars compacta have degenerated and 80% of the striatal dopamines are lost (Bernheimer et al., 1973; Hoehn & Yahr, 1967). During the first few years following the initiation of treatment, the symptoms are usually stable but as the disease progresses, the motor symptoms get worse and additional non-motor dysfunctions appear, such as depression and dementia (Hughes, Daniel, Kilford, & Lees, 1992) (Table 2.1).

Presence of ubiquitylated intraneuronal protein inclusions enriched in  $\alpha$ -Syn in the cytoplasm of neurons (Lewy bodies) and thread-like proteinacious inclusions within neurites (Lewy neurites), are one of the neuropathological hallmarks invariably associated with idiopathic PD as well as familial PD (Spillantini et al., 1997). Lewy bodies and neurites are not restricted to the substantia nigra pars compacta but can also be found in other brain regions and in the peripheral autonomic nervous system as the disease progresses (Braak et al., 2003).

**Table 2.1: Cardinal and secondary clinical features of Parkinson’s disease (Toulouse & Sullivan, 2008).**

<b>Cardinal features</b>	<b>Secondary symptoms</b>
Tremour at rest Rigidity Bradykinesia/hypokinesia/akinesia Flexed posture/loss of postural reflexes Freezing	<p>Neuropsychiatric symptoms: Dementia, depression, anhedonia, apathy, anxiety, slowness of thought, psychosis</p> <p>Autonomic dysfunctions: Neurogenic bladder, erectile dysfunction, constipation</p> <p>Sleep disturbances: Sleep fragmentation, rapid eye movement (REM) sleep disturbances, excessive daytime sleepiness, nocturnal akinesia/tremour restless legs syndrome/periodic limb movements in sleep</p> <p>Sensory symptoms: Diminished sense of smell, pain, numbness, paresthesiae</p>

### 2.2.2 The synucleopathies

Interestingly, the discovery of  $\alpha$ -Syn in Lewy bodies in PD was followed quickly by its detection in cellular inclusions in several other neurodegenerative diseases including cortical Lewy body dementia (Baba et al., 1998), multiple system atrophy (MSA) together with Shy-Drager syndrome, striatonigral degeneration, and olivopontocerebellar atrophy (Fujiwara et al., 2002), amyotrophic lateral sclerosis (ALS) (Mezey et al., 1998), and Hallervorden-Spatz syndrome, now referred to as neurodegeneration with brain iron accumulation type 1 (NBIA 1) (Saito et al., 2000). Collectively, the neurodegenerative diseases that share  $\alpha$ -Syn pathology as a primary feature have come to be known as synucleopathies (Dev et al., 2003).

### 2.2.3 Familial PD-associated mutants of $\alpha$ -Syn

The etiology of PD is mainly vague even though some genetic and environmental factors have been described as contributing factors. Approximately 5-10% of cases are estimated to be caused by inheritable genetic mutations (Dauer & Przedborski, 2003; Samii, Nutt, & Ransom, 2004). Linkage data has identified at least twelve loci, named PARK, whereby several of the genes with pathogenic mutations with specific pattern of inheritance have now been identified. These include two autosomal dominant genes,  $\alpha$ -Syn (*SNCA*), leucine-rich repeat kinase 2 (*LRRK2*) (Kruger et al., 1998; Paisan-Ruiz et al., 2004; Polymeropoulos et al., 1997; Zimprich et al., 2004), and three autosomal recessive genes, *Parkin*, *DJ-1* and PTEN-induced putative kinase 1 (*PINK1*) (Bonifati et al., 2003; Kitada et al., 1998; Valente et al., 2004). In addition, there are a few genes for which the pattern of inheritance is uncertain or for which there has been no independent confirmation. These include the ubiquitin C-terminal hydrolase-L1 (*UCH-L1*), *NR4A2*, *synphylin-1* and *Htra2* (Le et al., 2003; Leroy et al., 1998; Marx et al., 2003; Strauss et al., 2005). There are also four remaining loci (PARK3, PARK9, PARK10 and PARK11) for which linkage has been identified; however, the causative genes have not yet been discovered (Gasser et al., 1998; Hicks et al., 2002; Pankratz et al., 2002).

$\alpha$ -Syn has been implicated in the pathogenesis of PD due to the causal relationship between genetic mutations and disease. Beginning in 1997,  $\alpha$ -Syn was discovered to have more extensive significance to neurodegenerative diseases as Polymeropoulos et al. (1997) reported that a large Italian family

(Contorsi kindred) and 3 unrelated families of Greek origin were afflicted by an autosomal dominant form of PD associated with a point mutation (G209A) in the *SNCA* gene coding for  $\alpha$ -Syn, which causes an Alanine to Threonine substitution at position 53 (A53T). Despite the mutation was found only in this small population, the very high penetrance of this mutation for the Parkinsonian phenotype made the finding extraordinary. Thereafter, the A53T mutation was identified in several additional PD kindreds (Athanasiadou et al., 1999; Papadimitriou et al., 1999; Spira, Sharpe, Halliday, Cavanagh, & Nicholson, 2001).

Soon after, another familial autosomal dominant form of PD linked to an  $\alpha$ -Syn gene mutation (G to C transversion at position 88), which leads to an Alanine to Proline substitution at residue 30 (A30P) was identified in a German kindred (Kruger et al., 1998). A third  $\alpha$ -Syn gene mutation (G188A) causing an amino acid change from Glutamate to Lysine at residue 46 (E46K) was then discovered in a Spanish kindred manifesting classical PD or PD with features of dementia associated with widespread Lewy pathology (Zarranz et al., 2004) (Figure 2.5).

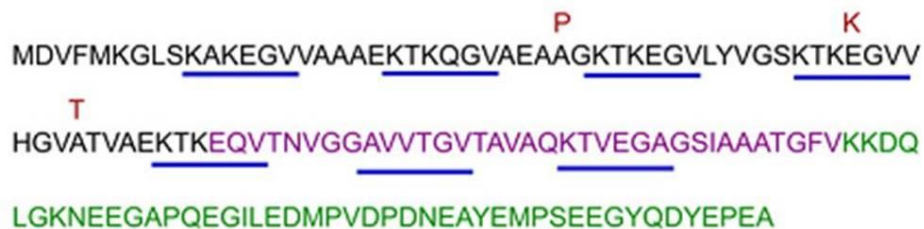


**Figure 2.5: Amino acid sequence of  $\alpha$ -Syn.**  $\alpha$ -Syn is composed of (1) an amino-terminal domain (black) with several imperfect KTKEGV motifs (blue underline); (2) a hydrophobic center (purple) and (3) a carboxy-terminus (green). Three familial mutations  $\alpha$ -Syn (red) have been identified in patients with PD (Waxman & Giasson, 2008).

Acceleration of oligomerisation is a shared property of all these three  $\alpha$ -Syn mutations linked to early-onset Parkinson's disease, suggesting that oligomeric states of  $\alpha$ -Syn may be the toxic species involved in the pathogenesis of PD rather than the insoluble fibrils (Conway et al., 2000; Zarranz et al., 2004). Both A53T and A30P mutants show an alteration in the secondary structure preferences of the polypeptide chain whereas E46K mutant causes a reduction in the net charge of the protein through sequence changes, resulting in an increased propensity to form annular protofibrils, which are capable of permeabilising cellular membranes by forming pore-like structures (Lashuel et al., 2002; Li, Uversky, & Fink, 2001; Rospigliosi et al., 2009). Such pores could affect the membranes of synaptic vesicles and disrupt the vesicular storage of dopamine (Volles & Lansbury, 2002). They could also damage mitochondria, leading to dissipation of the transmembrane potential and ultimately to the release of proapoptotic proteins, predisposing neuronal cells to death (Tanaka et al., 2001).

In addition, short chromosomal duplications or triplication containing the *SNCA* gene, plus relatively short flanking regions on chromosome 4, were discovered in patients with PD, indicating that a 50% increase in the expression of  $\alpha$ -Syn is sufficient to cause disease (Chartier-Harlin et al., 2004; Singleton et al., 2003). Altogether, these findings provide direct evidence that  $\alpha$ -Syn plays a pivotal role in the pathogenesis of PD.

#### **2.2.4 Environmental chemical inducers of Parkinsonism syndrome**

The environmental hypothesis of PD began with the discovery of MPTP in causing severe Parkinsonism syndrome in a cohort of young adult drug users in the early 1980s and has since developed to include a variety of environmental agents (Langston & Ballard, 1983). Agricultural chemicals have come under intense scrutiny due to their global application and widespread implications on human health. Both epidemiological and toxicological studies have provided evidence that certain pesticides have the potential to selectively damage the dopaminergic neurons, contributing to the development of PD (De Lau & Breteler, 2006). The use of pesticides including paraquat, rotenone, dieldrin, and maneb in toxicant-based models of PD has become increasingly popular and provided intriguing details on the neurodegenerative process (Dreschel & Patel, 2008).

##### **2.2.4.1 Rotenone**

Rotenone, a naturally occurring insecticide extracted from *Leguminosa* plants, is commonly used for small-scale organic farming and for piscicidal use to kill fish perceived as pests in lakes and reservoirs (Jones & Miller, 2008). Due to its highly lipophilic property, it easily crosses the blood-brain barrier, and accumulates in subcellular organelles including the mitochondria (Talpade, Greene, Higgins, & Greenamyre, 2000). The chemical structure of rotenone is shown in Figure 2.6.

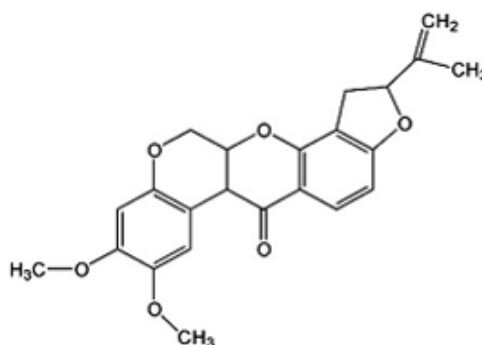


**Figure 2.6: Chemical structure of rotenone (International Programme on Chemical Safety, 2010).**

Rotenone exerts its toxic effect through the inhibition of mitochondrial complex I (NADH dehydrogenase). Specifically, it inhibits the transfer of electrons from iron-sulfur centers in complex I to ubiquinone and thereby interferes with NADH from being converted into usable cellular energy (ATP) (Sherer et al., 2003a). Moreover, following rotenone-induced inhibition, the electron flow through complex I is slowed at upstream sites that are prone to electron leakage. With electrons remaining in the site for a longer period of time than normal, molecular oxygen can react via a one-electron reduction to produce superoxide which is then released in the mitochondria (Drechsel & Patel, 2008).

Several studies showed that rotenone increases the mitochondrial reactive oxygen species (ROS) production, which mediate cytochrome *c* release and caspase-dependent apoptotic cell death (Ahmadi et al., 2003; Lee et al., 2008; Pei, Liou, & Chen, 2003). A recent report also demonstrated that ROS induced by rotenone involved nitration of the tyrosine residues of vesicular monoamine transporter 2 (VMAT2), which is responsible for packing dopamine and other monoamines into synaptic vesicles at nerve terminals. Functional inhibition

and accumulation of aggregate-like formations of VMAT2 by rotenone consequently leads to redistribution of dopamine to the cytosol, whose prooxidant conditions potentiate apoptosis of dopaminergic SH-SY5Y cells (Watabe & Nakaki, 2008). Furthermore, rotenone was shown to induce caspase-independent cell death (Li et al., 2005). Rotenone has also been demonstrated to induce activation of glycogen synthase kinase-3 (GSK-3), c-Jun N-terminal kinases (JNKs) and p38 kinases, whose activity seems to promote the progression of apoptosis (King & Jope, 2005; Newhouse et al., 2004).

Previously, the decrease of mitochondrial membrane potential and opening of the mitochondrial permeability transition pore have been shown to be involved in rotenone-induced apoptosis (Isenberg & Klaunig, 2000). Accordingly, Bcl-2 overexpression inhibits mitochondrial membrane potential changes and protects against apoptosis induced by rotenone (Tada-Oikawa, Hiraku, Kawanishi, & Kawanishi, 2003).

Taken together, rotenone-induced complex I inhibition results in deficiencies in the mitochondrial respiratory chain, decreased ATP synthesis, generation of ROS, mitochondrial depolarisation and eventually initiation of cell death processes (Sherer et al., 2003a). The central nervous system is highly dependent on aerobic respiration and maintaining a sufficient rate of oxidative phosphorylation is particularly critical to the survival of neurons. It is believed that subtle changes in respiratory chain complex activity may contribute to mild, late-onset neurological disorders. Support for this notion comes from

observations of a 15-30% reduction in complex I activity in nonfamilial sporadic PD patients (Schapira et al., 1990). Thus, rotenone is widely used to generate Parkinsonian models due to its inhibition of mitochondrial complex I, which has been implicated in the pathogenesis of PD.

Previous *in vivo* studies revealed that rotenone-treated rat caused uniform inhibition of complex I throughout the brain and selective degeneration to the nigrostriatal dopaminergic pathway accompanied by up-regulation of  $\alpha$ -Syn-positive cytoplasmic inclusion (Betarbet et al., 2000). Selective oxidative stress in the striatum of rotenone-treated rats as measured by increased oxidative protein damage has also been demonstrated. Indeed, rotenone-exposed animals show behaviors consistent with PD, including decreased locomotion, flexed posture, and rigidity (Betarbet et al., 2000; Sherer et al., 2003a). Besides, rotenone-treated animals reproduced the glial pathology observed in PD where selective and extensive microglial activation was examined in the nigrostriatal pathway (Sherer et al., 2003b). Knockout studies in mice have further identified microglial NADPH oxidase-mediated ROS generation as a key contributor to rotenone neurotoxicity (Gao, Hong, Zhang, & Liu, 2002).

Although rotenone has represented a useful experimental model of neurotoxicity, it lacks significant specificity for the central nervous system. Moreover, based on its limited environmental use, short half-life, and limited bioavailability, it is unlikely that rotenone exposure has a significant impact on PD. Furthermore, there is no evidence of PD in association with rotenone exposure (Franco, Li, Rodriguez-Rocha, Burns, & Panayiotidis, 2010).

#### 2.2.4.2 Maneb

Maneb is an ethylene-(bis)-dithiocarbamate (EBDC) fungicide used in the control of early and late blights on potatoes and tomatoes and many other diseases of fruits, vegetables, field crops, and ornamentals. Maneb controls a wider range of crops and vegetation diseases than other fungicides (Extension Toxicology Network, 1996). The chemical structure of maneb is as shown in Figure 2.7. However, exposure to this pesticide has been linked to a range of neurobehavioural abnormalities, including hyperactivity, ataxia, convulsions, and sedation (Miller, 1982). Additionally, its adverse effects have been observed in glutamate and dopamine systems (Vaccari et al., 1998; Vaccari, Saba, Ruiu, Collu, & Devoto, 1996). It has also been shown that chronic high-level occupational exposure to maneb is associated with the development of Parkinsonian syndrome in human studies (Ferraz, Bertolucci, Pereira, Lima, & Andrade, 1988).

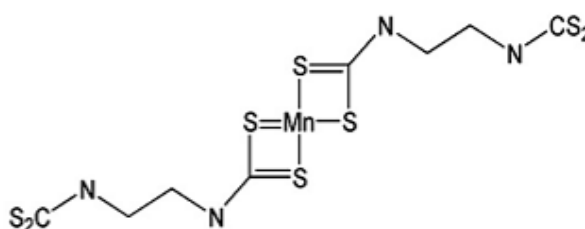


**Figure 2.7: Chemical structure of maneb (Drechsel & Patel, 2008).**

Low concentrations of maneb has been shown to lead to an increase in glutathione (GSH) and its oxidised form, glutathione disulphide (GSSG) (Barlow et al., 2005). GSH is one of the most abundant compounds in the brain (Mytilineou, Kramer, & Yabut, 2002) and it plays a critical role as a cellular antioxidant, reacting with free radicals nonenzymatically and also in the

reduction of peroxides, catalysed by glutathione peroxidase, forming the oxidised form, GSSG (Bharath, Hsu, Kaur, Rajagopalan, & Andersen, 2002). At high concentration, maneb cause deleterious effects on dopaminergic cells by disrupting the GSH system. It promotes autoxidation of dopamine and production of superoxide anion ( $O_2^{\cdot-}$ ), hydrogen peroxide ( $H_2O_2$ ) and quinone that can react with GSH in dopaminergic cells and hence decreases the level of GSH available to counter the oxidative situation and increases GSSG (Fitsanakis et al., 2002).

Diethyl-DTC is a known inhibitor of superoxide dismutase (SOD) (Heikkila, Cabbat, & Cohen, 1976), and was found to enhance the toxicity of MPTP due to this property (Corsini, Pintus, Chiueh, Weiss, & Kopin, 1985). Further studies have demonstrated that a range of DTCs, including maneb, when administered concurrently with known oxidative stressors like MPTP or paraquat, have yielded potentiated damage to dopaminergic systems, producing cell damage and loss even with otherwise non-toxic doses of these compounds (Takahashi, Rogerio, & Zanin, 1989; Thiruchelvam, Brockel, Richfield, Baggs, & CorySlechta, 2000; Walters, Irwin, Delfani, Langston, & Janson, 1999). A delicate balance exists between cell death and survival, is that oxidative stress pushes the system toward damage while antioxidant defenses promote survival (Schulz, Lindenau, Seyfried, & Dichgans, 2000). While compounds like MPTP, paraquat, and rotenone create imbalance through excessive production of ROS, maneb and other DTCs may be able create a state of enhanced susceptibility to oxidative damage via alterations in cellular antioxidant systems (including SOD and GSH) (Cereser, Boget, Parvaz, & Revol, 2001).

Structurally, maneb contains a major active fungicidal component, manganese that can serve as oxidative stressor (Snyder & Friedman, 1998). In the presence of water and oxygen, maneb rapidly degrades to ethylene thiourea which is a metal-free organic compound ( $C_3H_6N_2S$ ). Manganese would be liberated and become available via the decomposition of maneb. One particular target of the manganese metal is the mitochondria, where the manganese alters the calcium homeostasis. Thus, it inhibits mitochondrial complexes I and III and causes perturbation to the mitochondrial electron transport system (Gunter, Gavin, Aschner, & Gunter, 2006).

Domico, Zeevalk, Bernard, and Cooper (2006) demonstrated that maneb could act as uncoupler, resulting in the occurrence of mild to moderate mitochondrial uncoupling as revealed by oxygen consumption studies. Uncouplers of oxidative phosphorylation in mitochondria dissipate the proton gradient and prevent the coupling between the electron transport and phosphorylation reactions, thus inhibit ATP synthesis without affecting the respiratory chain and ATP synthase (Terada, 1990). Furthermore, the manganese metal impairs the functioning of some receptors and ionic channels of the plasma membrane, the systems for signal transduction and second messenger synthesis, some cellular enzymes, and other metalloproteins (Aschner & Aschner, 1991). Other mechanisms that have been suggested to explain the neurotoxicity of manganese include dopamine autoxidation, stimulation of free radicals and 6-hydroxydopamine (6-OHDA) production, and the reduction of levels of reduced GSH, glutathione peroxidase and catalase, which ultimately leads to severe oxidative stress (Dobson, Erikson, & Aschner, 2004).

### 2.2.5 Oxidative stress and mitochondrial dysfunction in PD

Oxidative damage to proteins, lipids, and nucleic acids has been found in the substantia nigra of patients with PD (Yacoubian & Standaert, 2008). Dexter et al. (1994) reported that a specific early marker of lipid peroxidation, cholesterol lipid hydroperoxides had a 10-fold increase in the PD substantia nigra compared to control subjects. An apparent selective increase in the level of DNA damage product including 8-hydroxy-2'-deoxyguanosine and 8-hydroxyguanine in the Parkinsonian brain has also been reported (Alam et al., 1997).

Moreover, increased total iron content seen in the substantia nigra of PD patients (Dexter et al., 1989) is thought to contribute to the free radical damage. The neurobiological importance of iron is dependent on its ferrous ( $\text{Fe}^{2+}$ ) and ferric ( $\text{Fe}^{3+}$ ) oxidation states as iron is capable of accepting and donating electrons, and participates in the oxidation-reduction reaction known as the Fenton reaction (Wessling-Resnick, 1999):



Iron levels must be well maintained within cells as excess iron causes enhanced generation of hydroxyl radicals via the Fenton reaction, and leads to cell damage (McCord, 1998). In Parkinsonian substantia nigra, iron content is elevated with a shift of the  $\text{Fe}^{2+}/\text{Fe}^{3+}$  ratio to the more oxidised form (Sofic et al., 1988). Microglial activation is a major source of the increased iron during

the disease process as it has been demonstrated that activated microglia can induce iron release from ferritin, resulting in free radicals production (Yoshida, Tanaka, Sotomatsu, & Hirai, 1995). Furthermore, free iron may promote the autoxidation of dopamine to its isoquinoline metabolites and generating superoxide and H<sub>2</sub>O<sub>2</sub>, which in turn generate reactive hydroxyl radicals (Berg et al., 2001). Iron-related oxidative stress also appears to augment  $\alpha$ -Syn aggregation and this relates the pathogenetically important role of iron to the major histopathological hallmark of PD (Hashimoto et al., 1999).

Several lines of evidences showed impairment of endogenous protective mechanisms in PD. The antioxidant protein, GSH levels were reduced in postmortem PD nigra (Perry & Yong, 1986; Sian et al., 1994; Sofic, Lange, Jellinger, & Riederer, 1992). Several genes linked to familial forms of PD, including *PINK1* and *DJ-1* also appear to be involved in protection against oxidative stress (Kim et al., 2005; Park et al., 2006). On the whole, both unregulated overproduction of reactive species and failure of cellular protective mechanisms appear to be operative in PD (Yacoubian & Standaert, 2008).

Mitochondrial dysfunction, implicated in the pathogenesis of PD, is another source for the production of ROS, which can then further damage mitochondria (Schapira, 2008). A few PD families show a maternal inheritance pattern consistent with abnormalities of mitochondrial DNA (Wooten et al., 1997), even though no specific mitochondrial DNA defect has been identified. The finding that the potent nigral mitochondrial toxin MPTP causes acute Parkinsonism further led to studies testing the possibility that mitochondrial

genetic factors contribute to the pathogenesis of PD (Langston & Ballard, 1983). It was shown that the catalytic activities for complex I (NADH dehydrogenase) are significantly reduced in the nigrostriatal system of PD patients (Hattori, Tanaka, Ozawa, & Mizuno, 1991). Genomic transplantation studies have demonstrated that the complex I defect is determined by mitochondrial DNA (Gu, Cooper, Taanman, & Schapira, 1998). Complex I activity is also reduced in neuroblastoma cybrids with mitochondrial genes from sporadic PD patients (Kosel, Hofhaus, Maassen, Vieregge, & Graeber, 1999) and these cybrids generate Lewy body inclusions over time, suggesting that defects in mitochondrial genes are likely to contribute to PD eventually (Trimmer, Borland, Keeney, Bennett, & Parker, 2004).

## **2.3 Cancer and apoptosis**

### **2.3.1 The Synucleins and cancer**

The involvement of Synuclein family in tumorigenesis came to light when  $\gamma$ -Syn, firstly named BCSG1 (Breast Cancer-Specific Gene 1) was shown to be overexpressed in advanced infiltrating carcinoma of the breast but not in normal or benign breast tissues (Ji et al., 1997).  $\gamma$ -Syn was further shown to be overexpressed in a high percentage of tumor tissues of diversified cancer types, including liver, esophagus, colon, gastric, lung, prostate, cervical cancer, but rarely expressed in tumor-matched nonneoplastic adjacent tissues. Expressions of *SNCG* protein in these cancer types all display stage-specific patterns of very low expression in stage I and high expression in stages II to IV (Liu et al., 2005).

Besides  $\gamma$ -Syn,  $\alpha$ - and  $\beta$ -Syn are also attractive candidates in oncogenesis, even though in a lesser extent. Bruening et al. (2000) reported that  $\alpha$ -,  $\beta$ -, and  $\gamma$ -Syn were not detectable in normal ovarian epithelium but were expressed in a high percentage of advanced staged ovarian carcinomas. Highly punctate  $\gamma$ -Syn expression was observed in some preneoplastic lesions of the ovary, suggesting that  $\gamma$ -Syn up-regulation may occur early in the development of ovarian carcinoma (Bruening et al., 2000).

Recently, Ye et al. (2010) found that  $\alpha$ -,  $\beta$ -, and  $\gamma$ -Syn were expressed in a high percentage of colorectal cancer.  $\gamma$ -Syn is valuable for evaluation of progression of colorectal cancer and it is now more sensitive to predict advanced stage and lymph node invasion by detection of  $\gamma$ -Syn protein combined with either  $\alpha$ - or  $\beta$ -Syn protein or both than by detection of  $\gamma$ -Syn only. Matsuo and Kamitani (2010) also reported that  $\alpha$ -Syn was highly expressed in 86% of the primary and 85% of the metastatic melanoma sections, as well as in 89% of nevus sections studied. However,  $\alpha$ -Syn was undetectable in non-melanocytic cutaneous carcinoma and normal skin.

### **2.3.2 Melanoma**

Melanoma is a malignant neoplasm of melanocytes, predominantly found in skin. Less common primary sites include the eye and mucosal surfaces. Melanin pigments, produced by melanocytes, are present in varying quantities in tumour cells and the extracellular tumour matrix, giving its characteristic dark colour (Jerant, Johnson, Sheridan, & Caffrey, 2000). Melanoma is one of the less common types of skin cancer but the most deadly of all, accounting for

majority (75%) of skin cancer related deaths. It is more frequently diagnosed in women than in men and is particularly common among Caucasians living in tropical or subtropical climates, with high rates of incidence in Australia, New Zealand, North America, and northern Europe (Parkin, Bray, Ferlay, & Pisani, 2002). Based on the statistics conducted by National Cancer Registry in 2006, there were 60 melanoma incidences per 100,000 populations in West Malaysia with the percentage of melanoma suffered by sex were 56.7% males and 43.4% females and about 62% sufferers were above the age of 50 years old. Among ethnic groups, Malays recorded the highest incidence of melanoma compared to Chinese and Indians (Omar, Mohd Ali, & Tamin, 2006).

Early signs of melanoma are changes to the shape or colour of existing moles or in the case of nodular melanoma, the appearance of a new lump anywhere on the skin. At later stages, the mole may itch, ulcerate or bleed. Early signs of melanoma are summarised by the mnemonic “ABCDE”: Asymmetry, Borders (irregular), Colour (variegated), Diameter (greater than 6mm), and Elevation (Friedman, Rigel, & Kopf, 1985). However, these classifications do not apply to the most dangerous form of melanoma, nodular melanoma which has its own classifications: elevated above the skin surface, firm to the touch and growing (Melanoma Education Foundation, 2010).

Metastatic melanoma may cause non-specific paraneoplastic symptoms including loss of appetite, nausea, vomiting and fatigue (Davis et al., 2010). Metastasis of early melanoma is possible, but relatively rare as less than a fifth of melanomas diagnosed early become metastatic. Despite many years of

intensive laboratory and clinical research, early surgical resection of thin tumours still provides the greatest chance for cure (Shapiro, 2002).

Treatment of melanoma once it has spread beyond the skin remains unsatisfactory. Patients with advanced disease, such as lymph node involvement and distant metastases, have 5-year survival rates of 50% and 10-20%, respectively (Ugurel, Tilgen, & Reinhold, 2003). This poor prognosis is largely due to the resistance of melanoma to available chemotherapeutic and biologic reagents, which has been attributed to its refractoriness to apoptosis (Hersey, 2002). The alkylating agent dacarbazine (DTIC) was the first chemotherapeutic drug used for advanced melanoma, and remains the only one approved by the Food and Drug Administration (FDA) as none of the chemotherapeutic drugs tried, including nitrosoureas (carmustine, lomustine), vinca alkaloids (vincristine, vinblastine), platinum compounds (cisplatin, carboplatin) and taxanes (Taxol, docetaxel) showed improvement over DTIC (Anderson, Buzaid, & Legha, 1995; Becker, Kampgen, & Brocker, 2000). Experiments using melanoma xenografts derived from patient tumors in immunodeficient mice have confirmed the resistance of melanoma cells to DTIC, cisplatin, and other chemotherapeutic drugs *in vivo* (Osieka, 1984).

Recently, epidemiological studies have reported co-occurrence of PD and melanoma. A large follow-up study in Denmark showed a two-fold higher incidence of malignant melanoma in patients who later developed Parkinson's disease than in general population (Olsen, Friis, & Frederiksen, 2006), whereas patients with Parkinson's disease were found to have increased risks for

subsequent development of malignant melanoma (Olsen et al., 2005). Melanoma prevalence also appears to be higher in patients with PD than in the general population in North America (Bertoni et al., 2010). Furthermore, a positive family history of melanoma was also reported to be associated with an excessive PD risk. These findings support the notion that melanoma and PD could share common genetic components and the genetic determinants of melanoma could be explored as susceptibility candidate genes for PD (Gao, Simon, Han, Schwarzschild, & Ascherio, 2009).

S-100, NK1/C3, HMB-45, and MART-1 are well known histological biomarkers for melanoma. S-100 and NK1/C3 proteins are expressed in almost all primary and metastatic malignant melanomas but unfortunately are expressed in many other malignant tumors and hence have limited specificity (Zubovits, Buzney, Yu, & Duncan, 2004). HMB-45 and MART-1 are melanocyte-specific proteins and are most commonly used as melanocytic markers (De Maziere et al., 2002; Raposo & Marks, 2007). Although HMB-45 is highly specific to melanoma, the clinical utility of HMB-45 is limited as it is not expressed by 20-40% of metastatic melanomas (Clarkson, Sturdgess, & Molyneux, 2001). MART-1 appeared to be the most useful histological biomarker for melanoma because its staining has a higher diagnostic accuracy than S-100, NK1/C3 and HMB-45 staining (Shidham et al., 2001; Zubovits et al., 2004). Recent work from Matsuo and Kamitani (2010) showed that  $\alpha$ -Syn is expressed in MART-1-negative melanoma and in more melanoma cases than MART-1, suggesting that  $\alpha$ -Syn might be a better histological biomarker for the diagnosis of melanoma.

### **2.3.3 Relationship between cancer development and dysregulation of apoptosis**

Cancer, referred to as malignant neoplasm, is a clonal disease originates from multistep accumulation of genetic or epigenetic changes in oncogenes and tumour suppressor (caretaker, gatekeeper and landscaper) genes, that compromise control of cell proliferation, survival, differentiation, migration and social interactions with neighboring cells and stroma (Pelengaris et al., 2006). In particular, these changes allow a normal cell to achieve the “hallmark” features of cancer, including capacity to proliferate irrespective of exogenous mitogens, refractoriness to growth-inhibitory signals, resistance to apoptosis, unrestricted proliferative potential (immortality), capacity to recruit a vasculature (angiogenesis) and ability to invade surrounding tissue and metastasise via lymph or blood, as neatly summarised by Hanahan and Weinberg (2000) (Figure 2.8). The malignant properties differentiate cancer from benign tumors, which are self-limited, localised and do not invade or metastasise (Weinberg, 2007).

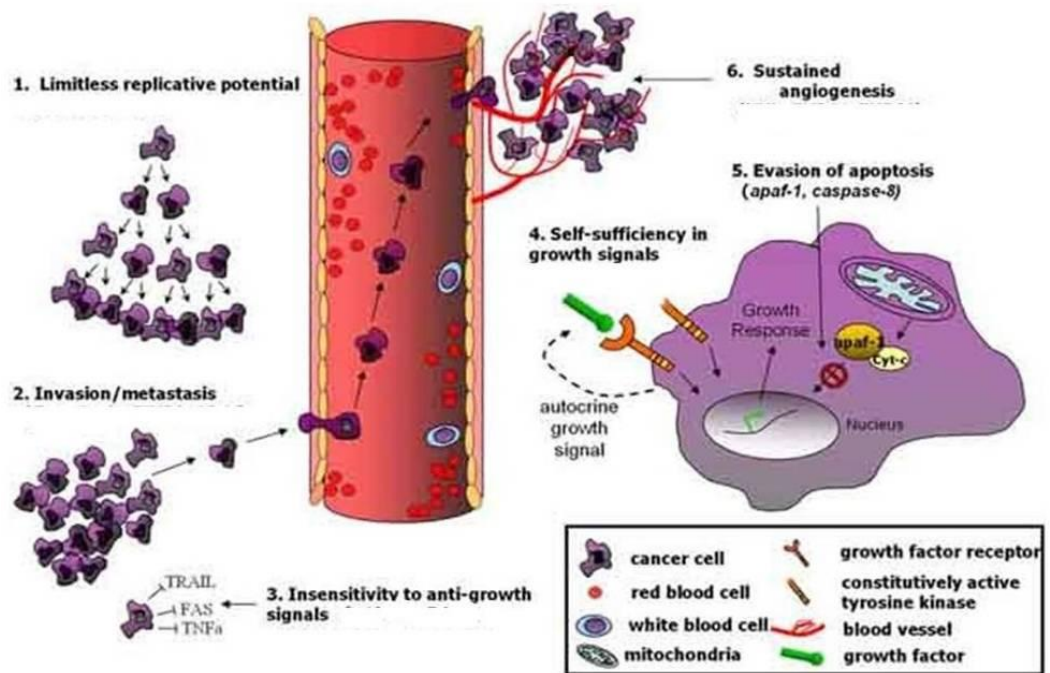


**Figure 2.8: The hallmarks of cancer (Balch et al., 2005).**

Dysregulation of apoptosis (programmed cell death) is a key process in cancer development and progression. Virtually all cancer cells bypass apoptosis through a variety of mechanisms involving dynamic interplays between oncogenes and/or mutated tumour suppressor genes. More than 50% of cancers are marked by a mutation in the tumour suppressor gene p53, a key pro-apoptotic regulator which, when mutated, facilitates tumourigenesis. Some viruses associated with cancers use tricks to prevent apoptosis of the cells they have transformed. Several human papilloma viruses have been implicated in causing cervical cancer. One of them produces a protein (E6) that binds and inactivates the apoptosis promoter p53 (Scheffner, Werness, Huibregtse, Levine, & Howley, 1990). Epstein-Barr virus, the cause of mononucleosis and some lymphomas produces a protein similar to Bcl-2 (a proto-oncogene product) or another protein that causes the cell to increase its own production

of Bcl-2 (Tsujimoto, 1989). These actions make the cell more resistant to apoptosis.

Even cancer cells produced without the participation of viruses may have tricks to avoid apoptosis. Some B-cell leukemias and lymphomas express high levels of Bcl-2, resulting from a translocation of the *BCL-2* gene into an enhancer region and thus blocking apoptotic signals they may receive (Nunez et al., 1989). Melanoma cells avoid apoptosis by inactivation of the apoptosis effector, Apoptotic Protease-Activating Factor 1 (Apaf-1) (Soengas et al., 2001). Some cancer cells, especially lung and colon cancer cells amplify the expression of a soluble decoy receptor, termed decoy receptor 3 (DcR3) that binds to FasL, plugging it up so it cannot bind Fas and thereby inhibits FasL-induced apoptosis (Pitti et al., 1998).

#### **2.3.4 Apoptotic pathways**

Apoptotic cell death is a genetically programmed mechanism that allows the cell to commit suicide (Hotchkiss, Strasser, McDunn, & Swanson, 2009). Apoptosis is critically important for the survival of multicellular organisms by getting rid of damaged or infected cells that may interfere with normal function (Vicencio et al., 2008). As illustrated in Figure 2.9, apoptosis is triggered through two main signalling pathways, the extrinsic and intrinsic (cell autonomous) pathways. The extrinsic pathway is mediated by a sub-group of Tumour Necrosis Factor receptors (TNFR) superfamily that includes TNFR, Fas and TNF-related apoptosis-inducing ligand (TRAIL) in response to multiple external pro-apoptotic signals. Activation of these so-called death

receptors leads to the recruitment and activation of initiator caspases such as caspases 8 or 10. The process involves the formation and activation of complexes such as the death inducing signalling complex (DISC), leading to the activation of an effector caspase, typically caspase 3. The active caspase 3 is responsible for the cleavage of a number of so-called death substrates that lead to the well-known characteristic hallmarks of an apoptotic cell including DNA fragmentation, nuclear fragmentation, membrane blebbing and other morphological and biochemical changes (Duprez, Wirawan, Vanden Berghe, & Vandenabeele, 2009).

On the other hand, the intrinsic pathway is initiated by cellular developmental cues or as a result of severe cellular stress (such as DNA damage or lack of oxygen, nutrients, or extracellular survival signals) and it is largely centred around and/or regulated by the mitochondria (Gupta, Kass, Szegezdi, & Joseph, 2009). The most widely studied form of intrinsic apoptosis is initiated by the stress-mediated release of cytochrome *c* from the mitochondria. Cytochrome *c* then binds to a procaspase-activating adaptor protein called Apaf-1, causing the Apaf-1 to oligomerise into a wheel-like heptamer called an apoptosome. The Apaf-1 proteins in the apoptosome then recruit initiator procaspase proteins (procaspase 9), which are activated by proximity in the apoptosome. The activated caspase 9 molecules then process downstream executioner procaspases, resulting in the activation of executioner caspase 3. This leads to the same type of apoptotic response as observed for the extrinsic pathway. Other pro-apoptotic proteins including Smac/Diablo (Second Mitochondrial-derived Activator of Caspase/Direct IAP-Binding protein with a Low pI) and

apoptosis inducing factor (AIF) are also released by the mitochondria (Brenner & Mak, 2009).

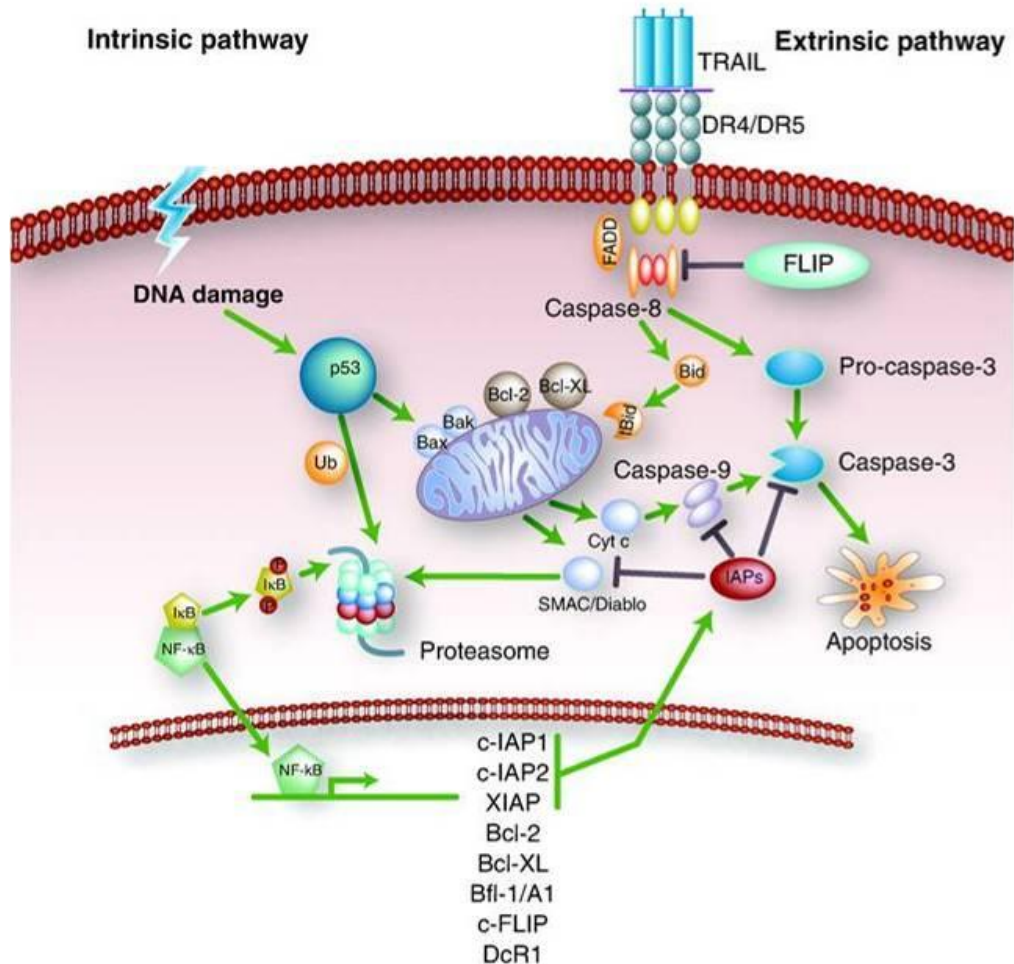


**Figure 2.9: Schematic representation of the main intrinsic and extrinsic apoptotic signalling pathways (De Vries, Gietema, & de Jong, 2006).**

Mammalian Bcl-2 proteins tightly regulate the intrinsic pathway of apoptosis mainly by controlling the formation of mitochondrial permeability transition pore, which leads to subsequent release of cytochrome *c* and other intermembrane mitochondrial proteins into the cytosol (Chao & Korsmeyer, 1998; Scarlett & Murphy, 1997; Yang et al., 1997). There are pro-apoptotic and anti-apoptotic Bcl-2 proteins that can bind to each other in various

combinations to form heterodimers, in which the two proteins inhibit each other's function. The balance between the activities of these two functional classes of Bcl-2 proteins largely determines whether a mammalian cell lives or dies by the intrinsic pathway of apoptosis (Brunelle & Letai, 2009).

The anti-apoptotic Bcl-2 proteins, including Bcl-2 and Bcl-xL, share four distinctive Bcl-2 homology (BH) domains (BH1-4). The pro-apoptotic Bcl-2 proteins consist of two subfamilies: the BH123 proteins and the BH3-only proteins. The main BH123 proteins are Bax and Bak, which are structurally similar to Bcl-2 but lack the BH4 domain. The BH3-only proteins including Bad, Bim, Bid, Puma and Noxa, share sequence homology with Bcl-2 in only the BH3 domain (Reed, Zha, Aime-Sempe, Takayama, & Wang, 1996) (Figure 2.10).

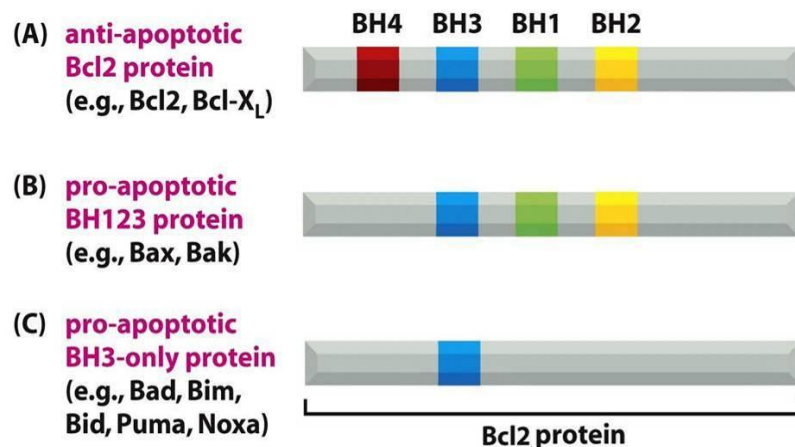


**Figure 2.10: The three classes of Bcl-2 proteins.** BH3 domain is the only BH domain shared by all Bcl-2 family members and it mediates the direct interactions between pro-apoptotic and anti-apoptotic family members (Alberts et al., 2008).

The pro-apoptotic BH123 protein, Bak is tightly bound to the mitochondrial outer membrane even in the absence of an apoptotic signal whereas Bax is mainly located in the cytosol and translocates to the mitochondria only after an apoptotic signal activates it (Wolter et al., 1997). The anti-apoptotic Bcl-2 proteins are also mainly located on the cytosolic surface of the outer mitochondrial membrane and preserving the membrane integrity mainly by binding to and inhibiting these pro-apoptotic Bcl-2 proteins either on the membrane or in cytosol (Dejean, Martinez-Caballero, Manon, & Kinnally, 2006; Sattler et al., 1997) (Figure 2.11). Moreover, the BH4 domain of Bcl-2 and Bcl-xL can bind to the C-terminal part of Apaf-1, thus inhibits Apaf-1-dependent caspase 9 activation (Hu, Benedict, Wu, Inohara, & Nunez, 1998).

In the presence of apoptotic stimulus, the BH3-only proteins bind to the long hydrophobic groove on anti-apoptotic Bcl-2 proteins via the BH3 domain and thereby neutralising their activity (Huang & Strasser, 2000). This binding and inhibition enables the pro-apoptotic BH123 proteins to become activated and aggregate to form oligomers in the mitochondrial outer membrane, resulting in the release of cytochrome *c* and other intermembrane protein that induce apoptosis (Luo, Budihardjo, Zou, Slaughter, & Wang, 1998; Uren et al., 2007; Willis et al., 2007). Some BH3-only protein may bind directly to Bax and Bak to help trigger the activation of these BH123 pro-apoptotic proteins (Kuwana et al., 2005; Walensky et al., 2006). Furthermore, activation of the intrinsic mitochondrial pathway can also occur following the activation of the extrinsic pathway. This has been shown to occur via the caspase 8 cleavage of the pro-apoptotic Bcl-2 member Bid to its activated tBid form (Brunelle & Letai, 2009).

These clearly demonstrate the central role of the mitochondria in the highly regulated and complex process of apoptosis.

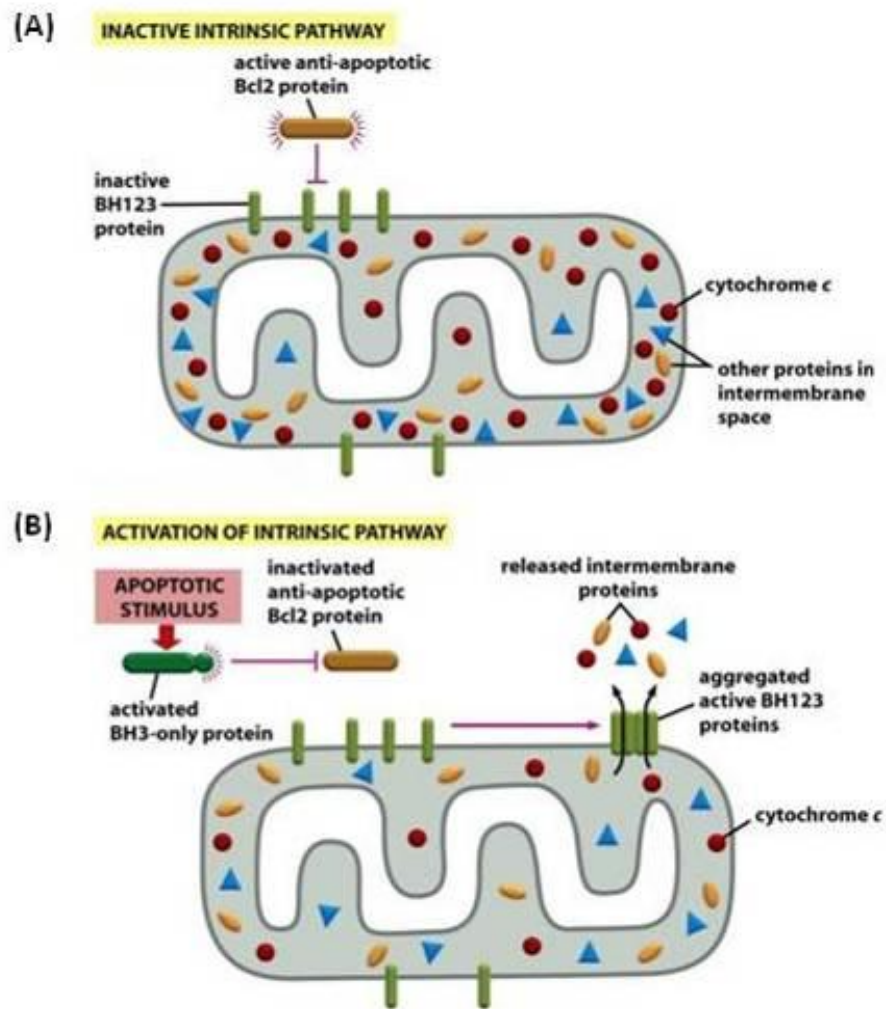


**Figure 2.11: The regulation of intrinsic pathway of apoptosis by pro-apoptotic BH-3 only and anti-apoptotic Bcl-2 proteins.** (A) In the absence of an apoptotic stimulus, anti-apoptotic Bcl-2 proteins bind to and inhibit the BH123 proteins on the mitochondrial outer membrane and in the cytosol. (B) In the presence of an apoptotic stimulus, BH3-only proteins are activated and bind to the anti-apoptotic Bcl-2 proteins so that they can no longer inhibit the BH123 proteins, which now become activated and aggregate in the outer mitochondrial membrane and promote the release of intermembrane mitochondrial proteins into the cytosol (Alberts et al., 2008).

### 2.3.5 Staurosporine-mediated apoptosis

Staurosporine, an indolo (2,3- $\alpha$ ) carbazole (Figure 2.12), was first discovered during the course of screening extracts of the bacterium *Streptomyces staurosporeus* for constituent alkaloids with protein kinase C inhibitory activity (Omura et al., 1977). Apart from its biological activities ranging from anti-fungal to anti-hypertensive, staurosporine, a protein kinase inhibitor, has been characterised as a strong inducer of apoptosis in many different mammalian cell types. These include cancer cell lines, lymphocytes, neurons, and other primary cell cultures (Yamaki et al., 2002).

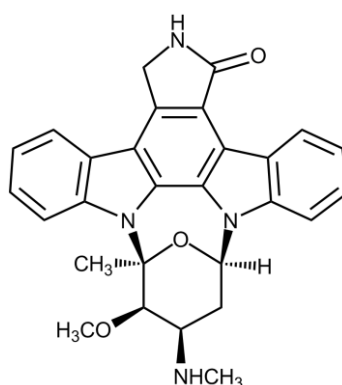


**Figure 2.12: Molecular structure of staurosporine (Scmeyer, 2008).**

The exact mechanism(s) by which staurosporine induces apoptosis remains elusive. It is generally believed that the mitochondrial apoptotic pathway plays a critical role in staurosporine-induced apoptosis (Tafani et al., 2002; Tafani, Minchenko, Serroni, & Farber, 2001) and this is further supported by a study demonstrating that overexpression of Bcl-2 and Bcl-xL and addition of caspase inhibitor were effective in protecting cells from apoptosis induced by low concentrations staurosporine (Yuste et al., 2002). While most reports showed a requirement for caspase activation in staurosporine-induced apoptosis, caspase-

independent mechanism was also suggested (Belmokhtar, Hillion, & Segal-Bendirdjian, 2001; Xue, Chiu, & Oleinick, 2003). Multiple mechanisms may therefore be involved in staurosporine-induced apoptosis and these may vary between different cell types.

Apparently, inhibition of protein kinases by staurosporine may have been responsible for induction of conformational changes in Bax and its translocation from the cytosol to mitochondria. Inhibition of Erk1/2 was shown to facilitate apoptosis induction in melanoma by promoting conformational changes of Bax and its relocation to mitochondria (Zhang, Borrow, Zhang, Nguyen, & Hersey, 2003). Overexpression of Akt was also shown to inhibit staurosporine-induced movement of Bax and apoptosis in HeLa cells (Tafani et al., 2001). Furthermore, staurosporine has been shown to inhibit the serine/threonine kinase Akt/protein kinase B leading to decreased phosphorylation of Bad (Zha, Harada, Yang, Jockel, & Korsmeyer, 1996). Bad is capable of forming heterodimers with the anti-apoptotic proteins Bcl-xL and Bcl-2 and antagonising their anti-apoptotic activity. Phosphorylated Bad cannot bind to either Bcl-xL or Bcl-2, so inhibition of Akt-mediated phosphorylation of Bad would increase sensitivity of cells to apoptosis (Yang et al., 1995).

## CHAPTER 3

### MATERIALS AND METHODS

#### 3.1 List of solution formulations

Formulations for the solutions used in this study are shown in Table 3.1.

**Table 3.1: List of solution formulations.**

<b>Solution</b>	<b>Formulation</b>
<b>Amido Black dye</b>	0.1% (w/v) Naphthol Blue Black, 10% (v/v) methanol, 2% (v/v) acetic acid
<b>Laemmli Dissociation Buffer</b>	125 mM Tris, 5% Sodium Dodecyl Sulfate (SDS), 0.02% bromophenol blue, 20% glycerol, 5% $\beta$ -mercaptoethanol, pH 6.8
<b>LB-ampicillin agar</b>	Tryptone 1%, Yeast extract 0.5%, NaCl 0.5%, 1.5% agar, pH 7.5, sterilisation by autoclaving, ampicillin is added to a final concentration of 50 $\mu$ g/ml when agar is cool
<b>LB medium</b>	Tryptone 1%, Yeast extract 0.5%, NaCl 0.5%, pH 7.5, sterilisation by autoclaving
<b>Lysis Buffer</b>	10 mM Tris/HCl, pH 7.8, 100 mM NaCl, 0.5% (w/v) sodium deoxycholate, 0.05% (v/v) nonidet-P40, 10 mM EDTA, 0.1 mM phenylmethylsulphonyl fluoride
<b>Phosphate Buffered Saline (PBS)</b>	150 mM NaCl, 2 mM $\text{NaH}_2\text{PO}_4$ , 20 mM $\text{Na}_2\text{HPO}_4$ , pH7.4
<b>Stripping buffer</b>	0.2 M Glycine, pH 2.2, 0.1% SDS, 1.0% Tween-20
<b>TAE buffer</b>	40 mM Tris/HCl, 10 mM sodium acetate, 2 mM EDTA, pH 8.0
<b>TE Buffer</b>	10 mM Tris-HCl, pH 7.5, 1 mM EDTA
<b>Transfer buffer</b>	150 mM Glycine, 20 mM Tris, 20% (v/v) methanol
<b>Tris-glycine electrophoresis buffer</b>	25 mM Tris/HCl, 190 mM glycine, 1% SDS, pH 8.6
<b>Tris buffered saline (TBS)</b>	150 mM NaCl, 10 mM Tris-HCl, pH 7.5

### 3.2 Molecular biology of $\alpha$ -Syn constructs

#### 3.2.1 Plasmid pCMV-Sport6 with full length human $\alpha$ -Syn cDNA

Plasmid pCMV-Sport6 (Figure 3.1) with full length human  $\alpha$ -Syn (GenBank ID: BC108275) cDNA (Clone ID: 6147966) inserted between *SalI* and *NotI* restriction sites was purchased from Open Biosystems, Huntsville, AL.

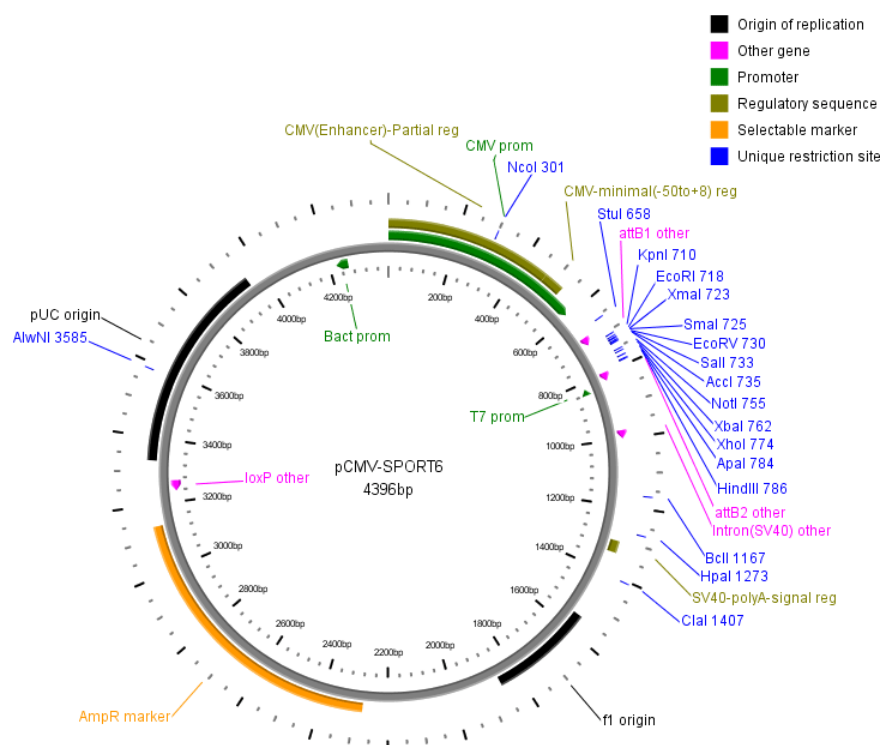


**Figure 3.1: Vector map of plasmid pCMV-Sport6 (Dong, Stothard, Forsythe, & Wishart, 2010).** The strong human cytomegalovirus (CMV) promoter regulatory region drives constitutive protein expression levels. This vector contains the pBR322 origin for replication in bacterial cells and the  $\beta$ -lactamase gene for ampicillin resistance selection in bacteria. Multiple cloning sites in the forward and reverse orientation facilitate molecular cloning (Invitrogen, 2004).

#### 3.2.2 Plasmid pBABE-hygro

Plasmid pBABE-hygro, a mammalian expression vector which has a backbone size of 5578 bp (Weinberg, 2009) was purchased from Addgene, Cambridge, MA (Figure 3.2). It was initially selected as a co-transfection plasmid with pCMV-Sport6- $\alpha$ -Syn as it contains a hygromycin resistance gene cloned in the

pBABE retroviral vector required for the growth of stably transfected mammalian cells (Cell Biolabs, 2008). For successful co-transfection, it is necessary for both vectors to be delivered into the same cell and to be equivalently integrated into the genome so that the cell would be stably expressing both gene of interest and selection marker.

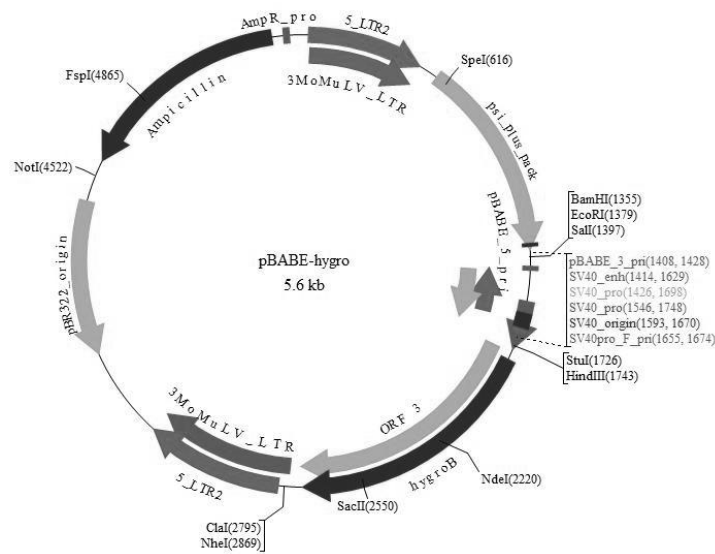


**Figure 3.2: Vector map of plasmid pBABE-hygro.** Plasmid pBABE-hygro contains the bacterial origin of replication (pBR322), ampicillin-resistance gene and hygromycin-resistance gene for selection of stably transfected mammalian cells (BVTech, 2005).

### 3.2.3 Design of primers for generation of $\alpha$ -Syn mutant constructs

Design of primers for generation of constructs expressing the three pathogenic mutations of  $\alpha$ -Syn (A30P, A53T and E46K) was done using Stratagene's web-based QuikChange<sup>®</sup> Primer Design Program, available online at <http://www.stratagene.com/qcprimerdesign>. The mutagenic primers designed are shown in Table 3.2. DNA primers were synthesised by Eurogentech AIT, Singapore.

**Table 3.2: Mutagenic primers used to create  $\alpha$ -Syn mutant constructs.**

<b>Primer</b>	<b>Primer Sequence (5' to 3')</b>
A30P	5'-GGGTGTGGCAGAAGCACCAGGAAAGACAAAAGA-3'
A30P_ ANTISENSE	5'-TCTTTTGTCTTTCCTGGTGCTTCTGCCACACCC-3'
A53T	5'-GAGTGGTGCATGGTGTGACGACAGTGGCTGAGAAGAC-3'
A53T_ ANTISENSE	5'-GTCTTCTCAGCCACTGTCGTCACACCATGCACCACTC-3'
E46K	5'-GGCTCCAAAACCAAGAAGGGAGTGGTGCATG-3'
E46K_ ANTISENSE	5'-CATGCACCACTCCCTTCTTGGTTTTGGAGCC-3'

### 3.2.4 Site-directed mutagenesis

#### 3.2.4.1 Mutant strand synthesis reaction (thermal cycling) and *DpnI* digestion of the amplification products

Site-directed Mutagenesis PCR was performed using QuikChange<sup>®</sup> Site-Directed Mutagenesis Kit (Stratagene Ltd., La Jolla, CA) according to manufacturer's manual, with minor modifications shown in Table 3.3. Incorporation of the oligonucleotide primers generated a mutated plasmid containing staggered nicks. Following temperature cycling, the product was treated with *DpnI*. The *DpnI* endonuclease is specific for methylated and hemimethylated DNA and hence was used to digest the parental DNA template and to select for mutation-containing synthesised DNA. The nicked vector DNA containing the desired mutation was then transformed into XL1-Blue supercompetent cells where the nicks in mutated plasmid were repaired *in vivo* during replication.

**Table 3.3: (a) PCR reagent mixture and (b) thermal cycling conditions for site-directed mutagenesis to generate  $\alpha$ -Syn mutant constructs.**

(a)

Reagent	Volume
10× reaction buffer	5 $\mu$ l
25 $\mu$ g/ml dsDNA template	1 $\mu$ l (25 ng)
125 $\mu$ g/ml forward primer	1 $\mu$ l (125 ng)
125 $\mu$ g/ml reverse primer	1 $\mu$ l (125 ng)
dNTP mix	1 $\mu$ l
DMSO	1.5 $\mu$ l
ddH <sub>2</sub> O	39.5 $\mu$ l
Total reaction	50 $\mu$ l
<i>Pfu</i> Turbo DNA polymerase (2.5 U/ $\mu$ l)	1 $\mu$ l

(b)

Segment	Cycles	Temperature	Time
1	1	95°C	30 sec
2	16	95°C	30 sec
		55°C	1 min
		68°C	10 min

### 3.2.4.2 Transformation of XL1-Blue supercompetent cells

XL1-Blue supercompetent cells were gently thawed on ice. For each sample reaction to be transformed, 50  $\mu$ l of the supercompetent cells was aliquoted to a prechilled 1 ml microcentrifuge tube. Then 4  $\mu$ l of the *Dpn*I-treated DNA from sample reaction were transferred to the aliquot of supercompetent cells. As an optional control, transformation efficiency of the XL1-Blue supercompetent cells was verified by adding 1  $\mu$ l of the pUC18 control plasmid (0.1 ng/ $\mu$ l) to a 50  $\mu$ l aliquot of the supercompetent cells. Transformation reactions were swirled gently to mix followed by incubation on ice for 30 min. The transformation reactions were then heat-pulsed for 45 sec at 42°C and placed on ice for 2 min before 950  $\mu$ l of prewarmed LB broth was added into each reaction. The transformation reactions were incubated at 37°C for 1 hr with

shaking at 250 rpm. Cells were pelleted by centrifugation at 10,000 rpm and 900 µl of LB broth was discarded while 100 µl of LB broth remained was used to resuspend the pellet to be spread on LB-ampicillin agar plates. Plates were then incubated at 37°C for overnight to allow transformed colonies to grow.

### **3.2.5 Plasmid extraction**

A single colony was picked from plate of transformants and inoculated in 5 ml LB medium containing 50 µg/ml ampicillin. The bacterial culture was incubated for 12-16 hr at 37°C with shaking at approximately 250 rpm. Bacterial cells were harvested by centrifugation at 6000 g for 15 min at 4°C and the supernatant was discarded. Plasmid DNA was isolated using PureLink Quick Plasmid Miniprep Kit (Invitrogen, Carlsbad, CA) or Plasmid Midi prep (Qiagen Ltd., Venlo, Netherlands) according to the protocol given in the manufacturer's handbook. In the end, plasmid DNA was eluted in 75 µl of TE buffer.

### **3.2.6 DNA quantification by spectrophotometry**

DNA concentration was determined by UV spectrophotometry with absorbance readings at 260 nm and 280 nm. The ratio of A<sub>260</sub>:A<sub>280</sub> (DNA: protein) should be greater than 1.8 for better purity. The concentration of the DNA was calculated as follows: (absorbance at 260 nm × dilution factor × 50) = µg/ml. Double stranded DNA at a concentration of 50 µg/ml has an absorbance at 260 nm = 1.

### **3.2.7 Restriction digestion of DNA**

A 50 µl reaction mix consisting of 1 µg of DNA, 0.5 µl of BSA (10 mg/ml), 5 µl 10× Buffer, 1 µl of *SalI* (Vivantis Inc., Chino, CA), and sterile distilled water topped up to 50 µl was incubated at 37°C for 2 hr. Reaction volume of 5 µl was mixed with 1 µl of 6× loading dye before being electrophoresed in a 1% agarose gel to confirm products of digestion.

### **3.2.8 Agarose gel electrophoresis**

Agarose powder (1.0 g) was weighed and mixed with 100 ml of 1× TAE to give a 1% agarose gel. Agarose solution was swirled to mix, microwaved to dissolve the agarose and left to cool on bench for 5 min. The gel was poured slowly into the gel mould with proper comb inserted and left to set for at least 30 min. Then 1× TAE buffer was poured into the gel tank to submerge the gel to 2-5 mm depth. Samples (1 µl of 6× loading dye was mixed with 5 µl DNA sample) were loaded onto gel alongside a 1 kb DNA ladder (Vivantis Inc., Chino, CA). Electrophoresis was carried out at constant voltage of 95 V for 30 min. The progress of the gel was monitored by reference to the marker dye. The electrophoresis was stopped when the bromophenol blue has electrophoresed 3/4 the length of the gel. The electrophoresed gel was visualised and photographed under a UV transilluminator (Syngene Bio Imaging, Frederick, MD) after staining with Gel Red (Biotium Inc., Hayward, CA).

### 3.2.9 Mammalian expression vector, pcDNA<sup>TM</sup>3.1D/V5-His-TOPO<sup>®</sup>

A 5.5 kb mammalian expression vector, pcDNA<sup>TM</sup>3.1D/V5-His-TOPO<sup>®</sup> (Invitrogen, Carlsbad, CA) designed to facilitate rapid directional cloning of blunt-end PCR products for expression in mammalian cells was used (Figure 3.3).

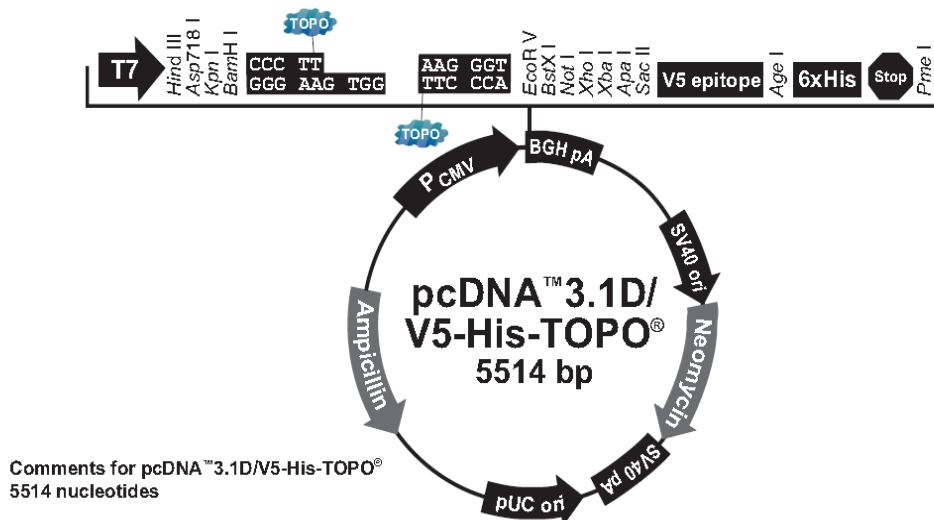


**Figure 3.3: Elements of pcDNA<sup>TM</sup>3.1D/V5-His-TOPO<sup>®</sup> vector.** CMV promoter: bases 232-819; TOPO<sup>®</sup> recognition site 1: bases 930-934; TOPO<sup>®</sup> recognition site 2: bases 939-943; SV40 early promoter and origin: bases 1833-2142; Neomycin resistance gene: bases 2217-3011; pUC origin: bases 3700-4373; Ampicillin resistance gene: bases 4518-5378 (Invitrogen, 2007).

### 3.2.10 Molecular cloning using pcDNA<sup>TM</sup>3.1 Directional TOPO<sup>®</sup> Expression Kit

#### 3.2.10.1 Design of PCR primers and generation of blunt end PCR products

The pcDNA<sup>TM</sup>3.1 Directional TOPO<sup>®</sup> Expression Kit (Invitrogen, Carlsbad, CA) was used to directionally clone blunt-end PCR product into the plasmid vector. PCR primers required to amplify the gene encoding for  $\alpha$ -Syn were first designed according to the manufacturer's manual (Table 3.4). The DNA primers were synthesised by Eurogentech AIT, Singapore. Blunt end PCR products were then produced using pCMV-Sport6-full length human  $\alpha$ -Syn

cDNA as DNA template. The preparation of PCR mixtures and thermal cycling conditions are presented in Table 3.5. The desired PCR products were then gel purified, as explained in Section 3.3.5.

**Table 3.4: PCR primers for amplification of gene encoding for  $\alpha$ -Syn.**

Primer	Sequence (5'→3')
Forward	5'-CACCATGGATGTATTCATGAAAGGA-3'
Reverse	5'-TTAGGCTTCAGGTTTCGTAGTC-3'

**Table 3.5: (a) PCR reaction mixture and (b) thermal cycling conditions applied to generate blunt end wild type and mutant  $\alpha$ -Syn cDNA fragments.**

(a)

Component	Volume/reaction	Final concentration
10× <i>Pfu</i> Buffer, containing 20 mM MgSO <sub>4</sub>	5 $\mu$ l	1×
Forward primer (100 $\mu$ M)	0.25 $\mu$ l	0.5 $\mu$ M
Reverse primer(100 $\mu$ M)	0.25 $\mu$ l	0.5 $\mu$ M
dNTP mix(10 mM each)	1 $\mu$ l	0.20 mM each
Template DNA(10 ng/ $\mu$ l)	1 $\mu$ l	10 ng
Sterile double-distilled water	42 $\mu$ l	-
<i>Pfu</i> Plus! DNA Polymerase, 5 U/ $\mu$ l (EURx, Gdansk, Poland)	0.5 $\mu$ l	2.5 U
<b>Total volume</b>	<b>50 <math>\mu</math>l</b>	<b>-</b>

(b)

Step	Temperature	Time	Number of cycles
Initial denaturation	95°C	5 min	1
Denaturation	95°C	30 sec	} 25
Annealing	53°C	30 sec	
Extension	72°C	1 min	
Final Extension	72°C	7 min	1
Cooling	4°C	Indefinite	1

### 3.2.10.2 TOPO<sup>®</sup> cloning reaction and transformation of DNA into One Shot<sup>®</sup> TOP10 Competent Cells

The reaction as shown in Table 3.6 was prepared, mixed gently and incubated for 5 min at room temperature. The reaction was placed on ice before proceeding to transformation. Two microlitres of the TOPO<sup>®</sup> cloning reaction mixture was added into a vial of 50 µl One Shot<sup>®</sup> TOP10 Chemically Competent *E. coli*, mixed gently and incubated on ice for 5 min. The cells were then heat-shocked for 30 sec at 42°C without shaking and the tube was immediately transferred to ice. Room temperature SOC medium (250 µl) provided by supplier was then added. The tube was capped tightly and the tube was shaken horizontally (200 rpm) at 37°C for 1 hr. Two hundred microlitres from each transformation was spread on a prewarmed LB-ampicillin agar plate and the plate was incubated overnight at 37°C.

**Table 3.6: TOPO<sup>®</sup> cloning reaction.**

<b>Reagents</b>	<b>Chemically competent <i>E. coli</i></b>
Fresh PCR products	1 µl
Salt solution	1 µl
Sterile water	3 µl
TOPO vector	1 µl
<b>Final volume</b>	<b>6 µl</b>

### 3.2.10.3 Analysing transformants

Several colonies were picked and cultured overnight in LB or SOB medium containing 50 µg/ml ampicillin. The plasmid DNA was isolated. The plasmids were analysed by restriction digest analysis using *XhoI* to confirm the presence and correct orientation of the insert before sending to an outsourced sequencing service provided by First BASE Laboratories Sdn Bhd, Selangor, Malaysia.

#### **3.2.10.4 Preparation of glycerol stock for long-term storage**

After the correct clone had been identified, the colony was purified and a glycerol stock was made for long-term storage while a stock of plasmid DNA was stored at -20°C. To prepare glycerol stock, the original colony was streaked out for single colony on LB-ampicillin plates. A single colony was isolated and inoculated into 2 ml of LB broth containing 50 µg/ml ampicillin. The culture was grown until it reached stationary phase before 0.85 ml of culture was mixed with 0.15 ml of sterile glycerol and transferred to a cryovial. The cryovial was then stored at -80°C.

### **3.3 Molecular biology of $\alpha$ -Syn gene silencing**

#### **3.3.1 Plasmid pLKO.1**

pLKO.1 is a replication-incompetent lentiviral vector chosen by the RNAi Consortium (TRC) for expression of short hairpin RNA (shRNA) (Moffat et al., 2006). pLKO.1-TRC cloning vector (Figure 3.4) along with pLKO.1-TRC control, the negative control vector containing non-hairpin insert and pLKO.1-scramble shRNA, the negative control vector containing scrambled shRNA were purchased from Addgene Inc., Cambridge, MA.

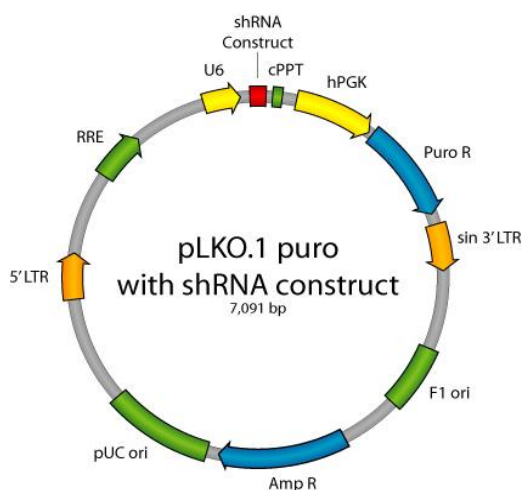


**Figure 3.4: Map of pLKO.1 containing a shRNA insert.** The original pLKO.1-TRC cloning vector has a 1.9 kb stuffer that is released by digestion with *AgeI* and *EcoRI*. shRNA oligonucleotides are cloned into the *AgeI* and *EcoRI* sites in place of the stuffer (Moffat et al., 2006).

### 3.3.2 Design of shRNA oligonucleotides for pLKO.1

The optimal 21-mer targets in the *SNCA* gene encoding for  $\alpha$ -Syn were determined for efficient gene silencing using the siRNA Selection Program hosted by Whitehead Institute for Biomedical Research, available online at <http://jura.wi.mit.edu/bioc/siRNAext/> (Yuan, Latek, Hossbach, Tuschl, & Lewitter, 2004). Firstly, 21-nucleotide sequences that match the pattern AA(N19) starting at 25-nucleotide downstream of the start codon (ATG), where N is any nucleotide, were determined. It was preferable for the 21-nucleotide sequences to have 36-52% GC content and not target the introns while the sense 3' end should have low stability with at least one A or T between position 15-19. Moreover, sequences with stretches of 4 or more nucleotide repeats, especially repeated Ts were avoided because poly (T) is a termination signal for RNA polymerase III. Sequences that did not fit the requirements were eliminated from consideration. At last, to minimise off-target mRNAs, the sequences were compared to the human genome database

using NCBI's BLAST program (Appendix A). Three target sequences that have at least 3 nucleotide mismatches to all unrelated genes were selected (Table 3.7).

**Table 3.7: 21-mer targets in the *SNCA* gene for efficient gene silencing.**

Name	21-mer target
HuAsynRNAi 1	5'-AAAGTGGCGGTTAGGATATAT-3'
HuAsynRNAi 2	5'-AATGAGTGA CTATAAGGATGG-3'
HuAsynRNAi 3	5'-AAGGACCAGTTGGGCAAGAAT-3'

As shown in Figure 3.5, each final shRNA construct requires the designing of two complementary oligonucleotides containing a sense (red) and an antisense (green) sequence, where the former is identical to the target gene mRNA so that once annealed, the dsDNA molecule obtained would have at the 5' a sticky end compatible with an *Age*I digested site, while at the 3' the end would be suitable for ligation with an *Eco*RI-digested site. The sense and antisense sequences are connected by a spacer capable of forming a loop. The final forward and reverse shRNA oligonucleotides designed are as shown in Table 3.8.

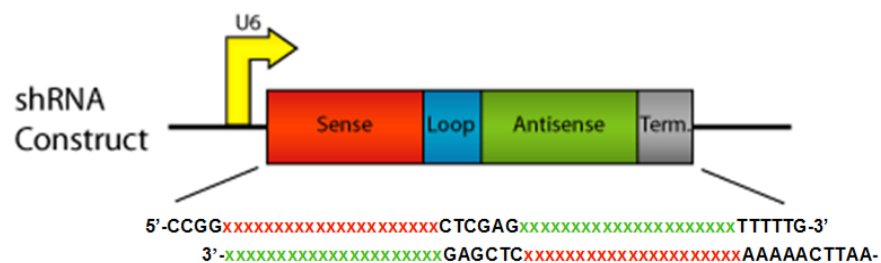


**Figure 3.5: Details of shRNA insert.** The U6 promoter directs RNA Polymerase III transcription of the shRNA. The shRNA contains 21 “sense” bases that are identical to the target gene, a loop and 21 “antisense” bases that are complementary to the “sense” bases (Moffat et al., 2006).

**Table 3.8: Forward and reverse shRNA oligonucleotides containing sense and antisense strands.**

Name	Forward oligonucleotide (5'-3')	Reverse oligonucleotide (5'-3')
HuAsynRNAi1	CCGGAAAGTGGCGGTT AGGATATATCTCGAGAT ATATCCTAACCGCCACT TTTTTTTG	AATTCAAAAAAAAAAGTG GCGGTTAGGATATATC TCGAGATATATCCTAA CCGCCACTTT
HuAsynRNAi2	CCGGAATGAGTACTA TAAGGATGGCTCGAGC CATCCTTATAGTCACTC ATTTTTTTG	AATTCAAAAAAAAAATGAG TGACTATAAGGATGGC TCGAGCCATCCTTATA GTCACTCATT
HuAsynRNAi3	CCGGAAGGACCAGTTG GGCAAGAATCTCGAGA TTCTTGCCCAACTGGTC CTTTTTTTG	AATTCAAAAAAAAAAGGAC CAGTTGGGCAAGAATC TCGAGATTCTTGCCCA ACTGGTCCTT

### 3.3.3 Annealing of shRNA oligonucleotides

The shRNA oligonucleotides were resuspended in sterile deionised H<sub>2</sub>O to a concentration of 100 µM and then the mixture shown in Table 3.9 was prepared and incubated at 95°C for 4 min in a water bath. The water bath was shut off and the water was allowed to cool to room temperature in a few hours as it is important for the cooling to occur slowly for the oligonucleotides to anneal.

**Table 3.9: Preparation of mixture for shRNA oligonucleotides annealing.**

Component	Volume
Forward oligonucleotide	9µl
Reverse oligonucleotide	9µl
10× annealing buffer	2µl

### 3.3.4 Double restriction digestion of pLKO.1-TRC cloning vector

In order to release the 1.9 kb stuffer, pLKO.1-TRC cloning vector was first digested with *AgeI* (New England Biolabs, Ipswich, MA). As shown in Table

3.10(a), the mixture was prepared and incubated at 37°C for 2 hr. The digested DNA was purified with GF-1 gel DNA recovery kit (Vivantis Inc., Chino, CA) and eluted in 30µl of sterile deionised H<sub>2</sub>O. The eluate was digested with *EcoRI* (New England Biolabs, Ipswich, MA) by preparing the mixture shown in Table 3.10(b) and incubating it at 37°C for 2 hr. The digested DNA was electrophoresed on 0.8% low melting point agarose gel. Two bands; one 7 kb and one 1.9 kb could be distinctly seen under UV illumination. The 7 kb band was then cut out and gel purified.

**Table 3.10: Reaction mixture for restriction digestion with (a) *AgeI* and (b) *EcoRI*.**

(a)	
<b>Component</b>	<b>Volume</b>
pLKO.1-TRC cloning vector (midiprep DNA)	6 µg
10× NEB buffer for <i>AgeI</i>	5 µl
<i>AgeI</i>	1 µl
ddH <sub>2</sub> O	to 50 µl

(b)	
<b>Component</b>	<b>Volume</b>
pLKO.1-TRC cloning vector digested with <i>AgeI</i>	30 µl
10× NEB buffer for <i>EcoRI</i>	5 µl
<i>EcoRI</i>	1 µl
ddH <sub>2</sub> O	14 µl

### 3.3.5 Purification of DNA from agarose gel

The DNA fragment of interest was excised from the agarose gel under UV light with a clean scalpel, placed in a sterile microcentrifuge tube and purified using GF-1 gel DNA recovery kit (Vivantis Inc., Chino, CA) as described in the manufacturer's handbook. The agarose was solubilised by incubation at 50°C with Gel DNA Binding Buffer, which provide the correct salt

concentration and pH to enhance binding of DNA onto a specially-treated glass filter membrane fixed into a column. The purified DNA was eluted with 30  $\mu$ l of sterile deionised water.

### **3.3.6 Preparation of competent *E. coli* DH5 $\alpha$ using Calcium Chloride**

A single colony was picked from the master stock plate of *E. coli* DH5 $\alpha$  using an inoculation loop and streaked on a new plate. The plate was incubated overnight at 37°C to allow the growth of bacteria. On the next day, a single colony was inoculated into 50 ml of LB Broth in a 250 ml conical flask and allowed for overnight incubation with shaking at 220 rpm. On the following day, 0.5 ml of the culture was transferred into 25 ml of LB Broth in 250 ml conical flask and incubated for 2-3 hr. The growth of culture was monitored every 45 min. Optical Density at 600 nm (OD<sub>600</sub>) of the culture was measured using the LB broth as a blank. The reading of absorbance has to lie between 0.6-1.0 and the best reading would be 0.6. Subsequently, bacteria were transferred to an ice-cold centrifuge tube and placed on ice. The tube was centrifuged at 9000 rpm for 10 min at 4°C. Supernatant was discarded and the collected pellet was resuspended with 10 ml of ice-cold MgCl<sub>2</sub>-CaCl<sub>2</sub> solution. The cells were centrifuged at 9000 rpm for 10 min at 4°C again and the pellet collected was resuspended with 2 ml of CaCl<sub>2</sub>. The cells were then kept on ice for 2 hr. Each 500  $\mu$ l of cells was aliquoted into separate microcentrifuge tubes and mixed with equal volume of sterile 40% glycerol before being stored at -80°C.

### 3.3.7 Ligation and transformation into *E. coli* DH5 $\alpha$

For cloning of the annealed oligonucleotides into pLKO.1-TRC cloning vector, the ligation mixture, as stated in Table 3.11 was prepared and incubated at 16°C for overnight. Four microlitres of ligation mixture was transformed into 100  $\mu$ l competent *E. coli* DH5 $\alpha$  cells and plated on LB-ampicillin agar plates.

**Table 3.11: Ligation mixture for cloning the inserts into pLKO.1-TRC cloning vector.**

Component	Volume
Annealed oligonucleotides	2 $\mu$ l
Digested pLKO.1-TRC cloning vector	50 ng
10 $\times$ T4 DNA ligase buffer	2 $\mu$ l
T4 DNA ligase	1 $\mu$ l
ddH <sub>2</sub> O	to 20 $\mu$ l

### 3.3.8 Screening for inserts

Colonies from each ligation were picked and inoculated into LB broth containing 50  $\mu$ g/ml ampicillin. The cultures were incubated at 37°C with shaking at 250 rpm overnight. The cultures were spun down and a miniprep kit was used to isolate DNA. A restriction digest with *Eco*RI and *Nco*I (New England Biolabs, Ipswich, MA) was conducted. The digestion products were electrophoresed on a 1% agarose gel and two fragments, a 2 kb fragment and a 5 kb fragment should be seen under UV illumination. The positive clones were sent to an outsourced sequencing service (First BASE Laboratories Sdn Bhd, Selangor, Malaysia) with pLKO.1 sequencing primer (5'-CAAGGCTGTTAGAGAGA TAATTGGA-3').

### **3.4 Cell culture**

#### **3.4.1 Maintenance of cell lines**

The cell lines used in this study were human neuroblastoma, SH-SY5Y and human melanoma, SK-MEL28, which was kindly donated by Dr. Lim Yang Mooi, Faculty of Medicine and Health Science, UTAR.

SH-SY5Y is one of three serially isolated neuroblast clones (SH-SY, SH-SY5, SH-SY5Y) of the human neuroblastoma cell line SK-N-SH which was established in December 1970 from the metastatic bone marrow biopsy of a 4 years old female. As shown in Figure 3.6(a), SH-SY5Y cells grow as clusters of neuroblastic cells with multiple, short, fine cell processes (neurites) (Biedler, Helson, & Spengler, 1973). SK-MEL28 is the skin melanoma cell line isolated from a 51 years old male with malignant melanoma by Carey and colleagues and it is a monoclonal and monolayer continuous culture with polygonal morphology, as shown in Figure 3.6(b) (Carey, Takahashi, Resnick, Oettgen, & Old, 1976).

Human neuroblastoma, SH-SY5Y and human melanoma, SK-MEL28 cell lines are anchorage-dependent cell cultures obtained from American Type Culture Collection (ATCC). These two cell lines were cultured in Minimum Essential Medium (MEM) (Cellgro<sup>®</sup> Media tech, Inc, Manassas, VA) supplemented with 10% (v/v) fetal bovine serum (FBS) (i-DNA Biotechnology Pte Ltd, Singapore) and 1% penicillin/streptomycin (Millipore, Billerica, MA) at 37°C in a 5% CO<sub>2</sub> humidified incubator.

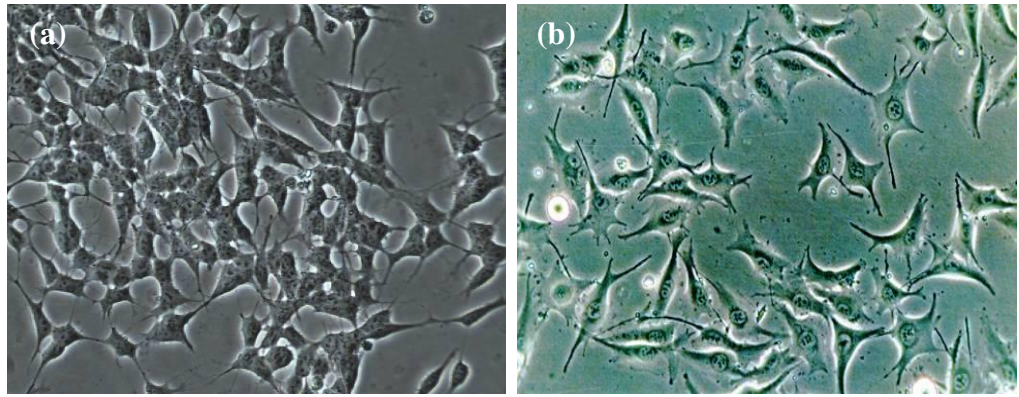


**Figure 3.6: Morphology of (a) SH-SY5Y (American Type Culture Collection, 2010) and (b) SK-MEL28 cells (Kikuchi, 1991).**

### **3.4.2 Cell passaging**

Subculture was carried out when cells reached confluence state. Spent medium was aspirated from culture flask and the adhering cell monolayer was washed once with 2 ml of Phosphate Buffered Saline (PBS) (OXOID Ltd, Hampshire, UK). One millilitre of 0.05% trypsin-EDTA (GIBCO Inc, Billings, MT) was added to cover the adhering cell layer. The flask was incubated at 37°C for 10 min and 2 ml of complete medium were added as soon as cells were detached to inhibit further trypsin activity that might damage cells. Cells were centrifuged at 1500 rpm for 5 min and the pelleted cells were resuspended in fresh medium. Appropriate volume of cells was transferred to new 25 cm<sup>2</sup> culture flasks (Orange Scientific, Braine-l'Alleud, Belgium) and fresh medium was added to each new culture. If necessary, subconfluent cultures were to be fed after 3-4 days by removing spent medium and adding fresh medium. Inverted microscope (Nikon Eclipse TS100, Melville, NY) was used to check the morphology of cell cultures.

### **3.4.3 Cryopreservation**

Cells were trypsinised, transferred into a 15 ml centrifuge tube and spun down at 1500 rpm for 5 min to pellet the cells. The supernatant was discarded and 950  $\mu$ l medium was added into the centrifuge tube to resuspend the cell pellet. Resuspended cell mixture was transferred to a cryovial (Nalgene, Rochester, NY) and 50  $\mu$ l of DMSO (Fisher Scientific Ltd, Leicestershire, UK), which serves as cryoprotective agent was added. The cryovial was then sealed with parafilm, labeled with date, passage, and cell line and transferred to the  $-80^{\circ}\text{C}$  freezing chamber. For long term storage, the cryovial was then transferred to the liquid nitrogen tank to be stored at  $-196^{\circ}\text{C}$ .

### **3.4.4 Stable transfection of cells**

Cells were trypsinised, pelleted, and resuspended in appropriate volume of OPTI-MEM<sup>®</sup> I (GIBCO Inc, Billings, MT) per transfection and transferred to a 4mm electroporation cuvette. Linearised DNA (20-30  $\mu$ g) was added to the cuvette and mixed thoroughly by inverting 5 times. Cuvette was then placed in an electroporator, ECM<sup>®</sup> 830 ElectroSquarePorator<sup>™</sup> (BTX Harvard Apparatus, Holliston, MA) and pulsed at cell-specific parameters. Electroporated cells were immediately transferred into 25  $\text{cm}^2$  culture flask supplemented with sufficient amount of growth medium. Stably expressing transfectants were selected 48 hr post-transfection using appropriate selective antibiotic. Selection process was carried out for a series of passaging by introducing fresh medium and antibiotic to the cells. Following 10-14 days, polyclonal pools of stably transfected cells were maintained. Protein expression was confirmed by Western blotting and immunofluorescence microscopy.

Linearised DNA was used as it could improve the transfection efficiency. Circular plasmid would recombine into the genome at a random position within the plasmid. Therefore, there is a relatively high likelihood that the expression cassette for the gene of interest will be destroyed, leading to antibiotic resistant clones. By linearising the plasmid, it could be determined at which position within the plasmid the recombination occurs and hence preserves the expression cassette for gene of interest in most cases. Linearised DNA also has higher tendency to be integrated into the genome than supercoiled DNA, thus facilitating stable expression of the construct.

#### **3.4.4.1 Generation of stable human $\alpha$ -Syn overexpressing cell lines by electroporation**

To generate stable cell lines overexpressing stable human  $\alpha$ -Syn, human neuroblastoma, SH-SY5Y cells were transfected with pcDNA<sup>TM</sup>3.1- $\alpha$ -Syn constructs [wild type human  $\alpha$ -Syn and three familial pathogenic  $\alpha$ -Syn mutants (A30P, A53T and E46K)], with pcDNA<sup>TM</sup>3.1 empty vector as negative control. The linearisation of the circular plasmid DNAs was carried out by a restriction digest with *Xho*I (EURx, Gdansk, Poland) at 37°C for 2 hr. The electroporation was done using the parameters stated in Table 3.12. Stably transfectants were then selected using 1 mg/ml G418 Sulfate (Geneticin) (A.G. Scientific Inc, San Diego, CA).

**Table 3.12: (a) Electroporation setting and (b) reaction mixture preparation for SH-SY5Y cells.**

(a)

<b>Electroporation settings</b>	
Choose Mode	LV
Set Voltage	230 V
Set Pulse Length	8 msec
Set Number of Pulses	1
Electrode Type	BTX Disposable Cuvette (4mm gap)
Desired Field Strength	575 V/cm

(b)

<b>Electroporation reaction mixture preparation</b>	
Cell Density	$1.5 \times 10^7$ cells/ml
Sample volume	800 $\mu$ l
DNA concentration	30 $\mu$ g
Temperature	Room temperature

#### **3.4.4.2 Transfection of SK-MEL28 cells by electroporation for $\alpha$ -Syn knockdown**

For  $\alpha$ -Syn knockdown, SK-MEL28 cells were transfected with pLKO.1-TRC control, pLKO.1-scramble shRNA and three pLKO.1 vectors, each cloned with different shRNA sequence targeting the human  $\alpha$ -Syn mRNA. The linearisation of the circular plasmid DNAs was carried out by a restriction digest with *Nco*I (New England Biolabs, Ipswich, MA) at 37°C for 2 hr. The electroporation was performed using the settings shown in Table 3.13. Stably expressing transfectants were selected using 3  $\mu$ g/ml Puromycin (BioWORLD, Dublin, OH).

**Table 3.13: (a) Electroporation setting and (b) reaction mixture preparation for SK-MEL28 cells.**

(a)

<b>Electroporation settings</b>	
Choose Mode	LV Mode (99 msec/500V)
Set Voltage	170 V
Set Pulse Length	70 msec
Set Number of Pulses	1
Chamber	BTX Disposable Cuvette (4mm gap)
Desired Field Strength:	425 V/cm

(b)

<b>Electroporation reaction mixture preparation</b>	
Cell Density	$1.5 \times 10^7$ cells/ml
Sample volume	400 $\mu$ l
DNA concentration	20 $\mu$ g
Temperature	Room temperature

### **3.5 Protein expression analysis**

#### **3.5.1 Preparation of cell lysates**

Cells were washed with PBS for at least 3 times. After the final rinse, cell scraper was used to collect the attached cells in PBS. Cell suspension was centrifuged at 1500 rpm for 5 min at 4°C and supernatant was discarded. For every  $1 \times 10^6$  cells, approximately 100  $\mu$ l of ice-cold Lysis Buffer was added to resuspend the pellet, ensuring no clumps remain. Protease inhibitor cocktail (Sigma Aldrich, St. Louis, MO) was added into the reaction mixture in a dilution factor of 1:100. The reaction mixture was transferred to a 1 ml microcentrifuge tube and was incubated on ice for 60 min. Cell debris was pelleted by centrifugation at 13,000 rpm for 10 min at 4°C. Supernatant was collected into an appropriately labelled tube. Protein concentration of lysate was quantified using Pierce<sup>®</sup> BCA Protein Assay Kit (Thermo Scientific,

Waltham, MA). The lysate could be used immediately or to be stored at -20°C or -80°C.

### **3.5.2 BCA Protein Assay**

The BCA protein assay applies a detergent-compatible formulation based on bicinchoninic acid (BCA) for the colourimetric detection and quantitation of total protein. This method combines the well-known reduction of  $\text{Cu}^{2+}$  to  $\text{Cu}^{1+}$  by protein in an alkaline medium (the biuret reaction) with the highly sensitive and selective colourimetric detection of the cuprous cation ( $\text{Cu}^{1+}$ ) using a unique reagent containing BCA. Bovine serum albumin (BSA) standards were prepared in the range of 0.2 to 1.0 mg/ml. Working reagent was prepared by mixing 50 parts of BCA™ Reagent A (sodium carbonate, sodium bicarbonate, bicinchoninic acid and sodium tartarate in 0.1 M sodium hydroxide) with 1 part of BCA™ Reagent B (4% cupric sulphate). Each unknown sample was diluted to 1:5 and 1:10 and 10 µl was added in duplicate wells as well as the BSA standards. Subsequently, 200 µl of working reagent was added to each well and the microplate was placed on a plate shaker for 30 sec to ensure thorough mixing of working reagent and samples. Plate was incubated at 37°C for 30 min and cooled to room temperature before measuring the absorbance at 562 nm on a microplate reader (Tecan Group Ltd, Mannedorf, Switzerland). The purple-coloured reaction product of this assay is formed by the chelation of two molecules of BCA with one cuprous ion. This water-soluble complex exhibits a strong absorbance at 562 nm that is nearly linear with increasing protein concentrations.

### 3.5.3 Sodium Dodecyl Sulphate-Polyacrylamide Gel Electrophoresis (SDS-PAGE)

For each SDS-PAGE gel, a small and a large glass plates were washed with 70% ethanol. An assembled sandwich of the glass plates and two spacers was then inserted into a gel-casting apparatus and was pushed all the way to the bottom of the holder before the screws were tightened. Table 3.14 gives the formulations for SDS-PAGE 15% resolving gel and 4% stacking gel.

**Table 3.14: Formulations for SDS-PAGE 15% resolving gel and 4% stacking gel.**

<b>Component</b>	<b>15% resolving gel</b>	<b>4% stacking gel</b>
30% acrylamide/bis solution (Bio-Rad Laboratories Inc, Hercules, CA)	4.95 ml	660 µl
1.5 M Tris (pH 8.8)	2.5 ml	-
1 M Tris (pH 6.8)	-	1.26 ml
H <sub>2</sub> O	2.4 ml	3 ml
10% SDS	100 µl	50 µl
10% APS (Promega, Madison, WI)	50 µl	25 µl
TEMED (Biobasic Inc, Ontario, Canada)	5 µl	5 µl
<b>Total Volume</b>	<b>10 ml</b>	<b>5 ml</b>

Resolving gel casting solution was prepared, swirled gently to mix and poured into the gel cassette. The cassette was filled to a level which allowed the comb to be inserted with 1 cm between the bottom of the wells and the top of the resolving gel. The gel was overlaid with 1-2 mm of water saturated n-butanol to exclude O<sub>2</sub> and ensure a flat interface between the resolving and stacking gels. The resolving gel was then allowed to polymerise for 30 min. A line would become visible at the top of the gel as it polymerises. Butanol was removed by inverting the gel and rinsing the top of the gel with water. The residual liquid was drained using filter paper. Stacking gel solution was then

prepared and the top of the gel cassette was filled with this mixture. The comb was inserted until the teeth were 1cm from the resolving gel. The comb should rest so that the top of the well dividers are level with the top of the short plate. This excludes air while ensuring that the dividers would fully separate the wells. The stacking gel was left to polymerise for 30-60 min and subsequently transferred to an electrophoresis tank which was filled with 1× Tris-glycine electrophoresis buffer. Protein samples (40 µg) were mixed with Laemmli dissociation buffer and boiled at 95°C for 5 min before being loaded onto the polyacrylamide gel alongside a broad range prestained protein molecular weight marker (Crystalgen Inc, Commack, NY). Electrophoresis was then conducted at constant 150 V for approximately 2 hr.

### **3.5.4 Western blot analysis**

#### **3.5.4.1 Semi-dry transfer**

Proteins resolved by SDS-PAGE were transferred to a polyvinylidene difluoride (PVDF) (Biotrace International PLC, Bridgend, UK) membrane using semi-dry transfer. In preparation of blotting, a PVDF membrane and two pieces of extra thick filter paper (required for each membrane sandwich) were first cut according to the dimensions of the gel and then completely immersed in transfer buffer for 15-30 min. Following electrophoresis, the gel was equilibrated in transfer buffer for removal of electrophoresis buffer salts and detergents and adjustment of gel to its final size prior to electrophoretic transfer. For assembly of the unit for standard transfer, a pre-soaked sheet of extra thick filter paper was placed onto the platinum anode. A centrifuge tube was rolled over the surface of the filter paper to exclude all air bubbles. The pre-wetted

blotting media (PVDF membrane) was placed on top of the filter paper and all air bubbles were rolled out. The equilibrated gel was then carefully placed on top of the transfer membrane and was aligned on the center of the membrane. All air bubbles were again rolled out before another piece of thick filter paper was placed on top of the gel. Then the cathode was placed onto the stack and the safety cover was positioned on the unit. The unit was plugged into the power supply. Subsequently, the power supply was turned on and the gel was transferred for 30 min at 15V. Once finished, the PVDF membrane could either be used immediately for blotting or be fixed in methanol, dried and stored at -20°C until further usage.

#### **3.5.4.2 Blotting of PVDF membrane**

The stored membrane was presoaked in PBS before incubating with 10 ml blocking buffer [5% w/v dried skimmed milk in PBS containing 0.1% (v/v) Tween-20 (PBS-T)] for 1 hr at room temperature with agitation. The membrane was rinsed and washed twice in PBS-T for 5 min. Incubation with primary antibody at appropriate dilutions, as shown in Table 3.15 was performed for 1 hr at room temperature or overnight at 4°C with agitation. The membrane was then washed with PBS-T three times for 5 min before incubation with secondary HRP conjugated rabbit anti-mouse IgG antibody (Calbiochem Inc, San Diego, CA) at appropriate dilution of 1:10,000 for 1 hr at room temperature with agitation. The membrane was then rinsed and washed as before in PBS-T, 10 min for three times to remove any unbound conjugate. There was a final 5 min wash in PBS before bound peroxidase conjugates were detected using Pierce<sup>®</sup> enhanced chemiluminescence (ECL) system (Thermo

Scientific, Waltham, MA) and visualised using FluorChem FC2 imager (Alpha Innotech Corp, San Leandro, CA).

**Table 3.15: Details of primary antibodies for Western blotting.**

Primary antibody	Source	Supplier	Dilution	Incubation condition
Anti- $\alpha$ -Syn, clone 7B12.2	mouse	Chemicon, Temecula, CA	1:1000 in PBS-T containing 2% BSA	Overnight at 4°C with gentle agitation
Anti-actin, clone C4	mouse	Millipore, Billerica, MA	1:5000 in PBS-T containing 2% BSA	1 hr at room temperature with gentle agitation

#### 3.5.4.3 Stripping and reprobing

The blot was placed in 10 ml of high-stringency stripping buffer for 10 min at room temperature to remove the bound primary and secondary antibodies. The membrane was washed with PBS-T twice for 10 min before reprobing using anti-actin antibody was performed to demonstrate equal loading amounts of total cell lysates.

#### 3.5.4.4 Amido Black staining of PVDF membrane

Optionally, after ECL, PVDF membrane was stained with Amido Black dye for 5 min before washing with distilled water and dried in air to check equal protein loading.

#### 3.5.5 Immunofluorescence microscopy

Cells were seeded onto coverslips and grown to 50% confluency for a period of 48-72 hr. Cells were fixed in 4% (w/v) paraformaldehyde (Sigma Aldrich, St.

Louis, MO) in PBS for 15 min at room temperature and permeabilised with 0.5% Triton X-100 (Fisher Scientific Ltd, Leicestershire, UK) in PBS for 5 min. Cells were then blocked with 2% goat serum (Sigma Aldrich, St. Louis, MO) in PBS for 1 hr at room temperature with agitation and incubated with primary antibody, anti- $\alpha$ -Syn clone 7B12.2 at dilution of 1:200 overnight at 4°C. The coverslips were then washed with PBS for 3 times and incubated with secondary antibody, goat anti-mouse IgG Dylight 488 conjugated (Thermo Scientific, Waltham, MA) at dilution of 1:100 for 1 hr away from light. After extensive washing with PBS, coverslips were then mounted on slides using buffered glycerol (90% glycerol in PBS). Individual cells were visualised using inverted-type fluorescence microscope (Nikon Eclipse TS100, Melville, NY).

### **3.6 Staurosporine treatment**

#### **3.6.1 MTT (3-(4, 5-Dimethylthiazol-2-yl)-2, 5-diphenyltetrazolium bromide) assay**

Staurosporine (Millipore, Billerica, MA) of 10mM master stock was prepared in DMSO. Untransfected and stably transfected SK-MEL28 and SH-SY5Y cells were plated on 96-well plates (BD Falcon, Franklin Lakes, NJ) at densities of  $1 \times 10^4$  and  $3 \times 10^4$  cells per well, respectively. After overnight incubation at 37°C in a humidified 5% CO<sub>2</sub> atmosphere, SK-MEL28 and SH-SY5Y cells were treated with staurosporine at different concentrations of 0.00  $\mu$ M, 0.50  $\mu$ M and 1.00  $\mu$ M and 0.00  $\mu$ M, 0.25  $\mu$ M and 0.50  $\mu$ M, respectively for 24 hr prior to an MTT assay. Untreated untransfected cells were used as control samples. Cell morphology was examined under the inverted microscope. Following 24 hr incubation, 20  $\mu$ l of aqueous MTT

solution (5 mg/ml) (Biobasic Inc, Ontario, Canada) was added into each well and was mixed by tapping gently on the side of the plate. The plate was then incubated at 37°C for 4 hr. The MTT solution was carefully decanted off and 100 µl DMSO was added into each well to solubilise the purple formazan crystals. The plate was kept in the dark and gently shaken for 15 min. The plate was then transferred to a microplate plate reader (Bio-Rad, Model 680 with Microplate Manager Software) and the absorbance was measured at wavelength of 550 nm. The intensity of colour produced is directly proportional to the number of viable cells.

### **3.6.2 Determination of median lethal dose (LD<sub>50</sub>)**

Percentage cell viability could be calculated from the absorbance values (Appendix B). Graph of percentage cell viability against the corresponding concentrations of drug was plotted. LD<sub>50</sub>, the concentration of a drug substance required to kill half the members of a tested population after a specified test duration was determined directly from the graph.

### **3.6.3 Detection of apoptotic markers level by Western blot analysis**

Untransfected and stably transfected SK-MEL28 and SH-SY5Y cells were seeded into 6-well plates at densities of  $2 \times 10^5$  and  $6 \times 10^5$  cells per well respectively. After overnight incubation, cells were treated with staurosporine at concentration of LD<sub>50</sub> for 24 hr. Untransfected cells served as control. Cell lysates were prepared, resolved on 15% SDS-PAGE gel and transferred to PVDF membranes for subsequent immunoblotting using the primary antibodies

and secondary antibody, as stated in Table 3.16. AlphaView 3.0 software (Alpha Innotech Corp, San Leandro, CA) was used for densitometry analysis.

**Table 3.16: Details of primary and secondary antibodies for detection of apoptotic markers following staurosporine treatment.**

Antibody	Source	Supplier	Dilution	Incubation condition
Primary antibodies against Bax, Bcl-2, Bcl-xL and cleaved caspase 9 (Asp 315)	Rabbit	Cell Signaling Technology, Inc, Beverly, MA	1:1000 in 5% w/v BSA, 1× TBS, 0.1% Tween-20	Overnight at 4°C with gentle shaking
Secondary antibody: Anti-Rabbit IgG (H+L) HRP Conjugate	Goat	Nacalai Tesque, Inc, Kyoto, Japan	1:10,000 in PBS-T in 2% w/v BSA	1 hr at room temperature with gentle shaking

#### 3.6.4 Staining DNA with Propidium Iodide for Flow Cytometric Analysis

SK-MEL28 and SH-SY5Y cells were seeded into 6-well plate with optimal seeding densities of  $2 \times 10^5$  cells/well and  $6 \times 10^5$  cells/well, respectively. After overnight incubation, cells were treated with staurosporine at the concentration of  $LC_{50}$  for 24 hr. Untransfected cells served as control. The cells were then harvested, washed once with 1 ml of PBS and centrifuged at 1000 rpm for 5 min. The cell pellet was then resuspended with 300  $\mu$ l of PBS and fixed with 700  $\mu$ l of ice-cold ethanol for at least 2 hr at 4°C. Ethanol was added dropwise while vortexing the cells to ensure fixation of cells and to minimise clumping. Fixed cells were pelleted by centrifugation at 2000 rpm for 5 min and washed once with PBS. The cells were then stained with 1 ml of PBS containing 10  $\mu$ g/ml of propidium iodide (Sigma Aldrich, St. Louis, MO) and 100  $\mu$ g/ml of RNase A (Fermentas Inc, Burlington, Canada) and were incubated for 30 min at 37°C. Samples were transferred to 5 ml polystyrene round-bottom tubes

(BD Falcon, Franklin Lakes, NJ) and stored in dark at 4°C until flow cytometric analysis within 24 hr. A laser-based flow cytometer (FACSCalibur, Becton Dickinson, Franklin Lakes, NJ) was used for this cellular DNA content analysis. Propidium iodide fluorescence could be detected in the FL2 channel. For each acquisition of flow cytometric analysis, 10,000 of cells were collected and the flow rate was kept under 400 events/sec. Results were displayed as dot plot and histograms. Percentages of cells in the sub G<sub>0</sub>, G<sub>0</sub>/G<sub>1</sub>, S, G<sub>2</sub>/M phases of the cycle were calculated using the Scripps Research Institute's WINMDI™ software.

### **3.7 *In vitro* model of Parkinson's disease**

#### **3.7.1 Environmental toxins treatment paradigm**

*In vitro* Parkinsonian models were generated by treating untransfected and stably transfected human neuroblastoma, SH-SY5Y cells with rotenone and maneb (Sigma Aldrich, St. Louis, MO). For acute treatment, untransfected and stably transfected SH-SY5Y cells were plated on 96-well plates at a density of  $3 \times 10^4$  cells per well, with 5% CO<sub>2</sub> in a humidified atmosphere overnight at 37°C. Cells were then incubated with varying serial concentration of rotenone (0.0 μM, 0.5 μM, 1.0 μM and 2.0 μM) or maneb (0 μM, 15 μM, 30 μM and 60 μM) for 48 hr prior to an MTT assay. While for chronic treatment, cultures were grown, fed twice per week with control medium or medium supplemented with 5 nM rotenone (Sherer et al., 2002) or 150 nM maneb and passaged approximately once a week on reaching confluence for up to 2 weeks before further assaying. Cells that had undergone chronic rotenone and maneb treatment were plated overnight and additionally subjected to an acute

oxidative insult through addition of H<sub>2</sub>O<sub>2</sub> (15 μM and 30 μM) (SYSTEM, Selangor, Malaysia) for 6 hr before MTT assay was carried out. Untreated untransfected cells served as control. LD<sub>50</sub>, the half-maximal (50%) lethal concentration was determined from the graph of cell viability against corresponding concentrations plotted.

### **3.7.2 Flow cytometric detection of reactive oxygen species level**

To evaluate intracellular H<sub>2</sub>O<sub>2</sub> level, untransfected and stably transfected SH-SY5Y cells were first seeded into 6-well plates at densities of  $4 \times 10^5$  cells per well respectively. After exposure in drug-free medium or medium containing rotenone or maneb at concentration of LD<sub>50</sub> for 48 hr, the treated cells were incubated with 5 μM DCFH-DA (Sigma Aldrich, St. Louis, MO) for 30 min at 37°C. After staining with DCFH-DA, the cells were trypsinised and washed twice with cold PBS. Then the cells were resuspended in PBS and kept on ice for immediate detection with a flow cytometer (FACSCalibur, Becton Dickinson, Franklin Lakes, NJ). The data were recorded using FL1 photomultiplier. The level of ROS generation was expressed as fluorescence intensity of DCF and 10,000 cells per sample were acquired for each flow cytometric analysis. The mean fluorescence intensity was determined using the data analysis program, Scripps Research Institute's WINMDI™ software. Dead cells and debris were excluded from the analysis by electronic gating of forward and side scatter measurements. Cells that had undergone chronic rotenone and maneb treatment were also plated overnight and additionally treated with 15 μM H<sub>2</sub>O<sub>2</sub> for 6 hr prior to DCFH-DA staining and flow cytometric detection.

### **3.7.3 Measurement of mitochondrial membrane potential**

In order to evaluate the mitochondrial respiratory function, the mitochondrial membrane potential was assessed by DiOC6(3) (Sigma Aldrich, St. Louis, MO) staining. Untransfected and stably transfected SH-SY5Y cells were seeded into 6-well plates at density of  $4 \times 10^5$  cells per well respectively. After incubation in drug-free medium or medium containing drugs ( $LD_{50}$ ) for 48 hr, the cells were treated with 40 nM DiOC6(3) for 15 min at 37°C away from light. Then the cells were harvested by trypsin and washed twice with cold PBS. After resuspended in cold PBS, the cells were analysed with flow cytometry using FL1 channel at an excitation wavelength of 488 nm and an emission wavelength of 525 nm. Acquisition was set for 10,000 events per sample. Percentages of cells with disrupted and normal mitochondrial membrane potential were calculated using the Scripps Research Institute's WINMDI™ software. Cells that had undergone chronic rotenone and maneb treatment were also plated overnight and additionally treated with 15  $\mu$ M  $H_2O_2$  for 6 hr prior to DiOC6(3) staining and flow cytometric detection.

### **3.8 Statistical analysis**

Quantitative data are expressed as arithmetic mean  $\pm$  standard error of mean (S.E.M) based on at least two separate experiments performed in triplicate (Appendix B). All results were subjected to statistical analysis with one-way-ANOVA followed by LSD's *post hoc* comparison test using Statistical Package for the Social Sciences (SPSS) software version 15.0 (SPSS Inc., Chicago, IL), in order to evaluate the significance of the differences. A p value  $< 0.05$  was considered as statistically significant.

## CHAPTER 4

### RESULTS

#### 4.1 Down-regulation of $\alpha$ -Syn expression in SK-MEL28 by RNAi

##### 4.1.1 Molecular cloning of shRNA sequences into pLKO.1-TRC cloning vector

The pLKO.1-TRC cloning vector first contained a 1.9 kb stuffer and it was released upon digestion with *EcoRI* and *AgeI* [Figure 4.1(a)]. The oligonucleotides designed contain the shRNA sequence flanked by sequences that were compatible with the sticky ends of *EcoRI* and *AgeI*. Forward and reverse oligonucleotides were annealed and then ligated into the pLKO.1 vector, producing a final plasmid that expresses the shRNA of interest [Figure 4.1(b)]. Plasmids that were successfully ligated were screened by restriction enzyme digestion involving *EcoRI* and *NcoI* [Figure 4.1(c)]. Two fragments, a 2 kb fragment and a 5 kb fragment could be seen. After identifying the positive clones, the presence and orientation of the inserts were verified by sending the isolated plasmids to an outsourced sequencing service provided by First BASE Laboratories, Selangor, Malaysia. The sequencing alignments for successful molecular cloning of shRNAs into pLKO.1-TRC cloning vector are shown in Figure 4.2.

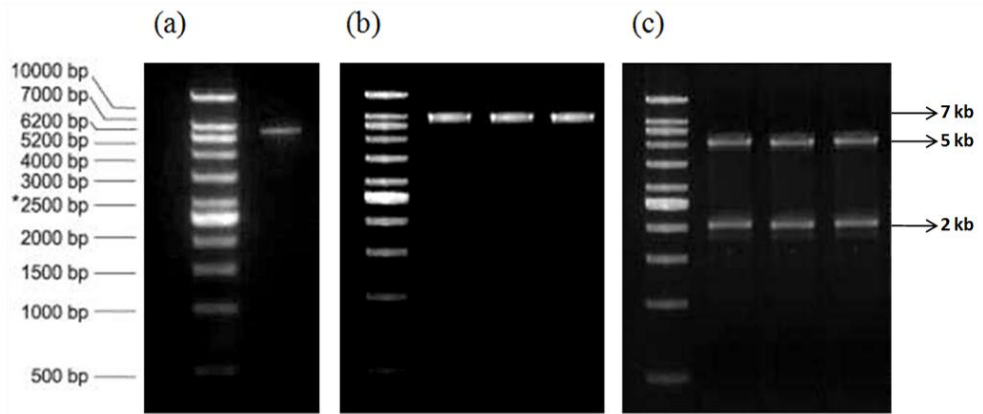


**Figure 4.1: Agarose electrophoresis gel pictures for shRNA molecular cloning.** (a) 7 kb band extracted by gel extraction after digestion of pLKO.1-TRC cloning vector with *AgeI* and *EcoRI*. (b) Linearised pLKO.1-TRC cloning vector with inserts. (c) Screening for inserts by conducting a restriction digest with *EcoRI* and *NcoI*. Two fragments, a 2 kb fragment and a 5 kb fragment were seen.

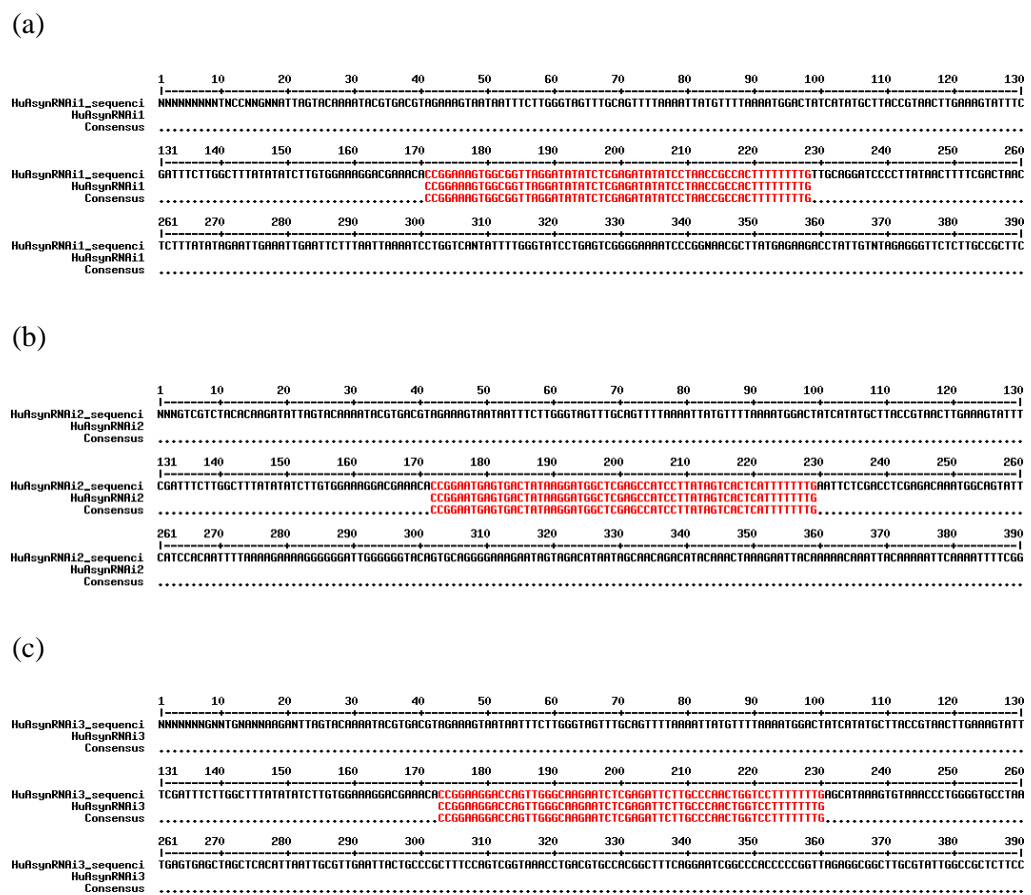


**Figure 4.2: Sequencing alignments produced by Multalin.** The presence and orientation of the inserts ligated into the pLKO.1 vector were verified by an outsourced sequencing service. (a) pLKO.1-HuAsynRNAi1 (b) pLKO.1-HuAsynRNAi2 (c) pLKO.1-HuAsynRNAi3.

#### **4.1.2 $\alpha$ -Syn-shRNA down-regulates $\alpha$ -Syn expression**

To get long-term suppression of gene expression, three shRNA sequences targeting human  $\alpha$ -Syn mRNA were cloned in the expression vector, pLKO.1, and were transfected into SK-MEL28 cells by electroporation, with pLKO.1-TRC control and pLKO.1-scramble shRNA as negative controls. Stably transfected cells were established by selection with puromycin and the expression of  $\alpha$ -Syn protein was then confirmed by Western blotting. Western blot revealed a single band of 19 kDa that is consistent with the monomeric  $\alpha$ -Syn for untransfected SK-MEL28 cells, which has been demonstrated by Matsuo and Kamitani (2010) to be highly expressing  $\alpha$ -Syn [Figure 4.3 (a)]. Compared with untransfected control,  $\alpha$ -Syn-shRNAs HuAsynRNAi1 and HuAsynRNAi2 were found to inhibit  $\alpha$ -Syn protein expression by 12.0% and 2.50% only, respectively, while  $\alpha$ -Syn-shRNA HuAsynRNAi3 inhibited  $\alpha$ -Syn protein expression significantly with approximately 49% reduction. pLKO.1-TRC control and pLKO.1-scramble shRNA had no effect on  $\alpha$ -Syn protein level [Figure 4.3(b)]. These result demonstrated that  $\alpha$ -Syn-shRNA transfection is an effective and long-term suppression method of endogenous  $\alpha$ -Syn. Human U6 promoter could effectively drive shRNA transcription in SK-MEL28 cells and shRNA HuAsynRNAi3 could successfully bring about knockdown of *SNCA* mRNA expression.

Immunofluorescence microscopy further confirmed expression of human  $\alpha$ -Syn in SK-MEL28 cells. As shown in Figure 4.4, untransfected SK-MEL28, pLKO.1-TRC control-transfected SK-MEL28 and pLKO.1-scramble shRNA-transfected SK-MEL28 exhibited a strong homogenous expression of  $\alpha$ -Syn,

whereas pLKO.1-HuAsynRNAi1-transfected SK-MEL28, pLKO.1-HuAsynRNAi2-transfected SK-MEL28 and pLKO.1-HuAsynRNAi3-transfected SK-MEL28 cells showed lower fluorescence intensity, indicative of lower  $\alpha$ -Syn immunoreactivity. The greatest reduction in fluorescence intensity was observed in pLKO.1-HuAsynRNAi3-transfected SK-MEL28. pLKO.1-HuAsynRNAi3-transfected SK-MEL28 with significant down-regulation of  $\alpha$ -Syn was then chosen to be used in subsequent experiments.

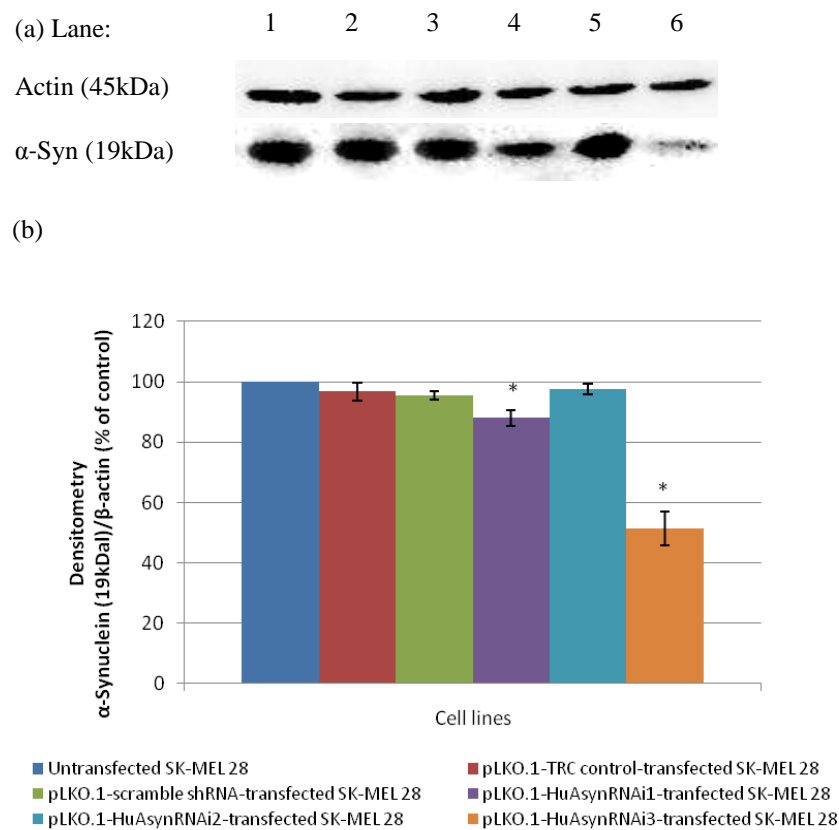


**Figure 4.3: Expression of  $\alpha$ -Syn in SK-MEL28 cells by (a) Western blot analysis and (b) the relative densitometry.** Lane 1: Untransfected SK-MEL28; Lane 2: pLKO.1-TRC control-transfected SK-MEL28; Lane 3: pLKO.1-scramble shRNA-transfected SK-MEL28; Lane 4: pLKO.1-HuAsynRNAi1-transfected SK-MEL28; Lane 5: pLKO.1-HuAsynRNAi2-transfected SK-MEL28; Lane 6: pLKO.1-HuAsynRNAi3-transfected SK-MEL28. Each bar represents mean  $\pm$  S.E.M of two different experiments. \* means  $p < 0.05$  compared with untransfected SK-MEL28 by one-way-ANOVA.

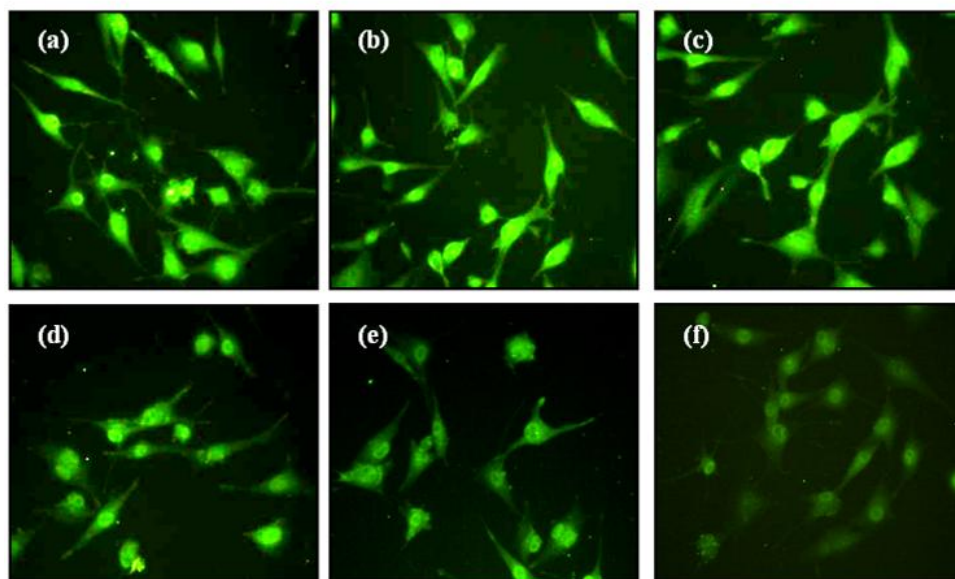


**Figure 4.4: Immunofluorescence microscopy depicting expression of human  $\alpha$ -Syn protein in SK-MEL28 cell lines.** (Magnification power = 100 $\times$ ). (a) Untransfected SK-MEL28 (b) pLKO.1-TRC control-transfected SK-MEL28 (c) pLKO.1-scramble shRNA-transfected SK-MEL28 (d) pLKO.1-HuAsynRNAi1-transfected SK-MEL28 (e) pLKO.1-HuAsynRNAi2-transfected SK-MEL28 (f) pLKO.1-HuAsynRNAi3-transfected SK-MEL28.

## 4.2 Effect of $\alpha$ -Syn knockdown against staurosporine insult

### 4.2.1 $\alpha$ -Syn knockdown enhances staurosporine-induced cyto-toxicity

To determine the effect of  $\alpha$ -Syn expression against staurosporine-induced cell death, the relative cyto-toxic response to staurosporine treatment in untransfected SK-MEL28, which served as control, pLKO.1-TRC control-transfected SK-MEL28, pLKO.1-scramble shRNA-transfected SK-MEL28 and pLKO.1-HuAsynRNAi 3-transfected SK-MEL28 were analysed. All four cell lines were exposed to 0.50  $\mu$ M and 1.00  $\mu$ M staurosporine for 24 hr before MTT assay was conducted. Based on MTT assay, a concentration-dependent decrease in cell viability was observed (Figure 4.5). Following exposure to 0.50  $\mu$ M and 1.00  $\mu$ M staurosporine, pLKO.1-HuAsynRNAi 3-transfected SK-MEL28 with  $\alpha$ -Syn expression being down-regulated significantly exhibited a

maximal decrease in cell viability ( $p < 0.05$ ) compared to untransfected control. LD<sub>50</sub> of staurosporine for untransfected SK-MEL28 cells was determined to be 0.50  $\mu\text{M}$  and this concentration was used for subsequent experiments. The result demonstrates that endogenously high  $\alpha\text{-Syn}$  expression can protect SK-MEL28 cells from staurosporine-induced cell death.

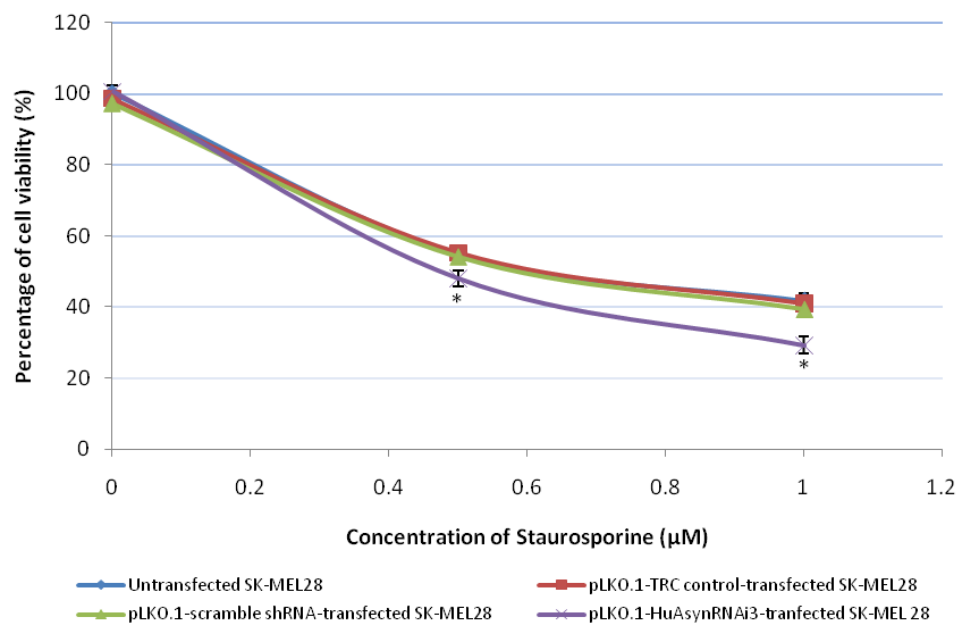
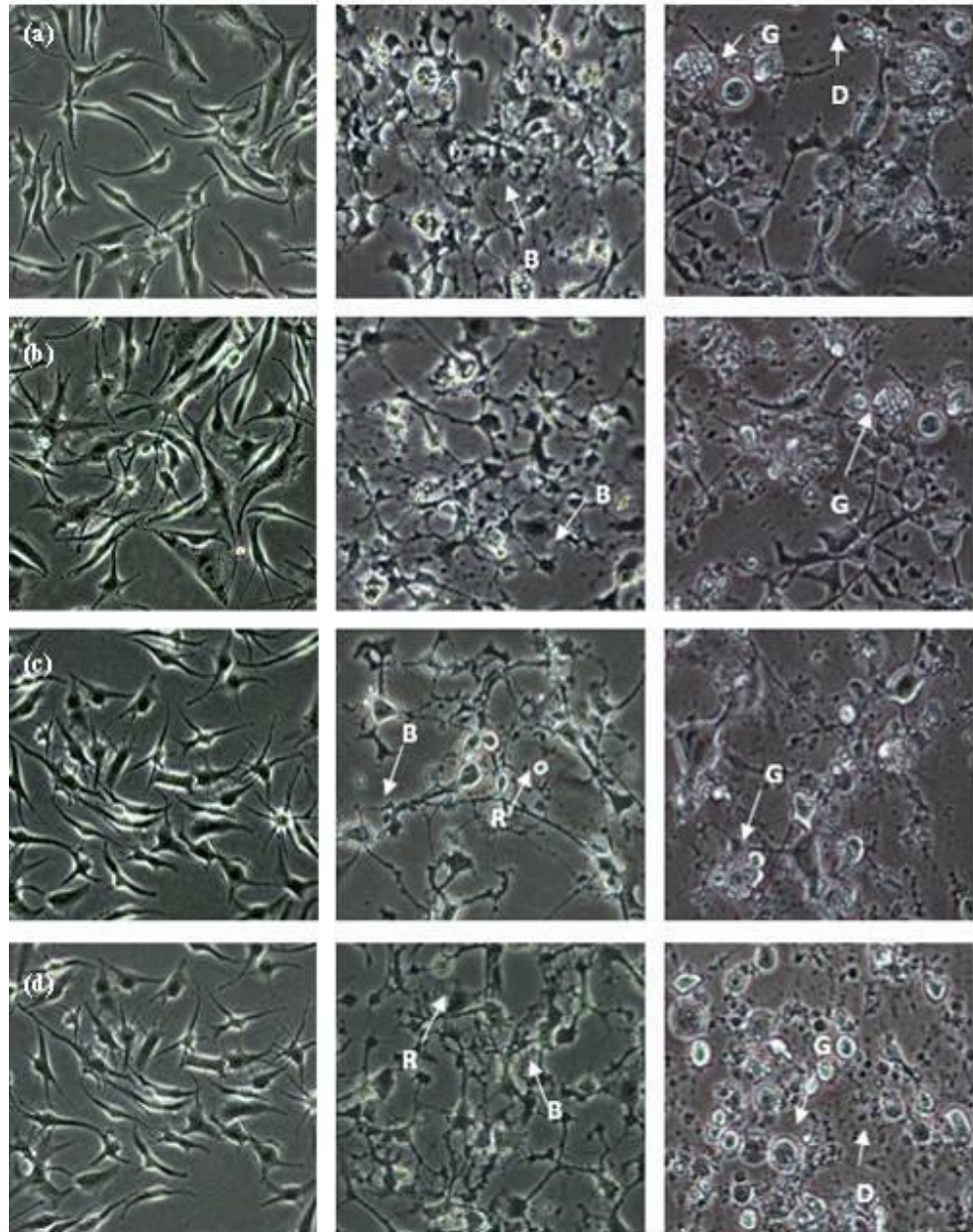


**Figure 4.5: Effect of staurosporine on percentage of cell viability of untransfected and stably transfected SK-MEL28.** Cells were exposed to staurosporine at two serial diluted concentrations (0.50 and 1.00  $\mu\text{M}$ ) for 24 hr before MTT assay was performed and absorbance was read at 550 nm. These results represent mean  $\pm$  S.E.M of three separate experiments. \* means  $p < 0.05$  compared to untransfected cells under each corresponding treatment by one-way-ANOVA.

#### **4.2.2 Observation of morphological changes in SK-MEL28 following staurosporine treatment**

Cyto-toxic effect of staurosporine administered elicited extensive morphological changes on SK-MEL28 cells and these could be easily discerned by observation under an inverted microscope. Generally, the morphological changes of the cells correlated to the quantitative results observed in cell viability studies. As shown in Figure 4.6, under normal condition, majority of the cells displayed standard morphology with well-defined membrane and exhibited usual anchorage properties. Upon treatment with 0.50  $\mu\text{M}$  staurosporine, vacuolation could be observed particularly around the nucleus and cells started to retract from surface of the flask. Membrane blebbing was also one of the characteristic remarks. Dead cells became shrunken, rounded up and edgy along with detachment from the surface. On the whole, as the concentration of staurosporine increased, the degree of confluence and number of attached, healthy cells gradually decreased. Following 1.00  $\mu\text{M}$  staurosporine treatment, heavily granulated cells could be largely observed as granulation may have been due to breaking down of cell organelles or nucleic material.



(i) 0.00  $\mu\text{M}$

(ii) 0.50  $\mu\text{M}$

(iii) 1.00  $\mu\text{M}$

**Figure 4.6: Morphological changes of SK-MEL28 cells after treatment with varying concentrations of staurosporine for 24 hr.** (Magnification power = 100 $\times$ ). R = rounded and shrunken cells, D = cell debris, G = granulated cells, B = membrane blebbing. (a) Untransfected SK-MEL28 (b) pLKO.1-TRC control-transfected SK-MEL28 (c) pLKO.1-scramble shRNA-transfected SK-MEL28 (d) pLKO.1-HuAsynRNAi3-transfected SK-MEL28.

### **4.2.3 Expression of apoptotic markers in SK-MEL28**

#### **4.2.3.1 $\alpha$ -Syn knockdown up-regulates Bax expression level in SK-MEL28**

To determine whether the knockdown of  $\alpha$ -Syn expression in SK-MEL28 could further elicit apoptotic stress induced by staurosporine, the expression of downstream pro- and anti-apoptotic molecules of the intrinsic (mitochondrial) apoptotic pathway, including Bax, Bcl-2, Bcl-xL and cleaved caspase 9 were investigated. SK-MEL28 cells were incubated in the absence or presence of 0.50  $\mu$ M staurosporine (LD<sub>50</sub>) for 24 hr before preparation of cell lysates and detection of apoptotic markers expression by Western blot analysis were carried out. Elevated protein level of Bax has been shown to promote apoptosis in response to numerous cell death-inducing stimuli (Oltvai & Korsmeyer, 1994). pLKO.1-HuAsynRNAi3-transfected SK-MEL28 had significantly greater endogenous Bax protein expression, as compared to untransfected SK-MEL28 (control), pLKO.1-TRC control-transfected SK-MEL28 and pLKO.1-scramble shRNA-transfected SK-MEL28 (Figure 4.7). After treatment with 0.50  $\mu$ M staurosporine, Bax protein expression was markedly increased. Higher Bax level could be observed in pLKO.1-HuAsynRNAi3-transfected SK-MEL28, as compared to that of untransfected SK-MEL28 (control), pLKO.1-TRC control-transfected SK-MEL28 and pLKO.1-scramble shRNA-transfected SK-MEL28. These results suggest that the endogenously high  $\alpha$ -Syn expression in SK-MEL28 can attenuate the up-regulation of Bax after being subjected to staurosporine treatment and thereby protects the cells from apoptotic cell death.

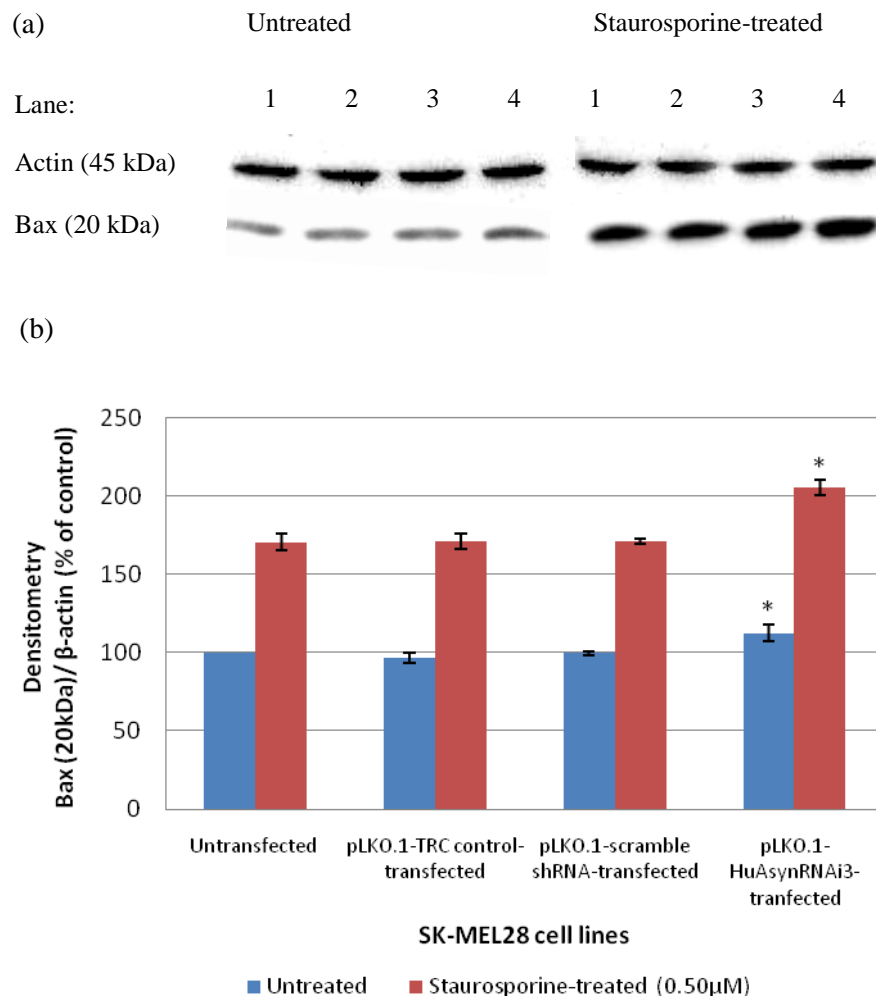


**Figure 4.7: Expression of Bax in SK-MEL28 cell lines by (a) Western blot analysis and (b) its relative densitometry.** Lane 1: Untransfected SK-MEL28; Lane 2: pLKO.1-TRC control-transfected SK-MEL28; Lane 3: pLKO.1-scramble shRNA-transfected SK-MEL28; Lane 4: pLKO.1-HuAsynRNAi3-transfected SK-MEL28. Cells were incubated in the absence or presence of 0.50 μM staurosporine for 24 hr and cell lysates were prepared and subjected to Western blot analysis. Error bars represent S.E.M from two independent experiments. \* means  $p < 0.05$  compared with untransfected cells under the same treatment by one-way-ANOVA.

#### **4.2.3.2 $\alpha$ -Syn knockdown down-regulates Bcl-2 expression level in SK-MEL28**

Bcl-2 has been shown to prevent both apoptotic and necrotic cell death induced by a variety of stimuli in several different systems (Zhang, Peng, Zhang, & Wu, 2003). As shown in Figure 4.8, pLKO.1-HuAsynRNAi3-transfected SK-MEL28 had significantly lower endogenous level of Bcl-2, as compared to untransfected SK-MEL28 (control), pLKO.1-TRC control-transfected SK-MEL28 and pLKO.1-scramble shRNA-transfected SK-MEL28. Bcl-2 protein expression in all four cell types was markedly increased after exposure to 0.50  $\mu$ M staurosporine for 24 hr. This increased expression of Bcl-2 should be a compensatory response of the cells against the staurosporine insult. However, following staurosporine treatment, pLKO.1-HuAsynRNAi3-transfected SK-MEL28 was shown to have significantly lower Bcl-2 expression, compared with untransfected SK-MEL28 (control), pLKO.1-TRC control-transfected SK-MEL28 and pLKO.1-scramble shRNA-transfected SK-MEL28. These results suggest that endogenously high  $\alpha$ -Syn expression in SK-MEL28 can lead to an increase of Bcl-2 expression and thereby protect the cells from staurosporine-induced cell death.

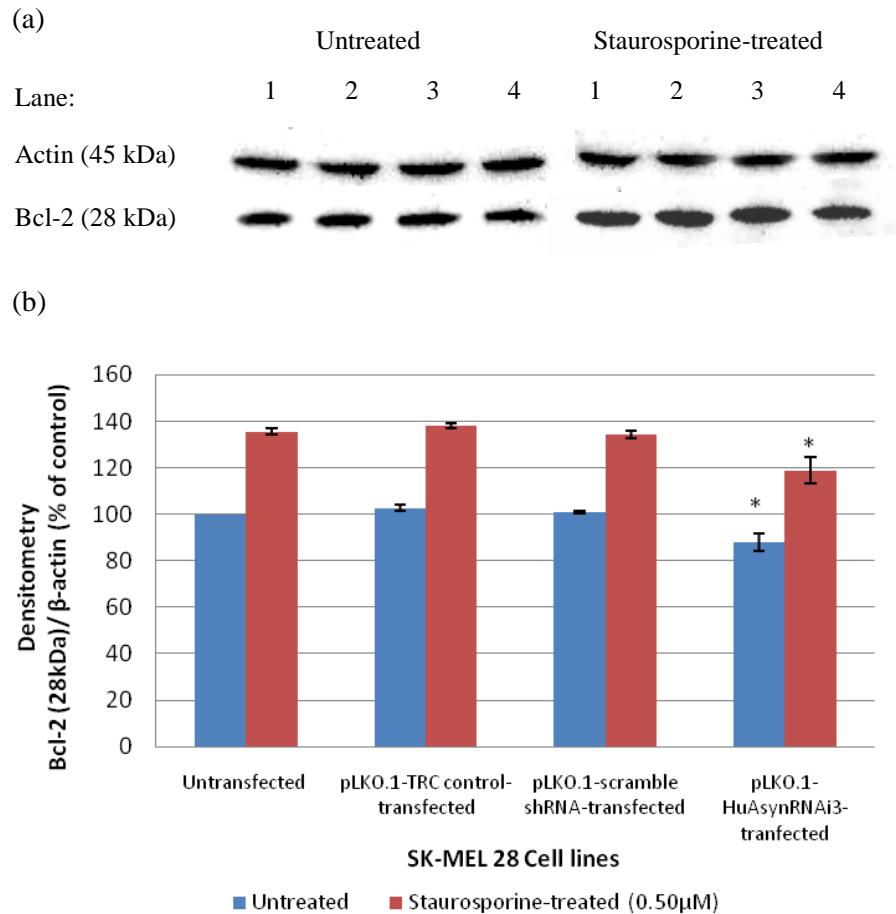


**Figure 4.8: Expression of Bcl-2 in SK-MEL28 cell lines by (a) Western blot analysis and (b) its relative densitometry.** Lane 1: Untransfected SK-MEL28; Lane 2: pLKO.1-TRC control-transfected SK-MEL28; Lane 3: pLKO.1-scramble shRNA-transfected SK-MEL28; Lane 4: pLKO.1-HuAsynRNAi3-transfected SK-MEL28. Cells were incubated in the absence or presence of 0.50  $\mu$ M staurosporine for 24 hr and cell lysates were prepared and subjected to Western blot analysis. Error bars represent S.E.M from two independent experiments. \* means  $p < 0.05$  compared with untransfected cells under the same treatment by one-way-ANOVA.

#### 4.2.3.3 $\alpha$ -Syn knockdown decreases Bcl-xL expression in SK-MEL28

Bcl-xL overexpression is responsible for the resistance of cells to staurosporine-induced apoptosis (Li et al., 2001). Among all four cell types tested, pLKO.1-HuAsynRNAi3-transfected SK-MEL28 had the lowest endogenous Bcl-xL protein expression, as compared to untransfected SK-MEL28 (control), pLKO.1-TRC control-transfected SK-MEL28 and pLKO.1-

scramble shRNA-transfected SK-MEL28 (Figure 4.9). After staurosporine treatment, the Bcl-xL level further decreased in the same trend. These results suggest that the endogenously high  $\alpha$ -Syn expression in SK-MEL28 can lead to greater Bcl-xL expression and thereby provides protective effect against staurosporine-induced cell death.

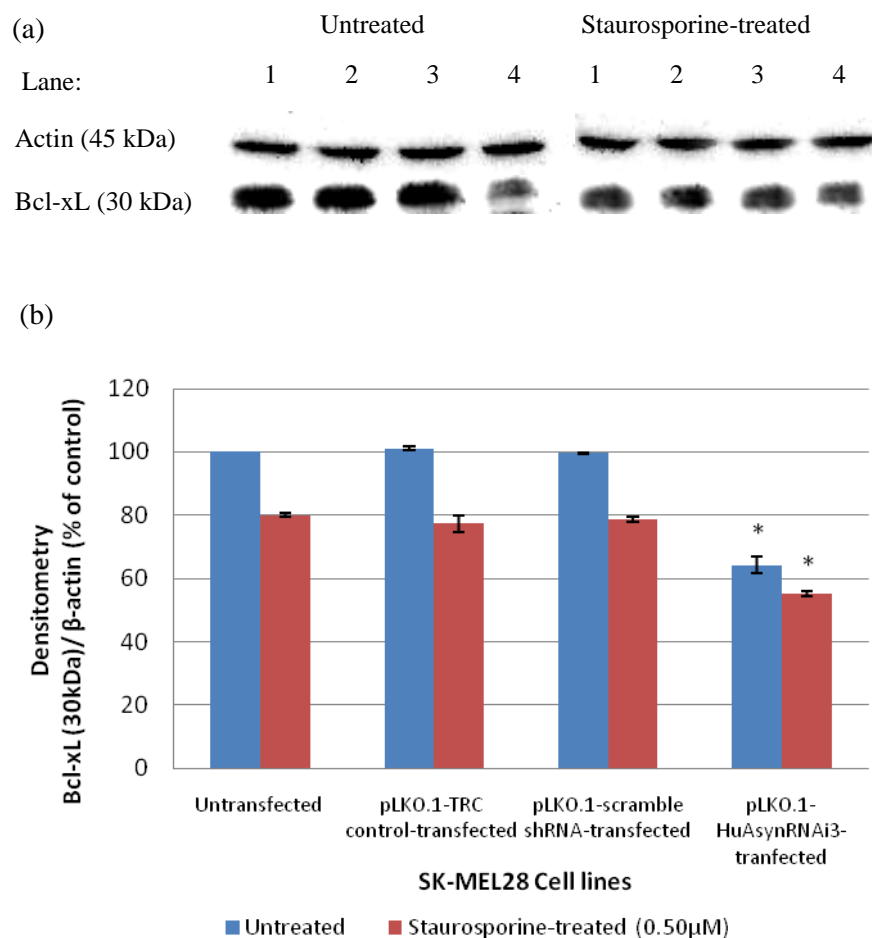


**Figure 4.9: Expression of Bcl-xL in SK-MEL28 cell lines by (a) Western blot analysis and (b) its relative densitometry.** Lane 1: Untransfected SK-MEL28; Lane 2: pLKO.1-TRC control-transfected SK-MEL28; Lane 3: pLKO.1-scramble shRNA-transfected SK-MEL28; Lane 4: pLKO.1-HuAsynRNAi3-transfected SK-MEL28. Cells were incubated in the absence or presence of 0.50  $\mu$ M staurosporine for 24 hr and cell lysates were prepared and subjected to Western blot analysis. Error bars represent S.E.M from two independent experiments. \* means  $p < 0.05$  compared with untransfected cells under the same treatment by one-way-ANOVA.

#### **4.2.3.4 $\alpha$ -Syn knockdown increases staurosporine-induced caspase 9 cleavage and activation in SK-MEL28**

Caspase 9 is an important member of the cysteine aspartic acid protease (caspase) family (Duan et al., 1996). Upon apoptotic stimulation, cytochrome *c* released from mitochondria associates with procaspase 9 (47 kDa)/Apaf-1. This complex processes procaspase 9 into a large active subunit (35 kDa or 17 kDa) and a small subunit (10 kDa) by self cleavage at Asp315 (Li et al., 1997). Cleaved caspase 9 further processes other caspase members, including caspase 3 and caspase 7 to initiate a caspase cascade, leading to programmed cell death (Slee et al., 1999). As shown in Figure 4.10, cleaved caspase 9 could only be detected in staurosporine-treated cells and pLKO.1-HuAsynRNAi3-transfected SK-MEL28 had the greatest cleaved caspase 9 level as compared to untransfected SK-MEL28 (control), pLKO.1-TRC control-transfected SK-MEL28 and pLKO.1-scramble shRNA-transfected SK-MEL28. These results suggest that endogenously high  $\alpha$ -Syn expression in SK-MEL28 can attenuate cleavage and activation of caspase 9 and thereby prevent staurosporine-induced cell death.

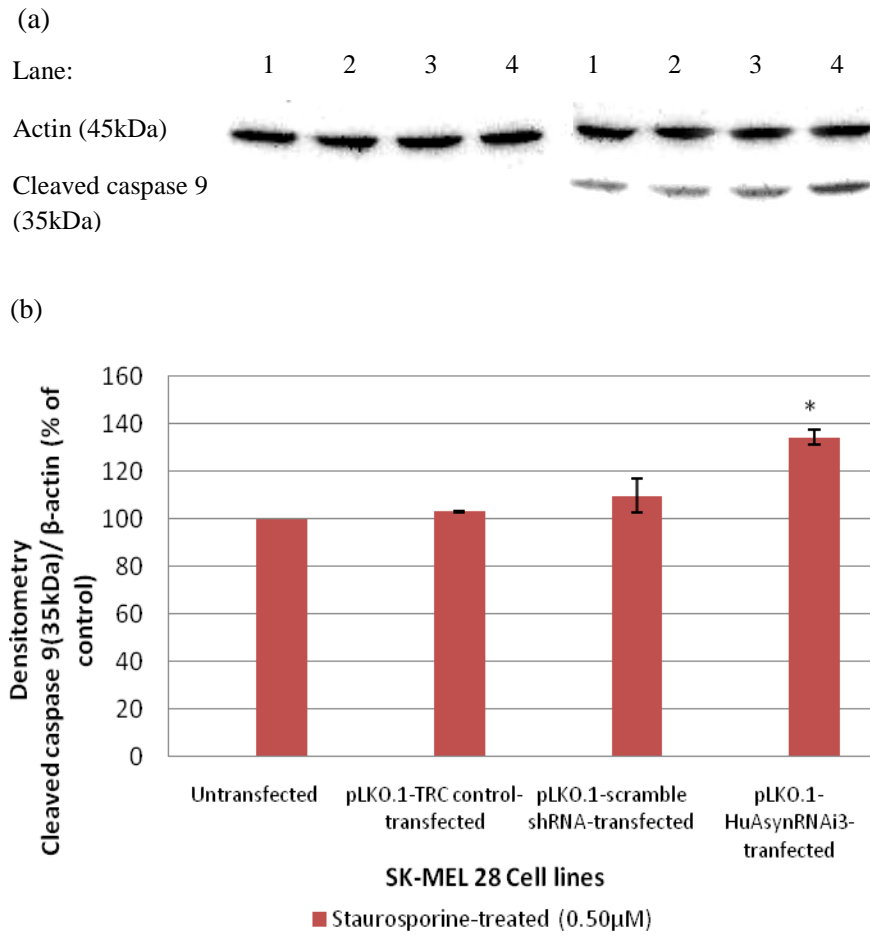


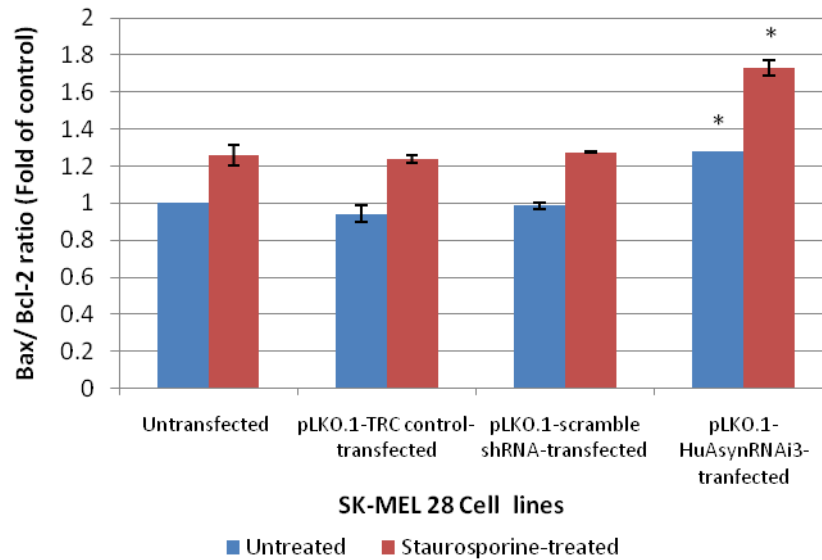
**Figure 4.10: Expression of cleaved caspase 9 in SK-MEL28 cell lines by (a) Western blot analysis and (b) its relative densitometry.** Lane 1: Untransfected SK-MEL28; Lane 2: pLKO.1-TRC control-transfected SK-MEL28; Lane 3: pLKO.1-scramble shRNA-transfected SK-MEL28; Lane 4: pLKO.1-HuAsynRNAi3-transfected SK-MEL28. Cells were incubated in the absence or presence of 0.50 μM staurosporine for 24 hr and cell lysates were prepared and subjected to Western blot analysis. Error bars represent S.E.M from two independent experiments. \* means  $p < 0.05$  compared with untransfected cells under the same treatment by one-way-ANOVA.

#### 4.2.3.5 $\alpha$ -Syn knockdown leads to elevated Bax/Bcl-2 and Bax/Bcl-xL ratios in SK-MEL28

Bax/Bcl-2 and Bax/Bcl-xL ratios determine the apoptotic potential of the cells. Elevated Bax/Bcl-2 and Bax/Bcl-xL ratios correspond with the onset of apoptosis (Chang et al., 2005; Raisova et al., 2001). As shown in Figure 4.11, pLKO.1-HuAsynRNAi3-transfected SK-MEL28 was shown to have

significantly elevated Bax/Bcl-2 and Bax/Bcl-xL ratios as compared to controls, both before and after staurosporine treatment. These results suggest that the endogenously high  $\alpha$ -Syn expression in SK-MEL28 causes the cells to be less prone to apoptotic cell death induced by staurosporine.

(a)



(b)

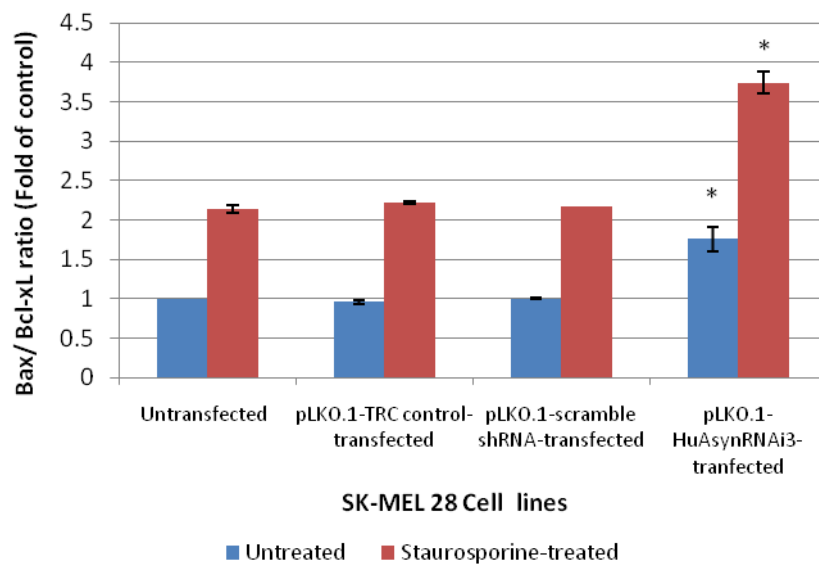


**Figure 4.11: Ratios of (a) Bax/Bcl-2 and (b) Bax/Bcl-xL in SK-MEL28 were quantified and plotted.** The Bcl-2 /Bax and Bcl-xL/Bax ratios in control (untreated and untransfected) cells were set as 1.00. Results represent mean  $\pm$  S.E.M of two independent experiments. \* means  $p < 0.05$  compared to untransfected cells under the same treatment by one-way-ANOVA.

#### 4.2.4 $\alpha$ -Syn knockdown reduces the proliferative index of SK-MEL28

To explore the possible roles of  $\alpha$ -Syn in controlling cell proliferation, the cell cycles of untransfected and stably transfected cells were examined by flow cytometric analysis with propidium iodide staining. The proliferative index (PI) was calculated using the formula:  $PI = (S+G_2)/(G_1+S+G_2)$  (Liang et al., 2007) (Appendix C). The mean proliferative index of pLKO.1-HuAsynRNAi3-transfected SK-MEL28, with  $\alpha$ -Syn expression being down-regulated was significantly lower than those of untransfected SK-MEL28 which serves as control, pLKO.1-TRC control-transfected SK-MEL28 and pLKO.1-scramble shRNA-transfected SK-MEL28 (Figure 4.12). These data suggest that the endogenously high  $\alpha$ -Syn expression could promote  $G_0/G_1$  to S transition and  $G_2/M$  in SK-MEL28, and therefore, might have contributed to the enhanced proliferation rate.

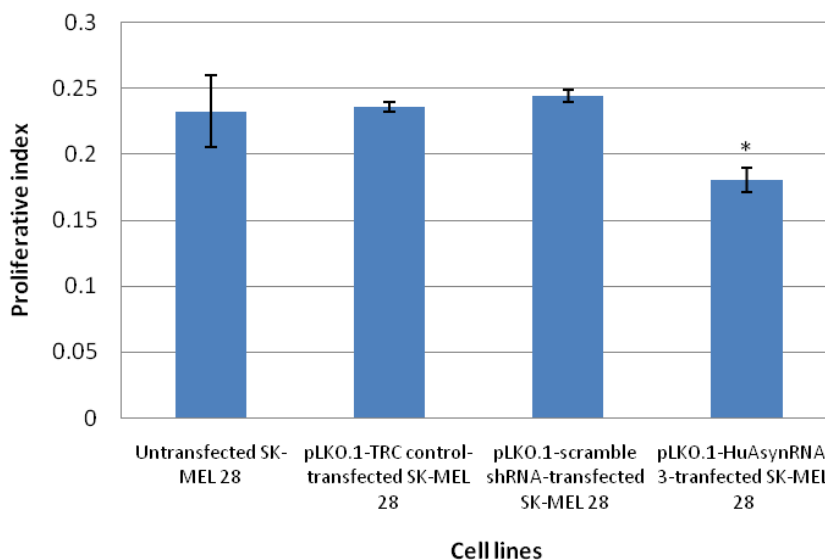


**Figure 4.12: Effect of  $\alpha$ -Syn knockdown on the proliferative index of SK-MEL28.** The cells were harvested, stained with propidium iodide and analysed by flow cytometry. Proliferative index was calculated using the equation  $(S+G_2)/(G_1+S+G_2)$ . These results represent mean  $\pm$  S.E.M of three independent experiments. \* means  $p < 0.05$  compared with untransfected SK-MEL28 by one-way-ANOVA.

As depicted in Figure 4.13, in general, treatment with staurosporine led to an increase of cells in the G<sub>2</sub>/M phase of cell cycle, with a corresponding decrease of cells in the G<sub>1</sub> and S phase of cell cycle when compared to untreated cells. However, no significant difference could be observed between the four cell types.

A sub G<sub>0</sub> hypodiploid peak is produced when low molecular weight DNA is lost after cell membrane permeability increases, resulting in decreased staining of apoptotic cells by DNA-specific fluorochromes, propidium iodide (Nicoletti, Migliorati, Pagliacci, Grignani, & Riccardi, 1991). Cells subjected to 0.50  $\mu$ M staurosporine treatment displayed an increase in the sub G<sub>0</sub> (hypodiploid) portion, as a consequence of partial DNA content loss due to fragmentation. pLKO.1-HuAsynRNAi3-transfected SK-MEL28 was shown to have slightly greater hypodiploid sub G<sub>0</sub> proportion as compared to untransfected SK-MEL28, pLKO.1-TRC control-transfected SK-MEL28 and pLKO.1-scramble shRNA-transfected SK-MEL28. These results suggest that staurosporine induces G<sub>2</sub>/M arrest, resulting in cell death in SK-MEL28.  $\alpha$ -Syn knockdown increases hypodiploid peak, a measure of the extent of DNA fragmentation, and hence of staurosporine-induced cell death.

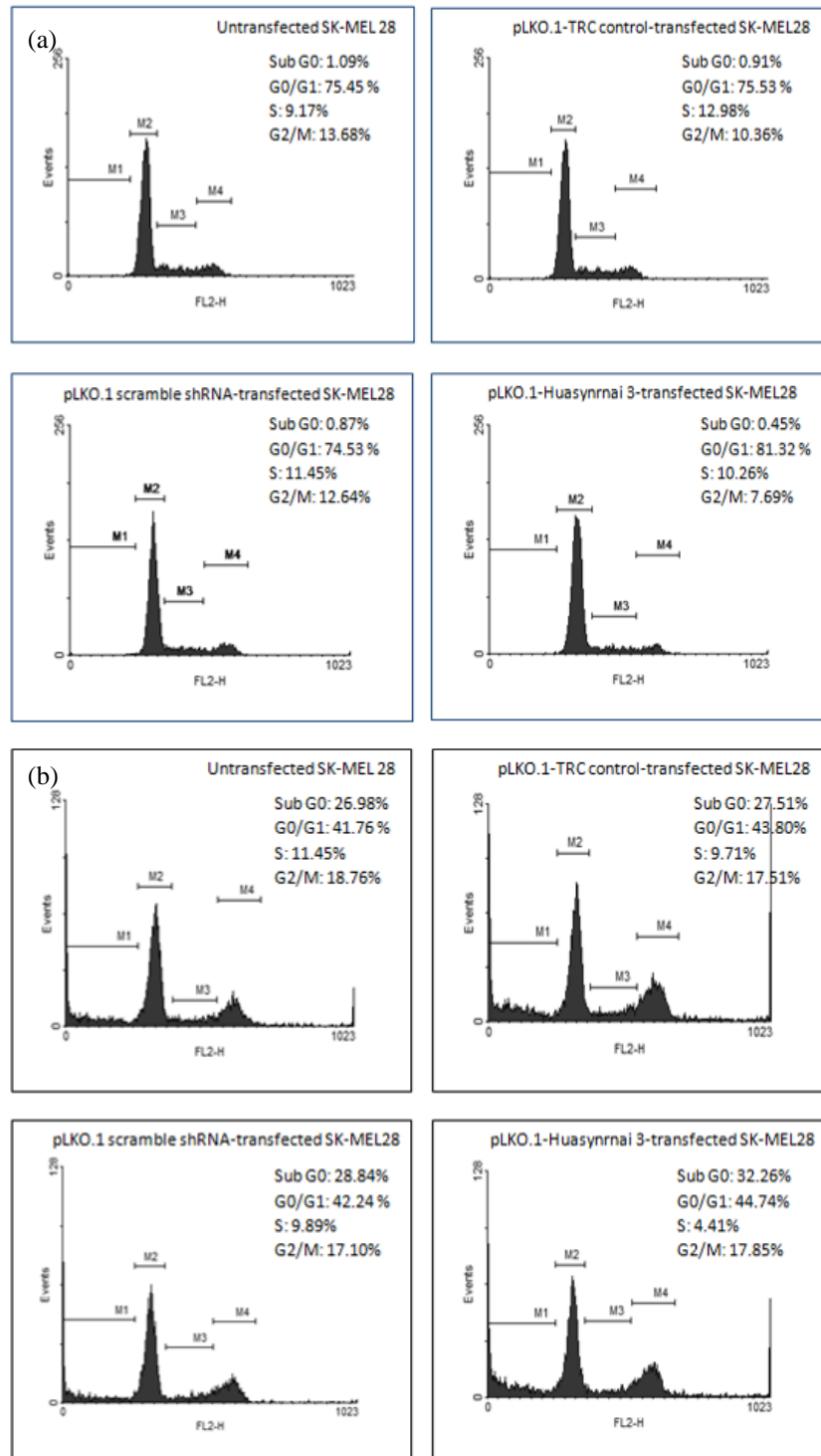


**Figure 4.13: Cell cycle distribution of (a) untreated and (b) staurosporine-treated SK-MEL28 cell lines.** SK-MEL28 cell lines were incubated in the absence or presence of staurosporine for 24 hr before being harvested, fixed with 70% ethanol for up to 2 hr followed by propidium iodide staining and flow cytometric analysis. The percentage of cells in each phase of the cell cycle was evaluated using the WinMDI software. Representative histograms from one experiment are shown. M1 = Sub Go phase, M2 = Go/G<sub>1</sub> phase, M3 = S phase, M4 = G<sub>2</sub>/M phase.

### **4.3 Overexpression of $\alpha$ -Syn in SH-SY5Y**

#### **4.3.1 Generation of mutant $\alpha$ -Syn construct by site-directed mutagenesis**

Using plasmid pCMV-Sport6 with wild type human  $\alpha$ -Syn cDNA construct, the A30P, A53T and E46K mutants were generated by PCR-based site-directed mutagenesis. Figure 4.14 shows the sequencing alignment for the successful generation of plasmid encoding the  $\alpha$ -Syn mutants. For  $\alpha$ -Syn mutant construct A30P, there was Alanine (GCA) to Proline (CCA) substitution at position 30. For  $\alpha$ -Syn mutant construct A53T, there was Alanine (GCA) to Threonine (ACG) mutations at amino acid 53. For  $\alpha$ -Syn mutant construct E46K, there was substitution of Glutamate (GAG) by Lysine (AAG) at position 46. For further confirmation, NCBI Blastx software was used to convert the nucleotide query sequence into protein sequences in all 6 reading frames. The translated protein products were then compared against the NCBI protein databases. As indicated in Figure 4.15, the translated sequences of the mutant  $\alpha$ -Syn constructs, A30P, A53T and E46K were verified as homologous to the human  $\alpha$ -Syn.

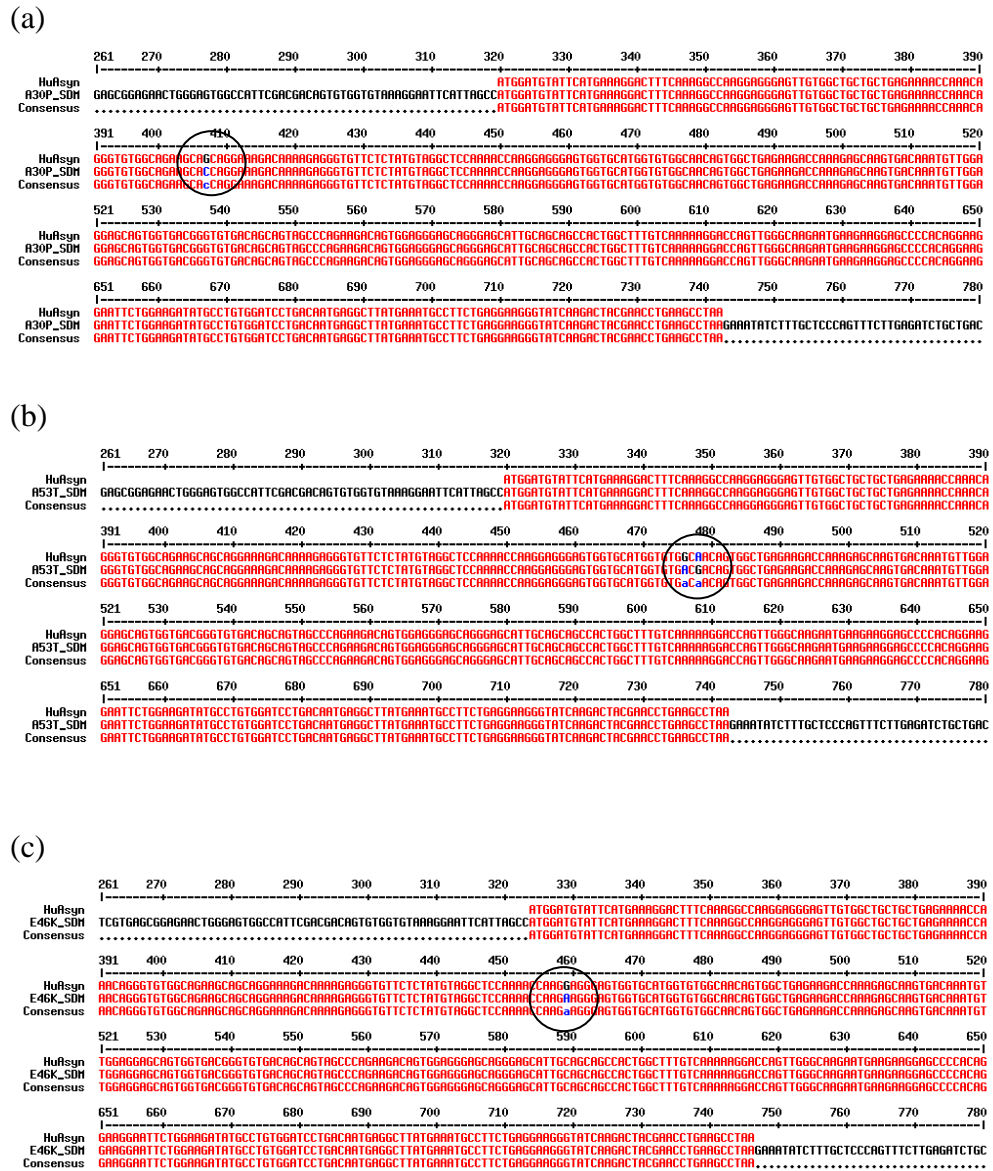


**Figure 4.14: Sequencing alignments produced by Multalin.** The generation of  $\alpha$ -Syn mutant constructs using site-directed mutagenesis were verified by an outsourced sequencing service. (a)  $\alpha$ -Syn mutant construct A30P (b)  $\alpha$ -Syn mutant construct A53T (c)  $\alpha$ -Syn mutant construct E46K.

(a)

```
>| gb|AAP36433.1| Homo sapiens synuclein, alpha (non A4 component of amyloid precursor)
[synthetic construct]
gb|AA29716.1| synuclein alpha [synthetic construct]
gb|AA29717.1| synuclein alpha [synthetic construct]
Length=141

Score = 207 bits (527), Expect = 2e-51
Identities = 139/140 (99%), Positives = 139/140 (99%), Gaps = 0/140 (0%)
Frame = +3

Query 318 MDVFMKGLSkakegfvvaaeektkQGVAAEAGKTKEGVLYVGSKTKEGTVHGVATVAEKTK 497
Sbjct 1 MDVFMKGLSKAKEGVVAAAEEKTKQGVAAEAGKTKEGVLYVGSKTKEGTVHGVATVAEKTK 60

Query 498 EQvtnvvggavvtgvtavaQKTVEGAGSIAAATGFVKKDQLGKNEEGAPQEGILEDMPVDP 677
Sbjct 61 EQVTNVGGAVVTGVTAVAQKTVEGAGSIAAATGFVKKDQLGKNEEGAPQEGILEDMPVDP 120

Query 678 DNEAYEMPSEEGYQDYEPEA 737
Sbjct 121 DNEAYEMPSEEGYQDYEPEA 140
```

(b)

```
>| gb|AAP36433.1| Homo sapiens synuclein, alpha (non A4 component of amyloid precursor)
[synthetic construct]
gb|AA29716.1| synuclein alpha [synthetic construct]
gb|AA29717.1| synuclein alpha [synthetic construct]
Length=141

Score = 207 bits (528), Expect = 1e-51
Identities = 139/140 (99%), Positives = 139/140 (99%), Gaps = 0/140 (0%)
Frame = +3

Query 321 MDVFMKGLSkakegfvvaaeektkQVAAEAGKTKEGVLYVGSKTKEGTVHGVATVAEKTK 500
Sbjct 1 MDVFMKGLSKAKEGVVAAAEEKTKQGVAAEAGKTKEGVLYVGSKTKEGTVHGVATVAEKTK 60

Query 501 EQvtnvvggavvtgvtavaQKTVEGAGSIAAATGFVKKDQLGKNEEGAPQEGILEDMPVDP 680
Sbjct 61 EQVTNVGGAVVTGVTAVAQKTVEGAGSIAAATGFVKKDQLGKNEEGAPQEGILEDMPVDP 120

Query 681 DNEAYEMPSEEGYQDYEPEA 740
Sbjct 121 DNEAYEMPSEEGYQDYEPEA 140
```

(c)

```
>| gb|AAP36433.1| Homo sapiens synuclein, alpha (non A4 component of amyloid precursor)
[synthetic construct]
gb|AA29716.1| synuclein alpha [synthetic construct]
gb|AA29717.1| synuclein alpha [synthetic construct]
Length=141

Score = 207 bits (528), Expect = 7e-52
Identities = 139/140 (99%), Positives = 140/140 (100%), Gaps = 0/140 (0%)
Frame = +2

Query 317 MDVFMKGLSkakegfvvaaeektkQVAAEAGKTKEGVLYVGSKTKKGGVTVGVATVAEKTK 496
Sbjct 1 MDVFMKGLSKAKEGVVAAAEEKTKQGVAAEAGKTKEGVLYVGSKTKKGGVTVGVATVAEKTK 60

Query 497 EQvtnvvggavvtgvtavaQKTVEGAGSIAAATGFVKKDQLGKNEEGAPQEGILEDMPVDP 676
Sbjct 61 EQVTNVGGAVVTGVTAVAQKTVEGAGSIAAATGFVKKDQLGKNEEGAPQEGILEDMPVDP 120

Query 677 DNEAYEMPSEEGYQDYEPEA 736
Sbjct 121 DNEAYEMPSEEGYQDYEPEA 140
```

**Figure 4.15: NCBI Blastx results.** (a)  $\alpha$ -Syn mutant construct A30P (b)  $\alpha$ -Syn mutant construct A53T (c)  $\alpha$ -Syn mutant construct E46K.

#### **4.3.2 Co-transfection using plasmid pCMV-Sport6- $\alpha$ -Syn and pBABE-hygro**

Plasmid pBABE-hygro was initially used as a co-transfection plasmid with pCMV-Sport6- $\alpha$ -Syn as it contains a hygromycin resistance gene cloned in the pBABE retroviral vector which gives the stably transfected mammalian cells selectable advantage (Cell Biolabs, 2008). For successful co-transfection, both vectors need to be delivered simultaneously into the same cell and to be integrated into the genome, allowing the cell to be stably expressing both gene of interest and selection marker.

However, in this study, after several attempts of co-transfection, the surviving hygromycin resistant clones obtained were found to have no or low expression of the protein of interest. Moreover, the low level of expression generally tended to decrease over time in culture due to the selective pressure depending solely on the expression cassette of antibiotic resistance gene (hygromycin B phosphotransferase). Even co-transfection done with high ratio of target plasmid/co-transfection plasmid did not improve the transfection outcome. To solve this problem, another mammalian expression vector, pcDNA<sup>TM</sup>3.1 which can carry both the gene of interest and selectable marker was used.

### 4.3.3 Molecular cloning of $\alpha$ -Syn constructs into plasmid vector pcDNA<sup>TM</sup>3.1

Blunt-end PCR product of wild type and mutant  $\alpha$ -Syn constructs with size of 422 bp were first produced [Figure 4.16 (a)] and were directionally cloned into the TOPO cloning site of pcDNA<sup>TM</sup>3.1 expression vector, downstream of a cytomegalovirus promoter using pcDNA<sup>TM</sup>3.1 Directional TOPO Expression Kit. Figure 4.16 (b) shows the linearised pcDNA<sup>TM</sup>3.1 empty vector with size of 5514 bp, pcDNA<sup>TM</sup>3.1-wild type  $\alpha$ Syn, pcDNA<sup>TM</sup>3.1- $\alpha$ Syn mutant A30P, pcDNA<sup>TM</sup>3.1- $\alpha$ Syn mutant A53T and pcDNA<sup>TM</sup>3.1- $\alpha$ Syn mutant E46K with size of 5936 bp, alongside with the 1 kb DNA ladder. The presence and orientation of the  $\alpha$ -Syn constructs cloned into the pcDNA<sup>TM</sup>3.1 vector were verified by sending the isolated plasmids to an outsourced sequencing service provided by First BASE Laboratories. Sequencing results are as shown in Figure 4.17.

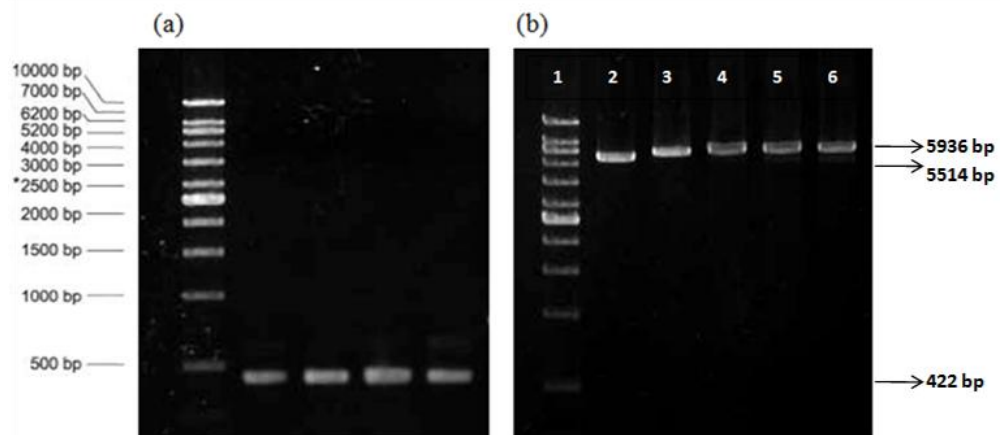
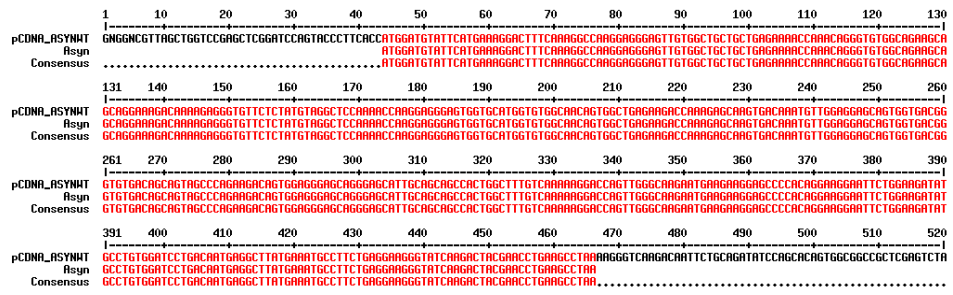
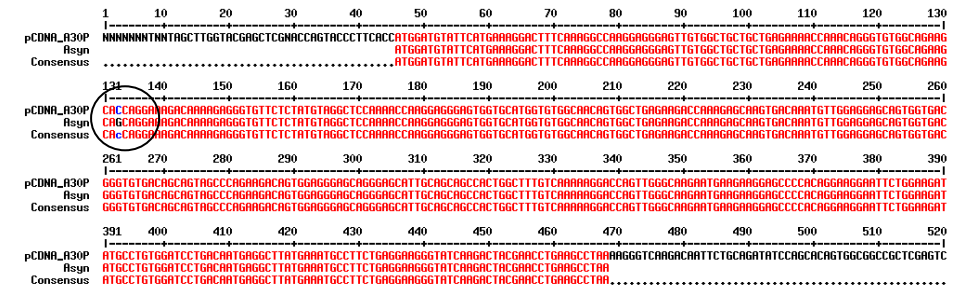


**Figure 4.16: Agarose electrophoresis gel pictures for molecular cloning of  $\alpha$ -Syn.** (a) Blunt-end  $\alpha$ -Syn PCR product with size of 422 bp that were to be directionally cloned into pcDNA<sup>TM</sup>3.1 plasmid vector. (b) Lane 1: 1 kb DNA ladder; Lane 2: linearised pcDNA<sup>TM</sup>3.1 empty vector with size of 5514 bp; Lane 3: pcDNA<sup>TM</sup>3.1-wild type  $\alpha$ Syn; Lane 4: pcDNA<sup>TM</sup>3.1- $\alpha$ Syn mutant A30P; Lane 5: pcDNA<sup>TM</sup>3.1- $\alpha$ Syn mutant A53T; Lane 6: pcDNA<sup>TM</sup>3.1- $\alpha$ Syn mutant E46K with size of 5936 bp.

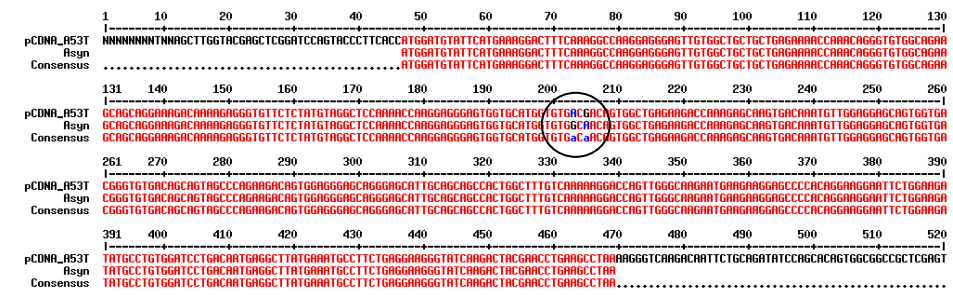
(a)



(b)



(c)



(d)

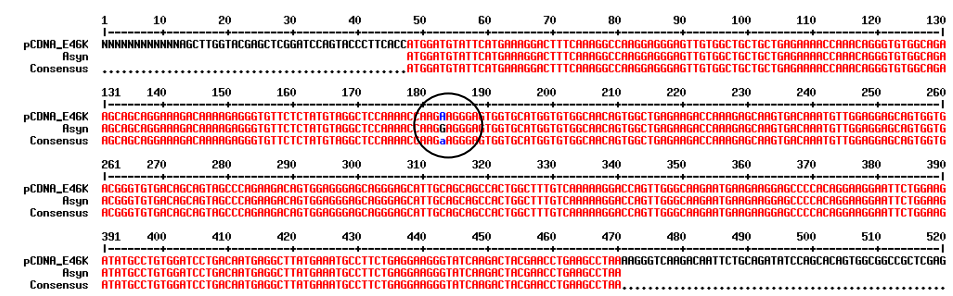


**Figure 4.17: Sequencing alignments produced by Multalin.** The presence and orientation of the  $\alpha$ -Syn constructs ligated into the pcDNA<sup>TM</sup>3.1 vector were verified by an outsourced sequencing service. (a) pcDNA<sup>TM</sup>3.1-wild type  $\alpha$ Syn (b) pcDNA<sup>TM</sup>3.1- $\alpha$ Syn mutant A30P (c) pcDNA<sup>TM</sup>3.1- $\alpha$ Syn mutant A53T (d) pcDNA<sup>TM</sup>3.1- $\alpha$ Syn mutant E46K.

#### **4.3.4 Generation of stable human $\alpha$ -Syn overexpressing cell lines**

To understand the physiological role of  $\alpha$ -Syn in neuronal cells, SH-SY5Y dopaminergic cells were engineered to be stably expressing wild type and mutant human  $\alpha$ -Syn protein, by transfection using a mammalian expression vector, pcDNA<sup>TM</sup>3.1. Stable transfectants were selected by G418 Sulfate (Geneticin). Another group of SH-SY5Y cells stably expressing the vector alone was also established and designated as mock-transfected cells, which serve as negative control. Constitutive and stable expression of  $\alpha$ -Syn was verified using Western blotting and immunofluorescence microscopy. Figure 4.18(a) shows strong expression of a 19 kDa human  $\alpha$ -Syn protein band in SH-SY5Y cells stably transfected with pcDNA<sup>TM</sup>3.1- $\alpha$ -Syn constructs but not in the untransfected and mock-transfected cells, as determined by Western blot analysis using a monoclonal antibody directed against human  $\alpha$ -Syn. Stable expression of human  $\alpha$ -Syn was further confirmed by immunocytochemical analysis [Figure 4.18(b)]. A bright immunofluorescence staining pattern in the  $\alpha$ -Syn overexpressing SH-SY5Y cells revealed that the  $\alpha$ -Syn protein was evenly distributed in the cells, whereas no immunoreactivity was detected in the untransfected and mock-transfected cells. In contrast to some previous studies (Iwata et al., 2003; Lee et al., 2004; Lu et al., 2010; Wu et al., 2009), endogenous  $\alpha$ -Syn was not detected in dopaminergic SH-SY5Y cells in this study, comparable to the results presented by Matsuo and Kamitani (2010) and Matsumoto et al. (2010). This discrepancy might be attributed to the different anti- $\alpha$ -Syn antibodies used as certain clones such as LB509, N19 and 2E3 have been shown to be more sensitive (Iwata et al., 2003; Lu et al., 2010; Wu et al., 2009) while 4D6 and 7B12.2 were unable to detect the endogenous  $\alpha$ -Syn in

SH-SY5Y cells (Matsuo & Kamitani, 2010). In this study, clone 7B12.2 was used and this explains the lack of sensitivity in detection of endogenous  $\alpha$ -Syn in SH-SY5Y.

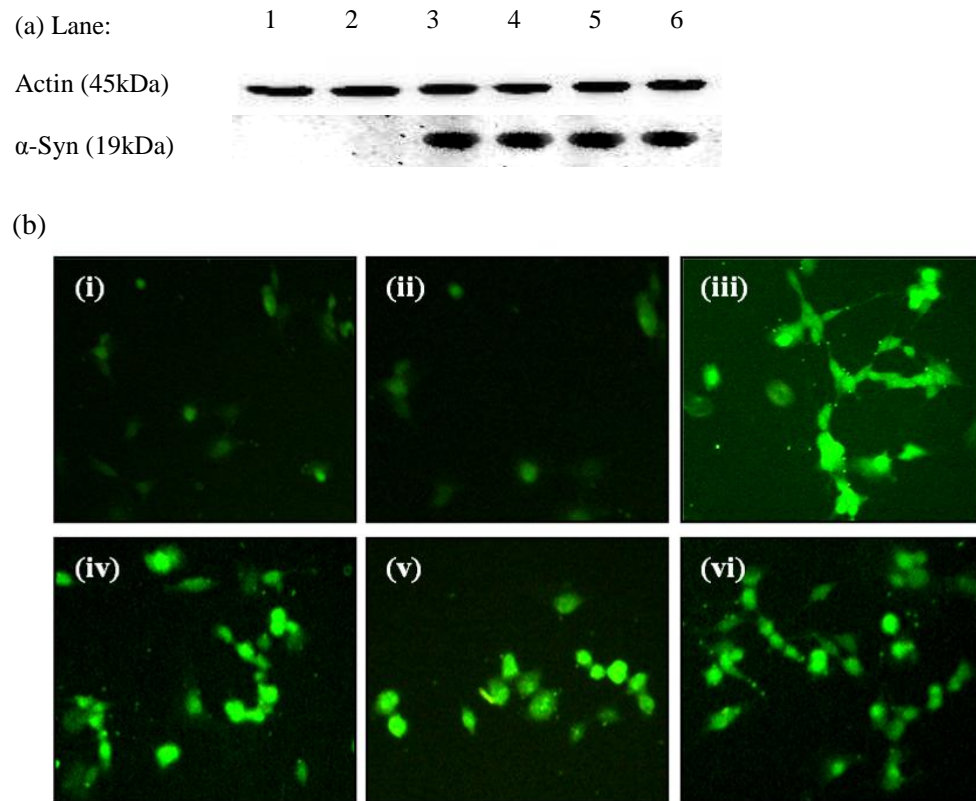


**Figure 4.18: Stable overexpression of human wild type or mutant  $\alpha$ -Syn in SH-SY5Y.** (a) Stable expression of  $\alpha$ -Syn was determined by Western blot analysis using anti- $\alpha$ -Syn antibody, clone 7B12.2; a 19 kDa band corresponding to the molecular mass of human  $\alpha$ -Syn protein was detected in  $\alpha$ -Syn overexpressing SH-SY5Y cells but not in untransfected and mock-transfected cells. Lane 1: Untransfected SH-SY5Y; Lane 2: Mock-transfected SH-SY5Y; Lane 3: pcDNA<sup>TM</sup>3.1-wild type  $\alpha$ Syn-transfected SH-SY5Y; Lane 4: pcDNA<sup>TM</sup>3.1- $\alpha$ Syn A30P-transfected SH-SY5Y; Lane 5: pcDNA<sup>TM</sup>3.1- $\alpha$ Syn A53T-transfected SH-SY5Y; Lane 6: pcDNA<sup>TM</sup>3.1- $\alpha$ Syn E46K-transfected SH-SY5Y. (b) Immunofluorescence microscopy bright staining revealed that  $\alpha$ -Syn was evenly distributed in stably transfected SH-SY5Y whereas no  $\alpha$ -Syn immunoreactivity was shown in both untransfected and mock-transfected cells. (Magnification power = 100 $\times$ ). (i) Untransfected SH-SY5Y; (ii) Mock-transfected SH-SY5Y; (iii) pcDNA<sup>TM</sup>3.1-wild type  $\alpha$ Syn-transfected SH-SY5Y; (iv) pcDNA<sup>TM</sup>3.1- $\alpha$ Syn A30P-transfected SH-SY5Y; (v) pcDNA<sup>TM</sup>3.1- $\alpha$ Syn A53T-transfected SH-SY5Y; (vi) pcDNA<sup>TM</sup>3.1- $\alpha$ Syn E46K-transfected SH-SY5Y.

#### **4.4 Effects of overexpression of wild type and mutant human $\alpha$ -Syn against staurosporine insult**

##### **4.4.1 Differential effects of overexpression of wild type and mutant human $\alpha$ -Syn on staurosporine-induced cell death in SH-SY5Y**

To determine the effect of  $\alpha$ -Syn overexpression on the cellular response to staurosporine-induced cell death, all six SH-SY5Y cell lines were exposed to 0.25  $\mu$ M or 0.50  $\mu$ M staurosporine for 24 hr before MTT assay was conducted. Exposure of these SH-SY5Y cells lines non- or overexpressing human  $\alpha$ -Syn to staurosporine resulted in a decrease in cell viability compared with the untreated group in each cell line. As shown in Figure 4.19, major differences in cell viability were found in the relative vulnerability after 0.25  $\mu$ M and 0.50  $\mu$ M staurosporine treatment: the viability of SH-SY5Y cells overexpressing wild type  $\alpha$ -Syn was significantly higher than that of control cells; while SH-SY5Y cells overexpressing mutant  $\alpha$ -Syn constructs (A30P, A53T and E46K) showed lower cell viability ( $p < 0.05$ ). LD<sub>50</sub> of staurosporine for untransfected SH-SY5Y cells was determined to be 0.15  $\mu$ M and this concentration was used for subsequent experiments. These data suggest that wild type  $\alpha$ -Syn may confer protective effect against apoptotic stressor while mutant  $\alpha$ -Syn constructs exacerbated the staurosporine-induced toxicity in SH-SY5Y.

##### **4.4.2 Observation of morphological changes in SH-SY5Y following staurosporine treatment**

The morphological changes of SH-SY5Y cells induced by staurosporine treatment are presented in Figure 4.20. In the absence of treatment, majority of the cells displayed standard morphology and exhibited usual anchorage properties. Upon treatment with staurosporine, cell underwent extensive

morphological aberrations including membrane blebbing, occasional stellate appearance, increased tendency to extend processes, exudation of cytoplasmic elements and cell fragmentation. Treatment of 0.25  $\mu\text{M}$  staurosporine initiated the cells to show neuritic like extension, round up and exhibit decreased adhesion to the tissue flask. On the whole, after 24 hr of 0.50  $\mu\text{M}$  staurosporine treatment, majority of cells were dead with rounded cell bodies containing only nuclei surrounded by cytoplasmic remnants. Moreover, vacuolar-granular degenerating cells could be observed.

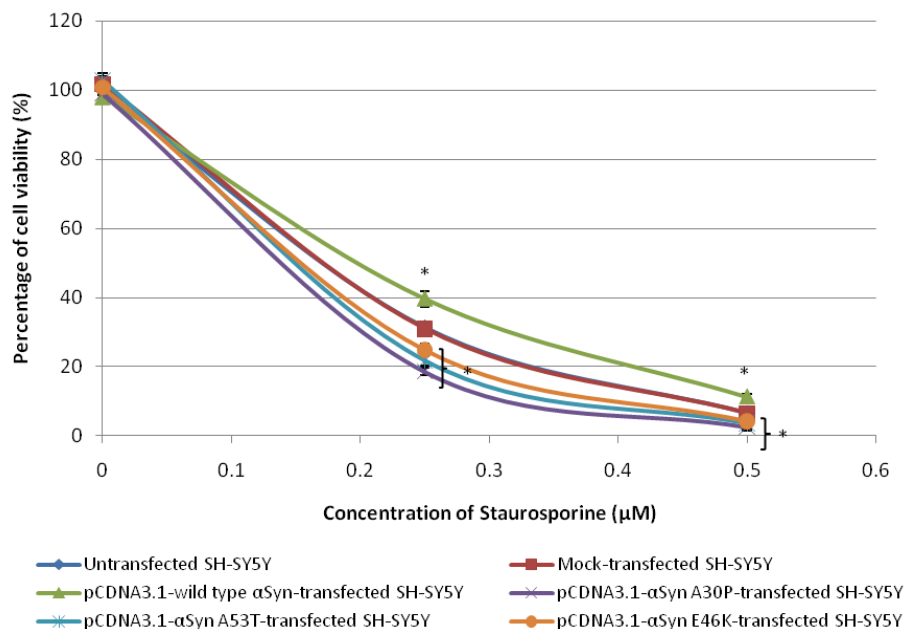


**Figure 4.19: Differential effects of staurosporine in untransfected SH-SY5Y and stably SH-SY5Y cells overexpressing different  $\alpha\text{-Syn}$ .** Cells were exposed to staurosporine at two serial diluted concentrations (0.25 and 0.50  $\mu\text{M}$ ) for 24 hr before MTT assay was performed and absorbance was read at 550 nm. Data represent mean  $\pm$  S.E.M of three separate experiments. \* means  $p < 0.05$  compared with untransfected SH-SY5Y cells under the same treatment condition by one-way-ANOVA.

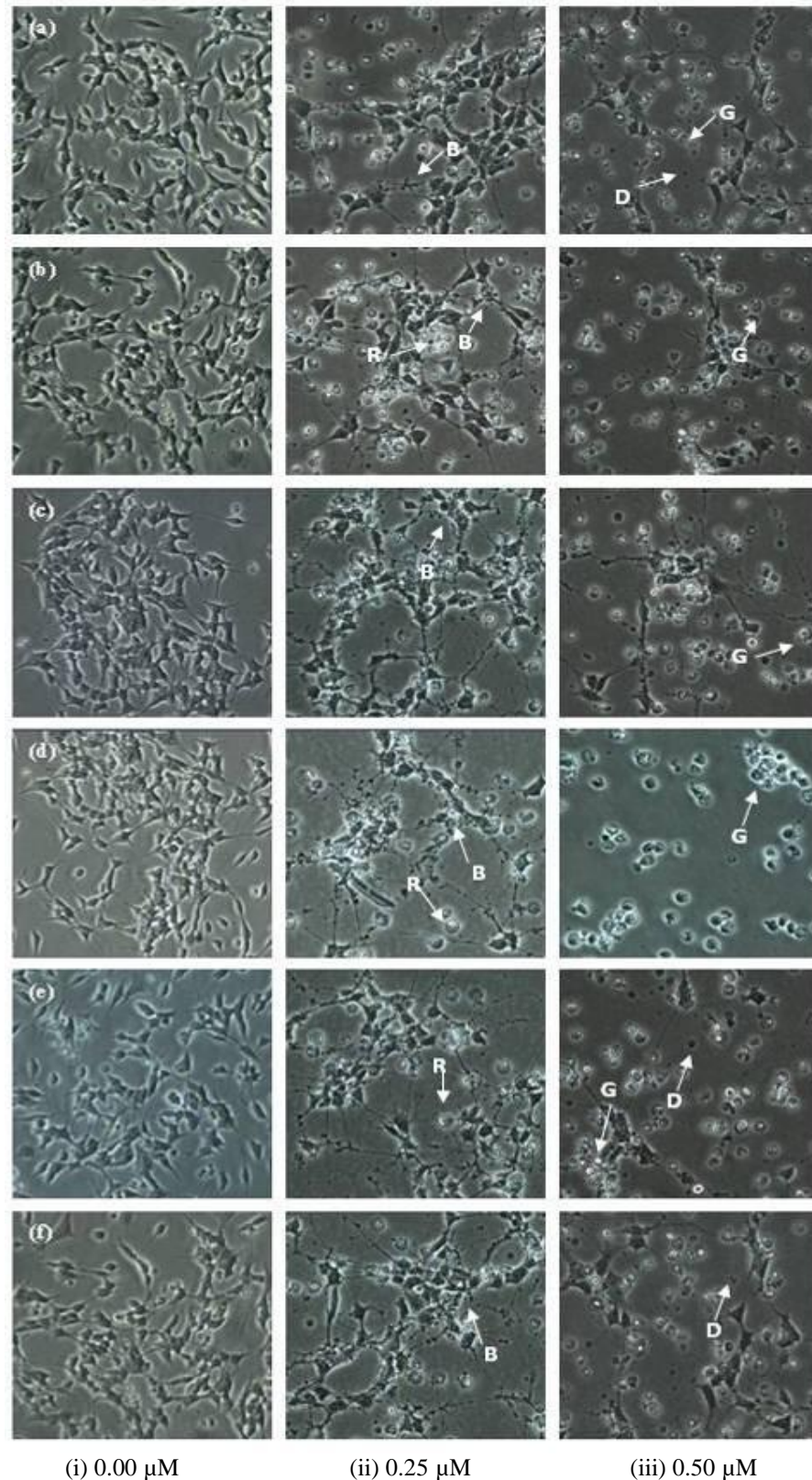


**Figure 4.20: Morphological changes of SH-SY5Y cells after treatment with varying concentrations of staurosporine for 24 hr.** (Magnification power = 100×). R = rounded and shrunken cells, D = cell debris, G = granulated cells, B = membrane blebbing. (a) Untransfected SH-SY5Y (b) Mock-transfected SH-SY5Y (c) pcDNA™3.1-wild type  $\alpha$ Syn-transfected SH-SY5Y (d) pcDNA™3.1- $\alpha$ Syn A30P-transfected SH-SY5Y (e) pcDNA™3.1- $\alpha$ Syn A53T-transfected SH-SY5Y (f) pcDNA™3.1- $\alpha$ Syn E46K-transfected SH-SY5Y.

### **4.4.3 Expression of apoptotic markers in SH-SY5Y**

#### **4.4.3.1 Wild type $\alpha$ -Syn overexpression suppresses Bax expression in SH-SY5Y following staurosporine treatment**

SH-SY5Y cells were incubated in the absence or presence of 0.15  $\mu$ M staurosporine (LD<sub>50</sub>) for 24 hr before preparation of cell lysates for detection of apoptotic markers expression by Western blot analysis. As shown in Figure 4.21, all SH-SY5Y cell lines expressing  $\alpha$ -Syn constructs had greater endogenous Bax protein expression as compared to that of untransfected SH-SY5Y, which served as control. Bax protein expression was markedly increased after treatment with staurosporine. However, lower Bax level could be observed in pcDNA<sup>TM</sup>3.1-wild type  $\alpha$ -Syn-transfected SH-SY5Y as compared to that of control. These data suggest that overexpression of all  $\alpha$ -Syn constructs leads to increased basal level of pro-apoptotic molecule, Bax in SH-SY5Y cells. However, wild type  $\alpha$ -Syn can partially suppress the Bax expression after staurosporine treatment.

#### **4.4.3.2 Mutant $\alpha$ -Syn overexpression leads to decreased Bcl-2 expression following staurosporine treatment in SH-SY5Y**

Since Bcl-2 plays critical roles in programmed cell death induced by a wide array of death signals, the levels of Bcl-2 in all six groups of SH-SY5Y cells were studied by Western blotting. Overall, the Bcl-2 protein expression increased after staurosporine treatment (Figure 4.22). Such up-regulation of Bcl-2 protein might imply a compensatory response of remaining neuronal cells to protect them from subsequent apoptosis. After staurosporine treatment, all SH-SY5Y cell lines expressing mutant  $\alpha$ -Syn constructs (A30P, A53T and E46K) had significantly lower level of Bcl-2 as compared to that of control.

Neuronal cells with lower Bcl-2 expression may be more vulnerable to apoptotic death. These data suggest that overexpression of mutant  $\alpha$ -Syn increases the cell susceptibility to toxic insult through modulation of Bcl-2.

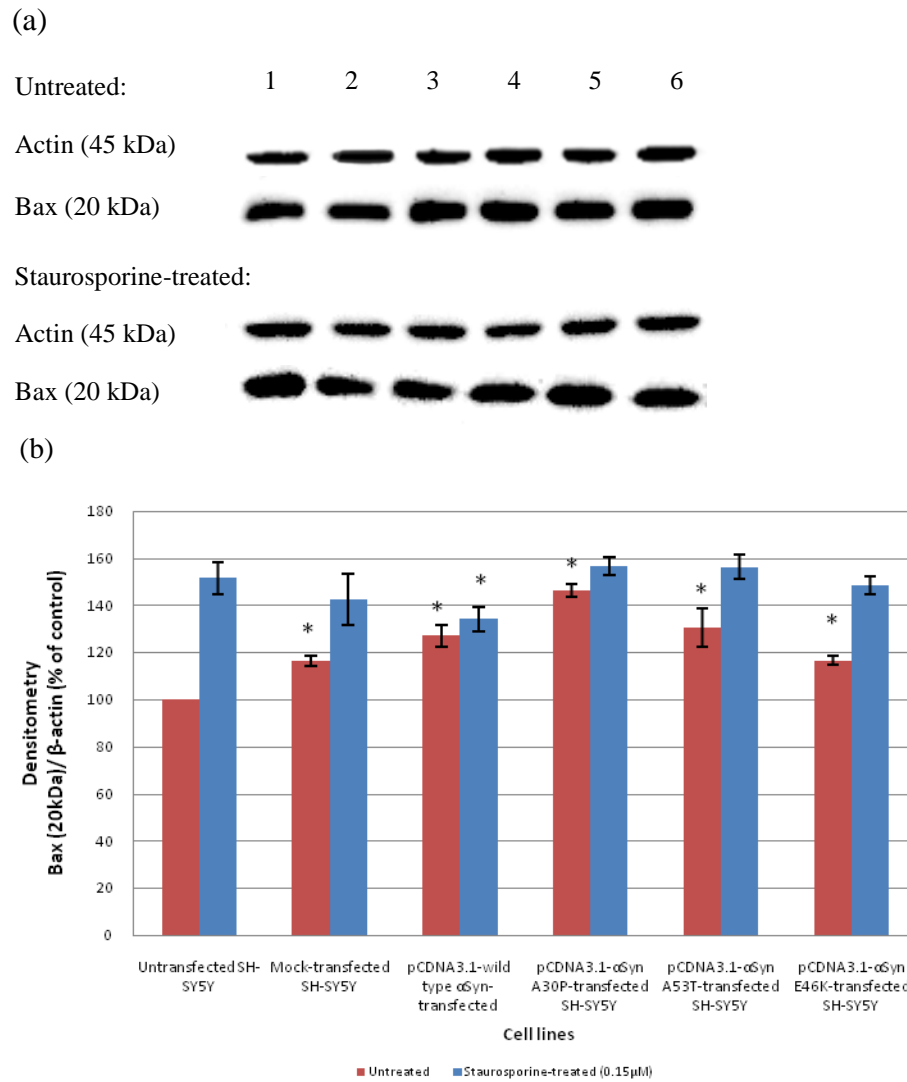


**Figure 4.21: Expression of Bax in SH-SY5Y cell lines by (a) Western blot analysis and (b) its relative densitometry.** Lane 1: Untransfected SH-SY5Y; Lane 2: Mock-transfected SH-SY5Y; Lane 3: pcDNA<sup>TM</sup>3.1-wild type  $\alpha$ Syn-transfected SH-SY5Y; Lane 4: pcDNA<sup>TM</sup>3.1- $\alpha$ Syn A30P-transfected SH-SY5Y; Lane 5: pcDNA<sup>TM</sup>3.1- $\alpha$ Syn A53T-transfected SH-SY5Y; Lane 6: pcDNA<sup>TM</sup>3.1- $\alpha$ Syn E46K-transfected SH-SY5Y. Cells were incubated in the absence or presence of 0.15  $\mu$ M staurosporine for 24 hr and cell lysates were prepared and subjected to Western blot analysis. Error bars represent S.E.M from two independent experiments. \* means  $p < 0.05$  compared with untransfected cells under the same treatment by one-way-ANOVA.

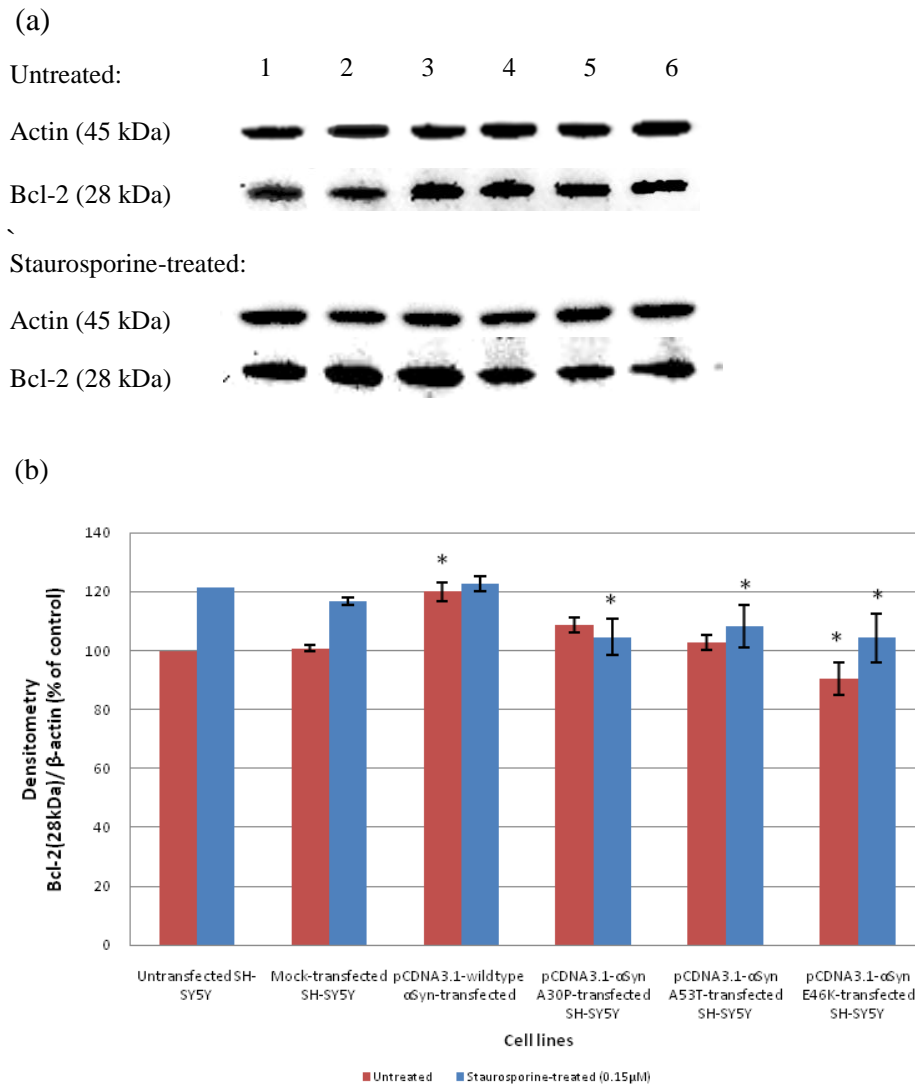


**Figure 4.22: Expression of Bcl-2 in SH-SY5Y cell lines by (a) Western blot analysis and (b) its relative densitometry.** Lane 1: Untransfected SH-SY5Y; Lane 2: Mock-transfected SH-SY5Y; Lane 3: pcDNA<sup>TM</sup>3.1-wild type  $\alpha$ Syn-transfected SH-SY5Y; Lane 4: pcDNA<sup>TM</sup>3.1- $\alpha$ Syn A30P-transfected SH-SY5Y; Lane 5: pcDNA<sup>TM</sup>3.1- $\alpha$ Syn A53T-transfected SH-SY5Y; Lane 6: pcDNA<sup>TM</sup>3.1- $\alpha$ Syn E46K-transfected SH-SY5Y. Cells were incubated in the absence or presence of 0.15  $\mu$ M staurosporine for 24 hr and cell lysates were prepared and subjected to Western blot analysis. Error bars represent S.E.M from two independent experiments. \* means  $p < 0.05$  compared with untransfected cells under the same treatment by one-way-ANOVA.

#### 4.4.3.3 Wild type $\alpha$ -Syn overexpression triggers greater basal Bcl-xL expression in SH-SY5Y

As shown in Figure 4.23, pcDNA<sup>TM</sup>3.1-wild type  $\alpha$ Syn-transfected SH-SY5Y had higher endogenous Bcl-xL protein expression, while the mutant  $\alpha$ -Syn

transfected cells had lower endogenous Bcl-xL level significantly, as compared to that of control. After staurosporine treatment, the Bcl-xL level further decreased in mutant  $\alpha$ -Syn transfected cells.

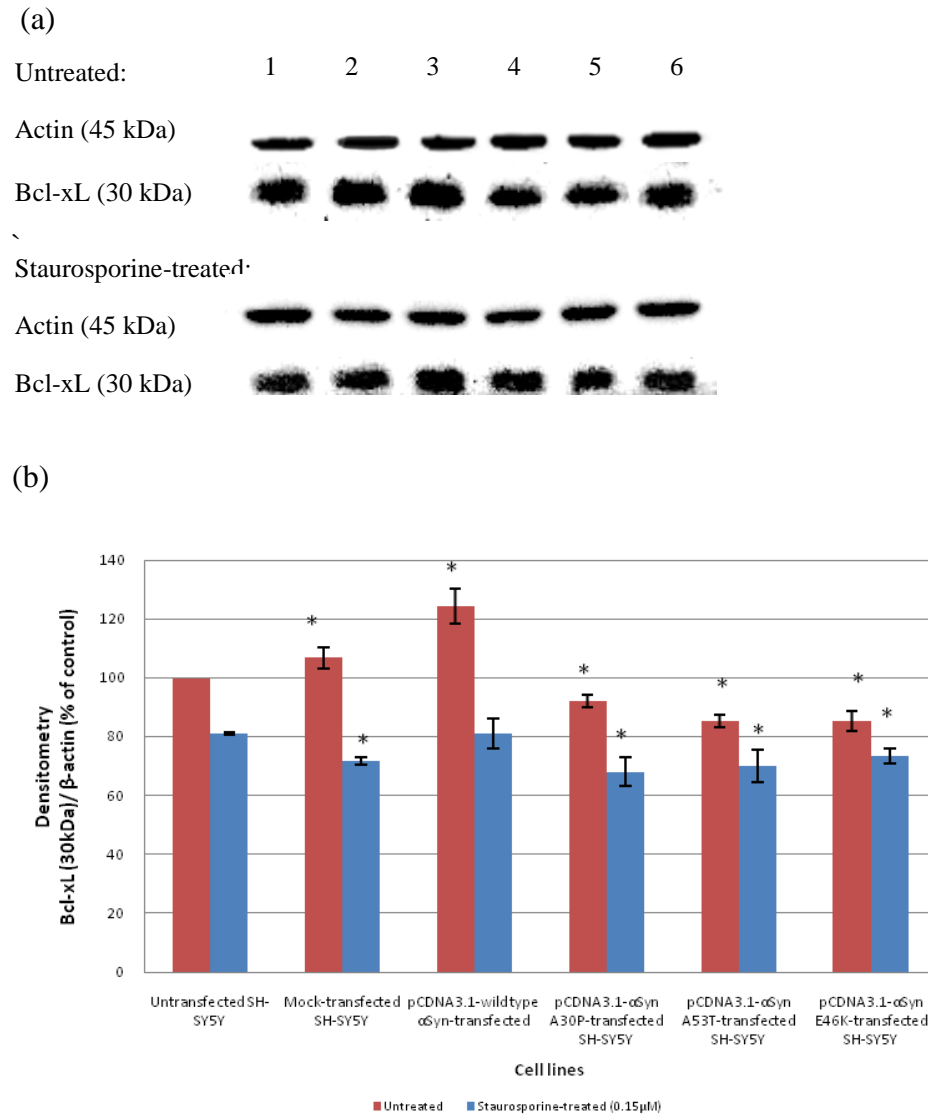


**Figure 4.23 Expression of Bcl-xL in SH-SY5Y cell lines by (a) Western blot analysis and (b) its relative densitometry.** Lane 1: Untransfected SH-SY5Y; Lane 2: Mock-transfected SH-SY5Y; Lane 3: pCDNA<sup>TM</sup>3.1-wild type  $\alpha$ Syn-transfected SH-SY5Y; Lane 4: pCDNA<sup>TM</sup>3.1- $\alpha$ Syn A30P-transfected SH-SY5Y; Lane 5: pCDNA<sup>TM</sup>3.1- $\alpha$ Syn A53T-transfected SH-SY5Y; Lane 6: pCDNA<sup>TM</sup>3.1- $\alpha$ Syn E46K-transfected SH-SY5Y. Cells were incubated in the absence or presence of 0.15  $\mu$ M staurosporine for 24 hr and cell lysates were prepared and subjected to Western blot analysis. Error bars represent S.E.M from two independent experiments. \* means  $p < 0.05$  compared with untransfected cells under the same treatment by one-way-ANOVA.

#### **4.4.3.4 Overexpression of mutant $\alpha$ -Syn increases cleavage and activation of caspase 9 in SH-SY5Y**

Similarly, cleaved caspase 9 could only be detected in staurosporine-treated SH-SY5Y cells (Figure 4.24). All  $\alpha$ -Syn mutants (A30P, A53T and E46K)-transfected SH-SY5Y cells had greater cleaved caspase 9 level compared with control. These results suggest that mutant  $\alpha$ -Syn overexpression in SH-SY5Y can exacerbate cleavage and activation of caspase 9 and thereby leads to prominent increase in staurosporine-induced cell death.

#### **4.4.3.5 Wild type $\alpha$ -Syn overexpression reduces the Bax/Bcl-2 and Bax/Bcl-xL ratios in SH-SY5Y following staurosporine treatment**

Bax/Bcl-2 and Bax/Bcl-xL ratios represent the apoptotic potential of the cells. (Chang et al., 2005; Raisova et al., 2001). At both endogenous level and after staurosporine treatment, SH-SY5Y cell lines expressing all three  $\alpha$ -Syn mutant constructs (A30P, A53T and E46K) had greater Bax/Bcl-2 and Bax/Bcl-xL ratios, as compared to the untransfected cells which served as control while these ratios were lower in cells expressing wild type  $\alpha$ -Syn (Figure 4.25). The data indicate that SH-SY5Y cells expressing wild type  $\alpha$ -Syn have lower apoptotic potential as compared to control, in contrary to the cells expressing  $\alpha$ -Syn mutants, which exhibit greater apoptotic potential.

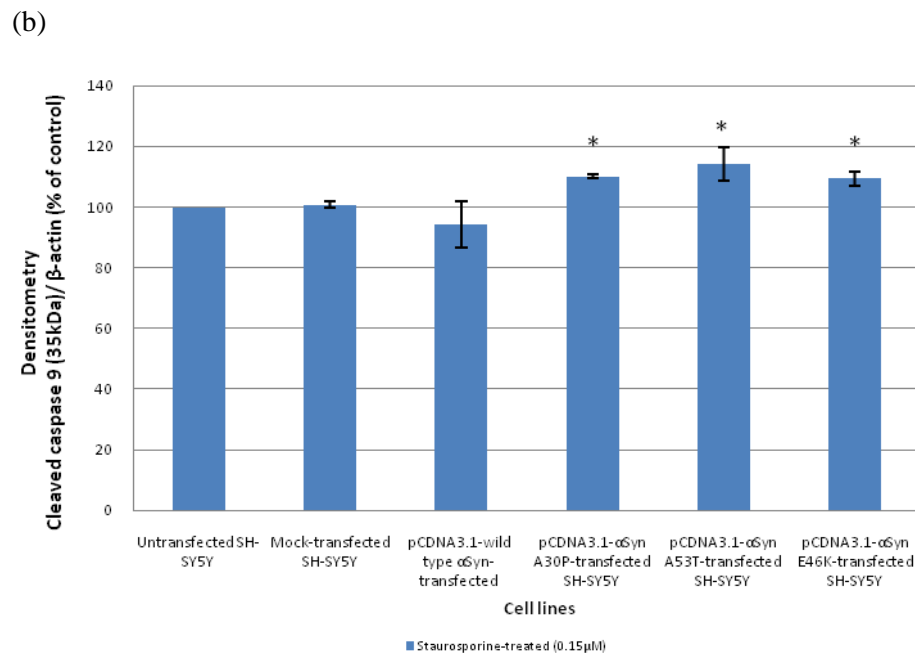
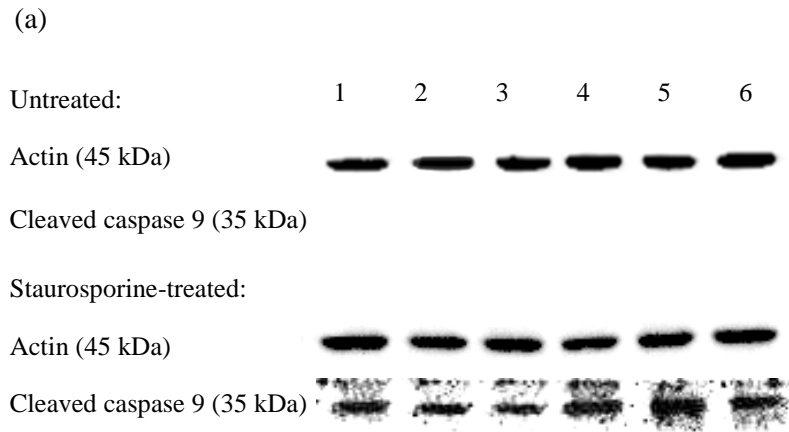
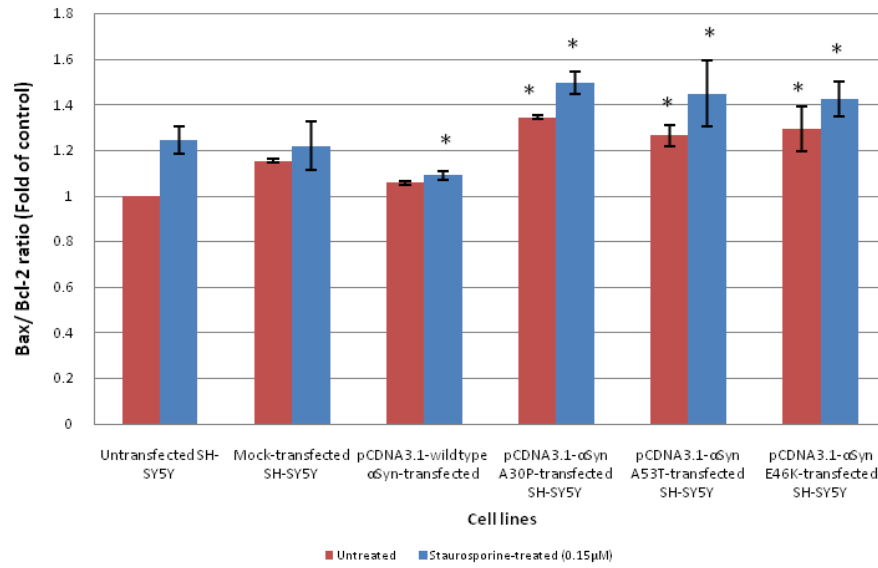


**Figure 4.24: Expression of cleaved caspase 9 in SH-SY5Y cell lines by (a) Western blot analysis and (b) its relative densitometry.** Lane 1: Untransfected SH-SY5Y; Lane 2: Mock-transfected SH-SY5Y; Lane 3: pcDNA<sup>TM</sup>3.1-wild type αSyn-transfected SH-SY5Y; Lane 4: pcDNA<sup>TM</sup>3.1-αSyn A30P-transfected SH-SY5Y; Lane 5: pcDNA<sup>TM</sup>3.1-αSyn A53T-transfected SH-SY5Y; Lane 6: pcDNA<sup>TM</sup>3.1-αSyn E46K-transfected SH-SY5Y. Cells were incubated in the absence or presence of 0.15 μM staurosporine for 24 hr and cell lysates were prepared and subjected to Western blot analysis. Error bars represent S.E.M from two independent experiments. \* means p < 0.05 compared with untransfected cells under the same treatment by one-way-ANOVA.

(a)



(b)

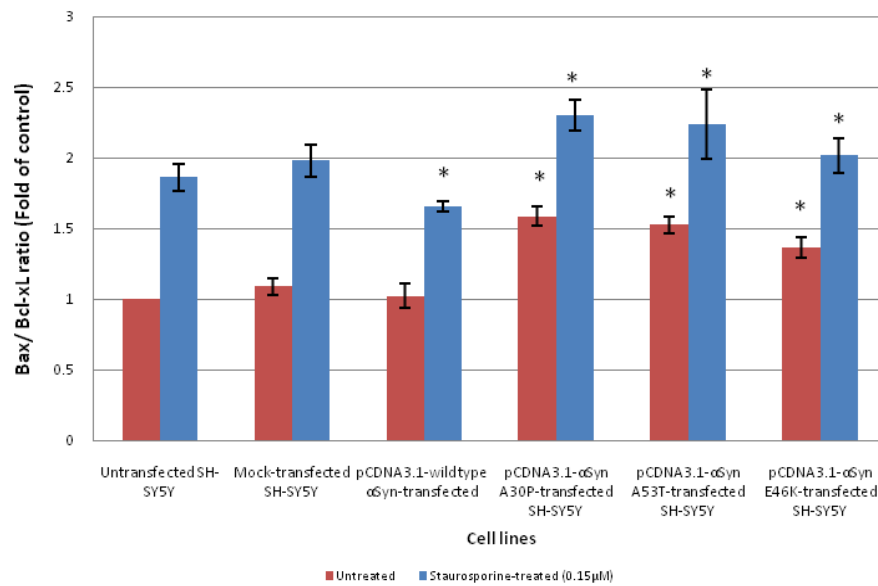


**Figure 4.25: Ratios of (a) Bax/Bcl-2 and (b) Bax/Bcl-xL in SH-SY5Y cell lines were quantified and plotted.** The Bcl-2/Bax and Bcl-xL/Bax ratios in control cell were set as 1.00. Results represent mean  $\pm$  S.E.M of two independent experiments. \* means  $p < 0.05$  compared to untransfected SH-SY5Y under the same treatment by one-way-ANOVA.

#### **4.4.4 Overexpression of mutant $\alpha$ -Syn reduces proliferative index of SH-SY5Y**

To investigate the differential roles of wild type and mutant  $\alpha$ -Syn overexpression in controlling cell proliferation in SH-SY5Y, flow cytometric cell cycle analysis was done using propidium iodide staining. The proliferative index (PI) was calculated as follows:  $PI = (S+G_2)/(G_1+ S+G_2)$  (Liang et al., 2007) (Appendix D). As shown in Figure 4.26, the mean proliferative index of pcDNA<sup>TM</sup>3.1-wild type  $\alpha$ Syn-transfected SH-SY5Y was slightly higher but did not differ significantly from those of untransfected SH-SY5Y and mock-transfected SH-SY5Y. On the contrary, SH-SY5Y cells overexpressing A30P, A53T and E46K mutants had significantly lower proliferative indices. These data suggest that overexpression of mutant  $\alpha$ -Syn constructs may suppress neuronal cell cycle progression, and thereby contribute to decrease in neuronal cell proliferation.

As shown in Figure 4.27 and 4.28, in general, treatment with staurosporine led to an increase of cells in the G<sub>2</sub>/M phase of cell cycle, with a corresponding decrease of cells in the G<sub>0</sub>/G<sub>1</sub> cell cycle when compared to untreated cells. However, no significant difference could be observed between the six cell types. Cells subjected to 0.15  $\mu$ M staurosporine treatment displayed an increase in the sub G<sub>0</sub> (hypodiploid) portion.  $\alpha$ -Syn mutants-transfected SH-SY5Y were shown to have slightly greater hypodiploid sub G<sub>0</sub> proportion as compared to untransfected SH-SY5Y. These results suggest that staurosporine also induces G<sub>2</sub>/M arrest, causing cell death in SH-SY5Y. Overexpression of  $\alpha$ -Syn mutants increases hypodiploid peak, a measure of the extent of DNA fragmentation, and hence of cell death.

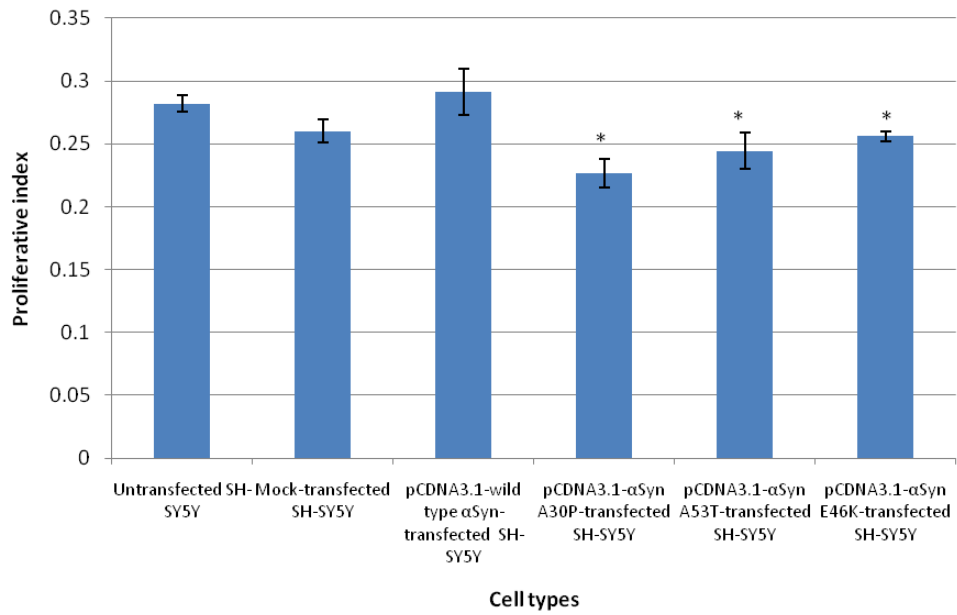


**Figure 4.26: Effect of  $\alpha$ -Syn overexpression on the proliferative index of SH-SY5Y.** The cells were harvested, stained with propidium iodide, and analysed by flow cytometry. Proliferative index was calculated using the equation:  $(S+G_2)/(G_1+S+G_2)$ . Results represent mean  $\pm$  S.E.M of three independent experiments. \* means  $p < 0.05$  compared with untransfected SH-SY5Y by one-way-ANOVA.

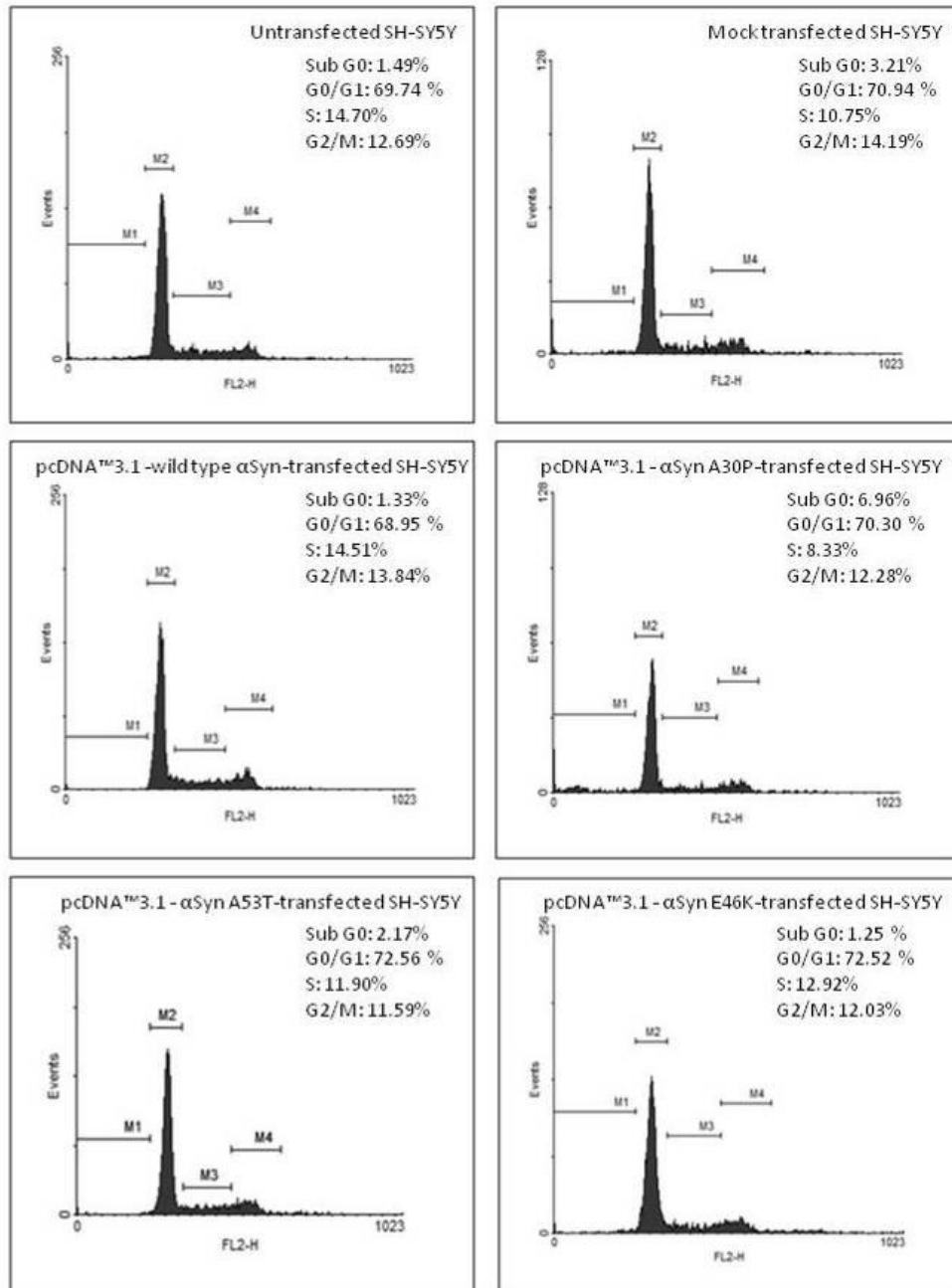


**Figure 4.27: Cell cycle distribution of untreated SH-SY5Y cell lines.** Untreated SH-SY5Y cell lines were incubated with drug-free medium for 24 hr before being harvested, fixed with 70% ethanol for up to 2 hr followed by propidium iodide staining and flow cytometric analysis. The percentage of cells in each phase of the cell cycle was evaluated using the WinMDI software. Representative histograms from one experiment are shown. M1= Sub Go phase, M2 = Go/G<sub>1</sub> phase, M3 = S phase, M4 = G<sub>2</sub>/M phase.

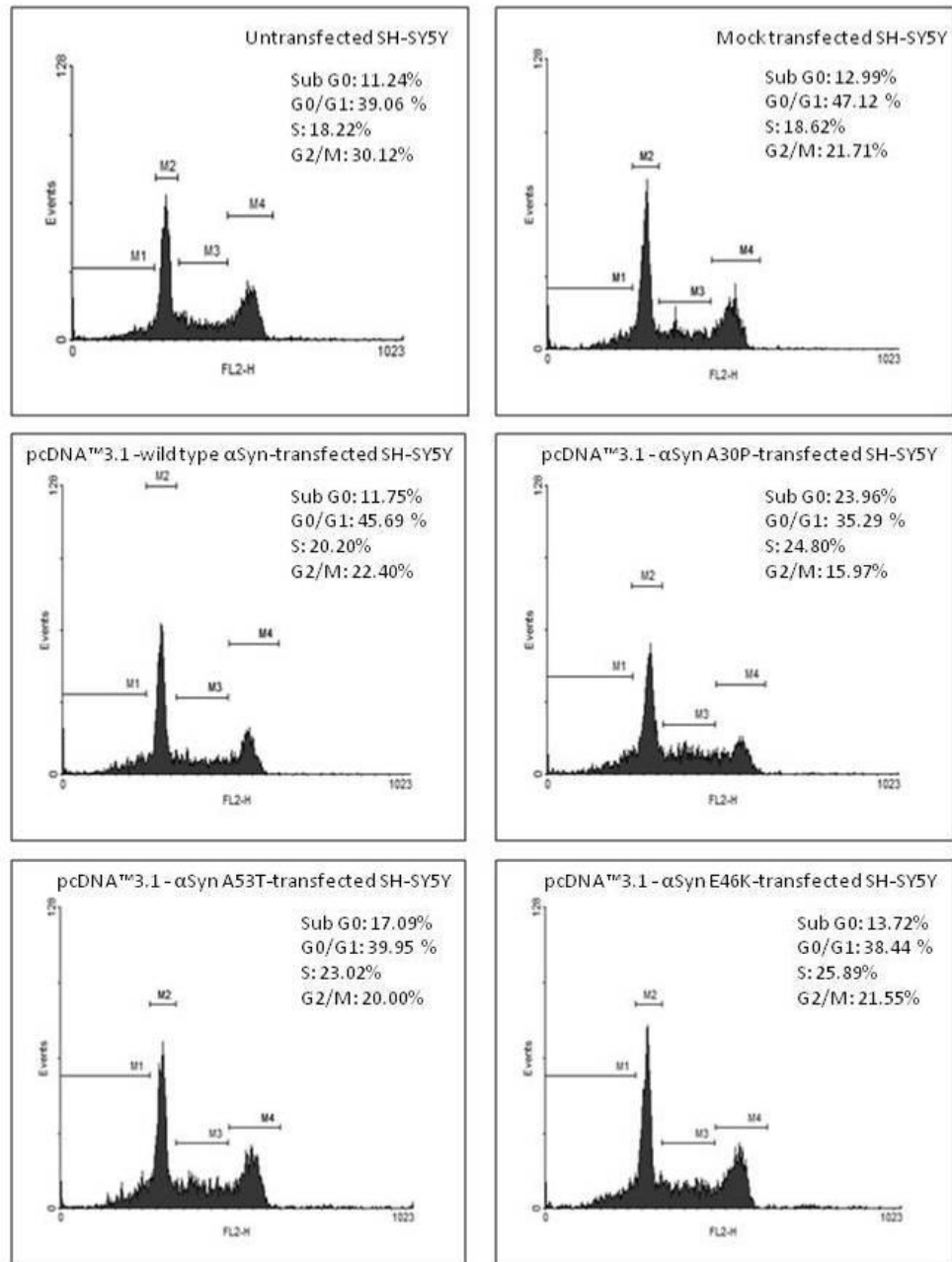


**Figure 4.28: Cell cycle distribution of staurosporine-treated SH-SY5Y cell lines.** Cells were treated with 0.15  $\mu$ M staurosporine for 24 hr before being harvested, fixed with 70% ethanol for up to 2 hr followed by propidium iodide staining and flow cytometric analysis. The percentage of cells in each phase of the cell cycle was evaluated using the WinMDI software. Representative histograms from one experiment are shown. M1 = Sub Go phase, M2 = Go/G<sub>1</sub> phase, M3 = S phase, M4 = G<sub>2</sub>/M phase.

#### **4.5 Effects of $\alpha$ -Syn overexpression against insults of environmental toxins, rotenone and maneb in SH-SY5Y**

##### **4.5.1 Differential effects of overexpression of wild type and mutant human $\alpha$ -Syn against acute rotenone-induced cell death in SH-SY5Y**

$\alpha$ -Syn plays a crucial role in the pathophysiology of dopaminergic neurodegeneration that occurs in Parkinson's disease. Both rotenone and maneb are the environmental toxins that could trigger physical symptoms associated with Parkinson's disease and are widely used to generate *in vitro* Parkinsonian models. To evaluate effects of overexpression of  $\alpha$ -Syn against rotenone insults, SH-SY5Y cell lines were exposed to rotenone at serial diluted concentrations (0.0  $\mu$ M, 0.5  $\mu$ M, 1.0  $\mu$ M and 2.0  $\mu$ M) for 48 hr before MTT assay was conducted. MTT result showed that rotenone markedly induced cell death of human dopaminergic SH-SY5Y cell lines in a concentration dependent manner. As shown in Figure 4.29, at 0.50  $\mu$ M rotenone treatment, wild type  $\alpha$ -Syn-transfected SH-SY5Y cells had significantly higher cell viability, as compared to control (untransfected cells) ( $p < 0.05$ ). Whereas  $\alpha$ -Syn mutants (A30P, A53T and E46K)-transfected SH-SY5Y showed lower cell viability following 0.50  $\mu$ M and 1.00  $\mu$ M rotenone treatment ( $p < 0.05$ ). LD<sub>50</sub> of rotenone for untransfected SH-SY5Y cells was determined to be 1.00  $\mu$ M and this LD<sub>50</sub> was then used for subsequent DCFH-DA and DiOC6(3) assays to determine rotenone induced-ROS generation and mitochondrial membrane potential changes, respectively. These data suggest that wild type  $\alpha$ -Syn confers protective effect against acute rotenone treatment while the mutant variants cause further rotenone-induced detrimental effects in SH-SY5Y.

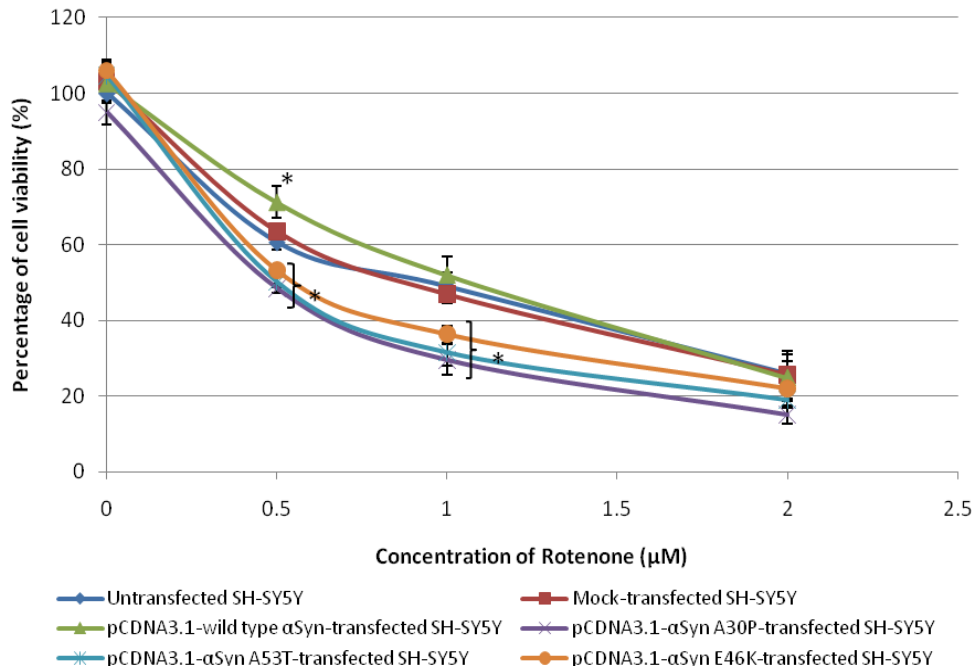


**Figure 4.29: Effects of acute rotenone treatment in untransfected SH-SY5Y and stably SH-SY5Y cells overexpressing different  $\alpha$ -Syn.** Cell viability was assessed by MTT assay after treatment with rotenone for 48 hr. Data represent mean  $\pm$  S.E.M of three separate experiments. \* means  $p < 0.05$  compared with untransfected SH-SY5Y cells under the same treatment condition by one-way-ANOVA).

#### 4.5.2 Differential effects of overexpression of wild type and mutant human $\alpha$ -Syn on acute maneb-induced cell death in SH-SY5Y

SH-SY5Y cell lines were exposed to maneb at serial diluted concentrations (0  $\mu$ M, 15  $\mu$ M, 30  $\mu$ M and 60  $\mu$ M) for 48 hr before MTT assay was conducted. MTT result shows a correlation between concentration and cell viability as the percentage of SH-SY5Y cell viability was inversely proportional to maneb concentrations (Figure 4.30). At 15  $\mu$ M maneb treatment, wild type  $\alpha$ -Syn-transfected SH-SY5Y cells had significantly higher cell viability, as compared to that of control (untransfected cells). Whereas  $\alpha$ -Syn mutants-transfected SH-SY5Y showed lower cell viability ( $p < 0.05$ ). LD<sub>50</sub> of maneb for untransfected SH-SY5Y cells was determined to be 30  $\mu$ M and this LD<sub>50</sub> was then used for

subsequent DCFH-DA and DiOC6(3) assays. These data suggest that wild type  $\alpha$ -Syn can rescue SH-SY5Y cells from maneb-induced cyto-toxicity while mutants of  $\alpha$ -Syn intensify the toxic insult.

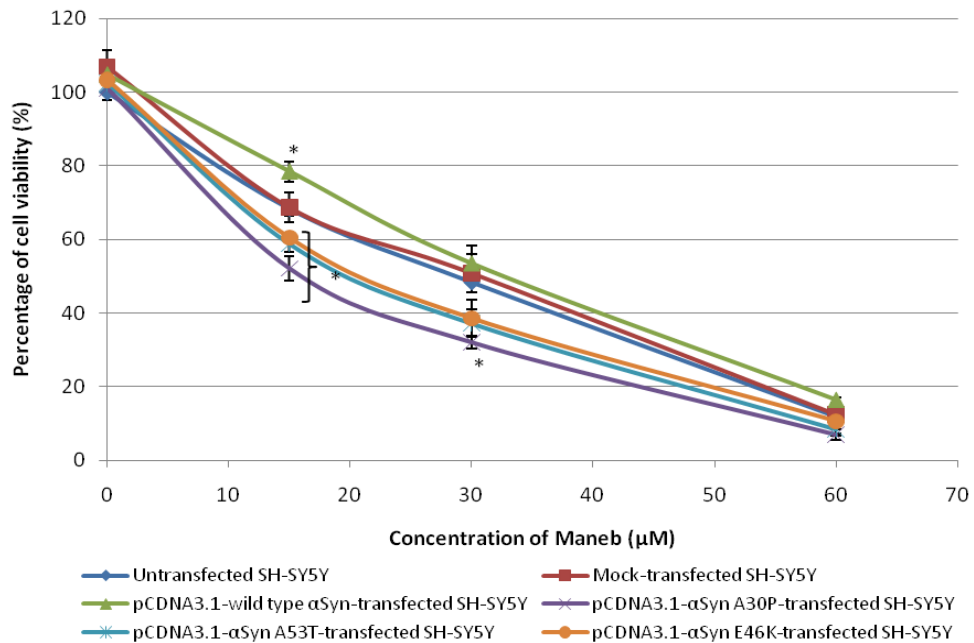


**Figure 4.30: Effects of acute maneb treatment in untransfected SH-SY5Y and stably SH-SY5Y cells overexpressing different  $\alpha$ -Syn.** Cell viability was assessed by MTT assay after treatment with maneb for 48 hr. Data represent mean  $\pm$  S.E.M of three separate experiments. \* means  $p < 0.05$  compared with untransfected SH-SY5Y cells under the same treatment condition by one-way-ANOVA.

#### 4.5.3 Differential effects of overexpression of wild type and mutant human $\alpha$ -Syn on $H_2O_2$ -induced cell death in SH-SY5Y that had been subjected to chronic rotenone treatment

$H_2O_2$  was chosen as an oxidative stressor because dopaminergic cells are normally exposed to  $H_2O_2$  during dopamine synthesis and catabolism. According to previous studies, chronic rotenone exposure was found to potentiate  $H_2O_2$ -induced cell death (Sherer et al., 2002). To determine whether  $\alpha$ -Syn overexpression modulates  $H_2O_2$  toxic insult following chronic rotenone

treatment, MTT assay was carried out after cells chronically treated with 5 nM rotenone were subjected to a 6-hr exposure to 15  $\mu\text{M}$  or 30  $\mu\text{M}$   $\text{H}_2\text{O}_2$ . This study did not detect any differences in rates of basal cell death resulting from chronic rotenone treatment (Figure 4.31). After exposure to 15  $\mu\text{M}$  or 30  $\mu\text{M}$   $\text{H}_2\text{O}_2$ , SH-SY5Y cells overexpressing wild type  $\alpha$ -Syn had significantly greater cell viability, as compared to that of control ( $p < 0.05$ ). Mutant  $\alpha$ -Syn transfected SH-SY5Y were shown to have lower viability than control, but it did not differ significantly. These results suggest that wild type form of  $\alpha$ -Syn but not the mutant variants has protective effect on the chronically rotenone-treated cells against subsequent  $\text{H}_2\text{O}_2$  insult.

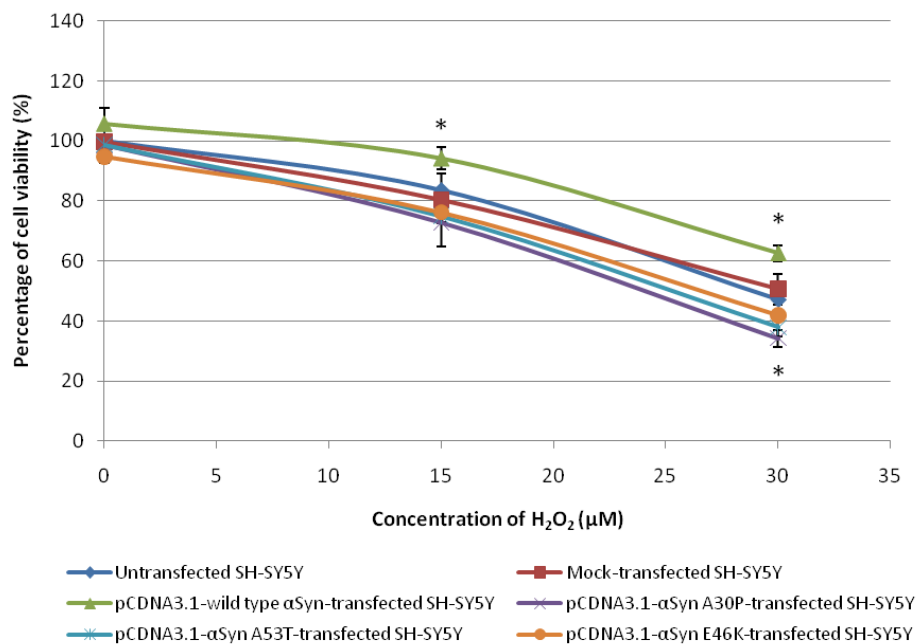


**Figure 4.31: Effects of  $\text{H}_2\text{O}_2$  in chronically rotenone-treated untransfected SH-SY5Y and stably SH-SY5Y cells overexpressing different  $\alpha$ -Syn.** Cell viability was assessed by MTT assay after treatment with  $\text{H}_2\text{O}_2$  for 6 hr. Data represent mean  $\pm$  S.E.M of three separate experiments. \* means  $p < 0.05$  compared with untransfected SH-SY5Y cells under the same treatment condition by one-way-ANOVA.

#### 4.5.4 Differential effects of overexpression of wild type and mutant human $\alpha$ -Syn on $H_2O_2$ -induced cell death in SH-SY5Y that had been subjected to chronic maneb treatment

MTT result showed that following chronic maneb treatment (150 nM), SH-SY5Y cells overexpressing wild type  $\alpha$ -Syn had significantly greater cell viability, as compared to that of control after subsequent exposure to 30  $\mu$ M  $H_2O_2$  ( $p < 0.05$ ) (Figure 4.32). Mutant  $\alpha$ -Syn A30P and A53T-transfected SH-SY5Y were shown to have significantly lower viability ( $p < 0.05$ ) while the percentage of cell viability of E46K-transfected SH-SY5Y was lower than that of control but did not differ significantly. These results suggest that wild type form of  $\alpha$ -Syn has protective effect on the chronically maneb-treated cells against subsequent  $H_2O_2$  insult while mutant  $\alpha$ -Syn A30P and A53T enhance the cells' susceptibility to the  $H_2O_2$  toxicity.

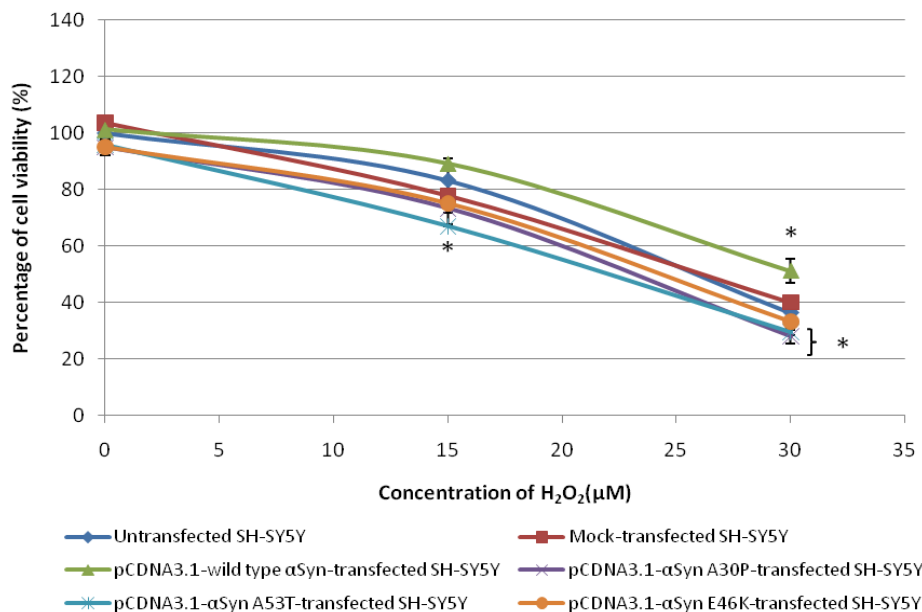


**Figure 4.32: Effects of  $H_2O_2$  in chronically maneb-treated untransfected SH-SY5Y and stably SH-SY5Y cells overexpressing different  $\alpha$ -Syn.** Cell viability was assessed by MTT assay after treatment with  $H_2O_2$  for 6 hr. Data represent mean  $\pm$  S.E.M of three separate experiments. \* means  $p < 0.05$  compared with untransfected SH-SY5Y cells under the same treatment condition by one-way-ANOVA.

#### **4.5.5 Differential effects of overexpression of wild type and mutant human $\alpha$ -Syn on rotenone and maneb-induced reactive oxygen species generation in SH-SY5Y**

To determine whether  $\alpha$ -Syn overexpression modulates rotenone and maneb-induced oxidative stress, the intracellular ROS generation was monitored using the redox-sensitive fluorophore, DCFH-DA following rotenone and maneb treatment. Non-fluorescent DCFH-DA is rapidly oxidised by ROS to the fluorescent derivative, DCF. Decreases or increases in DCF fluorescence were depicted as a shift in the histogram to either the left or right. A right shift of fluorescence indicates increased ROS generation and vice versa. The quantitative analysis of flow cytometric data revealed that exposure of SH-SY5Y cells to acute and chronic rotenone and maneb treatments resulted in an increase in ROS generation [Figure 4.33(a-g)].

As shown in Figure 4.34, compared with control, untreated wild type  $\alpha$ -Syn-transfected SH-SY5Y was shown to have lower fluorescence intensity, indicative of lower basal ROS level while untreated mutant  $\alpha$ -Syn-transfected SH-SY5Y had higher fluorescence intensity, which means greater basal ROS level. After acute rotenone, acute maneb and chronic rotenone treatments, wild type  $\alpha$ -Syn-transfected SH-SY5Y showed significantly lower ROS generation as compared to control, in contrast with mutant  $\alpha$ -Syn-transfected SH-SY5Y.

Interestingly, SH-SY5Y cells overexpressing the wild type form and the three familial mutants of  $\alpha$ -Syn were shown to have elevated ROS level as compared to controls after being subjected to chronic maneb treatment. However, wild type form of  $\alpha$ -Syn was shown to have reduced ROS generation following

subsequent H<sub>2</sub>O<sub>2</sub> insults right after the chronic treatments. Acute exposure to H<sub>2</sub>O<sub>2</sub> was associated with a significant increase in ROS generation in chronically rotenone or maneb-treated mutant  $\alpha$ -Syn expressing cells only. Overall, these data suggest that wild type  $\alpha$ -Syn blocks rotenone- and maneb-induced ROS production, in accordance with its protective effect against rotenone and maneb-induced decrease in cell viability. On the contrary, the A30P, A53T and E46K mutants increase rotenone- and maneb-induced ROS production and thus exhibit toxic effects on cell viability.

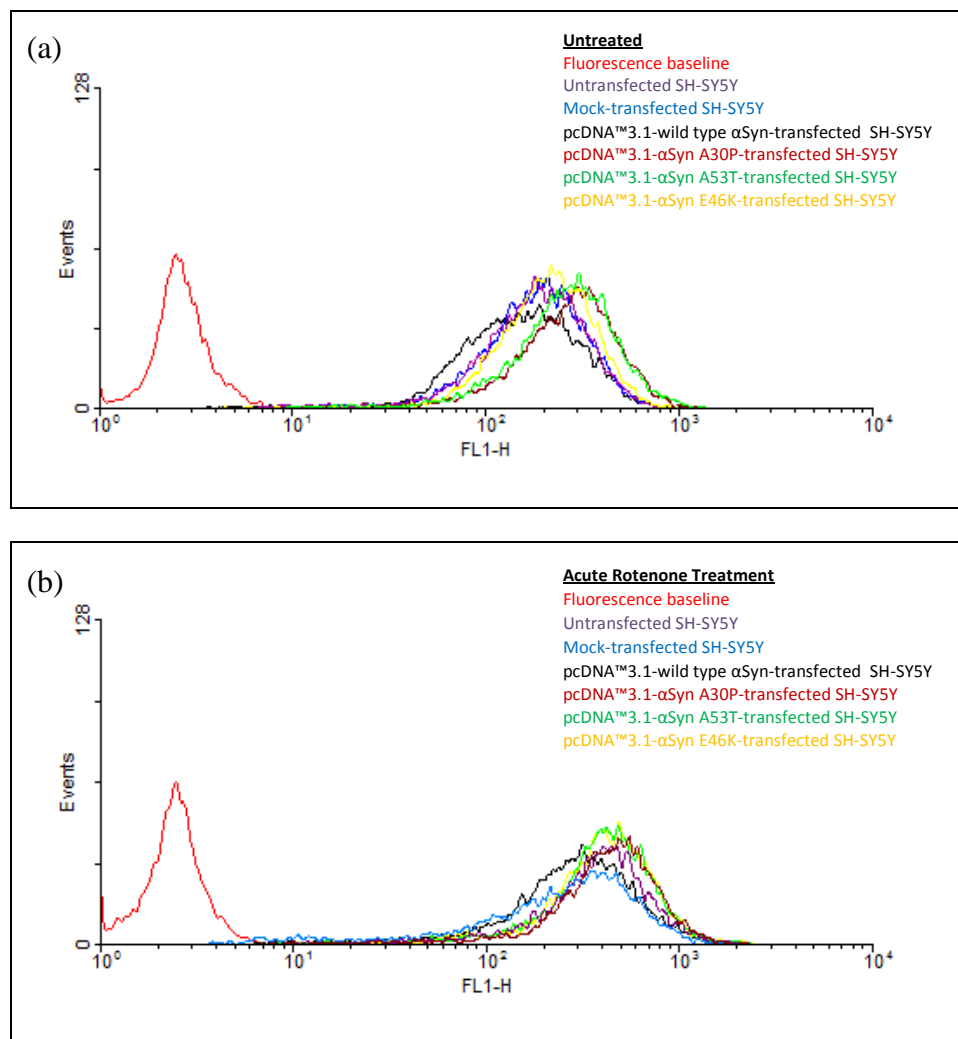


Figure 4.33: Legend on Page 130.

Figure 4.33 continued.

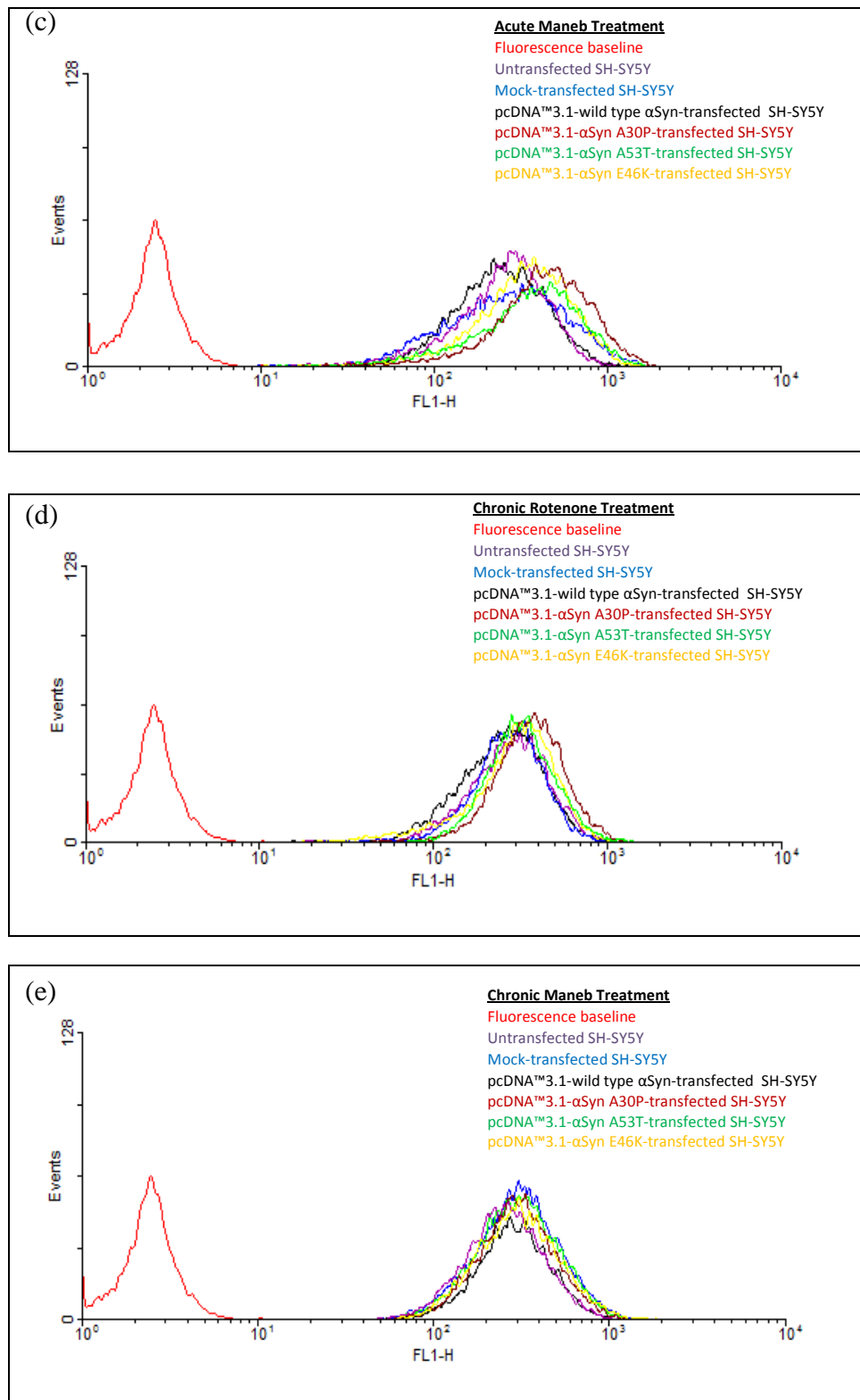
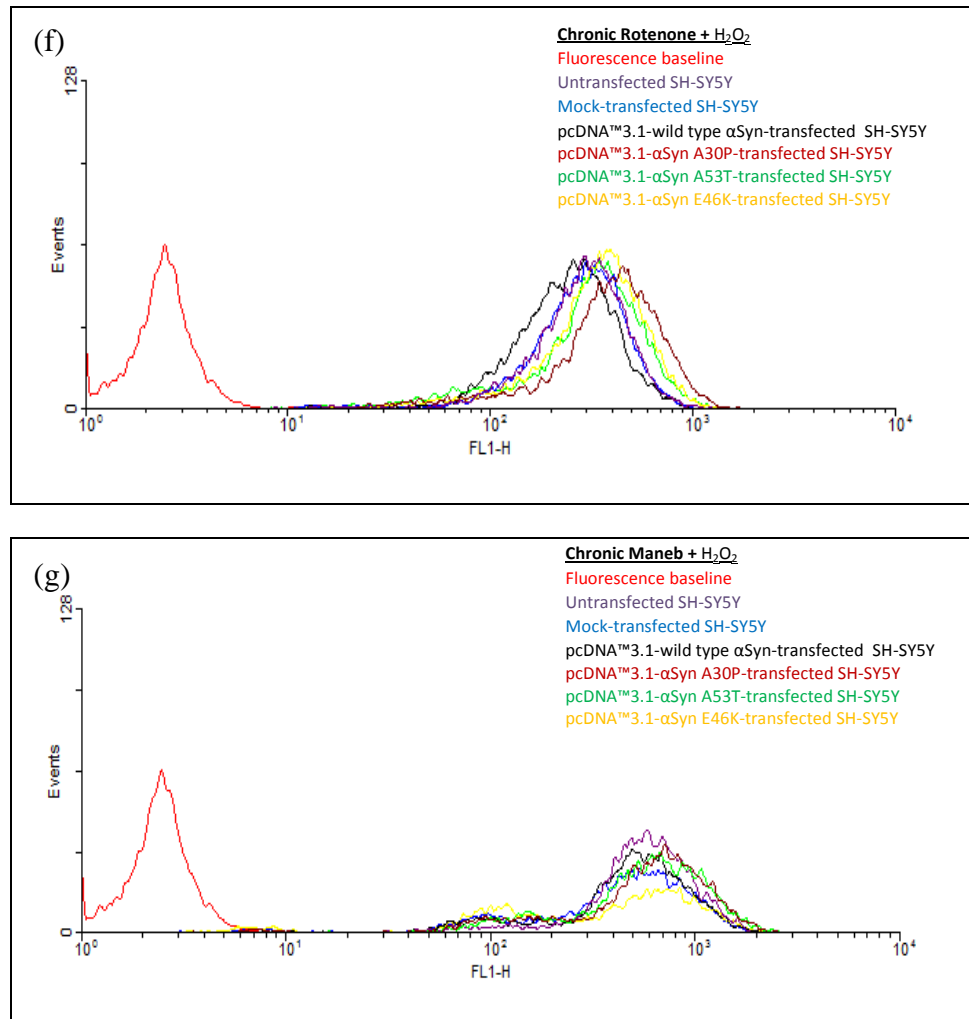
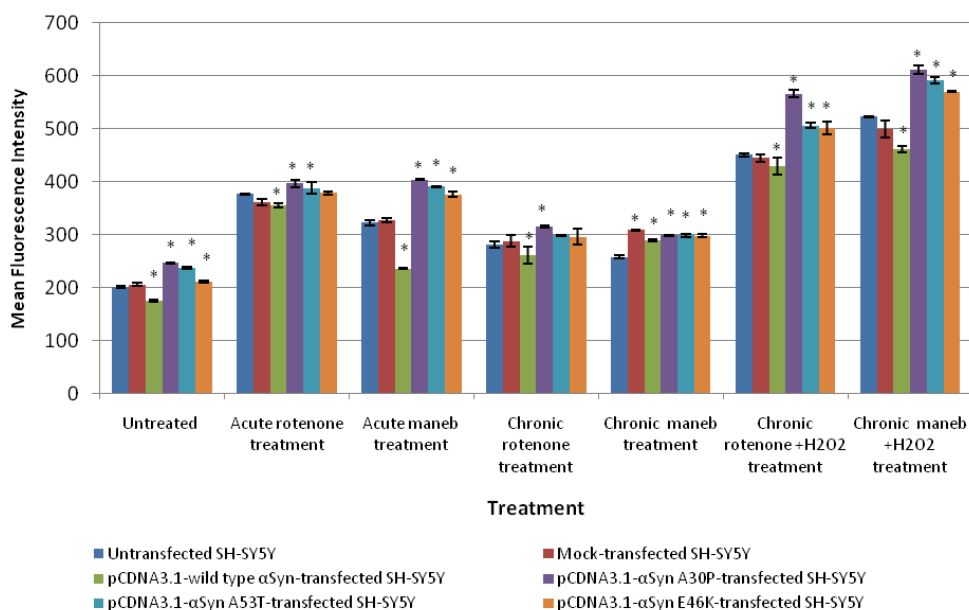


Figure 4.33: Legend on Page 130.

Figure 4.33 continued.



**Figure 4.33: Flow cytometric histograms of DCF show the effect of wild type and mutant  $\alpha$ -Syn on ROS generation of SH-SY5Y cells under various treatments.** (a) Untreated (b) Acute rotenone treatment (c) Acute mane b Treatment (d) Chronic rotenone treatment (e) Chronic mane b treatment (f) Chronic rotenone + H<sub>2</sub>O<sub>2</sub> (g) Chronic mane b + H<sub>2</sub>O<sub>2</sub>. After each treatment, cells were exposed to DCFH-DA, harvested and analysed by flow cytometry to determine the percentage of cells displaying an increase in ROS production (reflected by a rightward shift of the histogram). A representative histogram of three independent experiments is shown.



**Figure 4.34: Effect of wild type and mutant  $\alpha$ -Syn overexpression on ROS generation in SH-SY5Y cells.** Cells were incubated in drug-free or medium containing drugs/ $H_2O_2$  for a specific period of time, followed by DCFH-DA staining and flow cytometric analysis. Data represent mean  $\pm$  S.E.M of three separate experiments. \* means  $p < 0.05$ , compared with untransfected SH-SY5Y cells under the same treatment condition by one-way-ANOVA.

#### 4.5.6 Differential effects of overexpression of wild type and mutant human $\alpha$ -Syn on rotenone and maneb-induced mitochondrial membrane potential changes ( $\Delta\Psi_m$ ) in SH-SY5Y cells

In order to explore changes in mitochondrial function, the mitochondrial membrane potential ( $\Psi_m$ ) dissipation was measured by flow cytometry after exposing the cells to fluorescent probe, DiOC6(3). The polarisation status of the mitochondrial membrane is determined by an electrochemical gradient. Activation of the intrinsic (mitochondrial) apoptotic pathway can be assessed indirectly by determining whether the  $\Psi_m$  is reduced. In this procedure, cells were incubated with a lipophilic cation fluorochrome, DiOC6(3), which would accumulate in the mitochondrial matrix, driven by the  $\Psi_m$ . A reduction in fluorescence intensity indicated  $\Psi_m$  dissipation (Figure 4.35) and, therefore, the

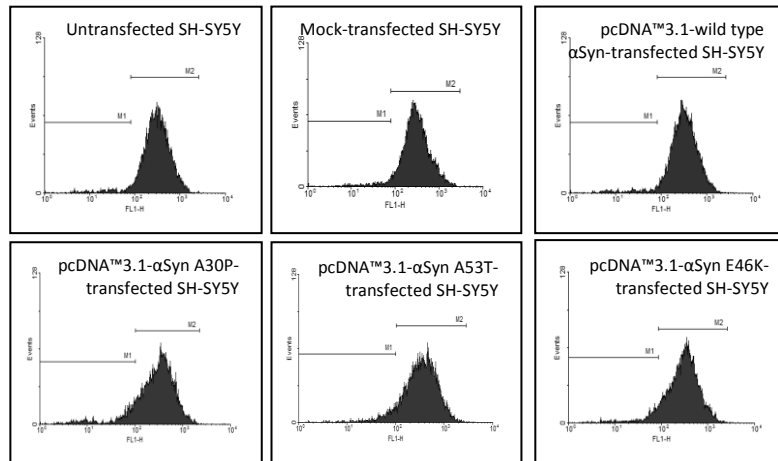
activation of the intrinsic apoptosis pathway (Charlot, Pretet, Haughey, & Mougin, 2004).

As shown in Figure 4.36, for SH-SY5Y cells overexpressing wild type  $\alpha$ -Syn, the percentage of cells showing low  $\Psi_m$  were either significantly lower after acute rotenone, chronic maneb and  $H_2O_2$  insult following chronic maneb treatment or of no significant difference following acute maneb, chronic rotenone and  $H_2O_2$  insult following chronic rotenone treatment, as compared to untransfected cells. The result showed that wild type  $\alpha$ -Syn expression prevented disruption of  $\Psi_m$ .

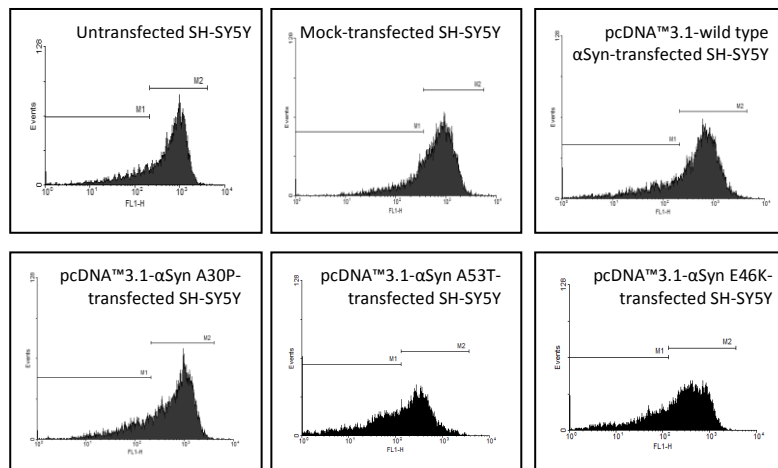
Generally, proportion of mutant A30P-transfected SH-SY5Y cells showing disrupted  $\Psi_m$  was greater than that of control under each treatment. However, the differences were only significant in cases of acute maneb, chronic maneb, chronic rotenone +  $H_2O_2$  and chronic maneb +  $H_2O_2$ .

For mutant A53T or E46K-transfected SH-SY5Y cells, proportion of cells with disrupted  $\Psi_m$  was significantly greater than that of control following each treatment. These data suggest that wild type  $\alpha$ -Syn but not mutant variants preserves the mitochondrial membrane potential in conditions known to compromise mitochondrial integrity thus protecting cells against apoptosis.

(a)



(b)



(c)

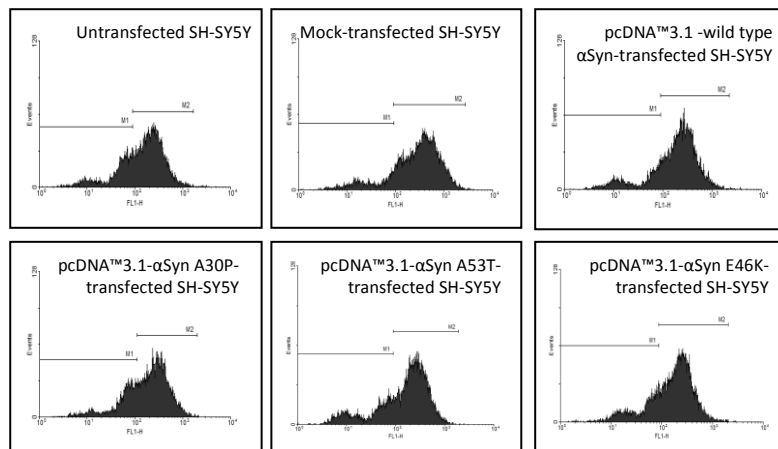
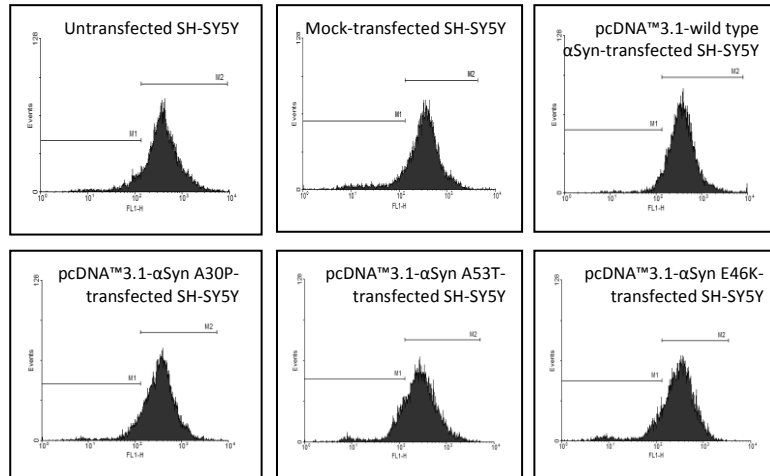


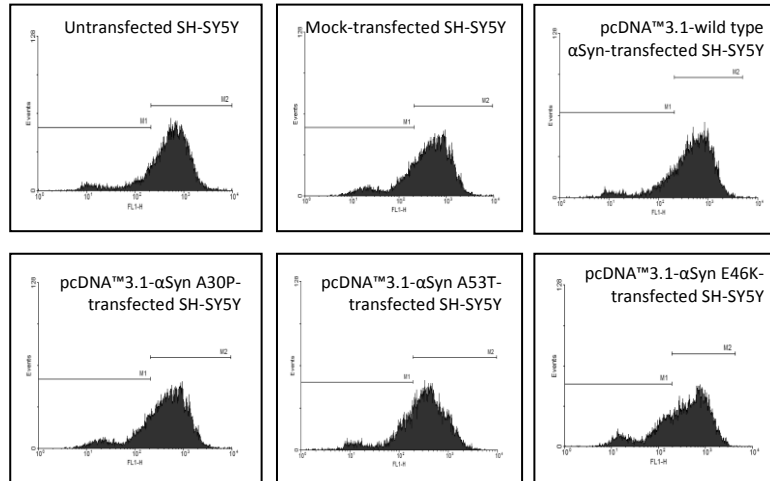
Figure 4.35: Legend on Page 135.

Figure 4.35 continued.

(d)



(e)



(f)

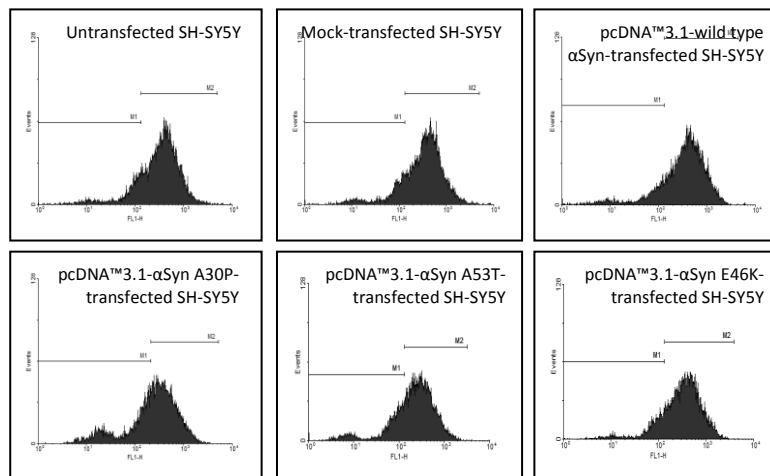
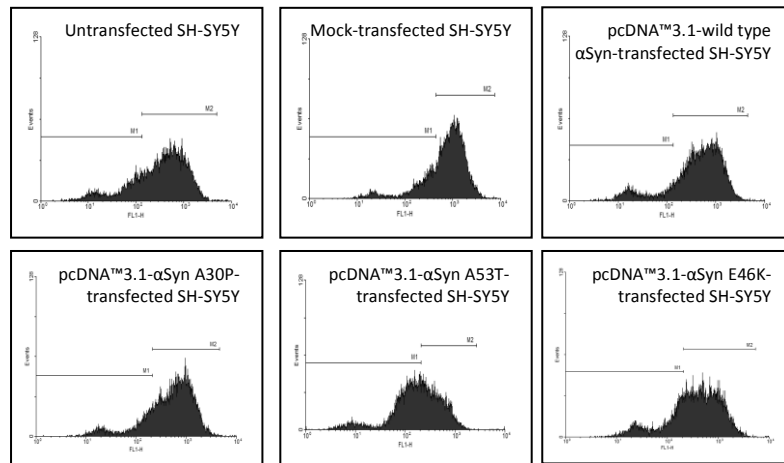


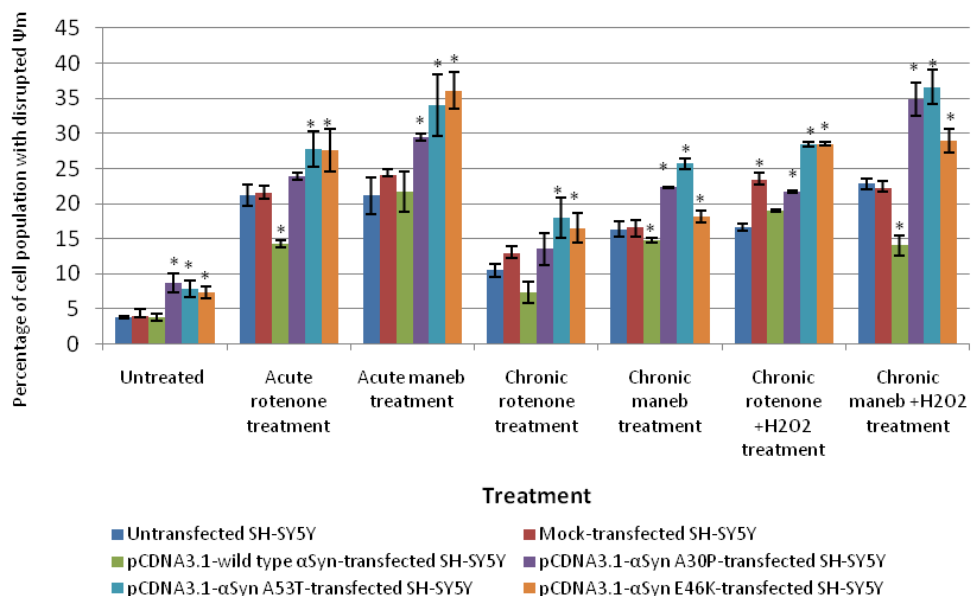
Figure 4.35: Legend on Page 135.

Figure 4.35 continued.

(g)



**Figure 4.35: Histograms of DiOC6(3) fluorescence, indicative of mitochondrial membrane potential changes ( $\Psi_m$ ).** SH-SY5Y cell lines were subjected to various treatments, (a) Untreated (b) Acute rotenone (c) Acute maneb (d) Chronic rotenone (e) Chronic rotenone +  $H_2O_2$  treatment (f) Chronic maneb (g) Chronic maneb +  $H_2O_2$  treatment and stained with DiOC6(3) prior to flow cytometry analysis. The M1 and M2 gates demarcate cell population with disrupted  $\Psi_m$  or with normal  $\Psi_m$  respectively. Representative histograms from one experiment are shown.



**Figure 4.36: Effects of wild type and mutant  $\alpha$ -Syn overexpression on mitochondrial membrane potential changes ( $\Delta\Psi_m$ ).** SH-SY5Y cell lines were subjected to various treatments and were stained with DiOC6(3). The intensity of fluorescence was evaluated by flow cytometry. Cells with a depolarisation of mitochondrial membrane showed a lower fluorescence compared with the control. Data represent percentage of cells with disrupted  $\Psi_m \pm$  S.E.M of three separate experiments. \* means  $p < 0.05$  compared to untransfected SH-SY5Y under corresponding treatment by one-way-ANOVA.

## CHAPTER 5

### DISCUSSION

#### 5.1 Gene silencing using RNA interference

##### 5.1.1 Knockdown efficiency of short hairpin RNAs

This study demonstrates that among the three shRNAs specially targeting  $\alpha$ -Syn mRNA, HuAsynRNAi3 appeared to be more effective than HuAsynRNAi1 and HuAsynRNAi2 in  $\alpha$ -Syn gene silencing. This might be related to the nature of the shRNA target sequence. Although the three target sequences have been verified to bear no homology to any sequence in the human genome database with their transcripts shRNA expected to have no interference on human genes, HuAsynRNAi3 which targeted the sequence, 5'-AAGGACCAGTTGGGCAAGAAT-3' might have minimised degradation of "off-target" mRNAs to the greatest extent while maximising the specific gene knockdown. Furthermore, this sequence has been confirmed to be valid for  $\alpha$ -Syn gene silencing by two previous reports (Sapru et al., 2006; Wu et al., 2009).

Moreover, one could speculate that the energy profile and secondary structure might influence the efficacy of shRNAs, as reported by Zhou and Zeng (2009). Functional shRNAs prefer high free energy states at both terminals. High free energy states of the two terminals were found to be the largest positive impact factor on shRNA efficacy. In addition, the accessibility of the 3' terminal is another key factor to shRNA effectiveness. Internal palindrome helps RNA molecules to form secondary structures. It was found that presence of more

possible palindromes involving the 3' terminal renders the shRNA to be less efficient as RNA secondary structure formed could limit the accessibility of the terminal and negatively impact shRNA efficacy (Zhou & Zeng, 2009).

Another determinant that affects the efficacy of these three shRNAs might be related to the properties of the target mRNA. It is suggested that extensive secondary structure in the mRNA, the presence of RNA-associated proteins and the specific subcellular localisation of the mRNA may render the transcript inaccessible to siRNA-incorporated RISC binding (Holen, Amarzguioui, Wiiger, Babaie, & Prydz, 2002).

### **5.1.2 Advantages of using shRNA versus siRNA**

In this study, stable  $\alpha$ -Syn gene silencing using shRNA-incorporated plasmids followed by puromycin selection was chosen to allow long-term knockdown studies. After stable transfection, the shRNA-incorporated plasmid gets randomly integrated into the genome and passed down to daughter cells after replication, allowing gene silencing to be inherited (Paddison, 2008).

Transfection of siRNA into cultured cells provides a fast and effective but only a short-term decrease in target gene expression. If the silencing effect is to be continuously seen, one would have to transfect it constantly, as siRNA gets degraded in the cells after a few days as it does not get passed down after cell division. This is consumable and expensive for large and continuous experiments (Donze & Picard, 2002).

Moreover, siRNA oligonucleotides are not applicable for many difficult-to-transfect cells types including SH-SY5Y cell line which was used in this study, as high transfection efficiency is required for effective knockdown. On the contrary, plasmids or viruses can deliver shRNA into any cell type and 100% transduction is possible when using viral delivery. Furthermore, plasmid vectors cloned with shRNA are economical as the integrated constructs provide an endless source of RNAi for stable knockdown (Clontech, 2008).

Usage of endogenous processing systems also gives shRNA an advantage over siRNA in terms of the propensity for induction of interferon response. However, its over-saturation of these systems has been shown to have other consequences that are more easily avoided by siRNA (Grimm et al., 2006). Overall, compared to siRNA, shRNA offers advantages in silencing longevity, delivery options and cost and hence it was chosen to be used in this study.

## **5.2 Assessment of anti-apoptotic property of $\alpha$ -Syn in both human melanoma and neuronal cell lines**

The role of  $\alpha$ -Syn has become an issue of debate as it remains contentious whether  $\alpha$ -Syn is cyto-toxic or cyto-protective. This study first analysed the possible cyto-toxic/-protective roles of  $\alpha$ -Syn in human melanoma, SK-MEL28 and neuronal, SH-SY5Y cells, by knockdown and overexpression, respectively and subjecting the cells to treatment of an apoptotic inducer, staurosporine.

### **5.2.1 Anti-apoptotic effect of $\alpha$ -Syn in human melanoma, SK-MEL28**

The main novel finding of the present study is that the endogenously high expression of  $\alpha$ -Syn is essential for survival of SK-MEL28 cells as its gene silencing by shRNA interference resulted in enhanced staurosporine-induced cyto-toxicity with greater levels of Bax/Bcl-2 and Bax/Bcl-xL ratios and cleaved caspase 9.  $\alpha$ -Syn is only recently discovered to be highly expressed in cancer cells. Therefore not many studies have elucidated its anti-apoptotic property in cancer cells. The protective effect shown by endogenously strong  $\alpha$ -Syn expression in SK-MEL28 cells against staurosporine toxicity can only be generally related to the well-known studies of another Synuclein family member,  $\gamma$ -Syn, which plays vital role in oncogenesis and to the anti-apoptotic property of  $\alpha$ -Syn in neuronal cell lines.

Both  $\alpha$ -Syn and  $\gamma$ -Syn share substantial sequence homology as each has a series of loosely repeated motifs throughout the first 93 amino acids and an acid region toward the C-terminal (Lavedan, 1998).  $\gamma$ -Syn has been reported to be 50% identical and 74% homologous to  $\alpha$ -Syn (Czekierdowski & Czekierdowska, 2007) (Figure 5.1). It was demonstrated that  $\alpha$ -Syn is highly expressed in the human melanoma cell line, SK-MEL28 but it is undetectable in non-melanocytic cutaneous carcinoma and normal cells (Matsuo & Kamitani, 2010). Whilst  $\gamma$ -Syn, initially termed as Breast Cancer-specific Gene 1, has been found at abundance levels in majority of advance-stage breast, ovarian, gastric, liver, colorectal, uterine and lung cancers, compared to its almost undetectable levels in normal or benign counterparts (Bruening et al., 2000;

Liu, Zhou, Boggs, Belinsky, & Liu, 2007; Morgan et al., 2009; Yanagawa et al., 2004; Ye et al., 2008; Zhao et al., 2006).

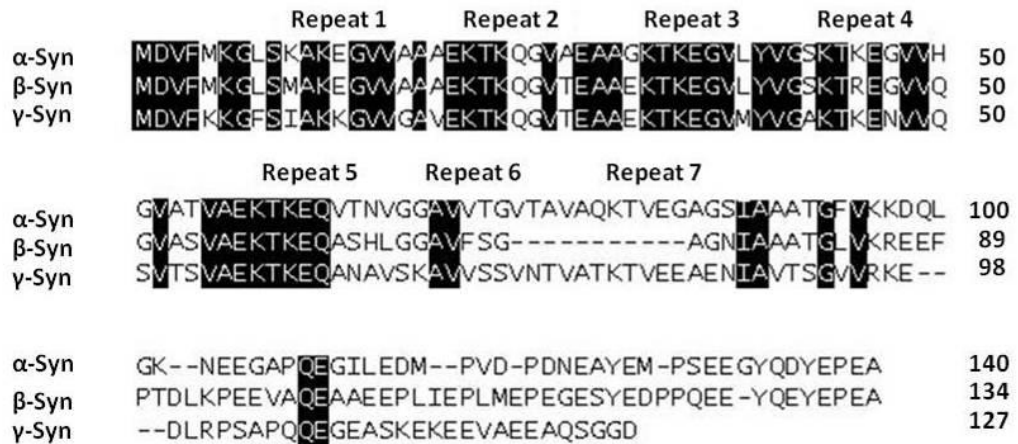


**Figure 5.1: Protein alignment for the human Synuclein proteins.** The highlighted regions indicated sequences conserved throughout the three Synuclein proteins. KTKEGV imperfect repeats are indicated (University of Pennsylvania Health System, 1999).

Oncogenic activation of  $\gamma$ -Syn was found to contribute to the development of breast and ovarian cancer by promoting tumour cell survival under adverse conditions and by providing resistance to certain chemotherapeutic drugs via modulation of MAPK pathway.  $\gamma$ -Syn is associated with two major MAPKs, i.e. ERK1/2 and JNK1, and it has been shown that overexpression of  $\gamma$ -Syn leads to constitutive activation of ERK1/2 and down-regulation of JNK1 in response to a host of environmental stress signals (Pan, Bruening, Giasson, Lee, & Godwin, 2002). Knockdown of  $\gamma$ -Syn sensitised human breast cancer cells to endoplasmic reticulum stress-induced apoptosis. Induction of apoptosis by endoplasmic reticulum stress when  $\gamma$ -Syn was down-regulated was reported to be dependent on modulation of JNK or involvement of caspase 3 and 7 activation (Hua et al., 2009). These data suggest that the up-regulation of both

$\alpha$ - and  $\gamma$ -Syn expression in these human malignancies promotes increase in cancer cell motility and disease progression. The mechanism underlying the anti-apoptotic effect of cellular  $\alpha$ -Syn in SK-MEL28 cells against staurosporine could be linked to the activation of ERK1/2 and down-regulation of JNK1, similar to that of  $\gamma$ -Syn in various malignancies.

### **5.2.2 Proposed anti-apoptotic and apoptotic mechanisms of wild type $\alpha$ -Syn**

The precise cellular mechanism underlying the anti-apoptotic function of  $\alpha$ -Syn remains to be elucidated. However, one could postulate on the involvement of the chaperoning property of  $\alpha$ -Syn. Studies have shown that  $\alpha$ -Syn shares a physical and functional homology with the chaperone protein 14-3-3; and its interactions with various cellular proteins like dephosphorylated Bad, protein kinase C (Ostrerova et al., 1999), tyrosine hydroxylase, the dopamine transporter Elk-1 (Iwata et al., 2001), ERK, PI3/Akt kinase (Seo et al., 2002), and cytochrome *c* (Gomez-Santos et al., 2002) have been thus far well established. These further support the concept that  $\alpha$ -Syn might counteract the activation of cell death signalling molecules during apoptotic insult.

To date, studies have suggested that the anti-apoptotic effect of wild type  $\alpha$ -Syn seems to be mediated through a variety of factor including decreased expression of p53 (Da Costa et al., 2002), a stimulation of the PI3/Akt signalling pathway (Seo et al., 2002), inactivation of JNK (Hashimoto et al. 2002), an increase in the expression levels of the anti-apoptotic protein Bcl-2, and an inhibition of the activity of pro-apoptotic proteins (Sidhu et al., 2004c)

(Figure 5.2). Thus, one could speculate that these few mechanisms might at least in some part be accounted for the anti-apoptotic properties exhibited by wild type  $\alpha$ -Syn against staurosporine treatment in this current study.

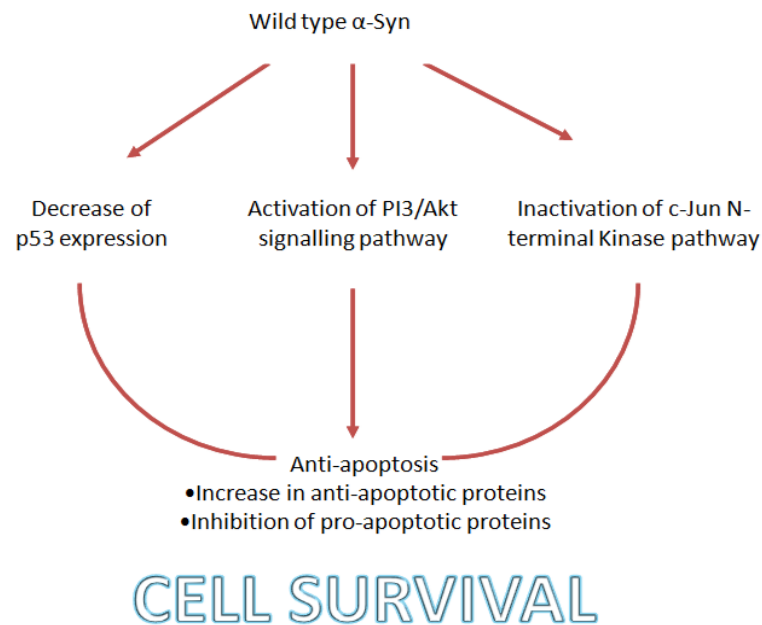


**Figure 5.2: A schematic representation of the anti-apoptotic mechanisms exhibited by wild type  $\alpha$ -Syn in previous literatures, which eventually lead to cell survival (Taken from Da Costa et al., 2002; Seo et al., 2002; Hashimoto et al. 2002; Sidhu et al., 2004c).**

However, clouding this issue are some studies reporting the toxicity of  $\alpha$ -Syn overexpression in a dopamine-dependent manner. Xu et al. (2002) reported that accumulation of  $\alpha$ -Syn in cultured human dopaminergic neurons results in apoptosis whereas in non-dopaminergic human cortical neurons,  $\alpha$ -Syn is not toxic but rather exhibits neuroprotective activity. Moreover, this dopamine-dependent neurotoxicity is mediated by 54-83 kDa soluble protein complexes that contain  $\alpha$ -Syn and 14-3-3 protein, a conserved regulatory molecule expressed in all eukaryotic cells. A recent study done by Bisaglia et al. (2010) also showed that  $\alpha$ -Syn overexpression increases dopamine toxicity in

dopaminergic BE(2)-M17 cells. Yet contrary to the above-mentioned dopamine-dependent toxicity,  $\alpha$ -Syn was shown to protect SH-SY5Y cells from dopamine toxicity (Colapinto et al., 2006).

The observed discrepancies among the findings of current and previous studies are likely to be due to the fact that different cell lines,  $\alpha$ -Syn overexpression mode (transient, inducible or stable), cell death-triggering agents, treatment conditions and choice of cyto-toxicity assay were used.

### **5.2.3 Differential effects of wild type and mutant $\alpha$ -Syn on human neuronal, SH-SY5Y following staurosporine treatment**

The present study also provides direct evidence by which cell viability comparison of wild type and mutant  $\alpha$ -Syn-expressing SH-SY5Y neuronal cells using MTT assay indicated that the former exhibited much less vulnerability while the latter were more sensitive in response to staurosporine toxicity.

In support of these data, a previous study demonstrates that wild type  $\alpha$ -Syn exerts an anti-apoptotic effect by drastically reducing the caspase 3 activation of TSM1 neocortical cell line upon three distinct apoptotic stimuli including staurosporine, etoposide, and ceramide C(2). This inhibitory control of the caspase response triggered by apoptotic agents was abolished by the PD-related pathogenic mutation A53T (Da Costa et al., 2000). Later on, another study done by Da Costa et al. (2002) also showed that  $\alpha$ -Syn drastically lowers basal and staurosporine-stimulated DNA fragmentation and number of terminal

deoxynucleotide transferase-mediated dUTP nick end labeling (TUNEL)-positive neurons. Interestingly,  $\alpha$ -Syn also diminishes both expression and transcriptional activity of p53, a tumour suppressor gene (Da Costa et al., 2002). Moreover, Hunya et al. (2008) reported that  $\alpha$ -Syn overexpression protects SH-SY5Y cells from classical apoptotic factors, amphotericin B and ruthenium red. On the other hand, overexpression of the mutant forms of  $\alpha$ -Syn (A30P and A53T) was found to sensitise ND7 neuronal cells to the effects of staurosporine (Zourlidou, Payne Smith, & Latchman, 2003).

#### **5.2.4 Modulation of expression levels of apoptotic markers by wild type and mutant $\alpha$ -Syn in SH-SY5Y**

This study demonstrates that wild type  $\alpha$ -Syn overexpression led to greater basal Bcl-2 and Bcl-xL levels in SH-SY5Y. Following staurosporine treatment, wild type  $\alpha$ -Syn overexpression suppressed Bax expression and thereby reduced the Bax/Bcl-2 and Bax/Bcl-xL ratios in SH-SY5Y, in accordance with its protective effect against staurosporine-induced cell death. This might be attributed to (1) the down-regulation of p53 expression as it has been reported that p53 directly up-regulates the transcriptional expression of Bax and indirectly down-regulates the expression of Bcl-2 (Miyashita et al., 1994) and (2) activation of PI3/Akt signalling pathway as it was previously reported that activated Akt stimulated changes in Bcl-2 and Bax expression and showed an anti-apoptotic effect in several different neuronal cell types. Activation of Akt has been shown to lead to phosphorylation of Bad, decreasing interaction of Bad with Bcl-xL and increasing the Bcl-xL/Bad ratio, eventually promoting neuronal cell survival (Seo et al., 2002). Also, as Kim, Ryu, and Song (2006)

demonstrated that JNK and p38 kinase-mediated phosphorylation leads to activation of Bax after staurosporine treatment, the suppression of Bax level by wild type  $\alpha$ -Syn overexpression against staurosporine insult in this study might be related to the inactivation of JNK.

In contrast, this study reveals that following staurosporine treatment, mutant  $\alpha$ -Syn expression caused a significant increase in the pro-apoptotic Bax protein and decrease in the levels of anti-apoptotic Bcl-2 and Bcl-xL protein, thus shifting the previous Bax/Bcl-2 and Bax/Bcl-xL ratios in favour of apoptosis. Overexpression of mutant  $\alpha$ -Syn but not wild type  $\alpha$ -Syn was also shown to increase cleavage and activation of caspase 9 in SH-SY5Y in response to staurosporine treatment. The lack of regulation of caspase 9 by wild type  $\alpha$ -Syn is in agreement with the previous study which showed that the expression of wild type  $\alpha$ -Syn, but not A30P and A53T  $\alpha$ -Syn, protects neuronal cell lines from apoptotic cell death with attenuation of caspase 3 activity without affecting the caspase 9 activity or the levels of cleaved caspase 3 (Li & Lee, 2005). It has been reported that there is involvement of caspase 3 and 9 (two downstream effectors of mitochondrial-dependent apoptosis) activation in A53T  $\alpha$ -Syn-induced cell death whereby the use of z-DEVD and z-LEHD, inhibitors of caspase 3 and 9, respectively, significantly protected against A53T  $\alpha$ -Syn-induced cell death (Smith et al., 2005). PC12 cells expressing mutant  $\alpha$ -Syn (A30P and A53T) showed increased sensitivity to apoptotic cell death accompanied by elevation of caspase 3 and 9 when treated with sub-toxic concentrations of an exogenous proteasome inhibitor (Tanaka et al., 2001).

Altogether, these data indicate that wild type  $\alpha$ -Syn exerts an anti-apoptotic effect in neurons that appears to be abolished by the PD-related mutation.

A study done by Nagano et al. (2001) which examined the association between  $\alpha$ -Syn and the following Bcl-2 family proteins: Bcl-2, Bcl-xL and Bax, revealed that wild type or mutant (A30P and A53T)  $\alpha$ -Syn does not bind to any of these members of the Bcl-2 family. Overall, these findings imply that  $\alpha$ -Syn-dependent protection involve an overall  $\alpha$ -Syn-dependent alteration in the signalling events that are upstream of the apoptotic cascade.

### **5.2.5 Attributed reasons for differential toxicity conferred by wild type and mutant $\alpha$ -Syn**

Based on the result of this study, it could be noted that the SH-SY5Y cells expressing all three mutant  $\alpha$ -Syn were significantly more vulnerable to toxic stimuli than cells expressing wild type  $\alpha$ -Syn. In general, the strength of toxicity of the three mutants are in the order of A30P>A53T>E46K. One common molecular feature that is proposed to relate to the increased pathogenicity and that differentiates the mutant proteins from wild type  $\alpha$ -Syn is their propensity to more rapidly form dityrosine-linked dimers under oxidative conditions and to oligomerise more rapidly (Krishnan et al., 2003). Some oligomeric species with annular shapes, which are the most toxic species of  $\alpha$ -Syn might form pores on intracellular cell membrane and hence induced cell death via disruption of cellular ion homeostasis (Danzer et al., 2007). Moreover,  $\alpha$ -Syn aggregation/oligomerisation is tightly associated with impairment of microtubule-dependent intracellular trafficking, ER stress and

Golgi fragmentation which eventually lead to cell death (Gosavi, Lee, Lee, Patel, & Lee, 2002; Lee, Khoshaghideh, Lee, & Lee, 2006).

The A53T and E46K  $\alpha$ -Syn proteins show increased rates of self-assembly and fibril formation (Conway, Harper, & Lansbury, 1998). This is consistent with studies reporting that the A53T  $\alpha$ -Syn preferentially adopts a  $\beta$ -sheet conformation (Bussell & Eliezer, 2001). These *in vitro* data suggest that the A53T and E46K  $\alpha$ -Syn mutations could be pathogenic due to their increased propensity to form pathological inclusions (Waxman & Giasson, 2008). Greenbaum et al. (2005) reported that A53T mutant increased the propensity of  $\alpha$ -Syn to fibrillise to a greater extent than the E46K mutation and this might explain the greater toxic potency of A53T compared with E46K, as shown in this current study.

While all three PD-linked  $\alpha$ -Syn mutations accelerate the formation of  $\alpha$ -Syn protofibrils, the A30P mutation was shown to delay the formation of amyloid fibrils (Conway et al., 2000). In support of the findings of this study, this means that the A30P protofibrils may have a longer life time and thus cause greater cumulative damage than other mutants. In addition, the A30P mutation appears to affect  $\alpha$ -Syn properties independent of protein aggregation. The A30P mutation may partially impaired the ability of  $\alpha$ -Syn to bind to brain vesicles (Jensen, Nielsen, Jakes, Dotti, & Goedert, 1998), likely due to a decreased likelihood to form  $\alpha$ -helices but does not significantly prevent  $\alpha$ -Syn localisation to presynaptic terminals (Kahle et al., 2000). Studies in mice indicate that A30P mutation is deficient in the ability of refolding SNARE

proteins which may be due to its reduced ability to interact with vesicles (Kahle et al., 2000). This A30P mutation can also directly impair the *in vitro* chaperone-like activity of  $\alpha$ -Syn (Souza et al., 2000b).

Aberrant  $\alpha$ -Syn degradation is implicated in Parkinson's disease pathogenesis because the protein accumulates in the Lewy inclusion bodies associated with the disease. Cuervo, Stefanis, Fredenburg, Lansbury, and Sulzer (2004) found that wild type  $\alpha$ -Syn was selectively translocated into lysosomes for degradation by the chaperone-mediated autophagy pathway. The pathogenic A53T and A30P  $\alpha$ -Syn mutants bound to the receptor for this pathway on the lysosomal membrane, but appeared to act as uptake blockers, inhibiting both their own degradation and that of other substrates. These data underlie the toxic gain-of-function by the mutants.

To explain the anti-apoptotic function of wild type  $\alpha$ -Syn by its chaperone activity, one could therefore envision that, under physiological conditions, wild type  $\alpha$ -Syn interacts with cellular intermediates of the apoptotic pathways. It should be noted in support of this concept that at the cellular level,  $\alpha$ -Syn is almost exclusively found to be associated with normal neurons but not with those exhibiting an apoptotic phenotype (Kholodilov et al., 1999b). It has been demonstrated that  $\alpha$ -Syn expression was up-regulated in a target injury model, suggesting that this could correspond to a compensatory response of neurons designed to promote their survival, in agreement with a physiological anti-apoptotic function (Kholodilov, Oo, & Burke, 1999a). In this context, mutated  $\alpha$ -Syn could accelerate the cell death due to the absence of wild type  $\alpha$ -Syn-

mediated-neuroprotection to apoptotic stimuli. Moreover, mutated  $\alpha$ -Syn has higher propensity to aggregate (Narhi et al., 1999) and to impair the protein aggregates degradation pathways (Cuervo et al., 2004) and would further trigger apoptotic cell death when aggregated (El-Agnaf et al., 1998). The presence of  $\alpha$ -Syn mutants likely reflect a gain-of-toxicity rather than a loss-of-function of the  $\alpha$ -Syn proteins (Dev et al., 2003). This explains the greater apoptotic cell death of the mutant  $\alpha$ -Syn transfected SH-SY5Y cells after being subjected to staurosporine insult in this current study.

### **5.3 Role of $\alpha$ -Syn on cell proliferation rate**

In this study, we could observe that knockdown of  $\alpha$ -Syn in SK-MEL28 and overexpression of mutant  $\alpha$ -Syn in SH-SY5Y reduced the cell proliferative indices. In support of these findings, overexpression of  $\alpha$ -Syn in PC12 cells resulted in enhanced proliferation rate and enrichment of cells in the S phase of the cell cycle. This was associated with increased accumulation of the mitotic factor cyclin B, down-regulation of the tumour suppressor retinoblastoma 2 and increased phosphorylation of ERK1/2, the key molecules in proliferation signalling (Lee et al., 2003). Moreover, it has been reported that wild type  $\alpha$ -Syn expression can lead to a decrease in expression of p53 (Da Costa et al., 2002). p53 can induce growth arrest by holding the cell cycle at the G<sub>1</sub>/S regulation point. Activated p53 binds to DNA and activates expression of several genes including WAF1/CIP1 encoding for p21. p21 then binds to the G<sub>1</sub>-S/CDK (CDK2) and S/CDK complexes (molecules important for the G<sub>1</sub>/S transition in the cell cycle) and inhibit their activity (Levine, 1997). The decreased proliferative indices caused by mutant  $\alpha$ -Syn may reflect the loss of

proliferative activity conferred by wild type  $\alpha$ -Syn. This study may have been an initial attempt in reporting the effect of mutant  $\alpha$ -Syn on cell cycle indices as there is no related previous literature. Therefore, it is suggested that wild type but not mutant  $\alpha$ -Syn expression could promote  $G_0/G_1$  to S transition and  $G_2/M$  and thus contribute to enhanced proliferation rate.

#### **5.4 $G_2/M$ phase arrest caused by staurosporine**

This study demonstrates that staurosporine treatment arrested both SK-MEL28 and SH-SY5Y cells in the  $G_2/M$  phase. Wang et al. (2004) reported that treatment with staurosporine led to a marked decrease in the cellular levels of Cdc2 protein and a small decrease in the levels of cyclin B. Decrease in protein levels of proliferating cell nuclear antigen (PCNA) and Cdc25C was also observed at the high concentration of staurosporine treatment. Moreover, staurosporine is found to be a potent inhibitor of  $p34^{cdc2}$  and  $p34^{cdc2}$ -like kinases and  $G_2/M$  phase arrest caused by staurosporine is due, at least in part, to the inhibition of the  $p34^{cdc2}$  kinases (Gadbois, Hamaguchi, Swank, & Bradbury, 1992). The accumulation of staurosporine-treated cells in the  $G_2/M$  phase in this study might be associated with the regulation of cell cycle related proteins. However, the exact mechanism was not examined in present study.

#### **5.5 $\alpha$ -Syn (gene) and toxicants (environmental) interactions in *in vitro* Parkinsonian SH-SY5Y cell culture model**

Parkinson's disease is likely to be caused by a combination of environmental exposures and genetic susceptibilities. Mitochondrial impairment at complex I, oxidative stress,  $\alpha$ -Syn aggregation and dysfunctional protein degradation have

been implicated in PD pathogenesis, but how they are related to each other is unclear (Waxman & Giasson, 2008). In this study, to further evaluate the pathogenesis of Parkinson's disease, human neuroblastoma SH-SY5Y cells were used as *in vitro* models which introduced both genetic factor ( $\alpha$ -Syn) and environmental factor (rotenone and maneb). This study investigated the effects of  $\alpha$ -Syn on SH-SY5Y cells after exposure to rotenone and maneb and the result might further extend fundamental understanding of the function of  $\alpha$ -Syn, in terms of both physiology and pathology.

The findings of this study indicate that wild type  $\alpha$ -Syn attenuated rotenone and maneb-induced cell death accompanied with reduced  $\Delta\Psi_m$  and ROS level whereas the mutant  $\alpha$ -Syn constructs exacerbated environmental toxins-induced cyto-toxicity in SH-SY5Y with augmented  $\Delta\Psi_m$  and ROS level. Several previous studies further support the protective role of wild type  $\alpha$ -Syn against environmental toxins. Jensen, Alter, and Omalley (2003) showed that wild type  $\alpha$ -Syn, but not its A30P or A53T mutants, can protect non-differentiated central nervous system dopaminergic cells from the neurotoxicity induced by either 1-Methyl-4-Phenylpyridinium ( $MPP^+$ ) (a metabolite of MPTP) or rotenone, the inhibitors of mitochondrial complex I that have been linked to the development of PD-like syndromes. Zhou et al. (2006) reported that the overexpression of mutants enhances toxicity of  $MPP^+$  and 6-OHDA in dopaminergic MN9D cells, whereas overexpression of wild type  $\alpha$ -Syn protected MN9D cells against  $MPP^+$  toxicity, but not against 6-OHDA. Furthermore,  $\alpha$ -Syn was reported to have the ability to interact with the pro-apoptotic proteins PKC $\delta$  and Bad following  $MPP^+$  treatment (Kaul,

Anantharam, Kanthasamy, & Kanthasamy, 2005). The association of  $\alpha$ -Syn with Bad in a stimulus-dependent manner may inhibit the pro-apoptotic functions of Bad. As shown in Figure 5.3, translocation of unphosphorylated Bad to the mitochondria is a prerequisite for the release of cytochrome *c* to initiate the apoptotic pathway. The observed decrease in cytochrome *c* release from  $\alpha$ -Syn cells has been attributed to the interaction of Bad and  $\alpha$ -Syn. Cytochrome *c*-mediated activation of caspase 3 is subsequently blocked and caspase 3-mediated proteolytic cleavage of PKC $\delta$  is attenuated.  $\alpha$ -Syn also binds to the pro-apoptotic kinase PKC $\delta$  and prevents proteolytic cleavage of PKC $\delta$  which significantly attenuates DNA fragmentation and cellular apoptosis (Kaul et al., 2005).

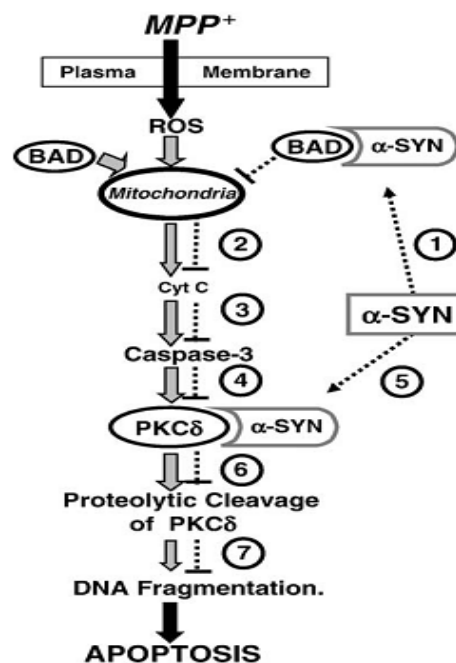


**Figure 5.3: A schematic model of  $\alpha$ -Syn-mediated dopaminergic protection from  $MPP^+$ -induced cyto-toxicity.** (1) Upon exposure to  $MPP^+$ ,  $\alpha$ -Syn binds to Bad in the cytoplasm and prevents its translocation to the mitochondria; (2) Bad-induced cytochrome *c* release is inhibited; (3) cytochrome *c*-mediated activation of caspase 3 is subsequently blocked; (4) caspase 3-mediated proteolytic cleavage of PKC $\delta$  is attenuated; (5)  $\alpha$ -Syn also binds to the pro-apoptotic kinase PKC $\delta$  and (6) prevents proteolytic cleavage of PKC $\delta$  which then attenuates (7) DNA fragmentation and cellular apoptosis (Kaul et al., 2005).

### **5.5.1 Possible mechanisms of rotenone and maneb-induced cell death**

Rotenone, known to inhibit mitochondrial complex I, induces apoptosis via activation of Bad in human dopaminergic SH-SY5Y cells. In rotenone-induced cell death, rotenone induced Bad dephosphorylation without changing the amount of Bad proteins (Watabe & Nakaki, 2004). In support of the results in this study, it is postulated that the wild type  $\alpha$ -Syn can interact with the dephosphorylated Bad and thereby displays protective effect against rotenone-induced cell death by suppressing translocation of dephosphorylated Bad to the mitochondria, subsequent release of cytochrome *c* and initiation of apoptotic pathway (Kaul et al., 2005).

Furthermore, rotenone has been shown to induce apoptosis in SH-SY5Y cells in a caspase-dependent way and through phosphorylation of c-Jun, JNK, and the p38 MAPK, indicative of activation of the p38 and JNK pathways (Newhouse et al., 2004). As previously reported, increased  $\alpha$ -Syn expression might protect cells from oxidative stress by inactivation of JNK via increased expression of scaffold protein c-Jun N-terminal kinase interacting protein-1/Islet-Brain1 (JIP-1b/IB1) (Hashimoto et al., 2002). In addition, a study showed that increased JIP-1b/IB1 expression protected dopaminergic cells from the PD-associated neurotoxin, MPTP (Xia et al., 2001). It is suggested that overexpression of wild type  $\alpha$ -Syn might protect neuronal cells against rotenone-induced damage by down-regulating the JNK pathway. However, these possibilities in current system would require further investigations.

Maneb has been reported to cause deleterious effects on dopaminergic cells at high concentration as it promotes the oxidation of catechols like dopamine, production of ROS and disruption of cellular antioxidant GSH system (Fitsanakis et al., 2002). In this current study, MTT assay showed that wild type  $\alpha$ -Syn gave protection whereas mutant  $\alpha$ -Syn enhanced the maneb-induced cell death in dopaminergic SH-SY5Y cells. One could speculate that the presence of wild type  $\alpha$ -Syn might tend to turn down the amount of cytoplasmic dopamine in dopaminergic nerve terminals, thereby limiting its conversion to highly reactive oxidative species and the resulting oxidative stress and partially protects from maneb induced-cell death. In contrast, in dopaminergic SH-SY5Y cells expressing mutant  $\alpha$ -Syn (A30P, A53T and E46K), a prior depletion of GSH would further impair the ability of the cellular system to recover after maneb was administered (Barlow et al., 2005).

### **5.5.2 Decreased basal level ROS in wild type $\alpha$ -Syn-transfected SH-SY5Y**

There were extensive previous studies reporting that  $\alpha$ -Syn increases intracellular ROS levels. Turnbull et al. (2001) reported that both solutions of full-length and a synthetic NAC peptide fragment of  $\alpha$ -Syn liberate  $H_2O_2$  and hydroxyl radicals upon incubation *in vitro* followed by addition of  $Fe^{2+}$ . Tabner, Turnbull, El-Agnaf, and Allsop (2002) further extended the study and suggested that  $H_2O_2$  accumulates by a metal-dependent mechanism during the incubation of  $\alpha$ -Syn and is subsequently converted to hydroxyl radicals upon addition of  $Fe^{2+}$  by Fenton's reaction. Junn and Mouradian (2002) also showed that all SH-SY5Y cell lines overexpressing wild type and particularly the two

mutant forms of  $\alpha$ -Syn (A30P and A53T) had increased ROS levels relative to control.

However in contrast to the above findings, the present study showed that untreated wild type  $\alpha$ -Syn-transfected SH-SY5Y had lower basal ROS level whereas untreated mutant  $\alpha$ -Syn-transfected SH-SY5Y had higher basal ROS level, compared to untransfected cells. The reasons for causing the discrepancy between these results with those of the above might be the different experimental methodologies used, including the usage of synthetic  $\alpha$ -Syn peptide, ferrous iron treatment, electron spin resonance spectroscopy for detection of free radicals and different expression plasmid.

### **5.5.3 Role of wild type $\alpha$ -Syn in counteracting rotenone- and maneb-mediated reactive oxygen species generation**

In order to explain the finding about suppression of basal ROS by wild type  $\alpha$ -Syn in SH-SY5Y cells, one could relate it to the physiological role of  $\alpha$ -Syn. As depicted in Figure 5.4, dopamine is synthesised in the cytoplasm and immediately sequestered into monoaminergic vesicles. If unstored, metabolism of free intracellular dopamine by monoamine oxidases produces  $H_2O_2$  and an inert metabolite, 3,4-dihydroxyphenylacetic acid (DOPAC) while its spontaneous autoxidation at normal intracellular pH that is, out of the acidic storage vesicles produces toxic and reactive dopamine-quinones, superoxide free radicals and  $H_2O_2$ .  $\alpha$ -Syn is highly enriched in presynaptic terminals, where 50% of it is associated with synaptic membranes and the other 50% is cytosolic. An important neuronal function of  $\alpha$ -Syn might be to regulate the

formation of synaptic vesicles from early endosomes through interactions with phospholipase D2 (PLD2). The A30P mutation abolishes the protein's ability to bind to small phospholipid vesicles, whereas the A53T mutation impairs its association with planar lipid membranes. Hence, mutations in  $\alpha$ -Syn might result in a reduced number of vesicles being available for dopamine storage, leading to an accumulation of free cytosolic dopamine and increased levels of basal oxidative stress (Lotharius & Brundin, 2002).

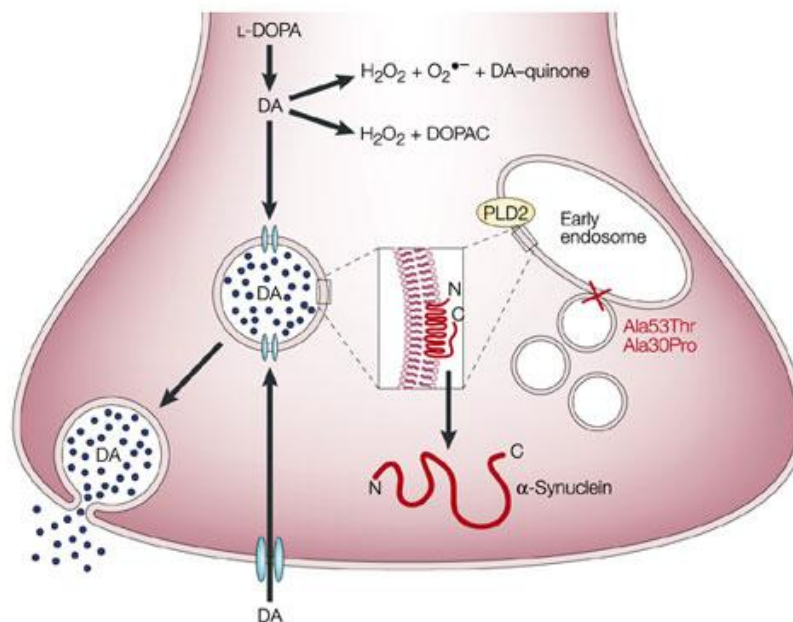


**Figure 5.4: A presynaptic terminal from a dopaminergic neuron depicting the potential function of  $\alpha$ -Syn in intracellular dopamine storage (Lotharius & Brundin, 2002).**

The result of this study also shows that both acute and chronic rotenone and maneb treatments caused ROS generation. Wild type  $\alpha$ -Syn blocked rotenone- and maneb-induced ROS production, in accordance with its protective effect against rotenone- and maneb-induced decrease in cell viability. On the contrary,

the A30P, A53T and E46K mutants increased rotenone- and maneb-induced ROS production and exhibited toxic effects on cell viability.

A previous study demonstrated that the ability of the mitochondrial respiratory chain complex I inhibitor rotenone to induce programmed cell death is closely related to its ability to induce mitochondrial ROS production. The induction of mitochondrial ROS production by rotenone had been attributed to the ability of rotenone to block mitochondrial respiratory chain complex I, NADH dehydrogenase, thereby increasing the formation of ubisemiquinone, the primary electron donor in mitochondrial superoxide generation (Li et al., 2003). Shamoto-Nagai et al. (2003) also stated that the binding of rotenone to the ubiquinone-binding sites of complex I would stimulate the production of ROS that is linked to the neurotoxic effects.

In support of the result of this study, a study done by Liu et al. (2006) showed that overexpression of  $\alpha$ -Syn in SH-SY5Y cells increased the activity of superoxide dismutase distinctly, reduced oxidative stress and significantly attenuated rotenone-induced cell apoptosis. Superoxide dismutases are metalloenzymes that catalyse the dismutation of superoxide radical into  $H_2O_2$  and molecular oxygen and consequently provide an important defence mechanism against superoxide radical toxicity (McCord & Fridovich, 1988). Hence, one could postulate that in this study, wild type  $\alpha$ -Syn blocked ROS generation by increasing the superoxide dismutase activity.

In accordance with the findings that maneb treatment increased ROS level in SH-SY5Y dopaminergic cells in this study, Fitsanakis et al. (2002) found that EBDCs including maneb can catalyse a one electron transfer from dopamine to molecular oxygen, resulting in generation of ROS products like superoxide and semiquinone species. Maneb also leads to increased levels of GSSG and altered heme-oxygenase-1 protein levels, providing evidence of an oxidative stress response in dopaminergic cultures (Barlow et al., 2005). It is suggested that the build-up of oxidative stress would be partially attenuated in the presence of wild type  $\alpha$ -Syn, which tends to decrease the amount of free dopamine inside neurons and the possible bio-conversion of dopamine into reactive and highly toxic species. By this means, the cells would be protected against maneb insult. To further support the role of wild type  $\alpha$ -Syn in attenuating ROS production, wild type  $\alpha$ -Syn, but not its A30P or A53T variants, were shown to have the ability to attenuate decrease of intracellular levels of reduced GSH after serum deprivation (Lee, Hyun, Halliwell, & Jenner, 2001).

#### **5.5.4 Role of wild type $\alpha$ -Syn in inhibiting rotenone- and maneb-mediated mitochondrial depolarisation**

This study demonstrates that both acute and chronic rotenone and maneb caused disruption of the mitochondrial transmembrane potential ( $\Delta\Psi_m$ ). Wild type  $\alpha$ -Syn but not mutant variants preserved the mitochondrial membrane potential in conditions known to compromise mitochondrial integrity thus protected SH-SY5Y cells against apoptotic cell death.

In support of these results, Dadakhujaev et al. (2010) reported that rotenone-dependent mitochondrial membrane potential loss was much more severe in

SH-SY5Y cells expressing the two  $\alpha$ -Syn mutants (A30P and A53T) than wild type  $\alpha$ -Syn or control. A recent study also demonstrated that after 1 and 2 weeks of low-dosage treatment, rotenone-induced cell death was attenuated in cell overexpressing wild type  $\alpha$ -Syn. The mitochondrial complex I activity was found to become greater and mitochondrial membrane swelling intensity was reduced, indicating that  $\alpha$ -Syn at least in some parts resists the rotenone-induced mitochondrial deficit (Lu et al., 2010). Acute neurotoxic effects of maneb in mesencephalic neuronal cultures are reported to be associated with perturbation in mitochondrial function as maneb acts as inhibitory uncouplers of the electron transport chain and prevents active mitochondrial respiration (Domico et al., 2006). However, no related studies concerning the effect of  $\alpha$ -Syn against maneb-induced mitochondrial dysfunction could be found. A previous study demonstrated that protection from MPP<sup>+</sup>, an inhibitor of mitochondrial complex I by wild type  $\alpha$ -Syn was directly correlated with the preservation of mitochondrial function. Specifically,  $\alpha$ -Syn rescued cells from MPP<sup>+</sup>-mediated decreases in mitochondrial dehydrogenase activity and loss of ATP levels by utilising ketosis (Jensen & Gai, 2001). Thus one could speculate that the same mechanism is used by wild type  $\alpha$ -Syn in conserving the mitochondrial function of SH-SY5Y cells following rotenone and maneb insults.

Conversely, a few studies reported that  $\alpha$ -Syn promotes mitochondrial deficits. Parihar, Parihar, Fujita, Hashimoto, and Ghafourifar (2008) showed that  $\alpha$ -Syn localises at the mitochondrial membrane, using SH-SY5Y cells overexpressing  $\alpha$ -Syn A53T mutant or wild type as well as isolated rat brain mitochondria.

Interaction of  $\alpha$ -Syn with mitochondria was demonstrated to cause release of cytochrome *c*, increase of mitochondrial calcium and nitric oxide, and oxidative modification of mitochondrial components. Hsu et al. (2000) demonstrated that  $\alpha$ -Syn overexpression in hypothalamic neuronal cell line (GT1-7) resulted in mitochondrial alterations accompanied by increased levels of free radicals.  $\alpha$ -Syn expression in HEK293 cells also enhances the mitochondrial sensitivity to rotenone (Orth, Tabrizi, Schapira, & Cooper, 2003). These discrepancies might be attributed to the different cell lines used, diverse expression levels of  $\alpha$ -Syn and changes of physiological function of  $\alpha$ -Syn upon toxic insults.

#### **5.6 Role of $\alpha$ -Syn against additional acute oxidative stress in chronic environmental toxins-treated *in vitro* Parkinsonian SH-SY5Y cell culture model**

Most data from environmental toxins-exposed dopaminergic cell cultures have been obtained after short term exposure of cells to relatively high concentration of environmental toxins and may not be relevant to the progressive nature of PD (Lu et al., 2010; Sherer et al., 2002). Therefore, in this study, the untransfected and stably transfected human neuroblastoma SH-SY5Y cells were exposed to low concentration of rotenone and maneb, respectively for up to two weeks before the effect of wild type and mutant  $\alpha$ -Syn on subsequent H<sub>2</sub>O<sub>2</sub>-induced cell death was examined.

Following chronic rotenone and maneb treatment, overexpression of wild type  $\alpha$ -Syn but not the mutant variants was found to rescue SH-SY5Y from the subsequent acute H<sub>2</sub>O<sub>2</sub> insult by blocking ROS production and preserving the

mitochondrial membrane potential. The current study demonstrates that in mild stress, the overexpression of wild type  $\alpha$ -Syn directly correlates with protection against subsequent acute toxicity.

In support to these results, Musgrove, King, and Dickson (2010) used a novel model of chronic oxidative stress in cultured dopaminergic and cortical neurons and reported neuroprotective up-regulation of endogenous  $\alpha$ -Syn in response to low dose toxicity, which then confers relative resistance to apoptosis following secondary insult. However, it is suggested that further increase of intracellular  $\alpha$ -Syn levels may drive abnormal accumulation of the protein, upon exposure additional insult. Quilty et al. (2006) also reported that the up-regulated  $\alpha$ -Syn in primary neural culture in response to chronic oxidative stress is associated with neuroprotection as the cells became more resistant to subsequent apoptotic changes. Furthermore, physiological concentrations of wild type  $\alpha$ -Syn, but not its A30P or A53T variants, were found to protect either cortical and hippocampal neurons, pheochromocytoma PC12 cells differentiated into catecholaminergic cells, NT-2/D1, SH-SY5Y and SK-N-MC neuroblastoma cells against the neurotoxicity induced by H<sub>2</sub>O<sub>2</sub>-induced oxidative stress (Lee et al., 2001; Seo et al., 2002). Moreover, induced overexpression of exogenously sourced  $\alpha$ -Syn is correlated to relative resilience against H<sub>2</sub>O<sub>2</sub>-induced oxidative stress via an inactivation of the pro-apoptotic JNK signalling pathway secondary to an increased expression and activity of JIP-1b/IB1, the scaffold protein of the JNK pathway in the GT1-7 cell line (Hashimoto et al., 2002).

## 5.7 Future studies and implications

Future studies might be directed to novel functional interactions between  $\alpha$ -Syn and the apoptosis cascade in SK-MEL28 melanoma and SH-SY5Y neuronal cells, considering the involvement of JNK and PI3/Akt signalling pathways. Further, it would be important to determine whether the anti-apoptotic property of human  $\alpha$ -Syn has *in vivo* relevance. A more detailed cell cycle analysis could be performed to assess the effect of wild type and mutant  $\alpha$ -Syn on cell cycle aberrations by studying the tumour suppressor gene expression, cyclin and cyclin-dependent kinase activity levels. Moreover, studies might be done to elucidate the exact in-depth mechanisms in connection to the differential effects of wild type and mutant  $\alpha$ -Syn against rotenone and maneb-induced neuronal cell death. Further investigation should reveal whether  $\alpha$ -Syn regulates the mitochondrial complex activity in dopaminergic neurons and also rigorously assess the involvement of antioxidant mechanism enzymes in the protective role of  $\alpha$ -Syn by examining the activity levels of superoxide dismutase, catalase, and glutathione peroxidase. These further investigations are essential to give insight into the biological function of  $\alpha$ -Syn in the pathogenesis of melanoma and Parkinson's disease.

As  $\alpha$ -Syn overexpression has been implicated to be involved in the melanoma cells' resistance to apoptosis which leads to cancer progression, the possibility of using  $\alpha$ -Syn as a potential target for melanoma drug therapy could be examined. Moreover, one could consider using  $\alpha$ -Syn as a target to overcome staurosporine-related drug resistance, for example in the case of a metastatic melanoma Mel-RM cell line, which is partially resistant to staurosporine (Xu,

Gillespie, & Hersey, 2004). It is also likely that  $\alpha$ -Syn could be developed into a histological biomarker for diagnosis and prognosis of different types of melanoma. However, as reported by Matsuo and Kamitani (2010),  $\alpha$ -Syn is expressed in both malignant and benign melanocytic lesions respectively so it cannot be used to distinguish between malignant and benign melanocytic skin lesions, but it is still constructive for the diagnosis of metastatic melanoma.

Thus far,  $\alpha$ -Syn has been extensively studied in many neuronal cell-based models but has yielded mixed results.  $\alpha$ -Syn was found to have either beneficial, adverse, or no effect on cell survival and/or susceptibility to certain insults. Therefore, understanding the function and underlying mechanisms of  $\alpha$ -Syn is indisputably a critical step before one could conclude that  $\alpha$ -Syn is the right target for Parkinson's disease. This present study extends the understanding regarding potential normative and pathological roles of  $\alpha$ -Syn as the findings suggest that the disease-causing mutations of  $\alpha$ -Syn observed in Parkinson's disease convert the protein from one which is able to modulate cell death, into a protein which has a damaging effect in neuronal cells exposed to a variety of death-inducing stimuli.

## CHAPTER 6

### CONCLUSIONS

In summary,  $\alpha$ -Syn gene knockdown was found to aggravate staurosporine-induced cyto-toxicity in SK-MEL28 cells. SH-SY5Y cells overexpressing wild type  $\alpha$ -Syn were less vulnerable while cells overexpressing  $\alpha$ -Syn mutant constructs (A30P, A53T and E46K) were more susceptible to staurosporine relative to untransfected cells. Overexpression of wild type  $\alpha$ -Syn attenuated acute and chronic maneb and rotenone-induced cell death accompanied with reduced  $\Delta\Psi_m$  and ROS level whereas the mutant  $\alpha$ -Syn constructs exacerbated environmental toxins-induced cyto-toxicity. After chronic rotenone and maneb treatment, overexpression of wild type  $\alpha$ -Syn but not the mutant variants was found to rescue SH-SY5Y from subsequent acute  $H_2O_2$  insult by blocking ROS production and preserving  $\Delta\Psi_m$ . Apart from showing that the wild type  $\alpha$ -Syn overexpression in SH-SY5Y cells has a tendency to resist rotenone and maneb insults, these findings provide a link between mutant  $\alpha$ -Syn and cell death by lowering the threshold of cells to oxidative and mitochondrial damage. These results suggest that the fundamental property of wild type  $\alpha$ -Syn may be protective and such property may be lost by its familial Parkinson's disease-linked mutations. Mutant  $\alpha$ -Syn not only caused the loss of protective function of wild type  $\alpha$ -Syn but also the gain-of-toxicity. This study, thus, provides fundamental insights concerning the role of  $\alpha$ -Syn in Parkinson's disease as well as in melanoma. The underlying influences of  $\alpha$ -Syn against staurosporine-induced apoptosis and rotenone- and maneb-induced

neurotoxicity were highlighted to facilitate prospective translation of  $\alpha$ -Syn discoveries into therapeutics for melanoma and Parkinson's disease.

## REFERENCES

- Abeliovich, A., Schmitz, Y., Farinas, I., Choi-Lundberg, D., Ho, W.H., Castillo, P.E., et al. (2000). Mice lacking alpha-synuclein display functional deficits in the nigrostriatal dopamine system. *Neuron*, *25*, 239-252.
- Ahmad, M., Attoub, S., Singh, M.N., Martin, F.L., & El-Agnaf, O.M.A. (2007).  $\gamma$ -Synuclein and the progression of cancer. *FASEB Journal*, *21*, 3419-3430.
- Ahmadi, F.A., Linseman, D.A., Grammatopoulos, T.N., Jones, S.M., Bouchard, R.J., Freed, C.R., et al. (2003). The pesticide rotenone induces caspase-3-mediated apoptosis in ventral mesencephalic dopaminergic neurons. *Journal of Neurochemistry*, *87*, 914-921.
- Alam, Z.I., Jenner, A., Daniel, S.E., Lees, A.J., Cairns, N., Marsden, C.D., et al. (1997). Oxidative DNA damage in the Parkinsonian brain: an apparent selective increase in 8-hydroxyguanine levels in substantia nigra. *Journal of Neurochemistry*, *69*, 1196-1203.
- Alberts, B., Johnson, A., Lewis, J., Raff, M., Roberts, K., & Walter, P. (2008). *Molecular Biology of the Cell* (4<sup>th</sup> edition). New York: Garland science, Taylor & Francis Group, LLC.
- American Type Culture Collection. (2010). ATCC Number: CRL-2266. Retrieved December 8, 2010, from <http://www.atcc.org/Attachments/1851.jpg>
- Anderson, C.M., Buzaid, A.C., & Legha, S.S. (1995). Systemic treatments for advanced cutaneous melanoma. *Oncology (Huntington)*, *9*, 1149-1158.
- Aschner, M., & Aschner, J.L. (1991). Manganese neurotoxicity: cellular effects and blood-brain barrier transport. *Neuroscience & Biobehavioral Reviews*, *15*, 333-340.
- Athanassiadou, A., Voutsinas, G., Psiouri, L., Leroy, E., Polymeropoulos, M.H., Ilias, A., et al. (1999). Genetic analysis of families with Parkinson disease that carry the Ala53Thr mutation in the gene encoding alpha-synuclein. *American Journal of Human Genetics*, *65*, 555-558.
- Baba, M., Nakajo, S., Tu, P. H., Tomita, T., Nakaya, K., Lee, V. M., et al. (1998). Aggregation of alpha-synuclein in Lewy bodies of sporadic Parkinson's disease and dementia with Lewy bodies. *American Journal of Pathology*, *152*, 879-884.
- Balch, C., Montgomery, J.S., Paik, H.I., Kim, S., Kim, S., Huang, T.H., et al. (2005). New anti-cancer strategies: epigenetic therapies and biomarkers. *Frontiers in Bioscience*, *10*, 1897-1931.

- Barlow, B.K., Lee, D.W., Cory-Slechta, D.A., & Opanashuk, L.A. (2005). Modulation of antioxidant defense systems by the environmental pesticide maneb in dopaminergic cells. *Neurotoxicology*, *26*, 63-75.
- Becker, J.C., Kampgen, E., & Brocker, E. (2000). Classical chemotherapy for metastatic melanoma. *Clinical and Experimental Dermatology*, *25*, 503-508.
- Belmokhtar, C.A., Hillion, J., & Segal-Bendirdjian, E. (2001). Staurosporine induces apoptosis through both caspase-dependent and caspase-independent mechanisms. *Oncogene*, *20*, 3354-3362.
- Berg, D., Gerlach, M., Youdim, M.B., Double, K.L., Zecca, L., Riederer, P., et al. (2001). Brain iron pathways and their relevance to Parkinson's disease. *Journal of Neurochemistry*, *79*, 225-236.
- Bernheimer, H., Birkmayer, W., Hornykiewicz, O., Jellinger, K., & Seitelberger, F. (1973). Brain dopamine and the syndromes of Parkinson and Huntington. Clinical, morphological and neurochemical correlations. *Journal of the Neurological Sciences*, *20*, 415-455.
- Bertoni, J.M., Arlette, J.P., Fernandez, H.H., Fitzer-Attas, C., Frei, K., Hassan, M.N., et al. (2010). Increased melanoma risk in Parkinson disease: a prospective clinicopathological study. *Archives of Neurology*, *67*, 347-352.
- Betarbet, R., Sherer, T.B., MacKenzie, G., Garcia-Osuna, M., Panov, A.V., & Greenamyre, J.T. (2000). Chronic systemic pesticide exposure reproduces features of Parkinson's disease. *Nature Neuroscience*, *3*, 1301-1306.
- Beyer, K. (2006). Alpha-synuclein structure, posttranslational modification and alternative splicing as aggregation enhancers. *Acta Neuropathologica*, *112*, 237-251.
- Bharath, S., Hsu, M., Kaur, D., Rajagopalan, S., & Andersen, J.K. (2002). Glutathione, iron and Parkinson's disease. *Biochemical Pharmacology*, *64*, 1037-1048.
- Biedler, J.L., Helson, L., & Spengler, B.A. (1973). Morphology and growth, tumorigenicity, and cytogenetics of human neuroblastoma cells in continuous culture. *Cancer Research*, *33*, 2643-2652.
- Biere, A.L., Wood, S.J., Wypych, J., Steavenson, S., Jiang, Y., Anafi, D., et al. (2000). Parkinson's disease-associated alpha-synuclein is more fibrillogenic than beta- and gamma-synuclein and cannot cross-seed its homologs. *Journal of Biological Chemistry*, *275*, 34574-34579.

- Bisaglia, M., Greggio, E., Maric, D., Miller, D.W., Cookson, M.R., & Bubacco, L. (2010). Alpha-synuclein overexpression increases dopamine toxicity in BE2-M17 cells. *BMC Neuroscience*, *11*, 41.
- Bonifati, V., Rizzu, P., van Baren, M.J., Schaap, O., Breedveld, G.J., Krieger, E., et al. (2003). Mutations in the DJ-1 gene associated with autosomal recessive early-onset Parkinsonism. *Science*, *299*, 256-259.
- Bonini, N.M., & Giasson, B.I. (2005). Snaring the function of alpha-synuclein. *Cell*, *123*, 359-361.
- Braak, H., Del Tredici, K., Rub, U., de Vos, R.A., Jansen Steur, E.N., & Braak, E. (2003). Staging of brain pathology related to sporadic Parkinson's disease. *Neurobiology of Aging*, *24*, 197-211.
- Brenner, D., & Mak, T.W. (2009). Mitochondrial cell death effectors. *Current Opinion in Cell Biology*, *21*, 871-877.
- Bruening, W., Giasson, B.I., Klein-Szanto, A.J., Lee, V.M., Trojanowski, J.Q., & Godwin, A.K. (2000). Synucleins are expressed in the majority of breast and ovarian carcinomas and in preneoplastic lesions of the ovary. *Cancer*, *88*, 2154-2163.
- Brunelle, J.K., & Letai, A. (2009). Control of mitochondrial apoptosis by the Bcl-2 family. *Journal of Cell Science*, *122*, 437-441.
- Buchman, V.L., Adu, J., Pinon, L.G., Ninkina, N.N., & Davies, A.M. (1998). Persyn, a member of the synuclein family, has a distinct pattern of expression in the developing nervous system. *Journal of Neuroscience*, *18*, 9335-9341.
- Bussell, R. Jr., & Eliezer, D. (2001). Residual structure and dynamics in Parkinson's disease-associated mutants of  $\alpha$ -synuclein. *Journal of Biological Chemistry*, *276*, 45996-46003.
- BVTech, Inc. (2005). Plasmid map of pBABE-hygro. Retrieved December 11, 2010, from <http://www.biovisualtech.com/bvplasmid/pBABE-hygro.htm>
- Cabin, D.E., Shimazu, K., Murphy, D., Cole, N.B., Gottschalk, W., McIlwain, K.L., et al. (2002). Synaptic vesicle depletion correlates with attenuated synaptic responses to prolonged repetitive stimulation in mice lacking alpha-synuclein. *Journal of Neuroscience*, *22*, 8797-8807.
- Carey, T.E., Takahashi, T., Resnick, L.A., Oettgen, H.F., & Old, L.J. (1976). Cell surface antigens of human malignant melanoma: mixed hemadsorption assays for humoral immunity to cultured autologous melanoma cells. *Proceedings of the National Academy of Sciences of the United States of America*, *73*, 3278-3282.

- Cell Biolabs. (2008). pBABE-Hygro Retroviral Vector. Retrieved December 8, 2010, from <http://www.cellbiolabs.com/PDFs/03ABB56A-3048-812A2ECED592116F51A8.pdf>
- Cereser, C., Boget, S., Parvaz, P., & Revol, A. (2001). Thiram-induced cytotoxicity is accompanied by a rapid and drastic oxidation of reduced glutathione with consecutive lipid peroxidation and cell death. *Toxicology*, *163*, 153-162.
- Chandra, S., Gallardo, G., Fernandez-Chacon, R., Schluter, O.M., & Sudhof, T.C. (2005). Alpha-synuclein cooperates with CSPalpha in preventing neurodegeneration. *Cell*, *123*, 383-396.
- Chang, J., Hsu, Y., Kuo, P., Kuo, Y., Chiang, L., & Lin, C. (2005). Increase of Bax/Bcl-XL ratio and arrest of cell cycle by luteolin in immortalized human hepatoma cell line. *Life Science*, *76*, 1883-1893.
- Chao, D.T., & Korsmeyer, S.J. (1998). BCL-2 family: regulators of cell death. *Annual Review of Immunology*, *16*, 395-419.
- Charlot, J.F., Pretet, J.L., Haughey, C., & Mouglin, C. (2004). Mitochondrial translocation of p53 and mitochondrial membrane potential ( $\Delta\Psi_m$ ) dissipation are early events in staurosporine-induced apoptosis of wild type and mutated p53 epithelial cells. *Apoptosis*, *9*, 333-343.
- Chartier-Harlin, M.C., Kachergus, J., Roumier, C., Mouroux, V., Douay, X., Lincoln, S., et al. (2004). Alpha-synuclein locus duplication as a cause of familial Parkinson's disease. *Lancet*, *364*, 1167-1169.
- Chen, L., Periquet, M., Wang, X., Negro, A., McLean, P.J., Hyman, B.T., et al. (2009). Tyrosine and serine phosphorylation of alpha-synuclein have opposing effects on neurotoxicity and soluble oligomer formation. *Journal of Clinical Investigation*, *119*, 3257-3265.
- Chen, N., & Reith, M.E. (2000). Structure and function of the dopamine transporter. *European Journal of Pharmacology*, *405*, 329-339.
- Chen, X., de Silva, H.A., Pettenati, M.J., Rao, P.N., St George-Hyslop, P., Roses, A.D., et al. (1995). The human NACP/alpha-synuclein gene: chromosome assignment to 4q21.3-q22 and TaqI RFLP analysis. *Genomics*, *26*, 425-427.
- Cheng, F., Vivacqua, G., & Yu, S. (2010). The role of alpha-synuclein in neurotransmission and synaptic plasticity. *Journal of Chemical Neuroanatomy*, doi:10.1016/j.jchemneu.2010.12.001

- Clarkson, K.S., Sturdge, I.C., & Molyneux, A.J. (2001). The usefulness of tyrosinase in the immunohistochemical assessment of melanocytic lesions: a comparison of the novel T311 antibody (anti-tyrosinase) with S-100, HMB45, and A103 (anti-melan-A). *Journal of Clinical Pathology*, *54*, 196-200.
- Clayton, D.F., & George, J.M. (1998). The synucleins: a family of proteins involved in synaptic function, plasticity, neurodegeneration and disease. *Trends in Neurosciences*, *21*, 249-254.
- Clontech. (2008). Multiple shRNA Delivery Options for RNAi. Retrieved December 5, 2010, from [http://www.clontech.com/images/ctq/JUL08UPD/UD862703\\_CTQ\\_Jul\\_08\\_US\\_7.pdf](http://www.clontech.com/images/ctq/JUL08UPD/UD862703_CTQ_Jul_08_US_7.pdf).
- Colapinto, M., Mila, S., Giraud, S., Stefanazzi, P., Molteni, M., Rossetti, C., et al. (2006). Alpha-Synuclein protects SH-SY5Y cells from dopamine toxicity. *Biochemical and Biophysical Research Communications*, *349*, 1294-1300.
- Conway, K.A., Harper, J.D., & Lansbury, P.T. (1998). Accelerated *in vitro* fibril formation by a mutant alpha-synuclein linked to early-onset Parkinson disease. *Nature Medicine*, *4*, 131-1320.
- Conway, K.A., Lee, S.J., Rochet, J.C., Ding, T.T., Williamson, R.E., & Lansbury, P.T. (2000). Acceleration of oligomerization, not fibrillization, is a shared property of both alpha-synuclein mutations linked to early-onset Parkinson's disease: implications for pathogenesis and therapy. *Proceedings of the National Academy of Sciences of the United States of America*, *97*, 571-576.
- Corsini, G.U., Pintus, S., Chiueh, C.C., Weiss, J.F., & Kopin, I.J. (1985). 1-Methyl-4-phenyl-1,2,3,6-tetrahydropyridine (MPTP) neurotoxicity in mice is enhanced by pretreatment with diethyldithiocarbamate. *European Journal of Pharmacology*, *119*, 127-128.
- Corti, O., Hampe, C., Darios, F., Ibanez, P., Ruberg, M., & Brice, A. (2005) Parkinson's disease: from causes to mechanisms. *Comptes Rendus Biologies*, *328*, 131-142.
- Crowther, R.A., Jakes, R., Spillantini, M.G., & Goedert, M. (1998). Synthetic filaments assembled from C-terminally truncated alpha-synuclein. *FEBS Letters*, *436*, 309-312.
- Cuervo, A.M., Stefanis, L., Fredenburg, R., Lansbury, P.T., & Sulzer, D. (2004). Impaired degradation of mutant  $\alpha$ -synuclein by chaperone-mediated autophagy. *Science*, *305*, 1292-1295.

- Czekierdowski, A., & Czekierdowska, S. (2007). SNCG (synuclein, gamma (breast cancer-specific protein 1)). Atlas of genetics and cytogenetics in oncology and haematology. Retrieved December 11, 2010, from <http://AtlasGeneticsOncology.org/Genes/SNCGID42343ch10q23.html>
- Da Costa, A.C., Ancolio, K., & Checler, F. (2000). Wild-type but not Parkinson's Disease-related Ala-53→ Thr mutant-synuclein protects neuronal cells from apoptotic stimuli. *Journal of Biological Chemistry*, 275, 24065-24069.
- Da Costa, A.C., Paitel, E., Vincent, B., & Checler, F. (2002). Alpha-synuclein lowers p53-dependent apoptotic response of neuronal cells. Abolishment by 6-hydroxydopamine and implication for Parkinson's disease. *Journal of Biological Chemistry*, 277, 50980-50984.
- Dadakhujayev, S., Noh, H.S., Jung, E.J., Cha, J.Y., Baek, S.M., Ha, J.H., et al. (2010). Autophagy protects the rotenone-induced cell death in alpha-synuclein overexpressing SH-SY5Y cells. *Neuroscience Letters*, 472, 47-52.
- Danzer, K.M., Haasen, D., Karow, A.R., Moussaud, S., Habeck, M., Giese, A., et al. (2007). Different species of  $\alpha$ -synuclein oligomers induce calcium influx and seeding. *Journal of Neuroscience*, 27, 9220-9232.
- Dauer, W., & Przedborski, S. (2003). Parkinson's disease: mechanisms and models. *Neuron*, 39, 889-909.
- Davis, J.L., Ripley, R.T., Frankel, T.L., Maric, I., Lozier, J.N., & Rosenberg, S.A. (2010). Paraneoplastic granulocytosis in metastatic melanoma. *Melanoma Research*, 20, 326-329.
- De Lau, L.M., & Breteler, M.M. (2006). Epidemiology of Parkinson's disease. *Lancet Neurology*, 5, 525-535.
- De Maziere, A.M., Muehlethaler, K., van Donselaar, E., Salvi, S., Davoust, J., Cerottini, J.C., et al. (2002). The melanocytic protein Melan-A/MART-1 has a subcellular localization distinct from typical melanosomal proteins. *Traffic*, 3, 678-693.
- De Vries, E.G., Gietema, J.A., & de Jong, S. (2006). Tumor necrosis factor-related apoptosis-inducing ligand pathway and its therapeutic implications. *Clinical Cancer Research*, 12, 2390-2393.
- Dejean, L.M., Martinez-Caballero, S., Manon, S., & Kinnally, K.W. (2006). Regulation of the mitochondrial apoptosis-induced channel, MAC, by BCL-2 family proteins. *Biochimica et Biophysica Acta*, 1762, 191- 201.

- Dev, K.K., Hofele, K., Barbieri, S., Buchman, V.L., & van der Putten, H. (2003). Part II: alpha-synuclein and its molecular pathophysiological role in neurodegenerative disease. *Neuropharmacology*, *45*, 14-44.
- Dexter, D.T., Holley, A.E., Flitter, W.D., Slater, T.F., Wells, F.R., Daniel, S.E., et al. (1994). Increased levels of lipid hydroperoxides in the Parkinsonian substantia nigra: an HPLC and ESR study. *Movement Disorder*, *9*, 92-97.
- Dexter, D.T., Wells, F.R., Lees, A.J., Agid, F., Agid, Y., Jenner, P., et al. (1989). Increased nigral iron content and alterations in other metal ions occurring in brain in Parkinson's disease. *Journal of Neurochemistry*, *52*, 1830-1836.
- Dobson, A.W., Erikson, K.M., & Aschner, M. (2004). Manganese neurotoxicity. *Annals of the New York Academy of Sciences*, *1012*, 115-128.
- Domico, L.M., Zeevalk, G.D., Bernard, L.P., & Cooper, K.R. (2006). Acute neurotoxic effects of mancozeb and maneb in mesencephalic neuronal cultures are associated with mitochondrial dysfunction. *NeuroToxicology*, *27*, 816-825.
- Dong, X., Stothard, P., Forsythe, I.J. & Wishart, D.S. (2010). Vector pCMV-SPORT6. Retrieved December 5, 2010 from <http://www.openbiosystems.com/vector/vectordetails.aspx?vid=24>
- Donze, O., & Picard, D. (2002). RNA interference in mammalian cells using siRNAs synthesized with T7 RNA polymerase. *Nucleic Acids Research*, *30*, e46.
- Drechsel, D.A., & Patel, M. (2008). Role of reactive oxygen species in the neurotoxicity of environmental agents implicated in Parkinson's disease. *Free Radical Biology & Medicine*, *44*, 1873-1886.
- Du, H.N., Tang, L., Luo, X.Y., Li, H.T., Hu, J., Zhou, J.W., et al. (2003). A peptide motif consisting of glycine, alanine, and valine is required for the fibrillization and cytotoxicity of human alpha synuclein. *Biochemistry*, *42*, 8870-8878.
- Duan, H., Orth, K., Chinnaiyan, A.M., Poirier, G.G., Froelich, C.J., He, W.W., et al. (1996). ICE-LAP6, a novel member of the ICE/Ced-3 gene family, is activated by the cytotoxic T cell protease granzyme B. *Journal of Biological Chemistry*, *271*, 16720-16724.
- Duprez, L., Wirawan, E., Vanden Berghe, T., & Vandenabeele, P. (2009). Major cell death pathways at a glance. *Microbes and Infection*, *11*, 1050-1062.

- El-Agnaf, O.M., & Irvine, G.B. (2000). Review: formation and properties of amyloid-like fibrils derived from alpha-synuclein and related proteins. *Journal of Structural Biology*, 130, 300-309.
- El-Agnaf, O.M., & Irvine, G.B. (2002). Aggregation and neurotoxicity of alpha synuclein and related peptides. *Biochemical Society Transactions*, 30, 559-565.
- El-Agnaf, O.M.A., Jakes, R., Curran, M.D., Middleton, D., Ingenito, R., Bianchi, E., et al. (1998). Aggregates from mutant and wild-type  $\alpha$ -synuclein proteins and NAC peptide induce apoptotic cell death in human neuroblastoma cells by formation of  $\beta$ -sheet and amyloid-like filaments. *FEBS Letters*, 440, 71-75.
- Eliezer, D., Kutluay, E., Bussell, R., & Browne, G. (2001). Conformational properties of alpha-synuclein in its free and lipid-associated states. *Journal of Molecular Biology*, 307, 1061-1073.
- Esposito, A., Dohm, C.P., Kermer, P., Bahr, M., & Woutersa, F.S. (2007).  $\alpha$ -Synuclein and its disease-related mutants interact differentially with the microtubule protein tau and associate with the actin cytoskeleton. *Neurobiology of Disease*, 26, 521-531.
- Extension Toxicology Network (EXTONET). (1996). Pesticide Information Profiles. Retrieved December 19, 2010, from <http://extoxnet.orst.edu/pips/maneb.htm>
- Ferraz, H.B., Bertolucci, P.H.F., Pereira, J.S., Lima, J.G.C., & Andrade, L.A.F. (1988). Chronic exposure to the fungicide maneb may produce symptoms and signs of CNS manganese intoxication. *Neurology*, 38, 550-553.
- Fitsanakis, V.A., Amarnath, V., Moore, J.T., Montine, K.S., Zhang, J., & Montine, T.J. (2002). Catalysis of catechol oxidation by metal-dithiocarbamate complexes in pesticides. *Free Radical Biology & Medicine*, 33, 1714-1723.
- Franco, R., Li, S., Rodriguez-Rocha, H., Burns, M., & Panayiotidis, M.I. (2010). Molecular mechanisms of pesticide-induced neurotoxicity: Relevance to Parkinson's disease. *Chemico-Biological Interactions*, 188, 289-300.
- Friedman, R.J., Rigel, D.S., & Kopf, A.W. (1985). Early detection of malignant melanoma: the role of physician examination and self-examination of the skin. *CA: A Cancer Journal for Clinicians*, 35, 130-151.
- Fujiwara, H., Hasegawa, M., Dohmae, N., Kawashima, A., Masliah, E., Goldberg, M. S., et al. (2002). Alpha-synuclein is phosphorylated in synucleinopathy lesions. *Nature Cell Biology*, 4, 160-164.

- Gadbois, D.M., Hamaguchi, J.R., Swank, R.A., & Bradbury, E.M. (1992). Staurosporine is a potent inhibitor of p34cdc2 and p34cdc2-like kinases. *Biochemical and Biophysical Research Communications*, 184, 80-85.
- Gao, H.M., Hong, J.S., Zhang, W., & Liu, B. (2002). Distinct role for microglia in rotenone-induced degeneration of dopaminergic neurons. *Journal of Neuroscience*, 22, 782-790.
- Gao, X., Simon, K.C., Han, J., Schwarzschild, M.A., & Ascherio, A. (2009). Family history of melanoma and Parkinson disease risk. *Neurology*, 73, 1286-1291.
- Gasser, T., Muller-Myhsok, B., Wszolek, Z.K., Oehlmann, R., Calne, D.B., Bonifati, V., et al. (1998). A susceptibility locus for Parkinson's disease maps to chromosome 2p13. *Nature Genetics*, 18, 262-265.
- Genetic Engineering & Biotechnology News. (2006). Next-Generation RNA Interference Scoring Efficient Knockdown with Mission shRNA Lentiviral Vector-Based shRNA Libraries. Retrieved December 20, 2010, from <http://www.genengnews.com/gen-articles/next-generation-rna-interference/1321/>
- George, J.M. (2001). The synucleins. *Genome Biology*, 3, 3002.1-3002.6.
- George, J.M., Jin, H., Woods, W.S., & Clayton, D.F. (1995). Characterization of a novel protein regulated during the critical period for song learning in the zebra finch. *Neuron*, 15, 361-372.
- Giasson, B.I., Duda, J.E., Murray, I.V., Chen, Q., Souza, J.M., Hurtig, H.I., et al. (2000). Oxidative damage linked to neurodegeneration by selective alpha-synuclein nitration in synucleinopathy lesions. *Science*, 290, 985-989.
- Giasson, B.I., Murray, I.V., Trojanowski, J.Q., & Lee, V.M. (2001). A hydrophobic stretch of 12 amino acid residues in the middle of alpha synuclein is essential for filament assembly. *Journal of Biological Chemistry*, 276, 2380-2386.
- Goda, Y. (1997). SNAREs and regulated vesicle exocytosis. *Proceedings of the National Academy of Sciences of the United States of America*, 94, 769-772.
- Goedert, M. (2001). Alpha-synuclein and neurodegenerative diseases. *Nature Reviews Neuroscience*, 2, 492-501.
- Goedert, M., Spillantini, M.G., & Davies, S.W. (1998). Filamentous nerve cell inclusions in neurodegenerative diseases. *Current Opinion in Neurobiology*, 8, 619-632.

- Gomez-Santos, C., Ferrer, I., Reiriz, J., Vinals, F., Barrachina, M., & Ambrosio, S. (2002). MPP<sup>+</sup> increases alpha-synuclein expression and ERK/MAP-kinase phosphorylation in human neuroblastoma SH-SY5Y cells. *Brain Research*, *935*, 32-39.
- Gosavi, N., Lee, H.J., Lee, J.S., Patel, S., & Lee, S.J. (2002). Golgi fragmentation occurs in the cells with prefibrillar alpha-synuclein aggregates and precedes the formation of fibrillar inclusion. *Journal of Biological Chemistry*, *277*, 48984-48992.
- Greenbaum, E.A., Graves, C.L., Mishizen-Eberz, A.J., Lupoli, M.A., Lynch, D.R., Englander, S.W., et al. (2005). The E46K mutation in alpha-synuclein increases amyloid fibril formation. *Journal of Biological Chemistry*, *280*, 7800-7807.
- Grimm, D., Streetz, K.L., Jopling, C.L., Storm, T.A., Pandey, K., Davis, C.R., et al. (2006). Fatality in mice due to oversaturation of cellular microRNA/short hairpin RNA pathways. *Nature*, *441*, 537-541.
- Gu, M., Cooper, J.M., Taanman, J.W., & Schapira, A.H. (1998). Mitochondrial DNA transmission of the mitochondrial defect in Parkinson's disease. *Annals of Neurology*, *44*, 177-186.
- Gunter, T.E., Gavin, C.E., Aschner, M., & Gunter, K.K. (2006). Speciation of manganese in cells and mitochondria: a search for the proximal cause of manganese neurotoxicity. *Neurotoxicity*, *27*, 765-776.
- Gupta, S., Kass, G.E., Szegezdi, E., & Joseph, B. (2009). The mitochondrial death pathway: promising therapeutic target in Diseases. *Journal of Cellular and Molecular Medicine*, *13*, 1004-1033.
- Hanahan, D., & Weinberg, R.A. (2000). The hallmarks of cancer. *Cell*, *100*, 57-70.
- Hashimoto, M., Hsu, L.J., Rockenstein, E., Takenouchi, T., Mallory, M., & Masliah, E. (2002). Alpha-synuclein protects against oxidative stress via inactivation of the c-Jun N-terminal kinase stress-signaling pathway in neuronal cells. *Journal of Biological Chemistry*, *277*, 11465-11472.
- Hashimoto, M., Hsu, L.J., Xia, Y., Takeda, A., Sisk, A., Sundsmo, M., et al. (1999). Oxidative stress induces amyloid-like aggregate formation of NACP/alpha-synuclein *in vitro*. *NeuroReport*, *10*, 717-721.
- Hattori, N., Tanaka, M., Ozawa, T., & Mizuno, Y. (1991). Immunohistochemical studies on complexes I, II, III, and IV of mitochondria in Parkinson's disease. *Annals of Neurology*, *30*, 563-571.
- Heikkila, R.E., Cabbat, F.S., & Cohen, G. (1976). *In vivo* inhibition of superoxide dismutase in mice by diethyldithiocarbamate. *Journal of Biological Chemistry*, *251*, 2182-2185.

- Hersey, P. (2002). Advances in the non-surgical treatment of melanoma. *Expert Opinion on Investigational Drugs*, *11*, 75-85.
- Hicks, A.A., Petursson, H., Jonsson, T., Stefansson, H., Johannsdottir, H.S., Sainz, J., et al. (2002). A susceptibility gene for late-onset idiopathic Parkinson's disease. *Annals of Neurology*, *52*, 549-555.
- Hodara, R., Norris, E.H., Giasson, B.I., Mishizen-Eberz, A.J., Lynch, D.R., Lee, V.M., et al. (2004). Functional consequences of alpha-synuclein tyrosine nitration: diminished binding to lipid vesicles and increased fibril formation. *Journal of Biological Chemistry*, *279*, 47746-47753.
- Hoehn, M.M., & Yahr, M.D. (1967). Parkinsonism: onset, progression and mortality. *Neurology*, *17*, 427-442.
- Holen, T., Amarzguioui, M., Wiiger, M.T., Babaie, E., & Prydz, H. (2002). Positional effects of short interfering RNAs targeting the human coagulation trigger tissue factor. *Nucleic Acids Research*, *30*, 1757-1766.
- Hotchkiss, R.S., Strasser, A., McDunn, J.E., & Swanson, P.E. (2009). Cell death. *The New England Journal of Medicine*, *361*, 1570-1583.
- Hsu, L.J., Sagara, Y., Arroyo, A., Rockenstein, E., Sisk, A., Mallory, M., et al. (2000). Alpha-synuclein promotes mitochondrial deficit and oxidative stress. *American Journal of Pathology*, *157*, 401-410.
- Hu, Y., Benedict, M.A., Wu, D., Inohara, N., & Nunez, G. (1998). Bcl-XL interacts with Apaf-1 and inhibits Apaf-1-dependent caspase-9 activation. *Proceedings of the National Academy of Sciences of the United States of America*, *95*, 4386-4391.
- Hua, H., Xu, L., Wang, J., Jing, J., Luo, T., & Jiang, Y. (2009). Up-regulation of gamma-synuclein contributes to cancer cell survival under endoplasmic reticulum stress. *The Journal of Pathology*, *217*, 507-515.
- Huang, D.C., & Strasser, A. (2000). BH3-only proteins—essential initiators of apoptotic cell death. *Cell*, *103*, 839-842.
- Hughes, A.J., Daniel, S.E., Kilford, L., & Lees, A.J. (1992). Accuracy of clinical diagnosis of idiopathic Parkinson's disease: a clinicopathological study of 100 cases. *Journal of Neurology, Neurosurgery & Psychiatry*, *55*, 181-184.
- Hunya, A., Foldi, I., Szegedi, V., Soos, K., Zarándi, M., Szabo, A., et al. (2008). Differences between normal and alpha-synuclein overexpressing SH-SY5Y neuroblastoma cells after Abeta(1-42) and NAC treatment. *Brain Research Bulletin*, *75*, 648-654.

- International Programme on Chemical Safety. (2010). Rotenone: Health and Safety Guide. Retrieved December 23, 2010, from <http://www.inchem.org/documents/hsg/hsg/hsg073.htm>
- Invitrogen. (2004). Instruction Manual: Custom cDNA Library in pCMV•SPORT 6.1. Retrieved December 5, 2010, from [http://www.invitrogen.jp/products/pdf/custom%20\\_pCMVSPORT6.1\\_library\\_man.pdf](http://www.invitrogen.jp/products/pdf/custom%20_pCMVSPORT6.1_library_man.pdf).
- Invitrogen. (2007). pcDNA™3.1D/ V5-His-TOPO®. Retrieved December 5, 2010, from [http://www.molecularlab.it/public/data/CRISTIAN/2007117134517\\_pcdna3\\_1dv5histopo\\_map.pdf](http://www.molecularlab.it/public/data/CRISTIAN/2007117134517_pcdna3_1dv5histopo_map.pdf).
- Isenberg, J.S., & Klaunig, J.E. (2000). Role of the mitochondrial membrane permeability transition (MPT) in rotenone-induced apoptosis in liver cells. *Toxicological Sciences*, 53, 340-251.
- Iwai, A., Masliah, E., Yoshimoto, M., Ge, N., Flanagan, L., de Silva, A., et al. (1995). The precursor protein of non-A $\beta$  component of Alzheimer's disease amyloid is a presynaptic protein of the central nervous system. *Neuron*, 14, 467-475.
- Iwata, A., Maruyama, M., Akagi, T., Hashikawa, T., Kanazawa, I., Tsuji, S., et al. (2003). Alpha-synuclein degradation by serine protease neurosin: implication for pathogenesis of synucleinopathies. *Human Molecular Genetics*, 12, 2625-2635.
- Iwata, A., Miura, S., Kanazawa, I., Sawada, M., & Nukina, N. (2001). Alpha synuclein forms a complex with transcription factor Elk-1. *Journal of Neurochemistry*, 77, 239-252.
- Jakes, R., Spillantini, M.G., & Goedert, M. (1994). Identification of two distinct synucleins from human brain. *FEBS Letters*, 345, 27-32.
- Jensen, P.H., & Gai, W.P. (2001). Alpha-synuclein: axonal transport, ligand interaction and neurodegeneration. *Advances in Experimental Medicine and Biology*, 487, 129-134.
- Jensen, P.H., Nielsen, M.S., Jakes, R., Dotti, C.G., & Goedert, M. (1998). Binding of alpha-synuclein to brain vesicles is abolished by familial Parkinson's disease mutation. *Journal of Biological Chemistry*, 273, 26292-26294.
- Jensen, P.J., Alter, B.J., & Omalley, K.L. (2003). Alpha-synuclein protects naive but not dbcAMP-treated dopaminergic cell types from 1-methyl-4-phenylpyridinium toxicity. *Journal of Neurochemistry*, 86, 196-209.
- Jerant, A.F., Johnson, J.T., Sheridan, C.D., & Caffrey, T.J. (2000). Early detection and treatment of skin cancer. *American Family Physician*, 62(2), 357-368, 375-376, 381-382.

- Ji, H., Liu, Y.E., Jia, T., Wang, M., Liu, J., Joseph, B.K., et al. (1997). Identification of a breast cancer-specific gene, SNCG, by direct differential complementary DNA sequencing. *Cancer Research*, *57*, 759-764.
- Jones, D.C., & Miller, G.W. (2008). The effects of environmental neurotoxicants on the dopaminergic system: A possible role in drug addiction. *Biochemical Pharmacology*, *76*, 569-581.
- Junn, E., & Mouradian, M.M. (2002). Human alpha-synuclein over-expression increases intracellular reactive oxygen species level. *Neuroscience Letters*, *320*, 146-150.
- Kahle, P.J., Neumann, M., Ozmen, L., Muller, V., Jacobsen, H., & Schindzielorz, A. (2000). Subcellular localization of wild-type and Parkinson's disease-associated mutant  $\alpha$ -synuclein in human and transgenic mouse brain. *Journal of Neuroscience*, *20*, 6365-6373.
- Kaul, S., Anantharam, V., Kanthasamy, A., & Kanthasamy, A.G. (2005). Wild-type [alpha]-synuclein interacts with pro-apoptotic proteins PKC[delta] and BAD to protect dopaminergic neuronal cells against MPP<sup>+</sup>-induced apoptotic cell death. *Molecular Brain Research*, *139*, 137-152.
- Kholodilov, N.G., Oo, T.F., & Burke, R.E. (1999a). Synuclein expression is decreased in rat substantia nigra following induction of apoptosis by intrastriatal 6-hydroxydopamine. *Neuroscience Letters*, *275*, 105-108.
- Kholodilov, N.G., Neystat, M., Oo, T.F., Lo, S.E., Larsen, K.E., Sulzer, D., et al. (1999b). Increased expression of rat synuclein in the substantia nigra pars compacta identified by mRNA differential display in a model of developmental target injury. *Journal of Neurochemistry*, *73*, 2586-2599.
- Kikuchi, H. (1991). TKG 0333: SK-MEL-28 (HIB 72). Retrieved December 8, 2010, from <http://www.idac.tohoku.ac.jp/dep/ccr/TKGdata/TKGvol03/TKG0333.html>
- Kim, B.J., Ryu, S.W., & Song, B.J. (2006). JNK- and p38 kinase-mediated phosphorylation of Bax leads to its activation and mitochondrial translocation and to apoptosis of human hepatoma HepG2 cells. *Journal of Biological Chemistry*, *281*, 21256-21265.
- Kim, R.H., Smith, P.D., Aleyasin, H., Hayley, S., Mount, M.P., Pownall, S., et al. (2005). Hypersensitivity of DJ-1-deficient mice to 1-methyl-4-phenyl-1,2,3,6-tetrahydropyridine (MPTP) and oxidative stress. *Proceedings of the National Academy of Sciences of the United States of America*, *102*, 5215-5220.

- Kim, T.D., Paik, S.R., & Yang, C.H. (2002). Structural and functional implications of C terminal regions of alpha-synuclein. *Biochemistry*, *41*, 13782-13790.
- King, T.D., & Jope, R.S. (2005). Inhibition of glycogen synthase kinase-3 protects cells from intrinsic but not extrinsic oxidative stress. *Neuroreport*, *16*, 597-601.
- Kitada, T., Asakawa, S., Hattori, N., Matsumine, H., Yamamura, Y., Minoshima, S., et al. (1998). Mutations in the parkin gene cause autosomal recessive juvenile Parkinsonism. *Nature*, *392*, 605-608.
- Kosel, S., Hofhaus, G., Maassen, A., Vieregge, P., & Graeber, M.B. (1999). Role of mitochondria in Parkinson's disease. *Biological Chemistry*, *380*, 865-870.
- Krishnan, S., Chi, E.Y., Wood, S.J., Kendrick, B.S., Li, C., Garzon-Rodriguez, W., et al. (2003). Oxidative dimer formation is the critical rate-limiting step for Parkinson's disease alpha-synuclein fibrillogenesis. *Biochemistry*, *42*, 829-837.
- Kruger, R., Kuhn, W.M.T., Voitalla, D., Graeber, M., Kösel, S., Przuntek, H., et al. (1998). Ala30Pro mutation in the gene encoding  $\alpha$ -synuclein in Parkinson's disease. *Nature Genetics*, *18*, 106-108.
- Kuwana, T., Bouchier-Hayes, L., Chipuk, J.E., Bonzon, C., Sullivan, B.A., Green, D.R., et al. (2005). BH3 domains of BH3-only proteins differentially regulate Bax-mediated mitochondrial membrane permeabilization both directly and indirectly. *Molecular Cell*, *17*, 525-535.
- Kuzuhara, S., Mori, H., Izumiyama, N., Yoshimura, M., & Ihara, Y. (1988) Lewy bodies are ubiquitinated - a light and electron-microscopic immunocytochemical study. *Acta Neuropathologica*, *75*, 345-353.
- Langston, J.W., & Ballard, P.A. Jr. (1983). Parkinson's disease in a chemist working with 1-methyl-4-phenyl-1,2,5,6-tetrahydropyridine. *The New England Journal of Medicine*, *309*, 310.
- Langston, J.W., Ballard, P., Tetrud, J.W., & Irwin, I. (1983). Chronic Parkinsonism in humans due to a product of meperidine analog synthesis. *Science*, *219*, 979-980.
- Lashuel, H.A., Petre, B.M., Wall, J., Simon, M., Nowak, R.J., Walz, T., et al. (2002). Alpha-synuclein, especially the Parkinson's disease-associated mutants, forms pore-like annular and tubular protofibrils. *Journal of Molecular Biology*, *322*, 1089-1092.
- Lavedan, C. (1998). The synuclein family. *Genome Research*, *8*, 871-880.

- Lavedan, C., Leroy, E., Dehejia, A., Buchholtz, S., Dutra, A., Nussbaum, R.L., et al. (1998). Identification, localization and characterization of the human gamma-synuclein gene. *Human Genetics*, *103*, 106-112.
- Le, W.D., Xu, P., Jankovic, J., Jiang, H., Appel, S.H., Smith, R.G., et al. (2003). Mutations in NR4A2 associated with familial Parkinson disease. *Nature Genetics*, *33*, 85-89.
- Lee, H.J., Khoshaghideh, F., Lee, S., & Lee, S.J. (2006). Impairment of microtubule-dependent trafficking by overexpression of alpha-synuclein. *European Journal of Neuroscience*, *24*, 3153-3162.
- Lee, H.J., Khoshaghideh, F., Patel, S., & Lee, S.J. (2004). Clearance of alpha-synuclein oligomeric intermediates via the lysosomal degradation pathway. *Journal of Neuroscience*, *24*, 1888-1896.
- Lee, J., Huang, M.S., Yang, I.C., Lai, T.C., Wang, J.L., Pang, V.F., et al. (2008). Essential roles of caspases and their upstream regulators in rotenone-induced apoptosis. *Biochemical and Biophysical Research Communications*, *371*, 33-38.
- Lee, M.H., Hyun, D.H., Halliwell, B., & Jenner, P. (2001). Effect of the overexpression of wild-type or mutant alpha-synuclein on cell susceptibility to insult. *Journal of Neurochemistry*, *76*, 998-1009.
- Lee, S.S., Kim, Y.M., Junn, E., Lee, G., Park, K.H., Tanaka, M., et al. (2003). Cell cycle aberrations by alpha-synuclein over-expression and cyclin B immunoreactivity in Lewy bodies. *Neurobiology of Aging*, *24*, 687-696.
- Leroy, E., Boyer, R., Auburger, G., Leube, B., Ulm, G., Mezey, E., et al. (1998). The ubiquitin pathway in Parkinson's disease. *Nature*, *395*, 451-452.
- Levine, A.J. (1997). p53, the cellular gatekeeper for growth and division. *Cell*, *88*, 323-331.
- Li, J., Spletter, M.L., Johnson, D.A., Wright, L.S., Svendsen, C.N., & Johnson, J.A. (2005). Rotenone-induced caspase 9/3-independent and -dependent cell death in undifferentiated and differentiated human neural stem cells. *Journal of Neurochemistry*, *92*, 462-476.
- Li, J., Uversky, V.N., & Fink, A.L. (2001). Effect of familial Parkinson's disease point mutations A30P and A53T on the structural properties, aggregation, and fibrillation of human alpha-synuclein. *Biochemistry*, *40*, 11604-11613.

- Li, N., Ragheb, K., Lawler, G., Sturgis, J., Rajwa, B., Melendez, J.A., et al. (2003). Mitochondrial complex I inhibitor rotenone induces apoptosis through enhancing mitochondrial reactive oxygen species production. *Journal of Biological Chemistry*, *278*, 8516-8525.
- Li, P., Nijhawan, D., Budihardjo, I., Srinivasula, S. M., Ahmad, M., Alnemri, E. S., et al. (1997). Cytochrome *c* and dATP-dependent formation of Apaf-1/caspase-9 complex initiates an apoptotic protease cascade. *Cell*, *91*, 479-489.
- Li, W., & Lee, M.K. (2005). Anti-apoptotic property of human  $\alpha$ -synuclein in neuronal cell lines is associated with the inhibition of caspase-3 but not caspase-9 activity. *Journal of Neurochemistry*, *93*, 1542-1550.
- Li, X., Marani, M., Mannucci, R., Kinsey, B., Andriani, F., Nicoletti, I., et al. (2001). Overexpression of BCL-X(L) underlies the molecular basis for resistance to staurosporine-induced apoptosis in PC-3 cells. *Cancer Research*, *61*, 1699-1706.
- Liang, J., Pan, Y., Zhang, D., Guo, C., Shi, Y., Wang, J., et al. (2007). Cellular prion protein promotes proliferation and G1/S transition of human gastric cancer cells SGC7901 and AGS. *FASEB Journal*, *21*, 2247-2256.
- Liu, H., Liu, W., Wu, Y., Zhou, Y., Xue, R., Luo, C., et al. (2005). Loss of epigenetic control of synuclein-gamma gene as a molecular indicator of metastasis in a wide range of human cancers. *Cancer Research*, *65*, 7635-7643.
- Liu, H., Zhou, Y., Boggs, S.E., Belinsky, S.A., & Liu, J. (2007). Cigarette smoke induces demethylation of prometastatic oncogene synuclein-gamma in lung cancer cells by downregulation of DNMT3B. *Oncogene*, *26*, 5900-5910.
- Liu, Y.Y., Zhao, H.Y., Zhao, C.L., Duan, C.L., Lu, L.L., & Yang, H. (2006). Overexpression of alpha-synuclein in SH-SY5Y cells partially protected against oxidative stress induced by rotenone. *Acta Physiologica Sinica*, *58*, 421-428.
- Lotharius, J., & Brundin, P. (2002). Impaired dopamine storage resulting from alpha synuclein mutations may contribute to the pathogenesis of Parkinson's disease. *Human Molecular Genetics*, *11*, 2395-2407.
- Lu, L., Gu, L., Liang, Y., Sun, X., Duan, C., & Yang, H. (2010). Dual effects of alpha-synuclein on neurotoxicity induced by low dosage of rotenone are dependent on exposure time in dopaminergic neuroblastoma cells. *Science China Life Sciences*, *53*, 590-597.

- Lundvig, D., Lindersson, E., & Jensen, P.H. (2005). Pathogenic effects of alpha-synuclein aggregation. *Molecular Brain Research*, 134, 3-17.
- Luo, X., Budihardjo, I., Zou, H., Slaughter, C., & Wang, X. (1998). Bid, a Bcl2 interacting protein, mediates cytochrome *c* release from mitochondria in response to activation of cell surface death receptors. *Cell*, 94, 481-490.
- Lyubchenko, Y.L., Kim, B.H., Krasnoslobodtsev, A.V., & Yu, J. (2010). Nanoimaging for protein misfolding diseases. *Wiley Interdisciplinary Reviews. Nanomedicine and Nanobiotechnology*, 2, 526-543.
- Maries, E., Dass, B., Collier, T.J., Kordower, J.H., & Steece-Collier, K. (2003). The role of alpha-synuclein in Parkinson's disease: insights from animal models. *Nature Reviews Neuroscience*, 4, 727-738.
- Maroteaux, L., Campanelli, J.T., & Scheller, R.H. (1988). Synuclein: a neuronspecific protein localized to the nucleus and presynaptic nerve terminal. *Journal of Neuroscience*, 8, 2804-2815.
- Marx, F.P., Holzmann, C., Strauss, K.M., Li, L., Eberhardt, O., Gerhardt, E., et al. (2003). Identification and functional characterization of a novel R621C mutation in the synphilin-1 gene in Parkinson's disease. *Human Molecular Genetics*, 12, 1223-1231.
- Matsumoto, L., Takuma, H., Tamaoka, A., Kurisaki, H., Date, H., Tsuji, S., et al. (2010). CpG demethylation enhances alpha-synuclein expression and affects the pathogenesis of Parkinson's disease. *PLoS ONE*, 5, e15522.
- Matsuo, Y., & Kamitani, T. (2010). Parkinson's disease-related protein,  $\alpha$ -Synuclein, in malignant melanoma. *PLoS ONE*, 5, e10481.
- McCord, J.M. (1998). Iron, free radicals, and oxidative injury. *Seminars in Hematology*, 35, 5-12.
- McCord, J.M., & Fridovich, I. (1988). Superoxide dismutase: the first twenty years (1968-1988). *Free Radical Biology & Medicine*, 5, 363-369.
- Meco, G., Bonifati, V., Vanacore, N., & Fabrizio, E. (1994). Parkinsonism after chronic exposure to the fungicide maneb (manganese ethylene-bis-dithiocarbamate). *Scandinavian Journal of Work, Environment & Health*, 20, 301-305.
- Melanoma Education Foundation. (2010). Finding melanoma early: warning signs & photos. Retrieved December 20, 2010, from <http://www.skincheck.org/Page4.htm>

- Mezey, E., Dehejia, A., Harta, G., Papp, M.I., Polymeropoulos, M.H., & Brownstein, M.J. (1998). Alpha synuclein in neurodegenerative disorders: murderer or accomplice? *Nature Medicine*, *4*, 755-757.
- Miller, D.B. (1982). Neurotoxicity of the pesticidal carbamates. *Neurobehavioral Toxicology & Teratology*, *4*, 779-787.
- Miyashita, T., Krajewski, S., Krajewska, M., Wang, H.G., Lin, H.K., Liebermann, D.A., et al. (1994). Tumour suppressor p53 is a regulator of bcl-2 and bax gene expression *in vitro* and *in vivo*. *Oncogene*, *9*, 1799-1805.
- Moffat, J., Grueneberg, D.A., Yang, X., Kim, S.Y., Kloepper, A.M., Hinkle, G., et al. (2006). A lentiviral RNAi library for human and mouse genes applied to an arrayed viral high-content screen. *Cell*, *124*, 1283-1298.
- Morgan, J., Hoekstra, A.V., Chapman-Davis, E., Hardt, J.L., Kim, J.J., & Buttin, B.M. (2009). Synuclein-gamma (SNCG) may be a novel prognostic biomarker in uterine papillary serous carcinoma. *Gynecologic Oncology*, *114*, 293-298.
- Moron, J.A., Zakharova, I., Ferrer, J.V., Merrill, G.A., Hope, B., Lafer, E.M., et al. (2003). Mitogen-activated protein kinase regulates dopamine transporter surface expression and dopamine transport capacity. *Journal of Neuroscience*, *23*, 8480-8488.
- Moussa, C., Mahmoodian, F., Tomita, Y., & Sidhu, A. (2007). Dopamine differentially induces aggregation of A53T mutant and wild type  $\alpha$ -synuclein: Insights into the protein chemistry of Parkinson's disease. *Biochemical and Biophysical Research Communications*, *365*, 833-839.
- Murphy, D.D., Rueter, S.M., Trojanowski, J.Q., & Lee, V.M.Y. (2000). Synucleins are developmentally expressed, and alpha-synuclein regulates the size of the presynaptic vesicular pool in primary hippocampal neurons. *Journal of Neuroscience*, *20*, 3214-3220.
- Musgrove, R.E., King, A.E., & Dickson, T.C. (2010). Neuroprotective upregulation of endogenous alpha-synuclein precedes ubiquitination in cultured dopaminergic neurons. *Neurotoxicity Research*. Retrieved October 8, 2010, from <http://www.biomedsearch.com/nih/Neuroprotective-Upregulation-Endogenous-Alpha-Synuclein/20617407.html>
- Mytilineou, C., Kramer, B.C., & Yabut, J.A. (2002). Glutathione depletion and oxidative stress. *Parkinsonism & Related Disorders*, *8*, 385-387.
- Nagano, Y., Yamashita, H., Nakamura, T., Takahashi, T., Kondo, E., & Nakamura, S. (2001). Lack of binding observed between human alpha-synuclein and Bcl-2 protein family. *Neuroscience Letters*, *316*, 103-107.

- Nakajo, S., Tsukada, K., Omata, K., Nakamura, Y., & Nakaya, K. (1993). A new brain-specific 14-kDa protein is a phosphoprotein. Its complete amino acid sequence and evidence for phosphorylation. *European Journal of Biochemistry*, *217*, 1057-1063.
- Narhi, L., Wood, S.J., Steavenson, S., Jiang, Y., Wu, G.M., Anafi, D., et al. (1999). Both familial Parkinson's disease mutations accelerate  $\alpha$ -synuclein aggregation. *Journal of Biological Chemistry*, *274*, 9843-9846.
- Newhouse, K., Hsuan, S.L., Chang, S.H., Cai, B., Wang, Y., & Xia, Z. (2004). Rotenone-induced apoptosis is mediated by p38 and JNK MAP kinases in human dopaminergic SH-SY5Y cells. *Toxicological Sciences*, *79*, 137-146.
- Nicoletti, I., Migliorati, G., Pagliacci, M.C., Grignani, F., & Riccardi, C. (1991). A rapid and simple method for measuring thymocyte apoptosis by propidium iodide staining and flow cytometry. *Journal of Immunological Methods*, *139*, 271.
- Ninkina, N.N., Alimova-Kost, M.V., Paterson, J.W., Delaney, L., Cohen, B.B., Imreh, S., et al. (1998). Organization, expression and polymorphism of the human persyn gene. *Human Molecular Genetics*, *7*, 1417-1424.
- Nunez, G., Seto, M., Seremetis, S., Ferrero, D., Grignani, F., Korsmeyer, S.J., et al. (1989). Growth and tumor promoting effects of deregulated Bcl-2 in human B lymphoblastoid cells. *Proceedings of the National Academy of Sciences of the United States of America*, *86*, 4589-4593.
- Olsen, J.H., Friis, S., & Frederiksen, K. (2006). Malignant melanoma and other types of cancer preceding Parkinson disease. *Epidemiology*, *17*, 582-587.
- Olsen, J.H., Friis, S., Frederiksen, K., McLaughlin, J.K., Mellekjær, L., & Møller, H. (2005). Atypical cancer pattern in patients with Parkinson's disease. *British Journal of Cancer*, *92*, 201-205.
- Oltvai, Z.N., & Korsmeyer, S.J. (1994). Checkpoints of dueling dimers foil death wishes. *Cell*, *79*, 189-192.
- Omar, Z.A., Mohd Ali, Z., & Tamin, N.S.I. (Eds.). (2006). Malaysian cancer statistics - Data and figure Peninsular Malaysia 2006. National Cancer Registry, Ministry of Health Malaysia. Retrieved January 3, 2011, from [http://moh.gov.my/images/gallery/Report/Cancer/MalaysiaCancerStatistics\\_2006.pdf](http://moh.gov.my/images/gallery/Report/Cancer/MalaysiaCancerStatistics_2006.pdf)
- Omura, S., Iwai, Y., Hirano, A., Nakagawa, A., Awaya, J., Tsuchiya, H., et al. (1977). A new alkaloid AM-2282 of Streptomyces origin. Taxonomy, fermentation, isolation and preliminary characterization. *Journal of Antibiotics*, *30*, 275-282

- Orth, M., Tabrizi, S.J., Schapira, A.H., & Cooper, J.M. (2003). Alpha-synuclein expression in HEK293 cells enhances the mitochondrial sensitivity to rotenone. *Neuroscience Letters*, *351*, 29-32.
- Osieka, R. (1984). Studies on drug resistance in a human melanoma xenograft system. *Cancer Treatment Reviews*, *11*, 85-98.
- Ostrerova, N., Petrucelli, L., Farrer, M., Mehta, N., Choi, P., Hardy, J., et al. (1999). Alpha-Synuclein shares physical and functional homology with 14-3-3 proteins. *Journal of Neuroscience*, *19*, 5782-5791.
- Paddison, P.J. (2008). RNA interference in mammalian cell systems. *Current Topics in Microbiology and Immunology*, *320*, 1-19.
- Paisan-Ruiz, C., Jain, S., Evans, E.W., Gilks, W.P., Simon, J., van der Brug, M., et al. (2004). Cloning of the gene containing mutations that cause PARK8-linked Parkinson's disease. *Neuron*, *44*, 595-600.
- Paleologou, K.E., Oueslati, A., Shakked, G., Rospigliosi, C.C., Kim, H.Y., Lamberto, G.R., et al. (2010). Phosphorylation at S87 is enhanced in synucleinopathies, inhibits alpha-synuclein oligomerization, and influences synuclein-membrane interactions. *Journal of Neuroscience*, *30*, 3184-3198.
- Pan, Z.Z., Bruening, W., Giasson, B.I., Lee, V.M., & Godwin, A.K. (2002). Gamma-synuclein promotes cancer cell survival and inhibits stress- and chemotherapy drug-induced apoptosis by modulating MAPK pathways. *Journal of Biological Chemistry*, *277*, 35050-35060.
- Pankratz, N., Nichols, W.C., Uniacke, S.K., Halter, C., Rudolph, A., Shults, C., et al. (2002). Genome screen to identify susceptibility genes for Parkinson disease in a sample without parkin mutations. *American Journal of Human Genetics*, *71*, 124-135
- Papadimitriou, A., Veletza, V., Hadjigeorgiou, G.M., Patrikiou, A., Hirano, M., & Anastasopoulos, I. (1999). Mutated alpha-synuclein gene in two Greek kindreds with familial PD: incomplete penetrance? *Neurology*, *52*, 651-654.
- Parihar, M.S., Parihar, A., Fujita, M., Hashimoto, M., & Ghafourifar, P. (2008). Mitochondrial association of alpha-synuclein causes oxidative stress. *Cellular and Molecular Life Sciences*, *65*, 1272-1284.
- Park, J., Lee, S.B., Lee, S., Kim, Y., Song, S., Kim, S., et al. (2006). Mitochondrial dysfunction in *Drosophila* PINK1 mutants is complemented by parkin. *Nature*, *441*, 1157-1161.
- Parkin, D., Bray, F., Ferlay, J., & Pisani, P. (2002). Global cancer statistics. *CA: A Cancer Journal for Clinicians*, *55*, 74-108.

- Payton, J.E., Perrin, R.J., Clayton, D.F., & George, J.M. (2001). Protein-protein interactions of alpha-synuclein in brain homogenates and transfected cells. *Molecular Brain Research*, 95, 138-145.
- Pei, W., Liou, A.K., & Chen, J. (2003). Two caspase-mediated apoptotic pathways induced by rotenone toxicity in cortical neuronal cells. *FASEB Journal*, 17, 520-522.
- Pelengaris, S., Khan, M., Steward, W., Blasco, M., Yee, C., Shima, D., et al. (2006). *The molecular biology of cancer*. US: Blackwell Publishing Ltd.
- Perez, R.G., & Hastings, T.G. (2004). Could a loss of  $\alpha$ -synuclein function put dopaminergic neurons at risk? *Journal of Neurochemistry*, 89, 1318-1324.
- Perez, R.G., Waymire, J.C., Lin, E., Liu, J.J., Guo, F., & Zigmond, M.J. (2002). A role for  $\alpha$ -synuclein in the regulation of dopamine biosynthesis. *Journal of Neuroscience*, 22, 3090-3099.
- Perrin, R.J., Woods, W.S., Clayton, D.F., & George, J.M. (2000). Interaction of human alpha-synuclein and Parkinson's disease variants with phospholipids. Structural analysis using site-directed mutagenesis. *Journal of Biological Chemistry*, 275, 34393-34398.
- Perry, T.L., & Yong, V.W. (1986). Idiopathic Parkinson's disease, progressive supranuclear palsy and glutathione metabolism in the substantia nigra of patients. *Neuroscience Letters*, 67, 269-274.
- Perutz, M.F., Pope, B.J., Owen, D., Wanker, E.E., & Scherzinger, E. (2002). Aggregation of proteins with expanded glutamine and alanine repeats of the glutamine-rich and asparagine-rich domains of Sup35 and of the amyloid beta-peptide of amyloid plaques. *Proceedings of the National Academy of Sciences of the United States of America*, 99, 5596-5600.
- Pitti, R.M., Marsters, S.A., Lawrence, D.A., Roy, M., Kischkel, F.C., Dowd, P., et al. (1998). Genomic amplification of a decoy receptor for Fas ligand in lung and colon cancer. *Nature*, 396, 699-703.
- Polymeropoulos, M.H., Lavedan, C., Leroy, E., Ide, S.E., Dehejia, A., Dutra, A., et al. (1997). Mutation in the alpha-synuclein gene identified in families with Parkinson's disease. *Science*, 276, 2045-2047.
- Quilty, M.C., King, A.E., Gai, W.P., Pountney, D.L., West, A.K., Vickers, J.C., et al. (2006). Alpha-synuclein is upregulated in neurones in response to chronic oxidative stress and is associated with neuroprotection. *Experimental Neurology*, 199, 249-256.

- Raisova, M., Hossini, A.M., Eberle, J., Riebeling, C., Wieder, T., Sturm, I., et al. (2001). The Bax/Bcl-2 ratio determines the susceptibility of human melanoma cells to CD95/Fas-mediated apoptosis. *Journal of Investigative Dermatology*, 117, 333-340.
- Raposo, G., & Marks, M.S. (2007). Melanosomes-dark organelles enlighten endosomal membrane transport. *Nature Reviews Molecular Cell Biology*, 8, 786-797.
- RCSB Protein Data Bank. (2009). Human micelle-bound alpha-synuclein. Retrieved January 1, 2011, from <http://www.rcsb.org/pdb/explore/explore.do?structureId=1XQ8>
- Reed, J.C., Zha, H., Aime-Sempe, C., Takayama, S., & Wang, H.G. (1996). Structure-function analysis of Bcl-2 family proteins. Regulators of programmed cell death. *Advances in Experimental Medicine and Biology*, 406, 99-112.
- Rospigliosi, C.C., McClendon, S., Schmid, A.W., Ramlall, T.F., Barré, P., Lashuel, H.A., et al. (2009). E46K Parkinson's-linked mutation enhances C-terminal-to-N-terminal contacts in alpha-synuclein. *Journal of Molecular Biology*, 388, 1022-1032.
- Saito, Y., Kawai, M., Inoue, K., Sasaki, R., Arai, H., Nanba, E., et al. (2000). Widespread expression of alpha-synuclein and tau immunoreactivity in Hallervorden-Spatz syndrome with protracted clinical course. *Journal of Neurological Science*, 177, 48-59.
- Samii, A., Nutt, J.G., & Ransom, B.R. (2004). Parkinson's disease. *Lancet*, 363, 1783-1793.
- Sapru, M.K., Yates, J.W., Hogan, S., Jiang, L., Halter, J., & Bohn, M.C. (2006). Silencing of human  $\alpha$ -synuclein *in vitro* and in rat brain using lentiviral-mediated RNAi. *Experimental Neurology*, 198, 382-390.
- Sattler, M., Liang, H., Nettlesheim, D., Meadows, R.P., Harlan, J.E., Eberstadt, M., et al. (1997). Structure of Bcl-xL-Bak peptide complex: recognition between regulators of apoptosis. *Science*, 275, 983-986.
- Scarlett, J.L., & Murphy, M.P. (1997). Release of apoptogenic proteins from the mitochondrial intermembrane space during the mitochondrial permeability transition. *FEBS Letters*, 418, 282-286.
- Schapira, A.H. (2008). Mitochondria in the aetiology and pathogenesis of Parkinson's disease. *Lancet Neurology*, 7, 97-109.
- Schapira, A.H., Cooper, J.M., Dexter, D., Clark, J.B., Jenner, P., & Marsden, C.D. (1990). Mitochondrial complex I deficiency in Parkinson's disease. *Journal of Neurochemistry*, 54, 823-827.

- Scheffner, M., Werness, B.A., Huibregtse, J.M., Levine, A.J., & Howley, P.M. (1990). The E6 oncoprotein encoded by human papillomavirus types 16 and 18 promotes the degradation of p53. *Cell*, *63*, 1129-1136.
- Schulz, J.B., Lindenau, J., Seyfried, J., & Dichgans, J. (2000). Glutathione, oxidative stress and neurodegeneration. *European Journal of Biochemistry*, *267*, 4904-4911.
- Scmeyer. (2008). The pan-kinase inhibitor staurosporine. Retrieved December 20, 2010, from <http://commons.wikimedia.org/wiki/File:Staurosporine1.png>
- Seo, J.H., Rah, J.C., Choi, S.H., Shin, J.K., Min, K., Kim, H.S., et al. (2002). Alpha-synuclein regulates neuronal survival via Bcl-2 family expression and PI3/Akt kinase pathway. *FASEB Journal*, *16*, 1826-1828.
- Serpell, L.C., Berriman, J., Jakes, R., Goedert, M., & Crowther, R.A. (2000). Fiber diffraction of synthetic alpha-synuclein filaments shows amyloid-like cross-beta conformation. *Proceedings of the National Academy of Sciences of the United States of America*, *97*, 4897-4902.
- Shamoto-Nagai, M., Maruyama, W., Kato, Y., Isobe, K., Tanaka, M., Naoi, M., et al. (2003). An inhibitor of mitochondrial complex I, rotenone, inactivates proteasome by oxidative modification and induces aggregation of oxidized proteins in SHSY5Y cells. *Journal of Neuroscience Research*, *74*, 589-597.
- Shapiro, R.L. (2002). Surgical approaches to malignant melanoma: Practical guidelines. *Dermatologic Clinics*, *20*, 681-699.
- Sharon, R., Goldberg, M.S., Bar-Josef, I., Betensky, R.A., Shen, J., & Selkoe, D.J. (2001). Alpha-Synuclein occurs in lipid-rich high molecular weight complexes, binds fatty acids, and shows homology to the fatty acid-binding proteins. *Proceedings of the National Academy of Sciences of the United States of America*, *98*, 9110-9115.
- Sherer, T.B., Betarbet, R., Stout, A.K., Lund, S., Baptista, M., Panov, A.V., et al. (2002). An *in vitro* model of Parkinson's disease: linking mitochondrial impairment to altered  $\alpha$ -synuclein metabolism and oxidative damage. *Journal of Neuroscience*, *22*, 7006-7015.
- Sherer, T.B., Betarbet, R., Testa, C.M., Seo, B.B., Richardson, J.R., Kim, J.H., et al. (2003a). Mechanism of toxicity in rotenone models of Parkinson's disease. *Journal of Neuroscience*, *23*, 10756-10764.
- Sherer, T.B., Kim, J.H., Betarbet, R., & Greenamyre, J.T. (2003b). Subcutaneous rotenone exposure causes highly selective dopaminergic degeneration and alpha-synuclein aggregation. *Experimental Neurology*, *179*, 9-16.

- Shibayama-Imazu, T., Ogane, K., Hasegawa, Y., Nakajo, S., Shioda, S., Ochiai, H., et al. (1998). Distribution of PNP 14 ( $\beta$ -synuclein) in neuroendocrine tissues: localization in Sertoli cells. *Molecular Reproduction and Development*, 50, 163-169.
- Shidham, V.B., Qi, D.Y., Acker, S., Kampalath, B., Chang, C.C., George, V., et al. (2001). Evaluation of micrometastases in sentinel lymph nodes of cutaneous melanoma: higher diagnostic accuracy with Melan-A and MART-1 compared with S-100 protein and HMB-45. *American Journal of Surgical Pathology*, 25, 1039-1046.
- Sian, J., Dexter, D.T., Lees, A.J., Daniel, S., Agid, Y., Javoy-Agid, F., et al. (1994). Alterations in glutathione levels in Parkinson's disease and other neurodegenerative disorders affecting basal ganglia. *Annals of Neurology*, 36, 348-355.
- Sidhu, A., Wersinger, C., & Vernier, P. (2004a). Alpha-synuclein regulation of the dopaminergic transporter: a possible role in the pathogenesis of Parkinson's disease. *FEBS Letters*, 565, 1-5.
- Sidhu, A., Wersinger, C., & Vernier, P. (2004b). Does alpha-synuclein modulate dopaminergic synaptic content and tone at the synapse? *FASEB Journal*, 18, 637-647.
- Sidhu, A., Wersinger, C., Moussa, C.E., & Vernier, P. (2004c). The role of alpha-synuclein in both neuroprotection and neurodegeneration. *Annals of the New York Academy of Sciences*, 1035, 250-270.
- Singleton, A.B., Farrer, M., Johnson, J., Singleton, A., Hague, S., Kachergus, J., et al. (2003). Alpha-synuclein locus triplication causes Parkinson's disease. *Science*, 302, 841.
- Slee, E.A., Harte, M.T., Kluck, R.M., Wolf, B.B., Casiano, C.A., Newmeyer, D.D., et al. (1999). Ordering the cytochrome *c*-initiated caspase cascade: hierarchical activation of caspases-2, -3, -6, -7, -8, and -10 in a caspase-9-dependent manner. *Journal of Cell Biology*, 144, 281-292.
- Smith, W.W., Jiang, H., Pei, Z., Tanaka, Y., Morita, H., Sawa, A., et al. (2005). Endoplasmic reticulum stress and mitochondrial cell death pathways mediate A53T mutant alpha-synuclein-induced toxicity. *Human Molecular Genetics*, 14, 3801-3811.
- Snyder, R.D., & Friedman, M.B. (1998). Enhancement of cytotoxicity and clastogenicity of 1-DOPA and dopamine by manganese and copper. *Mutation Research*, 405, 1-8.
- Soengas, M.S., Capodici, P., Polsky, D., Mora, J., Esteller, M., Opitz-Araya, X., et al. (2001). Inactivation of the apoptosis effector Apaf-1 in malignant melanoma. *Nature*, 409, 207-211.

- Sofic, E., Lange, K.W., Jellinger, K., & Riederer, P. (1992). Reduced and oxidized glutathione in the substantia nigra of patients with Parkinson's disease. *Neuroscience Letters*, *142*, 128-130.
- Sofic, E., Riederer, P., Heinsen, H., Beckmann, H., Reynolds, G.P., Hebenstreit, G., et al. (1988). Increased iron (III) and total iron content in post mortem substantia nigra of Parkinsonian brain. *Journal of Neural Transmission*, *74*, 199-205.
- Souza, J.M., Giasson, B.I., Chen, Q., Lee, V.M., & Ischiropoulos, H. (2000a). Dityrosine cross-linking promotes formation of stable alpha-synuclein polymers. Implication of nitrative and oxidative stress in the pathogenesis of neurodegenerative synucleinopathies. *Journal of Biological Chemistry*, *275*, 18344-18349.
- Souza, J.M., Giasson, B.I., Lee, V.M., & Ischiropoulos, H. (2000b). Chaperone-like activity of synucleins. *FEBS Letters*, *474*, 116-119.
- Spillantini, M.G., Crowther, R.A., Jakes, R., Hasegawa, M., & Goedert, M. (1998). Alpha-synuclein in filamentous inclusions of Lewy bodies from Parkinson's disease and dementia with Lewy bodies. *Proceedings of the National Academy of Sciences of the United States of America*, *95*, 6469-6473.
- Spillantini, M.G., Divane, A., & Goedert, M. (1995). Assignment of human alpha-synuclein (SNCA) and beta-synuclein (SNCB) genes to chromosomes 4q21 and 5q35. *Genomics*, *27*, 379-381.
- Spillantini, M.G., Schmidt, M.L., Lee, V.M.Y., Trojanowski, J.Q., Jakes, R., & Goedert, M. (1997). Alpha-synuclein in Lewy bodies. *Nature*, *388*, 839-840.
- Spira, P.J., Sharpe, D.M., Halliday, G., Cavanagh, J., & Nicholson, G.A. (2001). Clinical and pathological features of a Parkinsonian syndrome in a family with an Ala53Thr alpha-synuclein mutation. *Annals of Neurology*, *49*, 313-319.
- Stephan, A., Davis, S., Salin, H., Dumas, S., Mallet, J., & Laroche, S. (2002). Age-dependent differential regulation of genes encoding APP and alpha-synuclein in hippocampal synaptic plasticity. *Hippocampus*, *12*, 55-62.
- Strauss, K.M., Martins, L.M., Plun-Favreau, H., Marx, F.P., Kautzmann, S., Berg, D., et al. (2005). Loss of function mutations in the gene encoding Omi/HtrA2 in Parkinson's disease. *Human Molecular Genetics*, *14*, 2099-2111.
- Surgucheva, I., McMahon, B., & Surguchov, A. (2006). Gamma-synuclein has a dynamic intracellular localization. *Cell Motility and the Cytoskeleton*, *63*, 447-458.

- Tabner, B.J., Turnbull, S., El-Agnaf, O.M.A., & Allsop, D. (2002). Formation of hydrogen peroxide and hydroxyl radicals from A $\beta$  and  $\alpha$ -synuclein as a possible mechanism of cell death in Alzheimer's disease and Parkinson's disease. *Free Radical Biology and Medicine*, *32*, 1076-1083.
- Tada-Oikawa, S., Hiraku, Y., Kawanishi, M., & Kawanishi, S. (2003). Mechanism for generation of hydrogen peroxide and change of mitochondrial membrane potential during rotenone-induced apoptosis. *Life Sciences*, *73*, 3277-3288.
- Tafani, M., Cohn, J.A., Karpnich, N.O., Rothman, R.J., Russo, M.A., & Farber, J.L. (2002). Regulation of intracellular pH mediates Bax activation in HeLa cells treated with staurosporine or tumor necrosis factor- $\alpha$ . *Journal of Biological Chemistry*, *277*, 49569-49576.
- Tafani, M., Minchenko, D.A., Serroni, A., & Farber, J.L. (2001). Induction of the mitochondrial permeability transition mediates the killing of HeLa cells by staurosporine. *Cancer Research*, *61*, 2459-2466.
- Takahashi, R.N., Rogerio, R., & Zanin, M. (1989). Maneb enhances MPTP neurotoxicity in mice. *Research Communications in Chemical Pathology and Pharmacology*, *66*, 167-170.
- Talpade, D.J., Greene, J.G., Higgins, D.S. Jr., & Greenamyre, J.T. (2000). *In vivo* labeling of mitochondrial complex I (NADH: ubiquinone oxidoreductase) in rat brain using [(3)H]dihydrorotenone. *Journal of Neurochemistry*, *75*, 2611-2621.
- Tanaka, Y., Engelender, S., Igarashi, S., Rao, R.K., Wanner, T., Tanzi, R.E., et al. (2001). Inducible expression of mutant alpha-synuclein decreases proteasome activity and increases sensitivity to mitochondria dependent apoptosis. *Human Molecular Genetics*, *10*, 919-926.
- Terada, H. (1990). Uncouplers of oxidative phosphorylation. *Environmental Health Perspectives*, *87*, 213-218.
- Thiruchelvam, M., Brockel, B.J., Richfield, E.K., Baggs, R.B., & CorySlechts, D.A. (2000). Potentiated and preferential effects of combined paraquat and maneab on nigrostriatal dopamine systems: environmental risk factors for Parkinson's disease? *Brain Research*, *873*, 225-234.
- Toulouse, A., & Sullivan, A.M. (2008). Progress in Parkinson's disease-where do we stand? *Progress in Neurobiology*, *85*, 376-392.
- Trimmer, P.A., Borland, M.K., Keeney, P.M., Bennett, J.P. Jr., & Parker, W.D. Jr. (2004). Parkinson's disease transgenic mitochondrial cybrids generate Lewy inclusion bodies. *Journal of Neurochemistry*, *88*, 800-812.

- Tsujimoto, Y. (1989). Overexpression of the human Bcl-2 gene product results in growth enhancement of Epstein-Barr virus immortalized B cells. *Proceedings of the National Academy of Sciences of the United States of America*, *86*, 1958-1962.
- Turnbull, S., Tabner, B.J., Moore, S., Davies, Y., El-Agnaf, O.M.A., & Allsop, D. (2001).  $\alpha$ -synuclein implicated in Parkinson's disease catalyses the formation of hydrogen peroxide *in vitro*. *Free Radical Biology and Medicine*, *30*, 1163-1170.
- Ueda, K., Fukushima, H., Masliah, E., Xia, Y., Iwai, A., Yoshimoto, M., et al. (1993). Molecular cloning of cDNA encoding an unrecognized component of amyloid in Alzheimer disease. *Proceedings of the National Academy of Sciences of the United States of America*, *90*, 11282-11286.
- Ugurel, S., Tilgen, W., & Reinhold, U. (2003). Chemosensitivity testing in malignant melanoma. *Recent Results in Cancer Research*, *161*, 81-92.
- University of Pennsylvania Health System. (1999). Tau and alpha-synuclein dysfunction and aberrant aggregates define distinct neurodegenerative diseases. Retrieved December 11, 2010, from <http://www.bio.davidson.edu/courses/genomics/2001/madden/assignment1.html>
- Uren, R.T., Dewson, G., Chen L, Coyne, S.C., Huang, D.C.S., Adams, J.M., et al. (2007). Mitochondrial permeabilization relies on BH3 ligands engaging multiple prosurvival Bcl-2 relatives, not Bak. *Journal of Cell Biology*, *177*, 277-287.
- Uversky, V.N. (2004). Neurotoxicant-induced animal models of Parkinson's disease: understanding the role of rotenone, maneb and paraquat in neurodegeneration. *Cell and Tissue Research*, *318*, 225-241.
- Uversky, V.N., Cooper, M.E., Bower, K.S., Li, J., & Fink, A.L. (2002). Accelerated alpha synuclein fibrillation in crowded milieu. *FEBS Letters*, *15*, 99-103.
- Vaccari, A., Ferraro, L., Saba, P., Ruiu, S., Mocci, I., Antonelli, T., et al. (1998). Differential mechanisms in the effects of disulfiram and diethyldithiocarbamate intoxication on striatal release and vesicular transport of glutamate. *Journal of Pharmacology and Experimental Therapeutics*, *285*, 961-967.
- Vaccari, A., Saba, P.L., Ruiu, S., Collu, M., & Devoto, P. (1996). Disulfiram and diethyldithiocarbamate intoxication affects the storage and release of striatal dopamine. *Toxicology and Applied Pharmacology*, *139*, 102-108.

- Valente, E.M., Abou-Sleiman, P.M., Caputo, V., Muqit, M.M., Harvey, K., Gispert, S., et al. (2004). Hereditary early-onset Parkinson's disease caused by mutations in PINK1. *Science*, *304*, 1158-1160.
- Vicencio, J.M., Galluzzi, L., Tajeddine, N., Ortiz, C., Criollo, A., Tasdemir, E., et al. (2008). Senescence, apoptosis or autophagy? When a damaged cell must decide its path-a mini-review. *Gerontology*, *54*, 92-99.
- Volles, M.J., & Lansbury, P.T. Jr. (2002). Vesicle permeabilization by protofibrillar alpha-synuclein is sensitive to Parkinson's disease-linked mutations and occurs by a pore-like mechanism. *Biochemistry*, *41*, 4595-4602.
- Walensky, L.D., Pitter, K., Morash, J., Oh, K.J., Barbuto, S., Fisher, J., et al. (2006). A stapled BID BH3 helix directly binds and activates BAX. *Molecular and Cellular Biology*, *24*, 199-210.
- Walters, T.L., Irwin, I., Delfani, K., Langston, J.W., & Janson, A.M. (1999). Diethylthiocarbamate causes nigral cell loss and dopamine depletion with nontoxic doses of MPTP. *Experimental Neurology*, *156*, 62-70.
- Wang, Y.F., Hsieh, Y.F., Lin, C.L., Lin, J.L., Chen, C.Y., Chiou, Y.H., et al. (2004). Staurosporine-induced G2/M arrest in primary effusion lymphoma BCBL-1 cells. *Annals of hematology*, *83*, 739-744.
- Watabe, M., & Nakaki, T. (2004). Rotenone induces apoptosis via activation of bad in human dopaminergic SH-SY5Y cells. *Journal of Pharmacology and Experimental Therapeutics*, *311*, 948-953.
- Watabe, M., & Nakaki, T. (2008). Mitochondrial complex I inhibitor rotenone inhibits and redistributes vesicular monoamine transporter 2 via nitration in human dopaminergic SH-SY5Y cells. *Molecular Pharmacology*, *74*, 933-940.
- Waxman, E.A., & Giasson, B.I. (2008). Molecular mechanisms of  $\alpha$ -Synuclein neurodegeneration. *Biochimica et Biophysica Acta*, *1792*, 616-624.
- Weinberg, B. (2009). Addgene plasmid 1765. Retrieved December 13, 2010, from <http://www.addgene.org/pgvec1?f=c&cmd=findpl&identifier=1765>
- Weinberg, R.A. (2007). *The biology of cancer*. London: Garland Science, Taylor & Francis Group, LLC.
- Weinreb, P.H., Zhen, W., Poon, A.W., Conway, K.A., & Lansbury, P.T.J. (1996). NACP, a protein implicated in Alzheimer's disease and learning, is natively unfolded. *Biochemistry*, *35*, 13709-13715.

- Wersinger, C., Banta, M., & Sidhu, A. (2004). Comparative analyses of alpha-synuclein expression levels in rat brain tissues and transfected cells. *Neuroscience Letters*, *358*, 95-98.
- Wersinger, C., Prou, P., Vernier, P., & Sidhu, A. (2003). Modulation of dopamine transporter function by alpha-synuclein is altered by impairment of cell adhesion and by induction of oxidative stress. *FASEB Journal*, *17*, 2151-2153.
- Wessling-Resnick, M. (1999). Biochemistry of iron uptake. *Critical Reviews in Biochemistry and Molecular Biology*, *34*, 285-314.
- Willis, S.N., Fletcher, J.I., Kaufmann, T., van Delft, M.F., Chen, L., Czabotar, P.E., et al. (2007). Apoptosis initiated when BH3 ligands engage multiple Bcl-2 homologs, not Bax or Bak. *Science*, *315*, 856-859.
- Wolter, K.G., Hsu, Y., Smith, C.L., Mechushtan, A., Xi, X., & Youle, R.J. (1997). Movement of BAX from cytosol to mitochondria during apoptosis. *Journal of Cell Biology*, *139*, 1281-1292.
- Wooten, G.F., Currie, L.J., Bennett, J.P., Harrison, M.B., Trugman, J.M., & Parker, W.D. Jr. (1997). Maternal inheritance in Parkinson's disease. *Annals of Neurology*, *41*, 265-268.
- Wu, F., Poon, W.S., Lu, G., Wang, A., Meng, H., Feng, L., et al. (2009). Alpha-synuclein knockdown attenuates MPP<sup>+</sup> induced mitochondrial dysfunction of SH-SY5Y cells. *Brain Research*, *1292*, 173-179.
- Xia, X.G., Harding, T., Weller, M., Bieneman, A., Uney, J.B., & Schulz, J.B. (2001). Gene transfer of the JNK interacting protein-1 protects dopaminergic neurons in the MPTP model of Parkinson's disease. *Proceedings of the National Academy of Sciences of the United States of America*, *98*, 10433-10438.
- Xu, D.Z., Gillespie, S.K., & Hersey, P. (2004). Staurosporine induces apoptosis of melanoma by both caspase-dependent and -independent apoptotic pathway. *Molecular Cancer Therapeutics*, *3*, 187-197.
- Xu, J., Kao, S.Y., Lee, F.J., Song, W., Jin, L.W., & Yankner, B.A. (2002). Dopamine-dependent neurotoxicity of alpha-synuclein: a mechanism for selective neurodegeneration in Parkinson disease. *Nature Medicine*, *8*, 600-606.
- Xue, L.Y., Chiu, S.M., & Oleinick, N.L. (2003). Staurosporine-induced death of MCF-7 human breast cancer cells: distinction between caspase-3-dependent steps of apoptosis and the critical lethal lesions. *Experimental Cell Research*, *283*, 135-145.

- Yacoubian, T.A., & Standaert, D.G. (2008). Targets for neuroprotection in Parkinson's disease. *Biochimica et Biophysica Acta*, 1792, 676-687.
- Yamaki, K., Hong, J., Hiraizumi, K., Ahn, J.W., Zee, O., & Ohuchi, K. (2002). Participation of various kinases in staurosporine induced apoptosis RAW 264.7 cells. *Journal of Pharmacy and Pharmacology*, 54, 1535-1544.
- Yanagawa, N., Tamura, G., Honda, T., Endoh, M., Nishizuka, S., & Motoyama, T. (2004). Demethylation of the synuclein gamma gene CpG island in primary gastric cancers and gastric cancer cell lines. *Clinical Cancer Research*, 10, 2447-2451.
- Yang, E., Zha, J., Jockel, J., Boise, L.H., Thompson, C.B., & Korsmeyer, S.J. (1995). Bad, a heterodimeric partner for Bcl-XL and Bcl-2, displaces Bax and promotes cell death. *Cell*, 80, 285-291.
- Yang, J., Liu, X., Bhalla, K., Kim, C.N., Ibrado, A.M., Cai, J., et al. (1997). Prevention of apoptosis by Bcl-2: release of cytochrome *c* from mitochondria blocked. *Science*, 275, 1129-1132.
- Ye, Q., Wang, T.F., Peng, Y.F., Xie, J., Feng, B., Qiu, M.Y., et al. (2010). Expression of alpha-, beta- and gamma-synuclein in colorectal cancer, and potential clinical significance in progression of the disease. *Oncology Reports*, 23, 429-436.
- Ye, Q., Zheng, M.H., Cai, Q., Feng, B., Chen, X.H., Yu, B.Q., et al. (2008). Aberrant expression and demethylation of gamma-synuclein in colorectal cancer, correlated with progression of the disease. *Cancer Science*, 99, 1924-1932.
- Yoshida, T., Tanaka, M., Sotomatsu, A., & Hirai, S. (1995). Activated microglia cause superoxide-mediated release of iron from ferritin. *Neuroscience Letters*, 190, 21-24.
- Yu, S., Li, X., Liu, G., Han, J., Zhang, C., Li, Y., et al. (2007). Extensive nuclear localization of alpha-synuclein in normal rat brain neurons revealed by a novel monoclonal antibody. *Neuroscience*, 145, 539- 555.
- Yuan, B., Latek, R., Hossbach, M., Tuschl, T., & Lewitter, F. (2004). siRNA selection server: an automated siRNA oligonucleotide prediction server. *Nucleic Acids Research*, 32, W130-W134.
- Yuan, Z., Zhao, X., Yan, F., Zhao, J., Liu, H., Xiong, S., et al. (2007). Beta-synuclein protein from *Xenopus laevis*: overexpression in *Escherichia coli* of the GST-tagged protein and production of polyclonal antibodies. *Biochemistry (Moscow)*, 72, 1270-1278.

- Yuste, V.J., Sanchez-Lopez, I., Sole, C., Encinas, M., Bayascas, J.R., Boix, J., et al. (2002). The prevention of the staurosporine-induced apoptosis by Bcl-X(L), but not by Bcl-2 or caspase inhibitors, allows the extensive differentiation of human neuroblastoma cells. *Journal of Neurochemistry*, *80*, 126-139.
- Zarranz, J.J., Alegre, J., Gomez-Esteban, J.C., Lezcano, E., Ros, R., Ampuero, I., et al. (2004). The new mutation, E46K, of alpha synuclein causes Parkinson and Lewy body dementia. *Annals of Neurology*, *55*, 164-173.
- Zha, J., Harada, H., Yang, E., Jockel, J., & Korsmeyer, S.J. (1996). Serine phosphorylation of death agonist BAD in response to survival factor results in binding to 14-3-3 not Bcl-X. *Cell*, *87*, 619-628.
- Zhang, B.F., Peng, F.F., Zhang, J.Z., & Wu, D.C. (2003). Staurosporine induces apoptosis in NG108-15 cells. *Acta Pharmacologica Sinica*, *24*, 663-669.
- Zhang, X.D., Borrow, J.M., Zhang, X.Y., Nguyen, T., & Hersey, P. (2003). Activation of ERK1/2 protects melanoma cells from TRAIL-induced apoptosis by inhibiting Smac/DIABLO release from mitochondria. *Oncogene*, *22*, 2869-2881.
- Zhao, W., Liu, H., Liu, W., Wu, Y., Chen, W., Jiang, B., et al. (2006). Abnormal activation of the synuclein-gamma gene in hepatocellular carcinomas by epigenetic alteration. *International Journal of Oncology*, *28*, 1081-1088.
- Zhou, H., & Zeng, X. (2009). Energy profile and secondary structure impact shRNA efficacy. *BMC Genomics*, *10*, Suppl 1:S9.
- Zhou, Z.D., Yap, B.P., Gung, A.Y., Leong, S.M., Ang, S.T., & Lim, T.M. (2006). Dopamine-related and caspase-independent apoptosis in dopaminergic neurons induced by overexpression of human wild type or mutant alpha-synuclein. *Experimental Cell Research*, *312*, 156-170.
- Zimprich, A., Biskup, S., Leitner, P., Lichtner, P., Farrer, M., Lincoln, S., et al. (2004). Mutations in LRRK2 cause autosomal-dominant Parkinsonism with pleomorphic pathology. *Neuron*, *44*, 601-607.
- Zourlidou, A., Payne Smith, M.D., & Latchman, D.S. (2003). Modulation of cell death by alpha-synuclein is stimulus-dependent in mammalian cells. *Neuroscience Letters*, *340*, 234-238.
- Zubovits, J., Buzney, E., Yu, L., & Duncan, L.M. (2004). HMB-45, S-100, NK1/C3, and MART-1 in metastatic melanoma. *Human Pathology*, *35*, 217-223.

## APPENDIX A

### (a) Determination of shRNA target sequence using siRNA Selection Program

#### siRNA Selection Program

- \* Enter your sequence in [Raw](#) or [FASTA](#) format below,

OR enter [GI](#) or [Accession number](#)

- \* [Choose the siRNA pattern:](#)

Recommended patterns	<a href="#">custom</a>
<input type="radio"/> N2[CG]N8[AUT]N8[AUT]N2	<input style="width: 100%;" type="text"/> <a href="#">Enter pattern with 23 bases</a>
<input checked="" type="radio"/> AAN19TT	
<input type="radio"/> NAN21	

- Filter criteria:

- \* GC percentage: from  to
- \* [exclude a run of](#)  [or more T or A in a row](#)
- \* [exclude a run of](#)  [or more Gs in a row](#)
- \* [include less than](#)  consecutive GC in a row.
- equal %(+/- ) for all 4 bases.

#### Choose siRNA Candidate(s)

- siRNA candidates after filtering the **base\_run**, **gc%**, and **base\_variation**: (The more oligos you choose, the longer time for you to get results.)

Oligo patterns: *A=AAN19TT; B=NAN19NN; C=N2[CG]N8[AU]N8[AU]N2; F=Custom*

	Position	Sequence	Patterns	GC%	Thermodynamic Values	SNPs	miRNA targets
<input checked="" type="checkbox"/>	1	2575-2597	S 5' : AGUGGCGGUUAGGAUUAU UU mRNA : AA AGTGGCGGTTAGGATATAT TT AS 3' : UU UCACCGCCAUCCUAUUA	A,B	42	-4.8 (-9.8, -5.0)	<a href="#">88[43]</a>
<input checked="" type="checkbox"/>	2	2600-2622	S 5' : UCUACCUAAAAGCAGCAUUA UU mRNA : AA TCTACCTAAAGCAGCATAT TT AS 3' : UU AGAUGGAUUUCGUCGUUA	A,B	37	-2.9 (-8.6, -5.7)	<a href="#">102[48]</a>
<input checked="" type="checkbox"/>	3	2527-2549	S 5' : GCAAGGAAAAGGAUUUGUUA UU mRNA : AA GCAAGGAAAAGGATTGTITA TT AS 3' : UU CGUCCUUUCCUAAACAAU	A,B	37	-2.5 (-9.7, -7.2)	<a href="#">696[98]</a>
<input checked="" type="checkbox"/>	4	2398-2420	S 5' : GGAUGGUUACCAUAGAAAC UU mRNA : AA GGATGGTTACCATAGAAAC TT AS 3' : UU CCUACCAUUGGUUUCUUUG	A,B	42	-2.3 (-10.0, -7.7)	<a href="#">427[94]</a>
<input checked="" type="checkbox"/>	5	2385-2407	S 5' : UGAGUGACUAUAAGGAUUG UU mRNA : AA TGAGTGACTATAAGGATGG TT AS 3' : UU ACUCACUGAUUCCUACC	A,B	42	0.0 (-9.4, -9.4)	<a href="#">112[52]</a>

2. Choose the alignment tool:

3. Choose the species:

4. Choose the database you would like to BLAST against:

5. Receive result

via email:

on web browser.

6.

(b) NCBI BLAST search and final selection of target sequences.

**View BLAST Results and Filter Results to reduce off-target effects**

To eliminate siRNAs that may produce off-target effects, we provide several filtering methods: [?](#)

**by Number of Matches:** [?](#) [EXAMPLE](#)

Eliminate siRNAs with off-target BLAST hits sharing more than  matched bases of the antisense strand

**by Positions:** [?](#) [EXAMPLE](#)

Eliminate siRNAs with off-target BLAST hits aligning with its antisense strand at the specified positions

2	3	4	5	6	7	8	9	10	11	12	13	14	15	16	17	18	19
<input checked="" type="checkbox"/>																	

The entrez\_gene ID for your specific target:  [How to get entrez\\_gene ID?](#)

No.	pos	siRNA	type	GC%	thermodynamics	SNP	blast
<input checked="" type="checkbox"/>	1	2575-2597	A,B	42	-4.8 (-9.8, -5.0)		<a href="#">LINK</a>
		S 5' : AGUGGCGGUUAGGAUUAU UU mRNA : AA AGTGGCGGTTAGGATATAT TT AS 3' : UU UCACCGCCAAUCCUAUUA					
<input checked="" type="checkbox"/>	2	2385-2407	A,B	42	0.0 (-9.4, -9.4)		<a href="#">LINK</a>
		S 5' : UGAGUGACUAUAAGGAUGG UU mRNA : AA TGAGTGACTATAAGGATGG TT AS 3' : UU ACUCACUGAUUCCUACC					

## APPENDIX B

### Formulas

(A) Calculation for Cell Viability:

$$\text{Cell Viability (\%)} = \frac{\text{S average} - \text{N average}}{\text{P average} - \text{N average}} \times 100 \%$$

S: Absorbance of sample

P: Absorbance of positive controls (blank cells)

N: Absorbance of negative controls (blank medium)

(B) Calculation for Standard Error of Mean:

$$SE_{\bar{x}} = \frac{s}{\sqrt{n}}$$

where  $s$  is the sample standard deviation

$n$  is the size (number of observations) of the sample.

$$\text{Standard Deviation, } s = \sqrt{\frac{\sum x^2}{n} - (\bar{x})^2}$$

$x$  : Independent value

$\bar{x}$  : Mean value

$n$ : Number of assays

## APPENDIX C

### Effect of $\alpha$ -Syn knockdown on cell cycle phase distribution and proliferative index of SK-MEL28

#### (a) Cell cycle phase distribution of SK-MEL28 cell lines.

Cell lines	Cell cycle phases	Untreated			Staurosporine-treated		
		Percentage gated Average $\pm$ SEM			Percentage gated Average $\pm$ SEM		
Untransfected SK-MEL28	Sub Go	1.09	$\pm$	0.35	26.98	$\pm$	3.83
	Go/G1	75.45	$\pm$	2.97	41.76	$\pm$	0.93
	S phase	9.17	$\pm$	2.44	11.45	$\pm$	0.77
	G2/M	13.68	$\pm$	3.90	18.76	$\pm$	2.30
pLKO.1-TRC control-transfected SK-MEL28	Sub Go	0.91	$\pm$	0.11	27.51	$\pm$	1.11
	Go/G1	75.53	$\pm$	0.36	43.80	$\pm$	0.11
	S phase	12.98	$\pm$	0.33	9.71	$\pm$	1.76
	G2/M	10.36	$\pm$	0.01	17.51	$\pm$	0.96
pLKO.1-scramble shRNA-transfected SK-MEL28	Sub Go	0.87	$\pm$	0.15	28.84	$\pm$	1.04
	Go/G1	74.53	$\pm$	0.59	42.24	$\pm$	1.87
	S phase	11.45	$\pm$	0.56	9.89	$\pm$	0.16
	G2/M	12.64	$\pm$	0.21	17.10	$\pm$	2.49
pLKO.1-HuAsynRNAi 3-transfected SK-MEL28	Sub Go	0.45	$\pm$	0.06	32.26	$\pm$	5.89
	Go/G1	81.32	$\pm$	0.94	44.74	$\pm$	1.49
	S phase	10.26	$\pm$	0.50	4.41	$\pm$	1.08
	G2/M	7.69	$\pm$	0.42	17.85	$\pm$	3.10

#### (b) Proliferative index of SK-MEL28 cell lines.

Untreated Cell lines	Proliferative index		
	Average $\pm$ SEM		
Untransfected SK-MEL28	0.233	$\pm$	0.027
pLKO.1-TRC control-transfected SK-MEL28	0.236	$\pm$	0.003
pLKO.1-scramble shRNA-transfected SK-MEL28	0.244	$\pm$	0.005
pLKO.1-HuAsynRNAi 3-transfected SK-MEL28	0.181	$\pm$	0.009

## APPENDIX D

### Effect of $\alpha$ -Syn overexpression on cell cycle phase distribution and proliferative index of SH-SY5Y

#### (a) Cell cycle distribution of SH-SY5Y cell lines.

Cell lines	Cell cycle phases	Untreated			Staurosporine-treated		
		Percentage gated Average $\pm$ SEM			Percentage gated Average $\pm$ SEM		
Untransfected SH-SY5Y	Sub Go	1.49	$\pm$	0.94	11.24	$\pm$	0.51
	Go/G1	69.74	$\pm$	0.80	39.06	$\pm$	0.27
	S phase	14.70	$\pm$	2.26	18.22	$\pm$	0.46
	G2/M	12.69	$\pm$	1.18	30.12	$\pm$	0.24
Mock-transfected SH-SY5Y	Sub Go	3.21	$\pm$	1.10	12.99	$\pm$	0.73
	Go/G1	70.94	$\pm$	0.63	47.12	$\pm$	4.02
	S phase	10.75	$\pm$	0.67	18.62	$\pm$	1.42
	G2/M	14.19	$\pm$	0.76	21.71	$\pm$	2.94
pcDNA <sup>TM</sup> 3.1 -wild type $\alpha$ Syn-transfected SH-SY5Y	Sub Go	1.33	$\pm$	0.13	11.75	$\pm$	0.47
	Go/G1	68.95	$\pm$	1.86	45.69	$\pm$	0.72
	S phase	14.51	$\pm$	0.69	20.20	$\pm$	1.95
	G2/M	13.84	$\pm$	1.06	22.40	$\pm$	0.59
pcDNA <sup>TM</sup> 3.1 - $\alpha$ Syn A30P- transfected SH-SY5Y	Sub Go	6.96	$\pm$	1.56	23.96	$\pm$	5.79
	Go/G1	70.30	$\pm$	1.58	35.29	$\pm$	4.38
	S phase	8.33	$\pm$	0.18	24.80	$\pm$	3.38
	G2/M	12.28	$\pm$	1.09	15.97	$\pm$	2.93
pcDNA <sup>TM</sup> 3.1 - $\alpha$ Syn A53T- transfected SH-SY5Y	Sub Go	2.17	$\pm$	0.54	17.09	$\pm$	0.44
	Go/G1	72.56	$\pm$	1.08	39.95	$\pm$	0.69
	S phase	11.90	$\pm$	1.78	23.02	$\pm$	1.21
	G2/M	11.59	$\pm$	1.19	20.00	$\pm$	1.51
pcDNA <sup>TM</sup> 3.1 - $\alpha$ Syn E46K- transfected SH-SY5Y	Sub Go	1.25	$\pm$	0.70	13.72	$\pm$	0.72
	Go/G1	72.52	$\pm$	0.06	38.44	$\pm$	0.45
	S phase	12.92	$\pm$	0.83	25.89	$\pm$	1.02
	G2/M	12.03	$\pm$	1.22	21.55	$\pm$	0.48

#### (b) Proliferative index of SH-SY5Y cell lines.

Untreated Cell lines	Proliferative index		
	Average $\pm$ SEM		
Untransfected SH-SY5Y	0.282	$\pm$	0.007
Mock-transfected SH-SY5Y	0.260	$\pm$	0.009
pcDNA <sup>TM</sup> 3.1-wild type $\alpha$ Syn-transfected SH-SY5Y	0.291	$\pm$	0.018
pcDNA <sup>TM</sup> 3.1- $\alpha$ Syn A30P-transfected SH-SY5Y	0.227	$\pm$	0.011
pcDNA <sup>TM</sup> 3.1- $\alpha$ Syn A53T-transfected SH-SY5Y	0.245	$\pm$	0.014
pcDNA <sup>TM</sup> 3.1- $\alpha$ Syn E46K-transfected SH-SY5Y	0.256	$\pm$	0.004